

COMPUTATIONAL MAPPING OF PHYTOCHEMICALS IN PLANTS /HERBAL EXTRACTS TO POTENTIAL LEAD COMPOUNDS

Thesis submitted in partial fulfilment of the requirements for the Degree of

DOCTOR OF PHILOSOPHY

By

**SHILPA SHARMA
(E19SOE816)**



**BENNETT
UNIVERSITY**
TIMES OF INDIA GROUP

Department of Biotechnology,
School of Engineering and Applied Sciences

Bennett University
(Established under UP Act No 24, 2016)
Plot Nos 8-11, Tech Zone II
Greater Noida-201310, Uttar Pradesh, India
July 2022

Dedicated to family, friends, and the research community

@ Copyright Bennett University, Greater Noida, India

August 2022

ALL Rights Reserved

DECLARATION BY THE SCHOLAR

I hereby declare that the work reported in the Ph.D. thesis entitled “**Computational mapping of phytochemicals in plants /herbal extracts to potential lead compounds**” submitted at Bennett University, Greater Noida, India, is an authentic record of my work carried out under the supervision of **Dr. Rajinder Singh Chauhan**. I have not submitted this work elsewhere for any other degree or diploma.

I am fully responsible for the contents of my Ph.D. Thesis.

Shilpa Sharma

Department of Biotechnology

Bennett University, Greater Noida, India

16.08.2022

SUPERVISOR'S CERTIFICATE

This is to certify that the work reported in the Ph.D. thesis entitled “**Computational mapping of phytochemicals in plants /herbal extracts to potential lead compounds**”, submitted by **Shilpa Sharma** at **Bennett University, Greater Noida, India**, is a bonafide record of her original work carried out under my supervision. This work has not been submitted elsewhere for any other degree or diploma.

Dr. Rajinder Singh Chauhan

Dean (Research & Consultancy) &

Prof. & Head, Department of Biotechnology

Date: 16.08.2022

ACKNOWLEDGEMENT

I feel proud and privileged to honour and place my gratitude to all those who have been supportive and encouraging throughout the completion of my Ph.D. thesis. First and foremost, I avail this opportunity to express my deep sense of gratitude and indebtedness to Prof. Rajinder Singh Chauhan, for introducing the present work and for his inspiring guidance, constructive criticism and valuable suggestion throughout my PhD work. I gratefully acknowledge his constant encouragement and help in different ways to complete my thesis successfully. I will remain indebted to him for pruning my personality and giving new dimension in the scientific field through his analytical scientific outlook. I really salute his great wisdom and personality.

A special note of thanks to my PhD committee members Dr. Shivani Goel, Dr. Vivek Kumar, Dr. Vinay Sheel Bansal, Dr. Deepa Khare, Dr. Sridhar Swaminathan, Dr. Deepika Vatsa for their fruitful suggestions during perusal of my doctoral work. I would like to extend my sincere gratitude to all the faculty members at Biotechnology department for their sustained help and suggestions. I owe my grateful thanks to technical staff of the department.

I am also indebted to all my friends and colleagues Anjali Kharb, Roma Pandey, Aditi Singh and Sumit Joshi, Research Associates Dr. Poornima Sharma and Dr. Dipto Bhattacharya for their help and insight into the study. I would like to express my special thanks to my batchmates and friends Ashish Sharma and Prateek Kumar for their sustained help and tremendous support throughout my research work.

I emphatically extend my sincere gratitude to Mr. Vineet Jain (Chancellor, BU), Dr. Prabhu Kumar Aggarwal (Vice Chancellor, BU), Mr. Sudhanshu Varma (Chief Operating Officer, BU), Col. (Retd) Guljit Singh Chadha (Registrar) and BU Information Technology and administration staff for providing fellowship and lab infrastructure to pursue a Doctorate Degree.

Finally, I am especially thankful to my family members who were always a source of strength, support and inspiration. Above all, I offer my humble obeisance to the Almighty, who provided me endurance and eventually rewarded me with the successful completion of my work.

“All may not be mentioned, but no one is forgotten”

LIST OF ABBREVIATIONS

3D	Three-dimensional
ACE2	Angiotensin-Converting Enzyme 2
AKT	serine/threonine protein kinase
BP	Biological Process
CASP3	Caspase-3
CASP8	Caspase-8
CC	Cellular Component
COX	Cyclooxygenase
CVD	Cardiovascular disease
CYPs	Cytochromes
DAVID	Database for Annotation, Visualization, and Integrated Discovery
EGFR	Epidermal growth factor receptor
FOS	Fos Proto-Oncogene
FOXO1	Forkhead Box O1
GO	Gene Ontology
GROMACS	GRoningen MACHine for Chemical Simulations
H-bonds	Hydrogen bonds
HCC	Hepatocellular carcinoma
HSP90	Heat shock protein 90
IGF1R	Insulin Like Growth Factor 1 Receptor
IL6	Interleukin-6
ISG15	Interferon-Stimulated gene 15
KEGG	Kyoto encyclopedia of genes and genomes
MD	Molecular dynamics
MF	Molecular Function
Mpro/3CLpro	Main protease/3-Chymotrypsin-like protease
NAFLD	Non-alcoholic fatty liver disease
NASH	Non-alcoholic steatohepatitis
NDUFs	NADH:Ubiquinone Oxidoreductase Core Subunit
NFKB	Nuclear factor kappa B
PDB	Protein Data Bank
P-gp	Permeability glycoprotein
PIK3CA	Phosphatidylinositol-4,5-Bisphosphate 3-Kinase Catalytic Subunit Alpha
PIK3CB	Phosphatidylinositol-4,5-Bisphosphate 3-Kinase Catalytic Subunit Beta
PLIP	Protein-Ligand Interaction Profiler
PLpro	Papain-Like protease
PNPLA3	Patatin Like Phospholipase Domain Containing 3

PPARA	Peroxisome proliferator-activated receptor alpha
PPARG	Peroxisome proliferator-activated receptor gamma
PPI	Protein-Protein Interaction
RBM	Receptor Binding Domain
RdRp	RNA dependent RNA polymerase
RMSD	Root Mean Square Deviation
RMSF	Root Mean Square Fluctuation
RoG	Radius of gyration
ROS	Reactive Oxygen Species
SASA	Solvent-Accessible Surface Area
SG-pro	Spike Glycoprotein
STRING	Search Tool for the Retrieval of Interacting Genes
T2D	Type 2 Diabetes
TGFB	Transforming growth factor beta-1
TM6SF2	Transmembrane 6 Superfamily Member 2
TNFA	Tumor necrosis factor alpha
TP53	Tumor Protein P53
TTD	Therapeutic Target Database
UBQC	Ubiquitin C
VEGFA	Vascular Endothelial Growth Factor A

LIST OF FIGURES

Figure No.	Caption	Page No.
1.1	Paradigm shifting from traditional to modern drug discovery process	4
1.2	Experimental pharmacokinetic profile of Picroside-I and Picroside-II	6
2.1	Bioassay-Guided Fractionation workflow	18
3.1	Workflow of experiments in the current study	40
3.2	Interaction within active binding pocket of Mpro, 3D and 2D visualization of interaction with molecules and Mpro residues. A. Mpro and Jatamansin complex B. Mpro and 6,7-dehydroferruginol complex. C. Mpro and Beta-sitosterol complex. D. Mpro and Phyllocladanol complex	45
3.3	Binding interaction in active site pocket of PLpro. A. PLpro and Lantadene D complex. B. PLpro and Abietatriene complex. C. PLpro and Friedelan-3-one complex	48
3.4	Interaction within active binding pocket of RdRp, 2D and 3D visualization of interaction. A. Reduced lantadene A – RdRp complex. B. Lantadene A – RdRp complex	51
3.5	Interaction within active pocket of RBD of spike glycoprotein. A. Lantadene B – SG-pro complex B. Lantadene A – SG-pro complex	53
3.6	Distribution of dataset based on number of violations of stated rules for drug-likeness	54
3.7	RMSD and RMSF profile of free Mpro and complexes. Native Mpro in black and complexes in red (Replica 1) and green (Replica 2) colour lines. A. Beta-Sitosterol – Mpro B. Jatamansin - Mpro C. 6,7-dehydroferruginol – Mpro D. Phyllocladanol – Mpro	59
3.8	Hydrogen Bond Analysis pf Mpro-complexes in two replications, Replica 1 (red) and Replica 2 (green). A. Jatamansin - Mpro B. Beta-Sitosterol – Mpro C. Phyllocladanol – Mpro D. 6,7-dehydroferruginol – Mpro	60
3.9	RMSD and RMSF profile of free PLpro and complexes. Native PLpro in black and complexes in red (Replica 1) and green (Replica 2) colour lines. A. Abietatriene – PLpro B. Lantadene D – PLpro C. Friedelan-3-one – PLpro	61

3.10	Hydrogen Bond Analysis of PLpro – Complexes in two replications, Replica 1 (red) and Replica 2 (green). A. Lantadene D – PLpro B. Friedelan-3-one – PLpro	62
3.11	RMSD and RMSF profile of free RdRp and complexes. Native RdRp in black, and complexes in red (Replica 1) and green (Replica 2). A. Lantadene A – RdRp B. Reduced Lantadene A – RdRp	63
3.12	Hydrogen Bond Analysis of RdRp – Complexes in two replications, Replica 1 (red) and Replica 2 (green). A. Lantadene A – RdRp B. Reduced Lantadene A – RdRp	64
3.13	RMSD and RMSF profile of free Spike and complexes. Native SGpro in black, complexes in red (Replica 1) and green (Replica 2). A. Lantadene A – SGpro B. Lantadene B – SGpro.	65
3.14	Hydrogen Bond Analysis of SGpro – Complexes in two replications, Replica 1 (red) and Replica 2 (green). A. Lantadene A – SGpro B. Lantadene B – SGpro	65
3.15	Binding energies evaluated from MM-PBSA method of selected complexes. Van der wall energy is indicating highest contribution in total free binding energy. ΔE_{vdw} , ΔE_{elec} , ΔE_{pol} , ΔE_{np} , and ΔE_{bind} represents van der wall energy, electrostatic energy, polar solvation energy, nonpolar solvation energy, and total binding energy respectively.	66
4.1	Workflow of network pharmacology strategy to capture <i>Picrorhiza kurroa</i> compounds and their mechanism in NAFLD/ NASH treatments	76
4.2	Compound-Target-Network of <i>Picrorhiza kurroa</i> compounds. Green rectangle represents the Picrosides; Light blue rectangle stands for Cucurbitacins; Top orange rectangle stands for Bioenhancers; Light green rectangle represents the other active compounds from extracts for important for NAFLD associated diseases; In center, light cyan triangles represent the predicted targets of all 24 compounds; and edges represents the interaction between compounds and corresponding targets whereas size of all nodes indicate the number of interactions	80
4.3	Venn diagram signifies the distribution of predicted targets according to corresponding compounds	86
4.4	Interactive-Network of targets. Purple color nodes indicate the <i>Picrorhiza kurroa</i> treating targets of NAFLD (shared targets) whereas, cyan color nodes indicate the additional interactive proteins came from Protein-Protein-Interaction Network	87

4.5	GO and KEGG enrichment analysis of shortlisted gene encoding targets involved in: (A) Biological Process, (B) Molecular Function (C) Cellular Component, (D&E) signaling and disease pathways. (A-D) represents the outcomes in color scales (according to different p-values) and the sizes of the dots represent the gene count of each term. (E) represents the distribution of targets in different pathways	89
4.6	A comprehensive network of compound-disease-pathway-associated diseases. Color codes for all the nodes given in text, edges represent the interaction between all nodes whereas size of nodes indicate the number of interactions	90
4.7	Mapping of critical protein targets to their role in corresponding progressive stages	92
4.8	Interaction of potential compounds of <i>Picrorhiza kurroa</i> with putative targets in therapeutics of NAFLD/ NASH. Binding affinity of corresponding complex is mentioned in the center of individual figure. Left: 3D visualization and Right: 2D visualization of interaction (A) PPARG and Picroside-I complex (B) PPARA and Vernicoside complex (C) IL6 and Rutin complex (D) TNFA and Picroside-IV (E) CASP3 and Verminoside complex (F) CASP8 and Cucurbitacin I complex (G) AKT and Astragaloside complex (H) EGFR and Picroside-III (I) TGFB and Cucurbitacin F (J) HSP90 and Rutin	93
4.9	Molecular dynamics simulation analysis. RMSD and RMSF profile of apo-proteins and respective complexes. Apo-protein is represented in black and complexes in red color lines	99

LIST OF TABLES

Table No.	Title	Page No.
2.1	Some popular examples of approved drugs from ethnopharmacology approach	17
2.2	Molecular docking tools and software and their corresponding algorithms	22
2.3	Pharmacokinetics of Extracts and Formulations (related to <i>Picrorhiza kurroa</i>)	27
2.4	Intravenous administration of picroside-I and picroside-II	29
2.5	Oral Administration of Picroside-I and Picroside-II	29
3.1	Grid Box Coordinates and Size Parameters used in grid box generation	37
3.2	Medicinal values of selected essential oils compounds and their corresponding plant species	41
3.3	Interactions between potential compounds and Main Protease of SARS-CoV-2	43
3.4	Binding interaction of known inhibitors with therapeutic targets of SARS-CoV-2	46
3.5	Interaction between potential compounds and Pappain-Like protease of SARS-CoV-2	47
3.6	Interaction between potential compounds and RNA dependent RNA polymerase of SARS-CoV-2	50
3.7	Interaction between potential compounds and Spike glycoprotein of SARS-CoV-2	52
3.8	Pharmacological properties of resulting essential oils compounds	56
3.9	Binding Free Energies calculated from MM-PBSA Method of different complexes	67
4.1	Structure similarity in compounds and drugs based on tanimoto coefficient	77
4.2	Prediction of physicochemical and ADMET properties of significant compounds in <i>Picrorhiza kurroa</i> extracts	81
4.3	Biological or Medicinal activity of compounds of <i>Picrorhiza kurroa</i>	83
4.4	Binding affinity and interactions of <i>Picrorhiza kurroa</i> compounds as well as reference compounds with their respective proteins	95

TABLE OF CONTENTS

Subject	Page No.
ABSTRACT	i
LIST OF ABBREVIATIONS	ii
LIST OF FIGURES	iv
LIST OF TABLES	vii
CHAPTER 1	1
INTRODUCTION	1
CHAPTER 2	10
REVIEW OF LITERATURE	10
2.1. Herbs as potential sources of drugs	11
2.1.1. Historical Perspective	11
2.1.2. Role of Phytomedicine in modern drug discovery	12
2.2. Downfall and Re-emergence of Plant-based compounds in drug discovery	14
2.3. Methods for the discovery of novel pharmacologically active Phytochemicals	16
2.3.1. Experimental approaches in plant-based drug discovery	16
2.3.1.1. Random screening approach	16
2.3.1.2. Ethnopharmacology approach	17
2.3.1.3. Bioassay-Guided Fractionation and Metabolomic Profiling	17
2.3.1.4. Combinatorial chemistry and high throughput screening	19
2.3.2. Computational methods and resources to prioritize phytochemicals as leads	19
2.3.2.1. Structure-based drug discovery	20
<i>2.3.2.1.1. Protein structure Elucidation</i>	20
<i>2.3.2.1.2. Molecular docking based virtual screening</i>	21
<i>2.3.2.1.3. Molecular Dynamics (MD) Simulations</i>	22
2.3.2.2. Ligand-based drug discovery	23
<i>2.3.2.2.1. Structure similarity Approach</i>	23
<i>2.3.2.2.2. Pharmacophore modeling</i>	23
<i>2.3.2.2.3. Quantitative structure–activity relationship</i>	24

2.3.2.3. Network pharmacology in drug discovery	24
2.4. Pharmacokinetics and its importance in drug discovery	24
2.4.1. Pharmacokinetic profile of major iridoid glycosides, Picroside-I and Picroside-II of <i>Picrorhiza kurroa</i> in extracts and formulations	25
2.4.2. Pharmacokinetic profile of Picroside-I and Picroside-II of <i>Picrorhiza kurroa</i> in isolated compounds	29
2.4.3. Metabolites from biotransformation of Picroside-I, Picroside-II, Extracts, and Formulations through oral and intravenous delivery	30
CHAPTER 3	31
IN SILICO IDENTIFICATION OF POTENTIAL VOLATILE COMPOUNDS IN ESSENTIAL OILS AS INHIBITORS AGAINST MAJOR PATHOGENICITY DETERMINANTS OF SARS-COV-2	31
3.1. INTRODUCTION	32
3.2. MATERIALS AND METHODS	35
3.2.1. Dataset preparation	35
3.2.2. Preparation of ligands and four major therapeutic proteins of SARS-CoV-2 for molecular docking study	36
3.2.3. Molecular docking analysis	36
3.2.4. Pharmacokinetic analysis of compounds	37
3.2.5. Molecular dynamics simulation	38
3.2.6. Binding free energy analysis	39
3.3. RESULTS AND DISCUSSION	41
3.3.1. Identification of potentially active compounds against major therapeutic targets of SARS-CoV-2 based on ligand – receptor interactions	43
3.3.1.1. Interaction analysis of screened hit molecules and main protease of SARS-CoV-2	43
3.3.1.2. Interaction analysis of screened hit molecules and papain-like protease of SARS-CoV-2	46
3.3.1.3. Interaction analysis of screened hit molecules and RNA dependent RNA polymerase of SARS-CoV-2	49

3.3.1.4. Interaction analysis of screened hit molecules and spike glycoprotein of SARS-CoV-2	51
3.3.2. Pharmacokinetics analysis of shortlisted essential oils compounds	54
3.3.3. Investigation of stability and flexibility of ligand – receptor complexes in virtual biological system	55
3.3.3.1. Molecular dynamics simulation of main protease complexes	58
3.3.3.2. Molecular dynamics simulation of papain-like protease complexes	60
3.3.3.3. Molecular dynamics simulation of RNA dependent RNA polymerase complexes	62
3.3.3.4. Molecular dynamics simulation of spike glycoprotein complexes	64
3.3.4. Binding Free Energy Analysis	66
3.4. CONCLUSIONS	67
CHAPTER 4	69
IDENTIFICATION OF ACTIVE COMPONENTS IN <i>Picrorhiza kurroa</i> EXTRACTS AND THEIR POSSIBLE MECHANISTIC ACTIONS FOR THE TREATMENT OF NAFLD/ NASH	69
4.1. INTRODUCTION	70
4.2. MATERIALS AND METHODS	72
4.2.1. Curation of significant compounds present in <i>Picrorhiza kurroa</i>	72
4.2.2. Structure similarity analysis of <i>Picrorhiza kurroa</i> compounds with approved drugs for liver diseases	72
4.2.3. <i>In silico</i> pharmacokinetic profiling of <i>Picrorhiza kurroa</i> compounds	72
4.2.4. Network Pharmacology	73
4.2.4.1. Shortlisting of active constituents of <i>Picrorhiza kurroa</i> and prediction of their putative corresponding gene/ protein targets	73
4.2.4.2. Screening biological targets of <i>Picrorhiza kurroa</i> compounds in treating NAFLD/ NASH	73
4.2.4.3. Capturing interactive protein targets of NAFLD/ NASH	73

4.2.4.4. Gene ontology and KEGG enrichment analysis of shortlisted proteins	74
4.2.4.5. Construction of Compound-Target-Disease-Pathways Network	74
4.2.5. Molecular docking and molecular dynamics simulation analysis	74
4.3. RESULTS AND DISCUSSION	77
4.3.1. Compound structure similarity with known drugs of liver diseases revealed presence of active compounds in <i>Picrorhiza kurroa</i>	77
4.3.2. <i>In silico</i> pharmacokinetic analysis of <i>Picrorhiza kurroa</i> compounds	78
4.3.3. Network pharmacology to unravel mechanisms of action of <i>Picrorhiza kurroa</i> compounds in possible treatment of NAFLD/ NASH	79
4.3.3.1. Gene/ Protein target prediction of <i>Picrorhiza kurroa</i> compounds and fishing targets of NAFLD/ NASH	79
4.3.3.2. Compounds – Targets Network analysis	80
4.3.3.2.1. Compounds in <i>Picrorhiza kurroa</i> extracts act in synergistic manner to treat complexities and co-morbidities of NAFLD/ NASH	80
4.3.3.2.2. Noticeable role of bioenhancers in bioavailability of picrosides through compound -target network	85
4.3.3.3. Protein – Protein Interaction (PPI) network of shared targets	87
4.3.3.4. Gene Ontology and KEGG enrichment analysis of shortlisted targets	88
4.3.3.5. Comprehensive Network (Compound – Target – Diseases – Pathways – Other associated diseases) Analysis	90
4.3.4. <i>In silico</i> validation of potential candidates using molecular docking and molecular dynamics simulation	91
4.4. CONCLUSIONS	100
CHAPTER 5	102
CONCLUSIONS AND FUTURE PROSPECTS	102
5.1. CONCLUSIONS	103

5.2. FUTURE PROSPECTS	103
REFERENCES	105
APPENDICES	154
LIST OF PUBLICATIONS	189

ABSTRACT

In the era of modern medicine and synthetic pharmaceuticals, herbal medications and phytonutrients have caught the interest of scientists and healthcare professionals working on drug development. Since most of the herbal extracts used in phytotherapy contain hundreds of different chemical compounds, limited number of which have been experimentally shown to have biological or medicinal effects, thus it would be advantageous to map active compounds in extracts to potential leads in order to create novel chemical entities in drug discovery. Owing to this, attempts have been made to identify possible drug from a variety of aromatic and medicinal plants using several computational approaches. We worked on two types of diseases, one related to viral infection i.e., coronavirus disease-19 (COVID-19) and the other associated with lifestyle i.e., Non-alcoholic fatty liver disease (NAFLD) that eventually progresses to more chronic stages and remains incurable. To deal with the rising threats of COVID-19 recurrence, an alternate therapeutic option, directly affecting the entry, multiplication and infection cycle of virus has been considered a priority. Hence, the efforts were made in current study to identify potential leads to be used as inhalation therapy as nasal swabs have been reported to transfer viral load prominently. The current investigation is a unique initial attempt whereby essential oils compounds have been computationally screened to neutralize SARS-COV-2 infection. Other disease problem the NAFLD has become a silent pandemic worldwide with no authorized medication available. For NAFLD we considered a potential hepatoprotective herb, *Picrorhiza kurroa*, in which the extracts are reported to provide therapeutic efficacy, but the individual compounds are less bioavailable. Hence, the aim of the study was to explore major compounds in *Picrorhiza kurroa* extracts towards identification of mechanistic actions to pinpoint the potential leads. The network pharmacology approach revealed the interactive behavior of proteins involved in NAFLD interaction by *Picrorhiza kurroa* compounds and suggested multi-target drug discovery for treatment of NAFLD by providing novel compounds as potential therapeutics.

CHAPTER 1
INTRODUCTION

Since ancient times, plants have been used to treat various types of diseases, and the use of plants as medicine by humans can be traced back thousands of years according to fossil records [1]. Generally, the plants produce secondary metabolites which they form for their defense mechanism against herbivores and environmental conditions. Therefore, plants contain several types of secondary metabolites or phytochemicals that work like drugs to neutralize the therapeutic targets of particular disease. In addition to this, Phytochemicals have some unique characteristics like these are biologically active pharmacophores in pharmaceuticals that show structurally diverse chemical scaffolds, which are ideal for lead selection and optimization, presence of stereogenic centers, occupying large chemical space which is not covered by synthetic compounds [2]. In past few decades, the enhancement in use of medicinal plants is seen for several ailments even used as prescription drugs [3]–[6]. According to recent report of last four decades (1981-2019) on approved drugs, approximately, 87% of drugs are from natural products or derived from them [7], [8].

Traditionally, the single plant extracts or combination of extracts from different plants (root extract, leaf extract, powdered seed extract, whole plant extract etc.) were used, which contains mixtures of various phytochemicals. All these compounds present in mixtures are not therapeutically active in isolated form or even do not show similar efficacy, only few of them exhibit medicinal value whereas other phytochemicals work in a synergistic way [9], [10], which is important to provide effective cure for complex diseases. Thus, research is required to identify which active components in mixtures of extracts are therapeutically active and explore the molecular basis of their therapeutic actions. Based on the previous knowledge several modern medicines have been developed either by directly isolating the compounds or their derivatives for example, morphine, caffeine, quinine, salicin, artemisinin, paclitaxel, etc. [11], [12].

The traditional drug discovery has been a long process taking around 10 to 15 years and costing around 2 to 3 billion USD for single drug to reach the market [13], [14]. Drug discovery process includes various steps such as identification of suitable therapeutic targets, hit identification from natural or synthetic sources, hit to lead development, lead optimization, preclinical and clinical trials (<https://www.fda.gov/>). Traditionally, the process was more challenging where the biologically active compounds were isolated through

fraction-based activity, which was slow, laborious, and occasionally unreliable. Afterwards, the advent of High Throughput Screening (HTS) shifted the paradigm from natural leads to synthetic leads, that boosted the popularity of biological testing, and combinatorial chemistry was advocated as a superior way to create "drug-like" molecules for HTS [11], [15]. However, combinatorial chemistry failed to produce the complex structures required for therapeutics as plants produce them naturally, and resulted into only a single new chemical entity (NCE) namely sorafenib approved by US Food and Drug Administration (FDA) in that time period [16]. With the advancements in techniques like pre-fractionation, LC-MS, nuclear magnetic resonance (NMR) spectroscopy etc., again drug discovery focused on phytochemicals [17]. Despite incredible efforts by scientists and the ongoing introduction of new procedures for the development of novel pharmaceuticals, clinical trial success rates were just 13 percent, with a high risk of drug attrition. Consequently, Leading pharmaceutical corporations and research organizations used computational approaches in preliminary investigations to speed up the drug discovery and development process, reducing costs and failures in the final stages [18], [19]. Rational drug design integrated with computational-aided drug discovery (CADD) approaches presented better understanding of binding affinities and molecular interactions of ligand-receptor complexes [20], [21], molecular dynamics simulation gave the idea of stability of complex in biological system for a period of simulation [22], supercomputing facilities speeded up the process of lead identification [23], and current advances in machine learning and artificial intelligence (AI) approaches have substantially benefitted in the learning and analysis of big data in drug discovery [24]. The drug discovery steps practiced in traditional and modern drug discovery have been presented in Figure 1.1. From CADD, many success stories have been documented and continues to play crucial role in drug designing and discovery process [25]. However, still there are gaps in novel and innovative computational methods and pipelines to identify active components and important synergistic compounds from crude extracts specifically for some complex diseases. As suggested by Thomford et al., [15] in a review that innovative drug discovery demands multidisciplinary approach involving existing as well as emerging technologies to compress such phytochemicals for development of new medications.

Subsequently, after extensive review of literatures and keeping in mind the above highlighted suggestions and issues, we opted to utilize multidisciplinary approach in lead identification

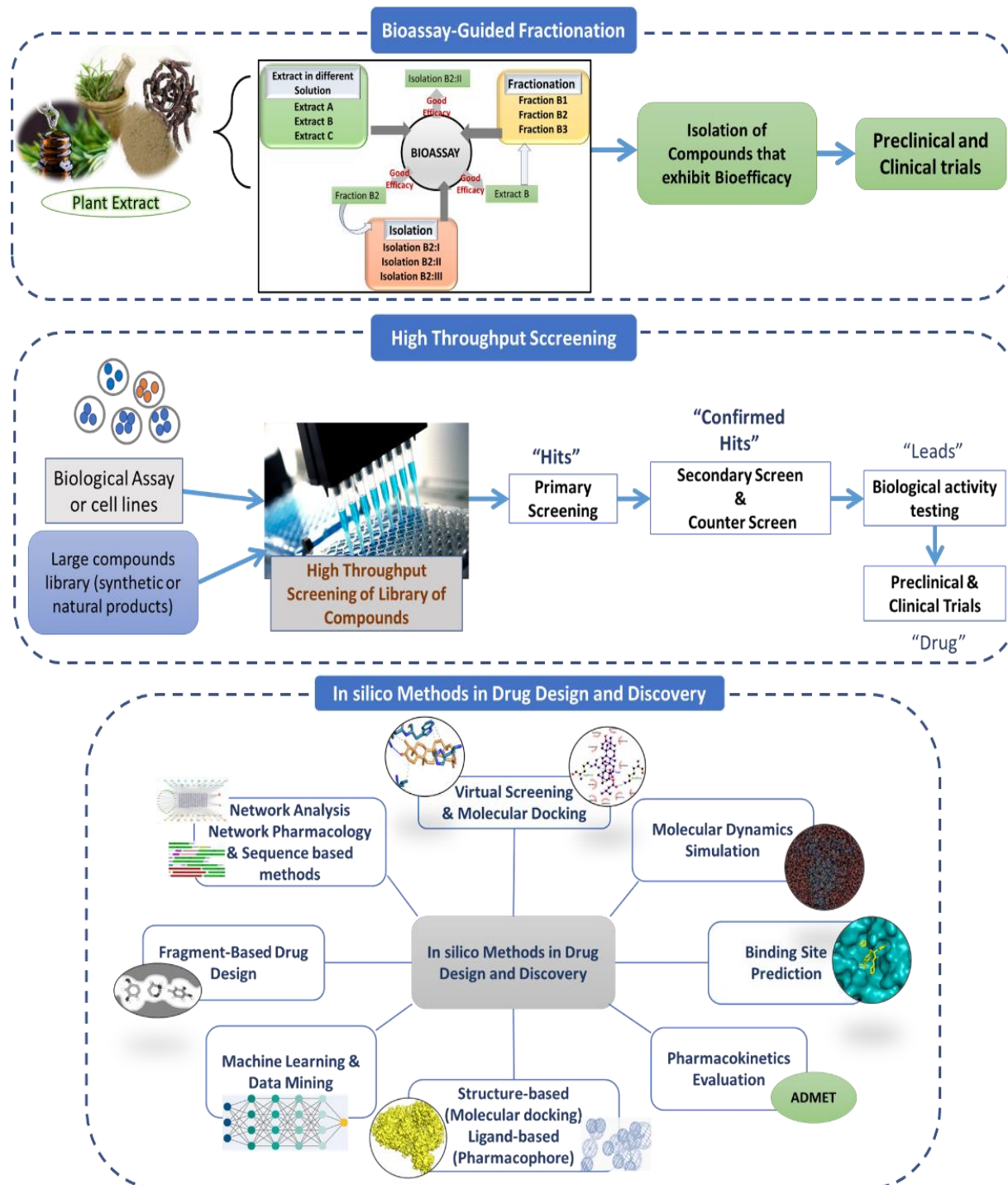


Figure 1.1: Paradigm shifting from traditional to modern drug discovery process

and concentrated on two crucial diseases with substantial medication demand for the treatment. These are two different types of diseases, one related to viral infection and the

other associated with lifestyle that progresses to more chronic stages and remains incurable. The global prevalence and the problems are discussed below for each disease.

In the last two years, we all witnessed global pandemic of Coronavirus disease 2019 (COVID-19), that claimed more than 6 million deaths around the world (<https://www.worldometers.info/>). Globalized vaccination programs alongside administration of repurposed drugs conferred a stronger and longer individual specific immune protection. However, rising threat of disease recurrence via evolution of novel viral variants posed recurrent threats of disease, therefore, a readily available phytopharmaceutical medication would have been the best option for COVID-19 treatment [26]. From the critical analysis of structural proteins of SARS-COV-2 virus, coupled with sufficient literature suggested four major therapeutic protein targets namely, main protease (Mpro), Papain-Like protease (PLpro) RNA-dependent-RNA-polymerase (RdRp) and the Spike-glycoprotein involved in virus's entrance, proliferation, and infection cycle. Till date, most of anti-viral drugs such as lopinavir, ritonavir, oseltamivir, favinapir and remdesivir have been tried against SARS-CoV-2 with limited success [27], [28] and also antiviral compounds and potential inhibitors have been studied [29]–[32]. The present study was, therefore, conceptualized to identify volatile phytochemicals that can be used as nasal therapy to directly block the binding site of SG-pro as well as other assisting proteins of SARS-COV-2 during entry into host nasal cells. The nasal swabs have been reported to carry massive SARS-CoV-2 viral loads in comparison to throat swabs in infected patients [33]. Plant based essential oils (EOs) are complex combination of volatile compounds belonging to various chemical classes, mainly terpenes and phenolics produced by mevalonate pathways and shikimate pathways respectively in aromatic plant species [34]. These compounds uniquely exhibit high vapor pressure at room temperature with several medicinal activities however, their use as of today has been limited to cosmetics and perfumery [35]. These molecules could be better counterparts in various respiratory diseases due to their unique characteristics [34], [36]. Thus, in this study, we used structure-based virtual screening of plants-derived essential oils (EO) compounds, followed by selective molecular dynamics simulation and binding free energy analysis of preferred receptor-ligand complexes, to suggest possible pharmacological leads as future SARS-CoV-2 therapeutics. Furthermore, we also proposed that combination nasal therapy with these volatile compounds might confer strong protection

against SARS-CoV-2 infection. Apart from this, recently SARS-CoV-2 has been reported to induce neurotropic damage to the brain via reaching olfactory lobes or the smelling epithelium in the brain [37], [38]. Thus, volatile compounds in EOs could be delivered through nasal delivery route and might even pass and target virus-infected brain lobes. Further detailed study is presented in chapter 3.

The other component of current study was non-alcoholic fatty liver disease (NAFLD), which is also considered as a serious public health concern, accounting for a large burden of hepatic and extrahepatic infections globally [39], [40]. According to reports, various comorbidities are associated with this disease such as chronic renal disease, cardiovascular disease, and considered as multisystem diseases [41] as well as it progresses to more severe stages like Non-alcoholic Steatohepatitis (NASH), Fibrosis, Cirrhosis, and eventually hepatocellular carcinoma, but surprisingly more deaths have been reported due to extra hepatic disorders. Furthermore, the complexities of this disease suggest the involvement of several pathogenic pathways and multiple targets, therefore, single- compound single-target approach has not

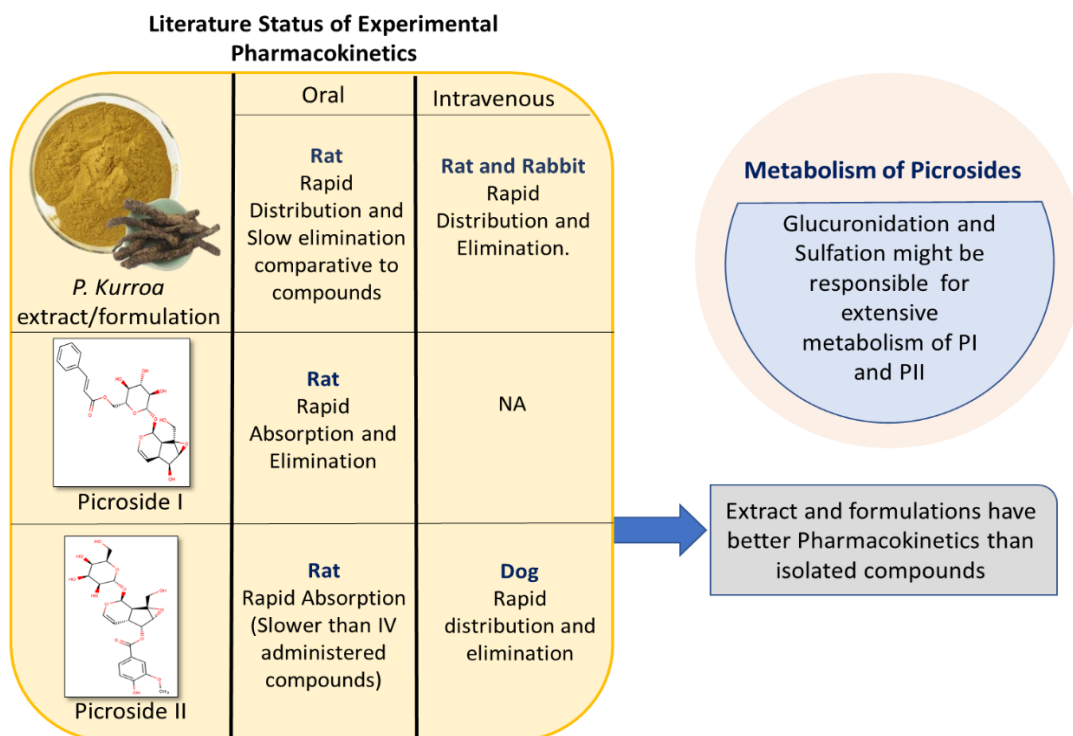


Figure 1.2 Experimental pharmacokinetic profile of Picroside-I and Picroside-II

been effective. The treatment of these liver pathologies has been quite challenging to the extent that no approved drug is available till date (<https://www.niddk.nih.gov>). Few herbal

medicines have been proven to be reported as hepatoprotective [42], [43]. *Picrorhiza kurroa* is one of those Himalayan medicinal herbs that is reported for various medicinal activities but extensively for hepatoprotective activity (Appendix Table A1). Its herbal formulations have been reported as potential hepatoprotective therapies against NAFLD/ NASH due to presence of mixtures of chemical constituents [44]–[46]. Even though, a few of signature components of *Picrorhiza kurroa* have shown hepatoprotective activity, however, their poor bioavailability has been major concern in translating into drugs [47]. It has been suggested that it might be because of hydrophilic nature and early metabolism and excretion via gut microbiota (Figure 1.2) [48]. Thus, to address above questions, we employed structural similarity and network pharmacology approaches and introduced multi-component-multi-target analysis to understand biological factors involved in pathology as well as to capture the mechanistic action of individual compounds in *Picrorhiza kurroa* by analyzing the connecting counterparts. Additionally, the potential leads have been shortlisted for major pathogenic targets directly engaged in disease pathways via different integrated computational techniques. The detailed investigation and methodology are demonstrated in chapter 4.

1.1. Research Gaps

From the literature, we recorded following gaps which have been addressed in the current study.

- In the era of antiviral intravenous and oral drugs, still there are gaps in discovery of potential leads for nasal delivery. Therefore, prioritizing plant-based essential oil compounds for inhalation therapy against SARS-COV-2 was considered a priority.
- Ayurvedic extracts are the mixtures of various metabolites, however, not all those compounds provide therapeutic activity rather few for which experimental knowledge is limited. As a result, urgent need has been realized to identify and map active compounds in crude herbal extracts into potential leads.

- NAFLD has been a silent pandemic for which no approved drugs are available. PicroLiv- a *Picrorhiza kurroa* based herbal formulation has been found to be effective for treating liver diseases, including NAFLD. However, major pharmacologically active compounds, Picroside-I and Picroside-II of *Picrorhiza kurroa* had shown less bioavailability and poor pharmacokinetics. Therefore, exploration of mechanistic action of active compounds from this herb was considered necessary to resolve poor bioavailability as well as to map potential therapeutic targets for NAFLD/ NASH. The following research objectives were proposed in light of above-mentioned gaps.

1.2. Research Objectives

- *In-silico* screening of plant-based essential oils compounds towards potential therapeutics against major proteins of SARS-COV-2.
- Computational mapping of *Picrorhiza kurroa* compounds to uncover potential therapeutic targets as well as their mechanistic action against non-alcoholic fatty liver disease (NAFLD) and non-alcoholic steatohepatitis (NASH)

1.3. Organization of Thesis

The entire research work is given in five chapters, and the thesis is organized as follows:

Chapter 1: This chapter covers the rationale for study, outlines the research problem, lists the research objectives, and provides a summary of the techniques employed to conduct the research.

Chapter 2: This chapter on Literature Review provides a thorough overview of conventional and existing methods for drug design and discovery. In this chapter, we also discussed the detailed computational approaches used in drug development.

Chapter 3: This chapter describes exploration of essential oils compounds from aromatic plant species for inhibition of major protein targets of SARS-CoV-2 using structure-based drug discovery, thereby proposing potential inhibitory compounds for inhalation therapy.

Chapter 4: This chapter is focused on study of mechanistic action of major active constituents of *Picrorhiza kurroa* effective in Non-alcoholic fatty liver disease and its further

progressive stages as well as addresses the bioavailability problem of some specific compounds from this herb via Network Pharmacology integrated with ligand and structure-based drug discovery.

Chapter 5: This chapter concludes the thesis by reviewing the work's significant accomplishments and proposing future directions for expanding the research.

CHAPTER 2
REVIEW OF LITERATURE

2.1. Herbs as potential sources of drugs

Plant based natural products acquired great interest of humankind as estimated in 1985 by World Health Organization (WHO), approximately 65% of people in the world have faith in plant derived naturally occurring products [49]. Natural products (NPs) and their derived compounds are in use for treatment of fatal diseases by traditional healers as well as for commercial purposes such as in cosmetics, dietary supplements and foods made from natural resources. The published article, reviews or literatures on natural products suggests that NPs have some important features that differentiate them from synthetic drugs such as high chemical diversity in molecules, biochemical specificity, and other essential molecular properties, therefore they can accelerate the number of potent lead structures which can be used as templates in drug designing process on the basis of biological activity [50]. According to study of Fabricant and Farnsworth (1985), there are 122 compounds with known chemical structures reported which were produced from 94 plant species. Among these compounds 80% have been shown to had ethnomedical usage that is equivalent to the present use of the active components of the plants [1], [49]. For instance, Berberine, a potential anti-inflammatory compound isolated from *Coptis chinensis Franch*, has already been in use traditionally for over 3000 years to treat inflammation and several infections. Quinine which was developed as antimalarial drug isolated from bark of *Cinchona* species has long been used to treat fever in amazon region and later introduced in Europe for the treatment of malaria [51]. Apart from this there are other successful compounds like berberine from *Berberis aristate*, Morphine from *Papaver somniferum*, Vinblastine, Vincristine from *Catharanthus roseus* and so on [52]. According to recent review, the interest of researchers has increased in last decade as a result a large numbers of medicinal plant databases have been developed and cited in the field of pharmacology and drug development [53].

2.1.1. Historical Perspective

Medicinal herbs have been used since ancient times for the treatment of many diseases and illnesses. The beginning of seeking medications in herbs/plants by humankind for the treatments is a result of many years of fights against several diseases. The knowledge of efficient components in herbs has been a product of hit and trial experiments for various centuries as documented by a range of sources, including written texts, ancient plant remedies

[54]. Traditional medicine practitioners were mainly dependent on herbs and used to recommend various ways of using herbs in ailments such as pills, ointments, snuffs, infusions and gargles [55]. The earliest records of plant based natural products have shown that thousands of plant-derived natural substances were recorded in Mesopotamia (2600 B.C.) that included oils extracted from *Cupressus sempervirens* (Cypress), *Papaver somniferum* (poppy juice), *Glycyrrhiza glabra* (licorice), and *Commiphora* species (myrrh) which are used to treat coughs, colds and inflammation. These products are still in use in modern era. Similarly, Egyptians also recorded plant derived substances from a plant named as *Ebers papyrus* in or around 2900 B.C., which is used to derive over 700 plant-based drugs in different forms [56]. The Chinese Materia Medica has been recorded in 1100 B. C. comprised of 52 prescriptions, thereafter Shennong Herbal recorded 365 drugs in or around ~100 B. C. then the work followed by Tang Herbal in 659 A. D. that contained 850 drugs [55]. Similarly, Charaka; Sushruta and Samhitas were documented dated before 1000 B.C. in Indian Ayurveda System with 341 and 516 drugs respectively [57]. Furthermore, the sensible use of herbal medications in ancient Western culture was greatly influenced by the Greeks and Romans. The Greek Scientist, Dioscorides (100 A.D.), recorded the collection, storage, and the uses of medicinal herbs, while Galen (130–200 CE.), a philosopher and pharmacist in Rome, worked on his complex prescriptions and formulae used in compounding drugs. Afterwards, in between approximately 5th and 12th century many of the European countries preferred this western knowledge while Arabs preferred Greco-Roman knowledge and extended it to comprise the use of their own resources in addition with Chinese and Indian herbs that were not known for Greco-Romans [51].

2.1.2. Role of Phytomedicine in modern drug discovery

Plants have long history of use in treatment of different types of diseases by traditional healers and played a vital role in this modern era. There are large number of drugs available which are derived from secondary metabolites of plants. A large and growing body of literature has reported the phytomedicines and modern drugs derived from plants specifically for different types of cancers [7], [58]–[60]. Moreover, the drugs have been developed for several diseases including different type of cancers, diabetes, cardiovascular diseases,

malaria, hypertension etc., based on the evidence of use of plants traditionally. Following are examples of some successful drugs contributing important role in ailment of humankind.

Artemisinin is a naturally occurring lead compound which was discovered in 1971 by Chinese scientists and reported in 1984 by Walter Reed Army Institute of Research (WRAIR) in an article published in *Journal of Natural Products* [61]. The analogs of artemisinin are used to treat malaria in various countries [62], and many of them were prepared for improving the activity of artemisinin, however, actual mechanism of action is still unknown. There are many controversies for mechanism of action that involve endoperoxide bridge with other components like iron that disturbs the detoxification process essential for parasites [63]. On the other hand, the study suggested artemisinin targets the malarial mitochondria and disrupts the significant function [64]. Reserpine is an anti-hypersensitive drug isolated from *Rauwolfia serpentina* majorly found in Himalayan areas, it used for the treatment of snakebite and other diseases. Other drugs are ephedrine, isolated from *Ephedra sinica* is used for the treatment of asthma. Salbutamol, salmeterol, and tubocurarine, are derived components which are isolated from *Chondrodendron* and *Curarea* species and these drugs are traditionally in use by a group of population in Amazon. In addition to the information, there are chemotherapeutic agents such as topotecan, irinotecan and belotecan, which are derived analogs of camptothecin isolated from *Camptotheca acuminata* [66]. Although its success could not remain on that peak and dropped early due to its severe side effect in bladder. There is recently reported first plant-derived tubulin interactive agent named as maytansine isolated from *Maytenus serrate* (Ethiopian tree). This chemical component documented as a modified weapon against monoclonal antibodies, as DM-1 and DM-4 (microbial precursors) act as warheads by linking with specific monoclonal antibodies against tumor-linked epitopes [51], [67]. Furthermore, the discussion would be incomplete without bringing up the blockbuster drug i.e., Paclitaxel (Taxol) which was the most promising plant-derived anticancer agent. The specific compound has been reported in various *Taxus* species (like *Taxus baccata*, *Taxus brevifolia*, *Taxus wallichiana*), the mechanism of action of taxanes was revealed by Schiff and his co-workers in 1979, they concluded that the taxanes inhibit cell growth by binding with microtubules and prevents their depolarization which is responsible for cell division [68]. Additionally, there are ongoing updates in the domain on how conventional medications are used and needed by diverse communities.

2.2. Downfall and Re-emergence of Plant-based compounds in drug discovery

Plant-based natural products have better advantages over synthetic compounds in terms of high biologically relevant chemical space and diverse scaffolds in phytochemicals. Moreover, they have higher molecular weights, a smaller number of Nitrogens, Sulphur, and Halogen atoms comparatively more Oxygen atoms, and these are also sterically more complex, with bridged tetrahedral carbon atoms, rings, and chiral centers [69]. The ratio of aromatic atoms and total atoms is lower in NPs while the number of solvated hydrogen bond donors and hydrogen bond acceptors are high as compared to synthetic molecules additionally, also contains universal distribution of octanol-water partition coefficient and diverse ring system [70]–[72]. The available characteristics of herbal products or plant derived natural products has accelerated the investigations of medicinal plants in pharmaceutical field to be a potent drug, also led to extraction of natural products that have become a successful pharmaceutical as discussed above, vincristine and vinblastine (anticancer drugs), codeine (painkillers), quinine (antimalarial drug) etc. Despite this, the use of natural products diminished in the major pharmaceutical industries. There are many reasons for this decreased importance of natural products at industrial level such as limited availability of bioactive phytochemicals due to exploitation of medicinal plants and herbs, seasonal supply of plant products also limited the time window of sample collection, herbs come in endangered category sometimes due to unsustainable harvesting techniques [73], [74], the optimization techniques were difficult in phytochemicals due to complexity and more chiral atoms than synthetic compounds [75]–[77] and the other reasons were incompatibility of phytochemicals with high throughput screening (HTS) and introduction of combinatorial chemistry which provided the view of simple and more drug-like screening libraries, both techniques will be explained in further sections. The advancement in genomics, proteomics, molecular and cellular biology also affected the use of natural products at industrial level, because it led to increase in the number of molecular or pathogenic targets. Due to the above-mentioned challenges, the plant-based drug discovery has been declined and demoted the interest of industries in herbal extracts and they shifted to synthetic libraries for screening [78], [79].

The re-emergence in the use of natural products has been noticed from the last two decades (~after 2000). The outcomes of vast synthetic chemical libraries used in HTS [80], fell short of expectations. The market acceptance rates of new medications decreased rather than increasing, where 45 drugs were approved in 1990 it became 21 drugs in 2010 [81], [82]. The reported reasons behind this declining trend in drugs were like modest portion of the chemical diversity is typically covered by synthetic compound libraries, less complexity and diversity in chemical structures, smaller number of chiral centers, high flexibility in synthetic libraries than natural compounds and these features make it less efficient in showing specific biological activity with specific proteins of disease [72], [79], [83]. Specifically, in the terms of plant-based drug discovery, well-documented ethnopharmacological information on the traditional usage of medicinal plants is accessible mostly, which might offer clues for molecules therapeutically useful in humans [54], [84], [85]. Therefore, most of the current drugs are inspired from the ancient knowledge of herbs in treatment as discussed in previous sections. Eventually, consideration of above-mentioned advantages and disadvantages of phytochemicals and synthetic compounds, even though the focus of industries on HTS approaches with synthetic libraries, phytocompounds still a valuable source of new chemical entities in drug discovery [86]. Hence, the new techniques were introduced to assist the process of drug discovery based on natural products. The scope increased due to advancements in techniques and equipments in relevant research fields, better understanding of disease pathways, elevation in number of therapeutic targets and improvement in natural lead optimization strategies [76], [77], [79], [87]. For instance, there was problematic issue in earlier days that extract of NPs contains mixtures of compounds which made difficult to separate desired components then this step was facilitated by introduction of HPLC-mass spectrometer (LC-MS) systems and accessibility of Natural product databases [79]. The other problem was structure elucidation, which used to be time consuming step in previous times when traditional spectroscopy was in existence [88]. After advancement in science, NMR spectroscopy was used to determine the chemical structure of molecule with high resolution. In addition, to identifying the biological activity profile of specific compounds against specific molecular targets SAR (Structure Activity Relationship) studies were conducted, which were initialized by using naturally existed biosynthetic congeners for example as noticed in the case of mannopeptimycins [89]–[91]. In addition to these developments, plant-

derived drug discovery was greatly aided by computational methodologies, as will be addressed in the following sections.

2.3. Methods for the discovery of novel pharmacologically active Phytochemicals

Additionally, the ethnomedical knowledge has enabled the identification of bioactive compounds for direct use in therapeutics hence contributed to health care globally. A number of challenges are associated with using medicinal plants as crude extracts. The amount of the desired compound(s) from medicinal plants may vary geographically and the season in which they can be collected. Moreover, bioactive molecules of many plants are associated with toxicity, and if the plant extract contains a lower content of bioactive compound(s) than usual, suboptimal dosage may not be effective. Also, Medicinal properties of many plants are also rapidly lost on storage. Furthermore, crude extracts may contain several undesired toxic compounds which may show harmful effects. Therefore, it is important to isolate and identify the bioactive molecules from plant extracts. Structural modification of isolated and identified bioactive compounds from plant extracts may allow an improvement in the efficacy and moderation of side effects. The experimental approaches used for choosing starting material and bioactive botanicals from mixture of extracts have been discussed briefly in following sections.

2.3.1. Experimental approaches in plant-based drug discovery

2.3.1.1. Random screening approach

Such approach of random sampling was motivated by capturing of unidentified herbal species existing in the nature. Initially the categorization was done based on the similar characteristics with the existing herb in the taxonomy exhibiting medicinal values. Hence, this approach involved selecting plants from any region with a high biodiversity and examining them for various biological activities. Since this technique did not rely on traditional or previous literary knowledge, those unidentified species could also be chosen if other plants or herbs from the same family to which they belonged had biological activity [92], [93]. This approach is helpful in identification of novel compounds and biological activity. Even though, there are limitations such as expensive process, low hit rates, a large

number of resources are wasted during the screening and testing in experiments at very preliminary stage.

2.3.1.2. Ethnopharmacology approach

This approach is based on conventional knowledge where the choice of the test material and the pharmacological assay are both based on the historical therapeutic usage of plants. In this method, the experimental research and observations of traditional medications and their biological activities are considered. It involved the concept of pharmacology, biochemistry, chemistry, botany etc. [1], [94]. Furthermore, some of the popular drugs discovered through this approach have been cataloged in Table 2.1. Despite these successes, there are still major challenges one of them is, the TCM and ayurveda both constitute the application of mixture of crude extracts that comprises several metabolites that raised the complexity in identification of exact bioactive component or synergistic compounds. This type of complementing effect of compounds in extracts might be advantageous for multifactorial diseases like dementia, diabetes, fatty liver diseases, etc. Although, this approach has been promising to capture candidate species with potent leads but still to answer the complexities of compound-target relationships certain advancements in the technology were required.

Table 2.1: Some popular examples of approved drugs from ethnopharmacology approach

Approved Drugs	Plants species	Diseases
Khellin	<i>Ammi visnaga</i>	Allergy and Asthma
Galegine (later metformin)	<i>Galega officinalis</i>	Diabetes
Papaverine (later verapamil)	<i>Papaver somniferum</i>	Antihypersensitive
Quinine (later chloroquine, mefloquine)	<i>Cinchona</i> species	Malaria
Artemisinin (later artemether)	<i>Artemisia annua</i>	Malaria
Digitoxin	<i>Digitalis purpurea</i>	Arrhythmias and Heart failure

2.3.1.3. Bioassay-Guided Fractionation and Metabolomic Profiling

The plant extracts possessing any biological activity are considered for iterative bioassay-guided fractionation cycles until the corresponding bioactive chemicals are obtained (Figure 2.1). In this method the pure extracts treated with different solvents (alcohol, methanol, water etc.) are tested for their biological activity followed by separation of phytocomponents based on their physicochemical properties and activity. Afterwards the extracts with good efficacy

selected for further fractionation process where inactive fractions are dropped, and active fractions taken forward for isolation by using different chromatographic techniques. Although this method results in better identification of desired compounds comparative to

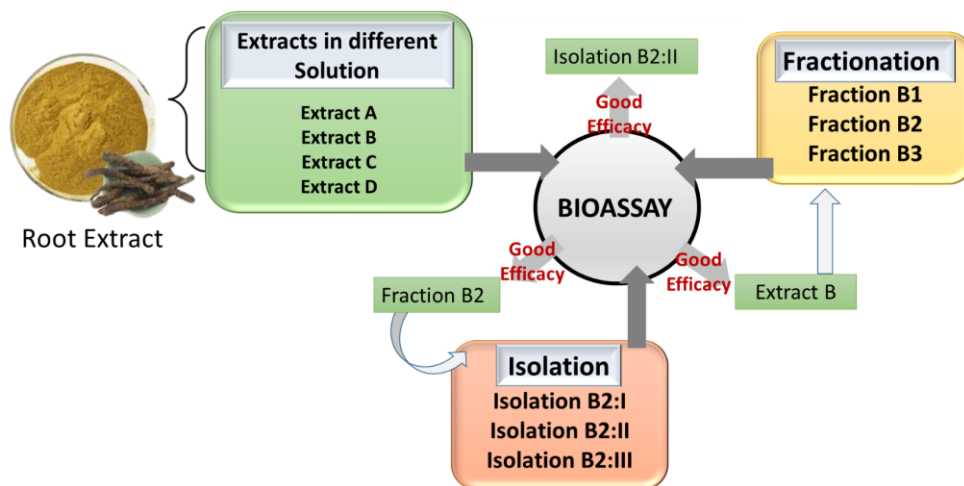


Figure 2.1: Bioassay-Guided Fractionation workflow

other methods, it is time-consuming, resource intensive and laborious task which is very difficult to isolate an active compound from hundreds of compounds [95], [96]. As mentioned, the extracts are complex mixtures, it is quite possible that bioactivity of extract might be due to additive or synergistic effects of other compounds therefore during fractionation interacted compounds are dropped off thus, in most cases the efficacy of bioactive compounds reduced in isolated form. To overcome these challenges an emerging metabolomic profiling which is used to identify the key precursors or end products (secondary metabolites) of cellular processes and enabled the quantification and identification of compounds at early stages therefore this approach shortens the time, efforts, and cost to some extent [97]. This method involves the highly sensitive techniques such as ultra-high performance liquid chromatography (UHPLC), gas chromatography (GC), high resolution – mass spectrometry (HR-MS), nuclear magnetic resonance (NMR) etc., [74]. In conclusion, metabolomic profiling is beneficial whereas bioactivity-guided fractionation may be unable to address the synergistic interaction of drugs. It is important to highlight that, extracts may be more effective than isolated compounds if botanicals have synergistic effects and are more stable and bioavailable in extracts. This suggests that herbal medicines or combinations of compounds may be useful, although more study is needed in this area [74], [98]–[101].

2.3.1.4. Combinatorial chemistry and high throughput screening

With the advancements in development of genome sequencing and structure elucidation techniques, it became possible to determine the structures of many proteins linked to disease processes [102]. Therefore, the emergence of new molecular targets demanded the novel molecular diversity for screening. Combinatorial chemistry is a strategy which was established to create a large synthetic chemical library for high-throughput screening against therapeutic targets [55]. Initially this technique emerged as a boon, due to involvement of robotic systems, tools like solid-phase synthesis thereby enabling the high-throughput approaches to investigate a library of millions of compounds. Despite assurances to the contrary, *de novo* combinatorial chemistry techniques to drug development have proved unsatisfactory in the past two decades, as seen by the diminishing quantity of NCEs [55]. Eventually, the trend shifted to generation of natural products like libraries where the structural resemblance to central scaffold of natural compound or phytochemical is synthesized or taken as starting material in order to synthesize a large and diverse chemical library that can yield potent leads. In support of this context Nicolaou et al., [103], [104] and stated as “We were particularly intrigued by the possibility that using scaffolds of natural origin, which presumably have undergone evolutionary selection over time, might confer favorable bioactivities and bioavailabilities to library members”. Afterwards, Nicolaou’s group proceeded with the development of various optimization strategies to alter the compound structures according to desired protein for neutralization. Hence it is clear that although, HTS approaches are effective in screening the multiple hits that may optimize to produce leads, the successful hit rate was very low and required time and investment extensively. Therefore, development of computational approaches with advancements in filtering methods in screening has been suggested to assist the drug discovery process by reducing the experimental time in initial phases [105], [106]. In light of the aforementioned context, the *in-silico* approaches are discussed in following sections.

2.3.2. Computational methods and resources to prioritize phytochemicals as leads

Since we have discussed all the experimental methods used in drug discovery clearly indicating the huge amount of time and cost required for drug discovery and development process, the computational-aided drug discovery (CADD) has played a vital role in reducing

the time and cost at initial stages by filtering out the undesirable and inactive compounds and prioritizing the potential leads for experimental assays [107]. CADD approach works as “virtual shortcut” in drug development process. CADD provides large number of hits compared to traditional HTS and combinatorial chemistry. This method is used mainly for three objectives, 1) screening of large libraries of compounds to smaller number of putative active compounds and inhibitors that can be subjected to experimental validations, 2) guide the modifications in compound structures to improve the ADMET properties, 3) developing new chemical structures by joining building blocks of functional groups for novel structures based on the desired target. To explain the CADD in detail it can be classified in two categories: Structure-Based (SB) and Ligand-Based (LB) drug discovery that is mainly based on knowledge of ligands and targets respectively.

2.3.2.1. Structure-based drug discovery

The most popular CADD methods are structure-based when the three-dimensional structure of a disease-related therapeutic target is known. Based on the target structure's understanding, the drugs are produced in SBDD. The essential premise of this method is the capability of compounds to interact with specific pathological target and exhibit physiological effect via binding within the specific binding pocket of the protein [106], [107]. Three-dimensional structures of disease related proteins are prerequisites for these techniques, the advancements in genomics, proteomics and biophysical techniques like X-ray crystallography and NMR spectroscopy enabled the elucidation of large number of proteins cataloged in protein databank (RCSB PDB). In this, two commonly used strategies are molecular docking, and de novo ligand designing. Apart from this, molecular dynamics simulations are used to further evaluate the ligand-receptor interactions and flexibility of complexes. The SBDD pipeline includes sequential levels like therapeutic target selection, preparation of ligand library and optimization, screening of compounds against the desired target, and evaluation of binding interaction through molecular docking thereafter, molecular dynamics simulation and binding free energy analysis [108].

2.3.2.1.1. Protein structure Elucidation

As mentioned above, structure-based drug discovery requires 3-D structure of protein targets. These commonly used protein structure determination techniques are x-ray crystallography, NMR spectroscopy and cryo-electron microscopy [109]. The experimental techniques have certain limitations like the x-ray crystallography is only feasible if the protein is crystalized therefore majority of protein targets are not elucidated yet whereas NMR spectroscopy is efficient only for smaller proteins. A continuous attempt is being made to overcome the challenges [110]. In case of unavailability of proteins structure and where target determination is not possible experimentally, computational methods are used. Computational methods determine structure from sequence thereby utilizing connecting links between sequence and structure. For protein structure prediction three types of computational methods are used namely, Homology modeling, ab-initio modeling, and threading [107]. Homology modeling is used to predict and model the protein structure based on the sequence similarity with known structures. Since the structures have been suggested to be more conserved than sequences during evolution this can aid in understanding the putative binding and functionally active sites as of known structure [111], [112]. Ideally, homology modeling can be used to model the structure of proteins which share more than 40 % sequence similarity with the known structure below this range the method is not reliable [113]. Threading techniques are used wherein sequence similarity is very less, but similar folds and domains observed [114], [115]. It is based on the concept of conserved fold and domain regions in the proteins structure during the period of evolution, diverse sequences have been observed but small change has been noticed in protein folds and domains [115]. Ab-initio or de novo modeling is performed when similar structures are not available. This method models the protein structure from scratch based on the sequence. There are various tools and servers available for protein structure modeling such as SWISS-MODEL [116], MODELLER [117], I-TASSER [118], HHpred [119], GenTHREADER [120], Rosetta [121] etc.

2.3.2.1.2. Molecular docking based virtual screening

This in silico method used to select the putative compounds from the library of hundreds or thousands of compounds by analyzing the binding interaction within the binding pocket of target proteins. The workflow for this is as follows, preparation of proteins and ligands or

optimized ligands, docking of ligand with target protein by generating the grid over the desired binding pocket, followed by ranking of compounds based on their binding energy and affinity with protein. The algorithm comprised in docking search for best confirmation of ligand as well as binding affinity in that particular pose. The tools used for molecular docking are based on different computational algorithms some of the popular tools are listed in Table 2.2.

Table 2.2: Molecular docking tools and software and their corresponding algorithms

Tool Name	Algorithm/scoring function
GOLD	Genetic algorithm
Glide	Exhaustive search
AutoDock and AutoDock Vina	Lamarckian genetic algorithm, empirical scoring
DOCK	Geometric matching
FlexX	Incremental build
eHits	Exhaustive search
Ligand fit	CHARMM force field-based docking

From this approach various drugs have been developed for example, inhibitors of HSP90 which is a therapeutic protein target in oncology, have been developed by Roughley et. al (2012), and Dorzolamide [122]. Recently, this technique is majorly used in development and searching of inhibitors for SARS-CoV-2, many studies have been reported that suggested novel inhibitors or repurposed drugs by utilizing the concept of SBDD [123].

2.3.2.1.3. Molecular Dynamics (MD) Simulations

Molecular dynamics (MD) simulations predict the detailed behavior of proteins in biomolecular system by evaluating the force field at individual atoms by other atoms and capture the movement of atoms throughout the simulation period. Importantly, these simulations can also forecast how biomolecules will react to alterations like mutations, phosphorylation, protonation, or the addition or removal of ligands at the atomic level [124]. Apart from this MD simulations are also used to examine the determined structure by X-ray, NMR, cryo-EM, and further to quantify the flexible regions of the protein and to correct the artifacts [125], There are various studies in all areas where MD simulations have been used extensively [126], [127].

Here we discussed some of the examples of the potential inhibitors and drugs developed from Structure-based high-throughput screening. Firstly, a protein kinase CK2 which is one of the

main targets in tumor was selected, then a library of 400, 000 compounds was screened against CK2 and 12 hits were captured and selected for in vitro studies. From these 12 hits a novel inhibitor of CK2 was identified with good biological activity [128], [129]. In other studies, antiviral inhibitors of Ebola virus have been found, also studies have been carried out for COVID [130], [131], Additionally, a new quinolinol that mimics the way p53 attaches to MDM2 and inhibits the MDM2-p53 interaction was discovered using this techniques [132]. There are many more examples where VHTS has been used in drug discovery studies [133]–[135].

2.3.2.2. Ligand-based drug discovery

The alternative of SBDD is ligand-based drug discovery (LBDD) where therapeutic protein target is not available and face challenges in homology modeling or ab-initio modeling, LBDD relies on knowledge of small molecules that bind to protein target to show the pharmacological activity [136], [137]. This approach can be classified as pharmacophore modeling, molecular structure similarity and quantitative structure–activity relationship (QSAR) [138].

2.3.2.2.1. Structure similarity Approach

The fundamental principle of similarity-based or fingerprint-based techniques is to choose new compounds for the target based on their chemical and physical resemblance to existing medications. Based on the idea that compounds with comparable structural characteristics often have similar binding characteristics, ligand similarity search techniques are straightforward yet efficient strategies [139], [140]. These similarity measures do not take into account information about activities of known binders of the target. It is completely based on 2-D or 3-D chemical similarity based on molecular fingerprints [70], [141].

2.3.2.2.2. Pharmacophore modeling

Pharmacophore modeling is a strategy in which models are built using the structural features of active ligands. On the other hand, the ligands can also be generated from the information of binding pocket if 3D structure of protein is known [142].

2.3.2.2.3. *Quantitative structure–activity relationship*

Quantitative structure–activity relationship (QSAR) methods are based on data that correlate activities of drug target interactions with various molecular descriptors. The QSAR method's underlying principle is that compounds with comparable structural characteristics often exhibit similar biological activity. [143]. These models demonstrate quantitatively how the structural characteristics of the ligand influence the activity response of a target that binds it. QSAR is obtained by calculating the correlation between experimentally determined biological activity and various properties of small ligand binders [144]. QSAR models can be used to predict the activity of new chemical analogs.

2.3.2.3. Network pharmacology in drug discovery

Network pharmacology (NP) is a new field in drug discovery that integrates system biology and genomic technology through computational biological tools. It is a method capable of describing intricate connections between biological systems, medications, and disorders. This approach is not only useful in identifying the multiple therapeutic targets of complex diseases but also multiple active compounds to neutralize the pharmacological activity of those proteins. This approach is extensively used to address the complexity of plant extracts where large number of compounds are present and to identify the active components of the extract, and the putative mechanism of action of compounds in treatments. Various studies have been done in this area [145]–[149].

2.4. Pharmacokinetics and its importance in drug discovery

Pharmacokinetics is the study of movement of drugs in the body. In other words, pharmacokinetics (PK) describes what the body does to the drug (Opposite to pharmacodynamics, which describes what the drug does to the body). PK comprises of four major components i.e., ADME (Absorption, Distribution, Metabolism and Elimination). Absorption is the process of movement of drug from site of administration to systemic circulation. If the route of administration is other than intravenous, drugs need to cross various cell membranes before getting accessible to systemic circulation. Thus, the dissolution and ability to permeate the epithelial cells of gastrointestinal tract are hurdles for orally administered drugs. After the drug enters in circulation, it is distributed to tissues

where the target lies for the drug by crossing the barriers. Metabolism is the enzymatic breakdown of a drug. In this process drug molecules are broken down to small molecules and converted to more hydrophilic inactive compounds that can be excreted from the body easily. These metabolites can be responsible for activity and toxicity of drug therefore study of metabolic pathway and PK of these metabolites is necessary. Finally, Elimination is transport of drug molecules into the urine, bile, faeces, etc. Drug Metabolism and Pharmacokinetics (DMPK) was mainly associated with the safety evaluation in last stages of drug discovery phase, i.e., clinical trials. Approximately, two decades ago, it was observed by the researchers that drug candidates failed in the development phases due to several reasons where poor pharmacokinetics was found to be major contributor. Thus, it was suggested that pharmacokinetic profiling of candidates at early stage of drug discovery and development process can eliminate the weak candidate at initial stage resulting in reduction of time and efforts in the process. In addition to good efficacy and activity, optimum pharmacokinetic profile and minimized drug-drug interaction can be chief components for successful drug candidate.

Despite these advantages, there are large number of plant-based compounds those face the problem of oral bioavailability including absorption, distribution through the blood stream, metabolism by several gut microbes and enzymes, excretion, and some toxicity especially in isolated form. This might be because of the complex nature of compounds, however there are successful drugs those exert a very complex structure such as paclitaxel. From the vast variety of medicinal herbs, *Picrorhiza kurroa* is a medicinal herb from Himalayan region which is highly reported for hepatoprotective activity although it is effective in several treatments like vitiligo, neural disorders, arthritis, diabetes etc. Two specific compounds from this herb have been studied extensively to check pharmacokinetics individually, as well as different formulation and extracts of the herb for pharmacokinetic profile.

2.4.1. Pharmacokinetic profile of major iridoid glycosides, Picroside-I and Picroside-II of *Picrorhiza kurroa* in extracts and formulations

The plant extract and formulations for these particular compounds have been majorly in use for various treatments. Therefore, to support the study various reports on pharmacokinetic behaviour of picrosides were recorded (Table 2.3). There were three formulations

administered intravenously among them only one exhibited the PK parameters whereas other two studies included determination and plasma-concentration of components in the form of graph only, the C_{max} and T_{max} were calculated manually from the graph. As described earlier same trend of pharmacokinetic behaviour of picrosides i.e., rapid distribution and elimination was observed by Lv et al. (2007) [150] and Vipul et al. (2005) [151]. The statistic in the table demonstrates that picroside-II in intravenously administered solution indicates larger systemic exposure and smaller elimination than picroside-I. In case of orally administered extract and formulations, picroside-I and picroside-II followed the increasing order of bioavailability in Extract, Picrolax capsule and Kutkin (concentration of picroside-II is different in all but following the same trend) [150], [152]. In addition to this, Oral absolute bioavailability estimation was also done by [153], whereas in other research proper oral bioavailability has not been calculated. Some sort of similarity in the manner of picroside data from mixture and isolated component concluded that the picroside-I and picroside-II are not causing any hindrance in each other fate.

Table 2.3: Pharmacokinetics of Extracts and Formulations (related to *Picrorhiza kurroa*)

Extract/ Formulation	Phytochemicals	Route of administrati on	Model Organism	Administered dose	Parameters	Picoside-I (P-I)	Picoside-II (P-II)	Refernces
Picroliv	P-I and kutkoside	Intravenous	Rabbit	30 mg/kg	Cmax (µg/ml)	~40*	~20 [kutkoside]*	[151]
Picroliv		Oral		100 mg/kg	Cmax (ng/ml)	206.10	152.62	[152]
TGpp (Total glycoside of Picrorhiza scrophulariiflor a Pennell)	P-I, P-II	Intravenous	Rat	36 mg/kg (5.04 mg/kg PI and 30.24 mg/kg)	Cmax (µg/ml)	~300*	~70*	[150]
					Tmax (min)	~ 0.5*	~0.5*	
Saline soluton	P-I, P-II, P-III	Intravenous	Rat	10 mg/kg.	F (%)	NA	0.254	[153]
					AUC (ng h/ml)	249.7	1465.8	
					MRT (h)	0.316	0.267	
					V _d (l/kg)	23.2	9.32	
					Cl (l/h/kg)	44.7	6.83	
					T 1/2 Beta (h)	0.35	0.94	
Kutkin	P-I, P-II	Oral	Rat	100mg/kg (45 mg/kg PI and 55 mg/kg PII)	Cmax (ng/mL)	206.1	152.6	[152]
					Tmax (h)	1.0	1.0	
					AUC (ng h/mL)	577.2	346.7	
					T _{1/2} (h)	37.2	29.5	
					V _d (L)	0.078	0.159	
<i>Picrorhiza kurroa</i> root extract	Various secondary metabolites	Oral	Rat	510 mg/kg (45 mg/kg PI, 32.3 mg/kg PII)	Cmax (ng/mL)	357.8	134.6	[152]
					Tmax (h)	1.0	1.04	
					AUC (ng h/mL)	1033.5	346.8	

					T _{1/2} (h)	56.1	33.5	
					V _d (L)	0.044	0.093	
Picrolax capsule	P-I, P-II	Oral	Rat	1585 mg/kg (45 mg/kg PI, 17.6 mg/kg PII)	C _{max} (ng/mL)	301.4	76.6	[152]
					T _{max} (h)	1.01	1.0	
					AUC (ng h/mL)	876.6	150.9	
					T _{1/2} (h)	50.6	15.2	
					V _d (L)	0.051	0.117	
Iridoid glycosides enriched extract	P-I, P-II, Apocyanin	Oral	Rat	50 mg/kg (5.7 % PI and 18.3 % PII)	C _{max} (ng/ml)	244.9	104.6	[154]
					T _{max} (h)	6	6	
					AUC (h ng/ml)	2524	1097.7	
					T _{1/2} (h)	14.4	8.14	
					V _d (L)	0.57	0.61	
Kutkin	P-I, P-II	Oral	Rat	100mg/kg (45 mg/kg PI and 55 mg/kg PII)	C _{max} (ng/ml)	172	16.6	[48]
					T _{max} (h)	1.0	1.0	
					AUC (ng h/ml)	530.2	61.2	
					T _{1/2} (h)	2.17	21.7	

*Not given in the paper, calculated value from the graph plot given in the paper

2.4.2. Pharmacokinetic profile of Picroside-I and Picroside-II of *Picrorhiza kurroa* in isolated compounds

According to previous studies done by various groups and institutes, the data is summarized for comparative study of pharmacokinetic and metabolic profiles of picrosides and to investigate the downfall in these compounds in spite of having several biological activities or medicinal value. From the literature, it has been observed that there were two pharmacokinetic studies available for intravenously administered picroside-II but not for picroside-I (Table 2.4). However, pharmacokinetic profile of picroside-I (IV administered) is existing from formulation not in isolated component (shown in Table 2.3). The data in the Table 2.4 suggested that picroside-I is rapidly distributed and eliminated from the body after intravenous administration as well as the picroside-II concentration in plasma is showing

Table 2.4: Intravenous administration of picroside-I and picroside-II

Administered dose	Model Organism	Parameters	Picroside-I (approx.)	Picroside-II (approx.)	References
5, 10 and 20 (mg/kg)	Dog	T1/2 β (min)	NA	27.8, 29.2 and 28.4	[155]
		AUC (μ g min/ml)		410.2, 797.0 and 1589.5	
		MRT (min)		25.8, 27.5 and 25.3	
		Cl (ml/min/kg)		12.4, 12.8 and 12.7	
		Vd (ml/kg)		318.9, 355.6 and 320.8	
2.5, 5 and 10 (mg/kg)	Dog	T1/2 α (min)	NA	6.10, 5.14 and 6.31	[156]
		T1/2 β (min)		26.02, 31.7 and 34.4	
		AUC (μ g min/ml)		253.9, 514.6 and 1148.2	

linearity and direct relation with dosage range. Likewise, there are less studies in context of Pharmacokinetic profile of orally administered isolated picroside-I and picroside-II (Table 2.5). The study of Xiong, et al., 2018 proposed rapid absorption and elimination of picroside-I [157]. The maximum plasma concentration of 137.65 ng/ml is achieved within 30 min and then eliminated within 3.47 h. MRT and AUC were also calculated in the data. Moreover, Ma et al., (2008) elucidated concentration – time profile of picroside-II in plasma [158]. However, PK parameters were not investigated in the paper. The value for C_{max} and T_{max} has been calculated by the given graph therefore the statistics can be different for them.

Table 2.5: Oral Administration of Picroside-I and Picroside-II

Administered Dose	Model organism	Parameters	Picroside-I (approx.)	Picroside-II (approx.)	References
100 mg/kg (P-I)	Rat	C _{max} (ng/ml)	137.6	NA	[157]

		Tmax (h)	0.50		
		MRT (h)	2.62		
		AUC (ng h/ml)	174.3		
		T1/2 β (h)	3.47		
40 mg/kg (P-II)	Rat	Cmax (ng/ml)	NA	~90*	[158]
		Tmax (min)		~15*	
		T _{1/2} (h)		<0.5	

*Not given in the paper, calculated value from the graph plot given in the paper

2.4.3. Metabolites from biotransformation of Picrosdie-I, Picroside-II, Extracts, and Formulations through oral and intravenous delivery

Metabolic profile is available only for orally administered picroside-I, picroside-II and extract (Iridoid glycosides enriched extract). The proposed metabolic pathways of picroside-I and picroside-II contained Phase I and Phase II reactions and their products in the form of sub-metabolites. The metabolites of picroside-I and picroside-II can be divided in four parts i.e phase I reaction metabolites, phase II reaction metabolites, phase I biotransformations of metabolites and phase II biotransformations of metabolites. The main metabolic pathways of picroside-I are reportedly hydrolysis, hydroxylation, deoxygenation, glucuronidation, and sulfate conjugation whereas picroside-II hydrolysis, deglycosylation, demethylation, glucuronidation, and sulfate conjugation (Appendix Figure A1 and A2). Furthermore, the metabolic profile of iridoid glycosides enriched extract indicated similar pathway as major metabolites were same as picroside-I and picroside-II. However, among 26 metabolites 15 were observed in plasma within 4 h and 3 after 8 h of administration and others were not absorbed at all. These changes in metabolic pattern in extract and plasma indicating the alteration in structure or fate of the metabolite in biological fluids.

CHAPTER 3
***IN SILICO* IDENTIFICATION OF POTENTIAL VOLATILE
COMPOUNDS IN ESSENTIAL OILS AS INHIBITORS
AGAINST MAJOR PATHOGENICITY DETERMINANTS OF
SARS-COV-2**

3.1. INTRODUCTION

The SARS-CoV-2 (COVID-19) pandemic has been documented in approximately 219 nations and territories, with vaccination being the only way to protect against the virus. However, their long-term effectiveness and high immune protection continue to raise concerns among general population. A COVID-19 drug repository which includes information on approved drugs, PubMed references, clinical trials, and details of mechanisms of drug action have been recently built from COVID-19 related datasets [159]. Coronaviruses belonging to the genera of Alphacoronavirus, Betacoronavirus, Gammacoronavirus, and Deltacoronavirus are composed of 27–32 kb of a single-stranded positive-sense RNA [160]. The genome is packed with a nucleocapsid protein and three structural proteins namely, the membrane protein, spike protein, and envelope protein. SARS-CoV-2 harbours four structural proteins and sixteen non-structural proteins (nsp1–16). One among these nsps, namely nsp12, is a RNA-dependent-RNA-polymerase (RdRp) indispensable to SARS-CoV-2 replication and transcription [160]. Cryo-electron microscopic structures have confirmed Nsp12-nsp7-nsp8 complex as the active replication/ transcription complex for the synthesis of SARS-CoV-2 RNA [161]. The polymerase motifs A-G in the palm sub-domain of RdRp is highly conserved and is usually targeted as a drug target active site. The homotrimeric transmembrane spike glycoprotein (SG-pro) of SARS-CoV-2 in open (receptor-accessible) conformation binds to angiotensin-converting enzyme 2 (ACE2) on host cells and fuses SARS-CoV-2 with the host cell membrane. The receptor binding domain (RBD) of SG-pro composed of loops, α helices, and short β 5 and β 6 strands, is considered the active site and drug target for anti-SARS-CoV-2 therapy. The main protease (Mpro) alternatively also termed as 3-Chymotrypsin-like protease (3CLpro) of SARS-CoV-2 hydrolyzes and internally processes the polyproteins pp1a and pp1ab translated from the viral RNA as well as mediates the replication and transcription of the viral gene. Mpro most probably functions as a homodimer and the cleft between domain I and II among the three domains of the Mpro protomer harbour the catalytic dyad residues, His41 and Cys145 (substrate-binding pocket) considered as the active site for anti-SARS-CoV-2 target. Papain-Like protease (PLpro) of SARS-CoV-2 functions as a deubiquitinating and deISGylating enzyme by removing ubiquitin and interferon-stimulated gene 15 (ISG15) from host cellular proteins.

Additionally, PLpro also cleaves and processes SARS-CoV-2 polyproteins like the Mpro. In a way, thus PLpro facilitates in evading the host immune system [162], [163].

As a result, finding alternative treatment options that directly disrupt the virus's entrance, proliferation, and infection cycle has been prioritized. For urgent requirement of drugs, the researchers focused on drug repurposing as already approved drugs had passed all the experimental and clinical tests that might reduce the drug discovery time [164]. For instance, lopinavir [165]–[167], remdesivir [168]–[170], ribavirin [171], [172], favipiravir [173]–[176], ritonavir [167], [177], interferon [175], [178], [179], chloroquine [27], [180], [181], hydroxychloroquine [182]–[185] have become suitable for treatment of SARS-CoV-2. Despite the aforementioned researches on repurposed antiviral drugs to minimize the effects of virus at initial phase of outbreak, the drugs eventually showed various side-effects [186], [187]. Hence, the research shifted to discover a specific drug then again phytochemicals played a crucial role in prioritizing the potential drug leads. Many phytochemicals based on their ethnomedical information along with *in-vitro* assays from different formulations and plants have been reported effective for SARS-CoV-2 [188]. For this, various *in-vitro*, *in-vivo* and *in-silico* approaches were used to identify the potential leads from library of phytochemicals. Based on the studies, a large number of phytochemicals have been shortlisted through computational studies as well as most of them have been evaluated in *in-vitro* and *in-vivo* experiments, the compounds like apigenin-7-O-rhamnoglucoside, herbacetin, and pectolinarin were reported to inhibit Mpro [189], Amentoflavone and Galocatechin gallate have been reported to be potential inhibitor of Mpro and PLpro [190]. Moreover, hesperidin from *Citrus aurantium* and stated for anti-oxidant and anti-inflammatory activity inhibited the formation of Spike and ACE2 complex which is required for viral entry in host [191], and major phytochemicals from *Nigella sativa*, *Swertia chirayita*, *Tinospora cordifolia* and *Withania somnifera* have been reported active against RdRp [192], [193]. Nallusamy et al. (2021) [194], have shown cyanin, Amentoflavone, agathisflavone, catechin-7-o-gallate and chlorogenicin to exhibit inhibitory activity against multiple proteins of SARS-CoV-2 as well as suggested potential sources of effective phytocompounds [195]. All the studies stated above were oral or intravenous drugs, however, at the time that the present work was initiated, there was no data on inhalation treatment instead of the fact that SARS-CoV-2 enters through nasal swabs and the main route of disease

progression is primarily through the lungs except a study steam inhalation therapy which was limited to small number of phytochemicals [33], [196]. Afterwards, in last year various studies came focusing on inhalation route. Since inhalation delivery of drugs is mostly preferred for various pulmonary diseases (such as asthma, cystic fibrosis, pneumonia etc.) wherein drugs directly reached to lungs by surpassing the liver first pass metabolism, gastrointestinal toxicity driven issues, and also minimizes pulmonary toxicity hence reducing the side effects at some extent [197]–[200]. Recently, Eedara et al., (2021), beautifully reviewed the potential inhalation therapeutics for treating SARS-CoV-2 infection [201]. Additionally, currently, a few pharmaceutical companies (for eg. Lupin and Glenmark Pharmaceuticals Ltd.) shifted the paradigm to repurposed inhalation drugs for COVID-19 [202], [203].

In our study the attempts have been made to shortlist the probable new chemical compounds from essential oils or aromatic plants for inhalation therapy. Since the essential oils are known to have a broad range of biological activity and medicinal values such as antibacterial, antiviral, anti-inflammatory, anticancer, antifungal etcetera [204]. Furthermore, these extremely volatile essential oil components are commonly categorized as lipophilic molecules and have high vapour pressure that may travel long distances, such as, from upper to lower airway tracts and eventually into the lungs. Some of the studies were published later on compounds from essential oils for treatment of SARS-CoV-2, these researches were mainly inclined to essential oil compounds exhibiting antiviral activity, eventually, the compounds from essential oils and aromatic plants namely, *Melissa officinalis*, *Zataria multiflora*, *Eugenia brasiliensis*, *Zingiber zerumbet*, *Cedrus libani*, and *Vetiveria zizanioides*, garlic essential oil, *Eucalyptus*, *Corymbia Lavandula* and *Lippia* species [32], [206]–[209].

In that direction, instead of only focusing on antiviral compounds, we searched through the literature on essential oils plants found in India and compiled 2,363 compounds from 1,050 aromatic plant species. Moreover, recently, investigators have examined the expression profiles of ACE2 in brain and concluded that SARS-CoV-2 caused neurological disorders reaching through olfactory nerves or blood circulation [37], [38], [210], [211].

Thus, our computational predictions of a drug lead prepared from any essential oil component molecule/s from our current study would prefer an intranasal/ respiratory tract for

administration and rapid delivery into SARS-CoV-2 infected cells. In the current investigation, the efforts have been made to shortlist the compounds and to predict the probable drug leads as potential therapeutics by using computational methods such as molecular docking, pharmacokinetic profiling, selective molecular dynamics simulation and binding free energy analysis. Besides, the molecules detected in this present analysis might even pass and target brain lobes rapidly due to faster delivery of nasal route. The workflow of screening and identification of drug leads for intranasal therapy have been demonstrated as schematic diagram in next section.

3.2. MATERIALS AND METHODS

3.2.1. Dataset preparation

In the current study, the target proteins of SARS-CoV-2 were searched from the literature where four proteins (Mpro, PLpro, SG-pro, RdRp) were selected for the study based on their established role in viral entry, replication, and life cycle. The three-dimensional (3D) structures of above-mentioned protein targets of SARS-CoV-2 submitted in RCSB Protein Data Bank (PDB) [212] in early 2020 were used. The x-ray crystallographic structures of Mpro (PDB ID: 6W63) [213] and PLpro (PDB ID: 6W9C) [214], with 2.1 and 2.7 Å resolution, respectively, were downloaded. Likewise, for SGpro and RdRp, 6VSB [215] and 7BTF [216] were downloaded which are solved structures from cryo-electron microscopy with resolution 3.5 and 2.9 Å, respectively. On the other hand, a total of 2473 chemical compounds belonging to a range of chemical classes from 1050 essential oils and aromatic plant species were manually recorded from existing literature and online repositories like EssOildb (<http://www.nipgr.ac.in/Essoildb/>, <https://essentialoils.org/db>) [217]. These aromatic plants and compounds have been used for a range of complex diseases, the details of medicinal values and related plant species given in section 3.3. Furthermore, the 3D structures of compounds were retrieved from chemical structure databases like Pubchem (<https://pubchem.ncbi.nlm.nih.gov/>) [218] and Chemspider (<http://www.chemspider.com/>) [219] using batch download services provided in the databases. A total of 2363 compound structures were downloaded in sdf format for further analysis. In addition to this, the known inhibitors Remdesivir (CID: 121304016) and Ribavirin (CID: 37542), X77 (N-(4-tert-

butylphenyl)-N-[(1R)-2-(cyclohexylamino)-2-oxo-1-(pyridin-3-yl)ethyl]-1H-imidazole-4-carboxamide) (CID: 145998279), and P85 (CID: 73659185) for these protein targets were also downloaded to utilize as a control. These structures were used as ligands in the screening study against four major targets (Mpro, PLpro, SG-pro and RdRp) of SARS-CoV-2.

3.2.2. Preparation of ligands and four major therapeutic proteins of SARS-CoV-2 for molecular docking study

Generally, prior to docking, protein crystal structures and ligands are prepared to add hydrogen atoms, reduce atomic conflicts, and execute additional operations not included in the x-ray crystal structure refining procedure, and in case of ligands it is done to assign bond orders and generate tautomers [220]. In this direction, firstly, the missing loops in structure of RdRp (897-910) and SG-pro (66-88, 95-99, 140-156, 176-186, 245-260, 443-460, 620-640, 672-686 and 828-852) were modelled using Swiss Model server [116]. Further, all four protein structures were prepared in AutoDock MGL tools [221] by removing undesired small molecule structures which are attached in the main structure during crystallization processes and water molecules which do not contribute to binding process, followed by addition of hydrogen atoms and atomic charges. On the other hand, the ligands (compound structures and known antagonists) were prepared by assigning bond orders, number of torsions to make it flexible during the docking process. Eventually, the resulted protein structures and ligands were converted to pdbqt format by utilizing AutoDock MGL tools 1.5.6 [221] and Raccoon [222], respectively for docking analysis.

3.2.3. Molecular docking analysis

Molecular docking of ligands and proteins was performed to evaluate the confirmation of ligands in the active site of desired protein based on ranking via scoring functions. A total of 2,363 compound structures (or ligands) were screened against all 4 protein targets through AutoDock vina [21] by using python scripts. A macromolecule grid box was generated around the corresponding active sites of receptors (Table 3.1). Resulting log files and output files were comprising nine different confirmations of the ligands with binding energy and RMSD of the corresponding poses. Compounds with the higher binding affinity within the active site binding pocket and good interaction were regarded as potential candidates. In

addition to this, two commercialized RdRp antagonists, remdesivir and ribavirin as well as known non-covalent Mpro inhibitor X77 and PLpro inhibitor P85 have been docked with Mpro, PLpro, RdRp, and SG-pro, independently to compare the binding affinity of EO compounds with well-known inhibitors and drugs. The visualization of complex comprising receptor and ligand was done in Pymol thereafter hydrogen bonding and other interactions of ligand and protein were also identified using Protein-Ligand Interaction Profiler (PLIP) and Ligplot.

Table 3.1: Grid Box Coordinates and Size Parameters used in grid box generation

Protein	Center (Å)			Box Dimensions (Å)		
	X	Y	Z	X	Y	Z
Mpro	-16.87	15.17	-26.6	60	70	70
PLpro	-25.12	30.28	35.53	66	112	54
RdRp	117.7	117.54	130.93	50	60	70
SG-pro	186.38	220.89	261.33	90	60	80

3.2.4. Pharmacokinetic analysis of compounds

The compounds exhibiting binding energy between -6.5 and -9.5 kcal/mol were checked initially for pharmacokinetic profile using SwissADME webserver [223]. Since the unacceptable Absorption, Distribution, Metabolism, Excretion, and Toxicity (ADMET) profile contributed to the failure of drugs in the last stages of drug development, it is suggested to check ADMET of compounds priorly [224], [225]. This program estimates physicochemical properties, water solubility, lipophilicity, pharmacokinetics and bioavailability of compounds by calculating a range of descriptors including molecular weight, number of heavy atoms, number of aromatic heavy atoms, number of rotatable bonds, number of hydrogen bond donors and acceptors, total polar surface area, LogP values, solubility values of given compounds and pharmacokinetic parameters such as gastrointestinal absorption, blood brain barrier permeation, and inhibitory effects of different Cytochromes P450 (CYPs) isoforms as interaction of CYPs and drug leads is suggested to consider and P-glycoprotein (P-gp) transporters [226]–[228]. Additionally, all compounds have been screened against the rules of drug-likeness like Lipinski’s rule [229], Egan’s rule [230], Veber’s rule [231], Ghose filter [232], Muegge filter [233] and finally selected

compounds were further evaluated for more stringent pharmacokinetic properties by using PkCSM webserver [234]. The study examined the violations of important drug-likeness rules, critical toxicity parameters like AMES toxicity, Hepatotoxicity. A list of violations for all compounds and for 645 compounds having free binding energies in the range of -6.5 to -9 kcal mol⁻¹ after initial autodock vina screening. Furthermore, EO compounds taken forward for molecular dynamics simulation were also evaluated for verification of their available pharmacokinetic properties using PkCSM.

3.2.5. Molecular dynamics simulation

Molecular Dynamics (MD) simulations are used to predict the movement of every atom over time means the stability and flexibility of receptor-ligand complex and interaction over the given time. All four protein targets and their corresponding shortlisted compounds were exposed to MD simulation using GRONINGEN MACHINE for CHEMICAL SIMULATIONS (GROMACS) with GROMOS96 54a7 force field [235] on gpu (nvidia dgx server). The ligand parameters and topology files were generated by utilizing PRODRG server [236]. Afterward the system was prepared Native protein and Complexes were subjected to Simple Point Charge (SPC) water molecules within a 1.0 nm dodecahedron box. Both ligand and protein topology files were compiled and put through neutralization by adding ions (Na⁺/Cl⁻). The GROMOS96 54a7 force field was used for energy minimization to relax the system and remove the initial clashes using 50,000 (maximum no. of steps) steps of steepest descent algorithm with tolerance of >1000kl/mol/nm. Minimized proteins and complexes were equilibrated in two steps under NVT (constant number of particles, volume, and temperature) followed by NPT (constant number of particles, pressure and temperature) [237]. Ultimately, MD simulation was performed for 100 nanoseconds (ns) with time frame of 2 femtosecond (fs) and trajectories were generated after every 10 picosecond (ps). The same MD simulation was performed in replicates with same parameters and conditions. The generated confirmations of protein-ligand complexes were investigated on the basis of their trajectories and other parameters like Hydrogen Bond analysis, Radius of gyration (RoG), Root Mean Square Deviation (RMSD) and Root Mean Square Fluctuation (RMSF), Pressure, and Temperature, curves. These parameters were evaluated by using GROMACS utilities

namely, gms_rms, gms_rmsf, gms_hbond etc. Final trajectories were evaluated using UCSF Chimera and graphs were generated using GROMACS tools and visualized in Grace.

3.2.6. Binding free energy analysis

The resulted complexes from MD simulations were subjected to evaluate the binding free energy using molecular mechanics Poisson-Boltzman surface area (mm_pbsa) method which gives the biomolecular interaction details with high correlation and better binding affinities between ligand and protein [238]. Since the complexes were shown converged in the last simulation steps, the last 10 ns trajectory consisting of 1000 frames was extracted from 100ns MD trajectory comprising 10000 frames of each of the complex. The MM-PBSA binding free energy of these complexes was calculated by utilizing g_mmpbsa script. [239], [240]. This method calculates binding energy by applying the following equation:

$$\Delta E_{be} = E_{complex} - (E_{receptor} + E_{ligand})$$

Where, $E_{complex}$ denotes total binding energy of complex, $E_{receptor}$ and E_{ligand} denote the total energy of receptor and ligand in solvent respectively. $E_{complex}$ is calculated as:

$$E_{complex} = (E_{MM}) + (E_{solvation})$$

$$E_{MM} = (E_{elec}) + (E_{vdw})$$

$$E_{solvation} = (E_{polar}) + (E_{nonpolar})$$

Where, E_{MM} represents molecular mechanic's energy in gas phase that is a sum of electrostatic and van der walls interaction energy and $E_{solvation}$ represents energy of solvation that is a sum of polar and nonpolar energy calculated by Poisson-Boltzmann model and solvent-accessible surface area (SASA) respectively. All the above experiments have been conducted sequentially as demonstrated in Figure. 3.1.

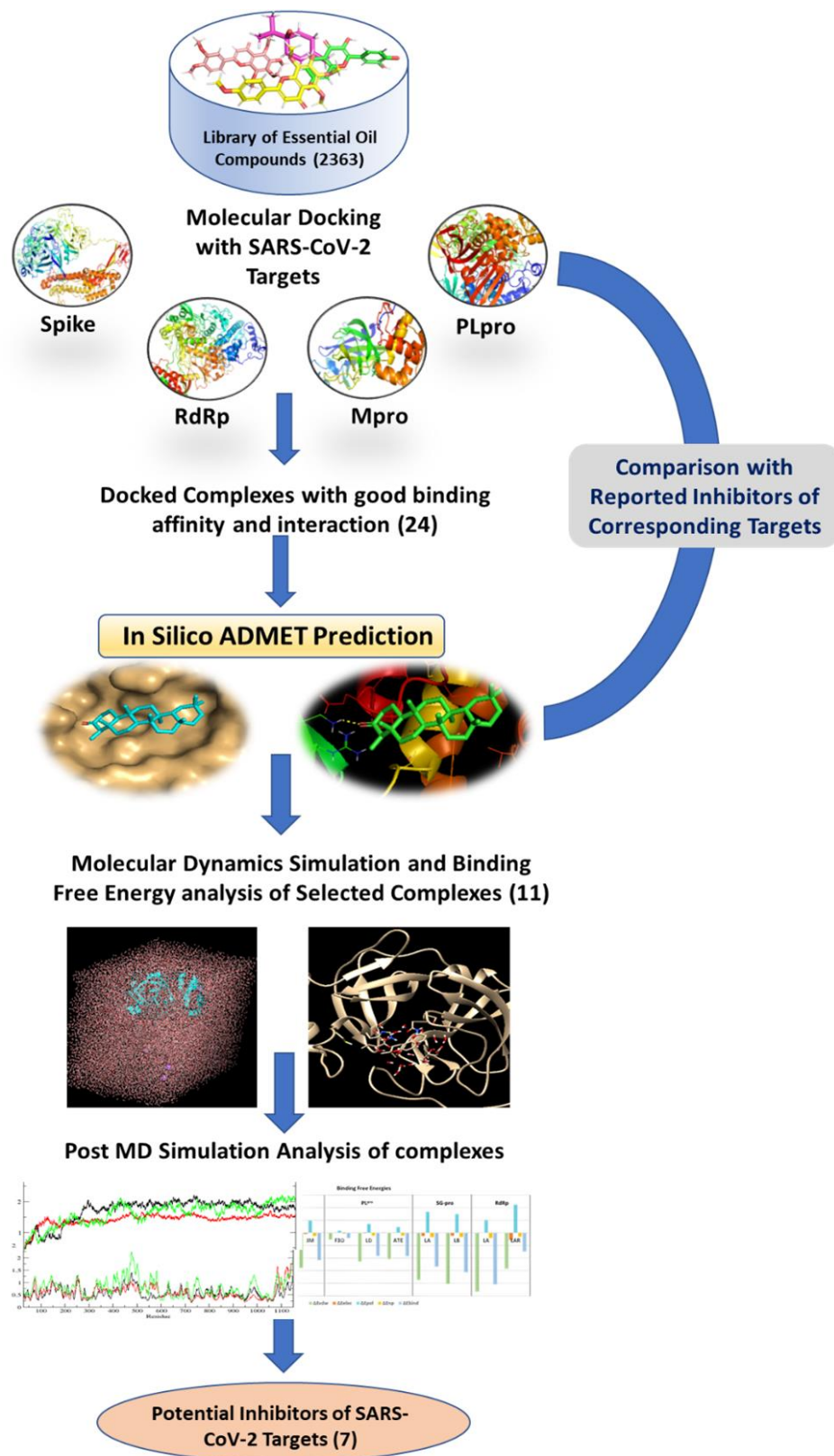


Figure 3.1: Workflow of experiments in the current study

3.3. RESULTS AND DISCUSSION

A total of 2,363 compounds were screened against four major protein targets of SARS-CoV-2 through docking simulation. Compounds within the binding energy range of -7 to -9.5 kcal/mol with their corresponding targets were docked further to replicate and evaluate the average value in two docking analysis. The results of docking were analyzed by studying and visualizing the interactions of ligands to the corresponding receptors. Compounds with strong binding affinity and interactions were eventually chosen for further investigation. Additionally, these molecules were reported to have a variety of therapeutic effects. Table 3.2 listed the biological activities as well as their corresponding plant species (some of them are listed), in fact, these compounds are also reported in other aromatic plant species that would be a very long list therefore not included in presented table. Furthermore, various pharmacological parameters like molecular weight, solubility, lipophilicity, hydrogen bond donors, and acceptors, and toxicity parameters like Ames toxicity, and hepatotoxicity have been suggested in previous studies [224], [226]. Hence, Pharmacokinetic properties of compounds were assessed to get information on drug-likeness of the shortlisted compounds. Structural stability of protein-ligand complexes in biological system has been predicted in molecular dynamics simulations by calculating RMSD, RMSF, Hydrogen Bonds (H-bond) and RoG of the newly formed predicted complex [241]. RMSD values indicate whether and when the complex is stabilized or equilibrated in a simulation window plotted with respect to time, residue-wise RMSF values around a stable average conformation signals residue-wise differences in fluctuation compared to the unbound protein or to a different ligand bound to the same receptor protein [241], persistence of H-bonds in the complex indicate the stability of ligand and protein throughout the simulation and also enhances the molecular interaction [241], [242] and RoG indicates the compactness of target protein throughout the simulation [243].

Table 3.2: Medicinal values of selected essential oils compounds and their corresponding plant species

Plant name	Plant Part	Compound	Medicinal Activity	References
<i>Nyctanthes arbor-tristis</i>	Stem	alpha-amyrin	Antiinflammatory, Antifungal, Antibacterial, Antioxidant	[244]–[246]
<i>Lantana camara</i>	Leaf	lantadene a	Antitumor, Antioxidant	[247]–[249]
<i>Nyctanthes arbor-tristis</i>	Stem	friedelan-3-one	Antimicrobial	[250]

<i>Lantana camara</i>	Leaf	lantadene b	Antitumor	[249]
<i>Lantana camara</i>	Leaf	reduced lantadene a	Anticancer	[251] [252]
<i>Nyctanthes arbor-tristis</i>	Stem	beta-amyrin	Antiinflammatory, Antioxidant	[245], [246]
<i>Nyctanthes arbor-tristis</i>	Stem	alpha-amyrone	Antioxidant, Antidiabetic, Antiinflammatory and Antihypersensitivity	[253], [254]
<i>Lantana camara</i>	Leaf	reduced lantadene b	Anticancer	[251] [252]
<i>Thymus carnosus</i>	Leaf	abietadiene	NA	
<i>Lantana camara</i>	Leaf	lantadene c	Antitumor	[249]
<i>Lantana camara</i>	Leaf	lantadene d	Antitumor	[247]
<i>Juniperus communis</i>	Leaf	abietatriene	Antitumor	[255], [256]
<i>Polylepis besseri</i>	Aerial part	abietol	Hepatoprotective	[257], [258]
<i>Cupressus funebris P</i>	unknown	6,7-dehydroferruginol	Antitumor, Antioxidant, Antifungal, Antibacterial,	[256], [259]
<i>Nardostychnus jatamansi</i>	unknown	beta-sitosterol	Antidiabetic, Anti-inflammatory, Antioxidant, Anticancer, Antimicrobial, Antihelminthic, Antimutagenic, Antimicrobial, Angiogenic, Immunomodulatory	[260]–[264]
<i>Eucalyptus urophylla</i>	Leaf	kaurene	Antibacterial	[265]
<i>Cupressus macrocarpa</i>	Leaf	phyllocladene	Antioxidant	[266]
<i>Nardostychnus jatamansi</i>		jatamansinol	Anticancer; Neuroprotective	[267], [268]
<i>Cupressus funebris P</i>	unknown	sandaracopimarinol	Antibacterial, Antioxidant, Antimicrobial	[269], [270]
<i>Cupressus macrocarpa</i>	Leaf, Fruit	phyllocladanol	NA	
<i>Nardostychnus jatamansi</i>		Oroselol	Antitumor, Antihepatitis	[271]
<i>Nardostychnus jatamansi</i>		jatamansin	NA	
<i>Smyrniun cordifolium</i>	Root	alpha-santonin	Antioxidant, Anti-inflammation, Anti-microbial, P-glycoprotein (P-gp) antagonist, Anti-ulcer, Antiviral, Anti-protozoal, Antinematode, Antipyretic	[272]
<i>Cupressus duclouxiana</i>	Leaf	ferruginol	Hepatoprotective, anti-malarial, antiviral, antioxidant, antibacterial, antitumor, antineoplastic	[257], [269], [270], [273]–[275]

3.3.1. Identification of potentially active compounds against major therapeutic targets of SARS-CoV-2 based on ligand – receptor interactions

In this section, I explained the interaction analysis of essential oils molecules resulting from molecular docking study. Since all compounds were docked to four major pathogenic protein targets namely, Mpro, PLpro, RdRp and SG-pro of SARS-CoV-2.

3.3.1.1. Interaction analysis of screened hit molecules and main protease of SARS-CoV-2

Ten compounds have been selected for Cysteine-like protease (CLpro) or Mpro, demonstrating acceptable binding affinity inside the binding pocket (Thr25-Asp289). After docking the compounds were visualized in PLIP and LigPLOT to explore interactions of ligand and protein in 3D and 2D. His41 and Cys145 are active site residues of the Mpro, as seen in the binding of the known inhibitor and as suggested by the literature [276].

All listed compounds for Mpro were found in the active site pocket, like the known inhibitor X77 (Table 3.3). As shown in the Table 3.3, binding pocket of Mpro comprised of amino acid residues namely, His41, Met49, Tyr54, Gly143, Ser144, Glu166, Gln192, Thr190, Thr199, Met276, Thr25, Cys44, Arg131, Lys137, Phe140, Leu141, Asn142, Cys145, His163, His164, Met165, Leu167, Pro168, Asp187, Arg188, Gln189, Thr190, Asp197, Thr198, Asn238, Tyr239, Gly275, Leu286, Leu287 and Asp289. The potentially hit complexes were investigated for their intermolecular interactions viz., hydrogen bonds, hydrophobic interactions, pi-pi stacking and salt bridges. All the mentioned molecules interact with similar binding pocket except lantadene B which was observed in nearby pocket however the binding affinity was high for this molecule.

Table 3.3: Interactions between potential compounds and Main Protease of SARS-CoV-2

Compound Name	Binding affinity	Binding residues	H-bonds	Hydrophobic	Salt-bridge
Lantadene B	-8.9	Met276, Gly275, Leu287, Leu286, Asp289, Tyr239, Thr199, Lys137, Asn238, Thr198, Asp197, Arg131	Thr199, Met276	Asp197, Leu272, Leu286, Leu287	Arg131, Lys137
Jatamansin	-7.8	His41, Asp187, Met49, Met165, Leu141, Asn142, Glu166, Phe140, Ser144, His163	Ser144, Glu166	His41, Met165, Glu166, Asp187	His41, His163
Alpha-santonin	-7.3	Gln166, His41, Cys44, Arg188, Asp187, Gln189, Met165	His41, Glu166	Met49, Gln189	

Ferruginol	-7.3	His41, Cys145, Met165, Arg188, Gln189, Glu166, Leu141, Asn142, Gly143, Ser144	Gly143	Met49, Met165, Gln189	
6,7-dehydroferruginol	-7.3	His41, Gln189, Arg188, Asp187, Met165, Met49, Leu141, Ser144, Gln166, His163, Asn142, Cys145, Gly143	Gly143	His41, Met165, Gln189	
Beta-sitosterol	-7.1	Thr25, Gln166, Leu167, Pro168, His41, Cys44, Met49, Arg188, Asp187, Gln189, Met165, Cys145	Glu166	His41, Met165, Glu166, Pro168, Gln189	
Jatamansinol	-7.1	His41, Arg188, Met49, Gln192, Pro168, Glu166, Gln189	Gln192		
Sandaracopimarinol	-7.1	Cys44, Asp187, Gln189, Arg188, His41, Thr25, Met49, Tyr54	Met49	Gln189	
Phyllocladanol	-7.1	Tyr54, Gln189, Asp187, Arg188, Met49, Glu166, Asn142, Met165, His41, His164	Tyr54	His41, Glu166, Met49	
Oroselol	-7	Gln192, Pro168, Thr190, Gln189, Arg188, Cys44, His41, Glu166, Met165, Leu167	Gln192, Thr190,	Met165, Leu167	His41

From listed ten compounds, four compounds namely jatamansin and beta-sitosterol from *Nardostychnus jatamansi*, 6,7-dehydroferruginol and phyllocladanol from *Cupressus funerbis P.* and *Cupressus macrocarpa P.* respectively, showed stable interactions with key residues (Figure 3.2). The binding affinities of these four compounds were -7.8, -7.1, -7.3 and -7.1 kcal/mol, respectively. Jatamansin displayed two hydrogen bonds with Ser144 and Glu166, as well as hydrophobic interactions with His41, Met165, Glu166 and Asp187 and salt bridges with His41 and His163 of Mpro. Moreover, beta-sitosterol, 6,7-dehydroferruginol and phyllocladanol exhibit H-bonding with Gly143, Glu166 and Tyr54 respectively, and strong hydrophobic interaction was also noticed including active site residue His41. The catalytic dyad residues were observed to be involved in 6,7-dehydroferruginol-Mpro and beta-sitosterol-Mpro complexes (Figure 3.2). As demonstrated in the Table 3.2, beta-sitosterol and 6,7-dehydroferruginol are already stated for medicinal activity like antifungal, antioxidant, anticancer, antibacterial etc., from the current analysis we can infer the additional potential antiviral activities of the abovementioned compounds. Apart from this, Ser144 of Mpro exhibit H-bonding with a distance of 2.66 Å in jatamansin-Mpro complex, while Glu166 of

Mpro with a distance of 2.89 Å in the beta-sitosterol-Mpro complex indicating compact bonding in jatamansin-Mpro complex. Since these compounds are targeting the active site

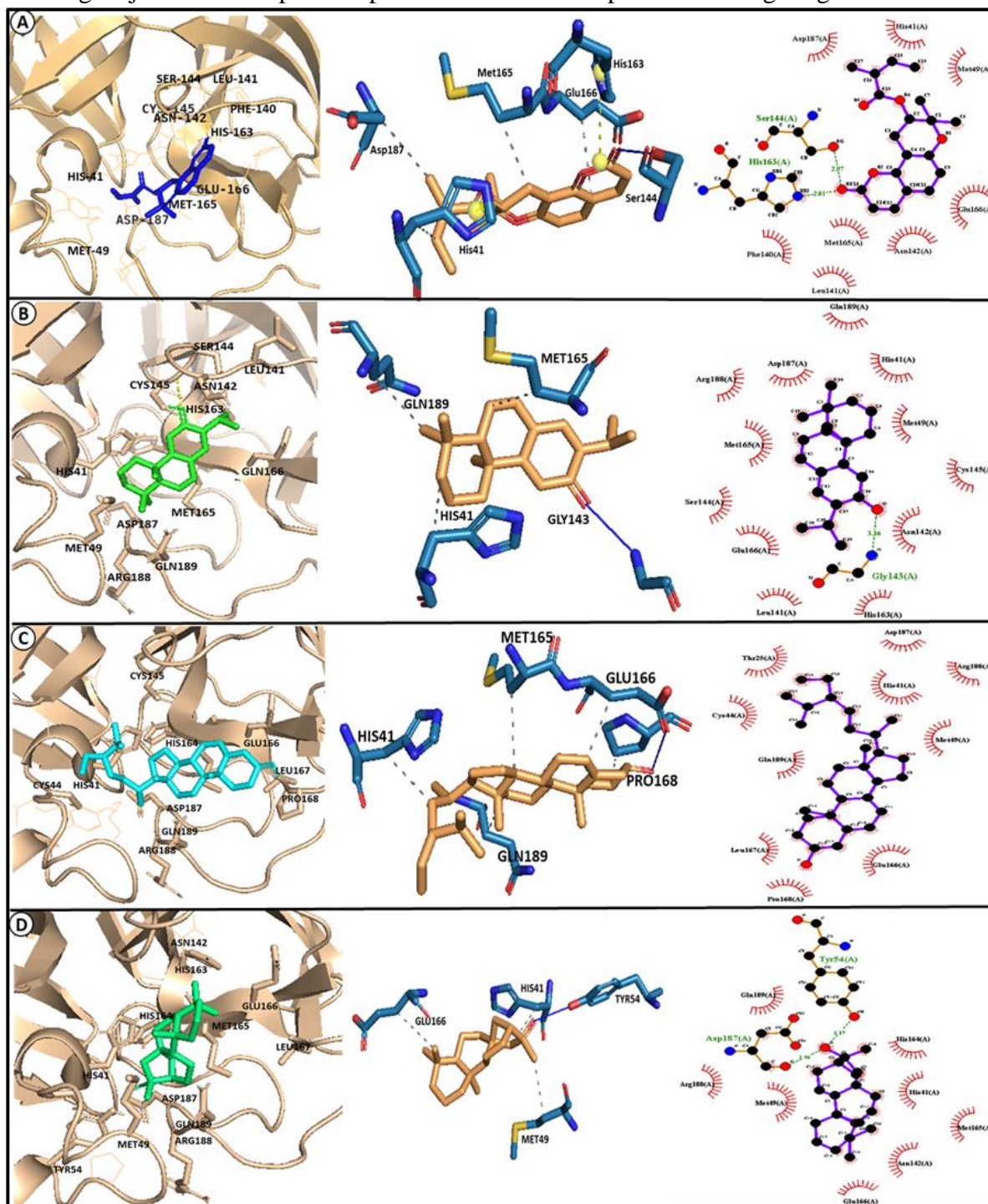


Figure.3.2: Interaction within active binding pocket of Mpro, 3D and 2D visualization of interaction with molecules and Mpro residues. A. Mpro and Jatamansin complex B. Mpro and 6,7-dehydroferruginol complex. C. Mpro and Beta-sitosterol complex. D. Mpro and Phyllocladanol complex.

residue and forming strong interaction within the pocket by showing additional interaction

with other adjacent residues, it is assumed that these molecules might be potential candidates. An unreported active site pocket in close vicinity to the reported active site was noted as most of the complexes with best docking score conformations such as Mpro complexes with reduced lantadene A, lantadene A, friedelan-3-one, lantadene C, lantadene D, lantadene B, reduced lantadene B, alpha-amyrone, beta-amyrin, and alpha-amyrin were not considered due to their binding with pockets other than the reported active site, however their docking energies ranged from -8.5 to -9.5 kcal/mol (Appendix Table A2). Comparative analysis with X77 presented that jatamansin has better affinity with Mpro than its well-known inhibitor, while only the highest docking energy of remdesivir-Mpro was comparable to jatamansin-Mpro, ribavirin, X77, and P85 complexes with Mpro exhibited a lower binding affinity compared to jatamansin-Mpro (Table 3.4).

Table: 3.4: Binding interaction of known inhibitors with therapeutic targets of SARS-CoV-2

SARS-CoV-2 Protein targets	Known drugs or inhibitors			
	Remdesivir	Ribavirin	P85	X77
Mpro	-7.8	-6.4	-7.1	-7.5
PLpro	-6.6	-5.7	-6.7	-6.8
RdRp	-7.5	-6.2	-7.7	-6.7
SG-pro	-8.1	-6.4	-8.6	-8.4

Thus, ten candidate compounds, lantadene B, jatamansin, alpha-santonin, ferruginol, 6,7-dehydroferruginol, beta-sitosterol, jatamansinol, sandaracopimarinol, phyllocladanol, and oroselol have been found to bind into or close to the reported active site of Mpro (Table 3.3). Among them, jatamansin, beta-sitosterol, 6,7-dehydroferruginol and phyllocladanol were taken forward for molecular dynamics simulation assessments after a careful observation of their binding modes with Mpro.

3.3.1.2. Interaction analysis of screened hit molecules and papain-like protease of SARS-CoV-2

PLpro is one of the important therapeutic targets of SARS-CoV-2 which primarily engages in escape mechanism for virus as it exhibits the DUB and DeISGylating activity therefore altering the mechanism of host innate immune system [162]. Inhibition of this enzyme is required to aid host in the release of chemokines and other antiviral agents against viral

infection. Four residues of PLpro namely, Trp107, Cys112, His273 and Asp287 are reported as catalytic sites [277]. In case of 3D structure with pdb id: 6w9c, active amino acids in the catalytic sites are Trp106, Trp109, Cys111, His272 and Asp286 [278]. Top molecules exhibiting good binding affinities have been presented in Appendix Table A3. The best binding affinity was observed in other than desired binding pocket at -7.8 kcal/mol (Appendix Table A3). A total of eight compounds from different plant species were selected based on their binding affinity and interaction in desired pocket (Table 3.5).

Table 3.5: Interaction between potential compounds and Pappain-Like protease of SARS-CoV-2

Compound Name	Binding affinity	Binding residues	H-bonds	Hydrophobic	pi-pi Interaction	Salt-bridge
lantadene d	-7.4	Leu 162, Asp164, Gly163, Tyr273, Tyr264, Asn267, Tyr268, Gln269, His272	Tyr268, Tyr264, Asp164	Leu162, Tyr264, Tyr268, Gln269		
abietatriene	-7	Trp106, Cys270, Asn109, His272, Asp286, Leu289, Asn267		Trp106, Leu289	Trp106, His272	
abietadiene	-7.1	Trp106, Cys270, Asn109, His272, Asp286, Leu289, Asn267		Trp106, Leu289		
lantadene c	-7.3	Arg166, Gln174, Glu203, Val202, Tyr207, Leu199, Leu185, Met208, Lys232		Leu185, Leu199, Val202, Glu203, Tyr207		Arg166
alpha-amyirin	-7.6	Tyr213, Glu214, Lys217, Phe258, Thr257, Gly256, Thr259, Lys306	Lys217	Glu214, Tyr305, Lys306		
abietol	-7.2	Glu252, Leu253, Lys254, Tyr305, Tyr213, Lys217, Glu214, Tyr251, Thr257	Thr257, Lys254, Glu252	Glu214, Lys254, Thr257, Tyr305		
lantadene a	-7.4	Tyr213, Glu214, Thr257, Tyr305, Thr259, Phe258, Ser278, Gly256, Lys306	Lys306	Glu214, Tyr305, Lys306		Lys217
friedelan-3-one	-7.1	Lys105, Trp106, Leu289, Asp286, Cys270, His272	Lys105	Lys105, Trp106, His272, Leu289		

Lantadene D from *Lantana camara* W, abietatriene from *Xeranthemum annuum* P or *Hyptis suaveolens* W, and friedelan-3-one from *Protium hebetatum* P showed desired interaction with active site residues of PLpro (Figure 3.3). Abietadiene, lantadene C, alpha-amyirin, abietol, and lantadene A are other shortlisted candidates that bound close to the reported

active site pocket of PLpro. Since lantadene D, abietatriene, and friedelan-3-one bound within the desired pocket were considered for further interaction analysis. Lantadene D showed binding score of -7.4 kcal/mol, where Tyr268, Tyr264, and Asp164 engaged in H-bond formation and Leu162, Gly163, Asn267, Tyr264, Tyr268, and Gln269 resorted to hydrophobic interactions in the reported active site of lantadene D-PLpro complex.

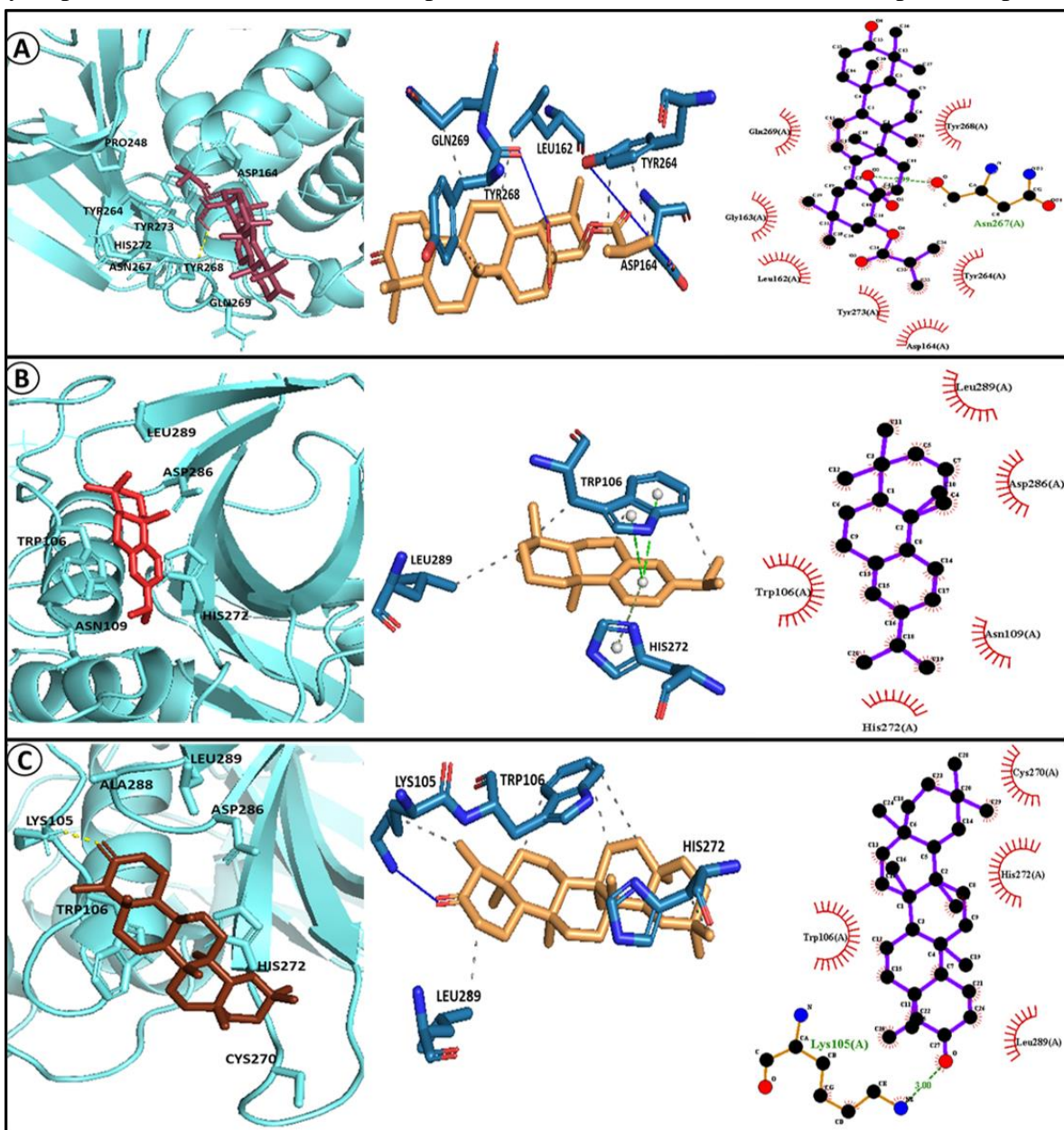


Figure 3.3: Binding interaction in active site pocket of PLpro. A. PLpro and Lantadene D complex. B. PLpro and Abietatriene complex. C. PLpro and Friedelan-3-one complex

However, since Trp107, Cys112, His273 and Asp287 are the reported catalytic sites in PLpro,

and lantadene D interacted close to His273 and Asp 287 by utilizing H-bonding and hydrophobic interactions in these regions (Figure 3.3 A). Although, abietatriene was observed to confer a binding affinity of -7 kcal/mol, the interactions with active site triad Trp106, Asn109 and His272, as well as with other residues sitting in pocket like Cys270, Asp286, Leu289 and Asn267 were noted in the abietatriene-PLpro complex. Abietatriene demonstrated extra pi-pi interaction with Trp106 and His272 in order to form stable complex (Figure 3.3 B). Likewise, friedelan-3-one docked to PLpro with a binding energy of -7.1 kcal/mol and demonstrated stability owing to Hydrogen bonds with Lys105 and hydrophobic interactions with Lys105, Trp106, His272, and Leu289 inside the active site pocket (Table 3.5, Figure 3.3 C). Furthermore, lantadene D and abietatriene proved to be potential for targeting PLpro. In comparative analysis with known molecules namely, remdesivir, ribavirin, X77, and P85 bestowed lower binding affinities compared to these compounds (Table 3.4). We can consider lantadene D in preference to abietatriene with respect to H-bonds and hydrophobic interactions while abietatriene exhibited pi-stacking and hydrophobic interactions. Moreover, other compounds which are not included could have better antiviral activity due to their higher binding affinities.

3.3.1.3. Interaction analysis of screened hit molecules and RNA dependent RNA polymerase of SARS-CoV-2

According to reported studies inhibition of RdRp is significant as the enzyme is proved to be crucial for viral replication by catalyzing replication from RNA template. The crystallographic structure (pdb id: 7BTF) used in the current study that exhibit Asp760 and Asp761 as the active sites of RdRp [216]. A total of 67 compounds were found to confer better binding affinity than remdesivir, albeit the binding pocket may be different. Therefore, from the top compounds seven were shortlisted based on close-knit binding as well as on preferable interactions to the previously reported active site of RdRp namely, reduced lantadene A, beta-amyrin, alpha-amyrin, alpha-amyrone, lantadene A, reduced lantadene B and kaurene (Table 3.6).

Table 3.6: Interaction between potential compounds and RNA dependent RNA polymerase of SARS-CoV-2

Compound Name	Binding affinity	Binding residues	H-bonds	Hydrophobic	pi-pi Interaction	Salt-bridge
reduced lantadene a	-8.5	Trp617, Asp623, Lys621, Cys622, Arg624, Arg553, Asp760, Asp761, Ser814, Asp618, Glu811, Tyr455	Trp617, Lys621	Tyr455, Lys621, Arg624, Glu811		Arg553, Lys621
beta-amyrin	-8.4	Trp617, Asp618, Cys622, Lys621, Asp623, Asp760, Asp761, Lys798, Glu811,	Lys621, Cys622	Glu811		
alpha-amyrin	-8.1	Trp617, Asp618, Tyr619, Pro620, Lys621, Lys798, Asp761, Lys798, Trp800, Glu811, Phe812, Ser814	Lys621	Glu811		
alpha-amyrenone	-7.9	Pro620, Lys621, Asp618, Trp617, Lys798, Trp800, Glu811, Asp761, Ser814	Lys621	Glu811		
lantadene a	-7.6	Trp617, Asp618, Arg555, Asp623, Thr556, Asn691, Arg553, Ser682, Asp760, Asp761, Glu811	Trp800	Arg555, Asp623		Arg553
reduced lantadene b	-7.5	Lys551, His439, Ser549, Arg555, Ile548, Arg858, Arg836, Ala547, Phe 441, Lys545, Ser814, Glu811	Ile548, Lys551	Phe441, Ile548		Lys545, Arg555
kaurene	-6.7	Trp617, Tyr619, Asp760, Asp761, Glu811, Trp800, Lys798		Lys798, Glu811		

Reduced lantadene A docked to the reported active pocket with the highest binding affinity of -8.5 kcal/mol whereas lantadene A with modest binding affinity of -7.6 kcal/mol, both were forming H-bonds, Hydrophobic and salt bridge interactions with the residues in active site pocket which indicate these molecules could be potent leads to inhibit the activity of RdRp (Figure 3.4). In the interaction evaluations of RdRp and reduced lantadene A, two H-bonds with Trp617 and Lys621, four hydrophobic interactions with Tyr455, Lys621, Arg624, and Glu811, while two salt bridges with Arg553 and Lys621 were noticed and LA exhibited H-bond with Trp800, hydrophobic interactions with Arg555 and Asp623, and additional salt bridge interaction with Arg553 (Table 3.7, Fig 3.4). On the other hand, friedelan-3-one, beta-amyrin, alpha-amyrenone, abieta-8,12-diene, isokaurene, khusinol, alpha-amyrin, abietatriene, kaur-16-ene, pimara-8,15-diene, isophyllocladene, dehydroabietal, nezukol, isohibaene, trans-totarol, abietadiene, rimuene, lantadene B, and (11E,13Z)-Labdadien-8-ol

were found to bind RdRp in undesired pockets with docking energies in the range of -8.1 to -9.1 kcal mol⁻¹ (Appendix Table A4). Interestingly, all compounds bound in active site

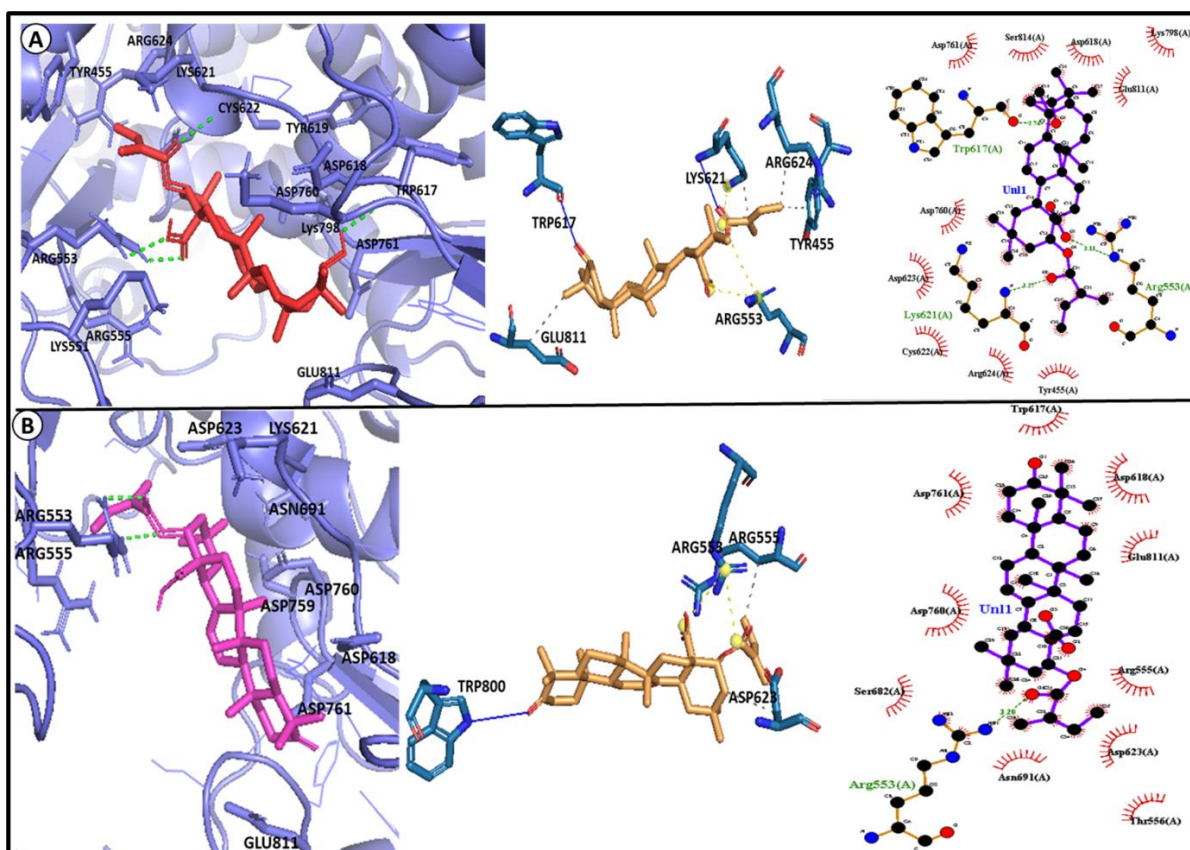


Figure 3.4: Interaction within active binding pocket of RdRp, 2D and 3D visualization of interaction. A. Reduced lantadene A – RdRp complex. B. Lantadene A – RdRp complex.

region showed higher docking score than reported antiviral drugs and inhibitors mentioned in the study (Table 3.4). The shortlisted compounds would probably be able to inhibit the activity of RdRp eventually inhibiting replication cycle, hence considered for further exploration.

3.3.1.4. Interaction analysis of screened hit molecules and spike glycoprotein of SARS-CoV-2

The spike is the significant protein in the entry mechanism of virus into the host. Receptor binding domain (RBD) of spike protein binds with ACE2 receptor present in lungs and invades the host cells [279]. Receptor binding domain is of ~200 residues (318-514), Since Gln498 directly binds to ACE2 receptor as described in another comparable x-ray

crystallographic structure (PDB ID: 6m0j) of Spike RBD, it is regarded as a crucial residue for binding [280], which is also confirmed by Singh et al. (2021) [281] where they shortlisted two potential compounds (Diacetylcurcumin and Dicafeoylquinic acid) inhibiting RBD of Spike at the binding sites of ACE2. The top binding affinities were observed in the range of -8.9 and -8 kcal/mol of Alpha-amyrone, beta-amyrin, reduced lantadene B, perfluorotributylamine, alpha-amyrin, friedelan-3-one, LAR, kaur-15-ene, beyerene, kaurene, isophyllocladene, lantadene A, lantadene B, lantadene C, and lantadene D (Appendix Table A5), however bound in different pockets. Based on desired active site pocket, 8 compounds were shortlisted (Table 3.7).

Table 3.7: Interaction between potential compounds and Spike glycoprotein of SARS-CoV-2

Compound Name	Binding affinity	Binding residues	H-bonds	Hydrophobic	Salt-bridge
beta-amyrin	-8	Asp428, Phe429, Thr430, Ser514, Phe464, Pro463, Glu516, Phe515	Asp428, Thr430	Phe464, Glu516	
phyllocladene	-7.9	Phe456, Lys458, Asn460, Ser469, Glu471, Arg454, Pro491, Phe490		Phe456, Lys458, Pro491	
reduced lantadene b	-7.9	Tyr396, Phe464, Ser514, Phe429, Asp428, Thr430, Phe515, Arg355, Glu516	Arg355, Thr430, Glu516	Arg355, Tyr396, Pro426, Phe464, Glu516	Arg355
beta-sitosterol	-7.8	Glu471, Ile472, Ala475, Tyr473, Cys488, Phe490, Asn487, Lys458, Phe456, Arg457, Leu455		Phe456, Glu471, Tyr473	
sandaracopimarinol	-7.8	Arg454, Leu455, Phe456, Asn460, Lys458, Glu471, Asn487, Pro491, Phe490	Leu455	Phe456, Lys458, Glu471, Pro491	
lantadene b	-7.3	Gly482, Gln493, Tyr495, Ser494, Gly496, Arg403, Tyr505, Asn501, Tyr449	Gly496	Tyr449, Tyr505	Arg403
lantadene a	-7.1	Arg403, Tyr495, Gly482, Gln493, Tyr449, Ser494, Gly496, Asn501, Tyr505	Ser494, Gly496	Tyr449, Tyr505	Arg403

lantadene d	-7	Leu455, Phe490, Phe456, Glu471, Ser 469, Ile472, Tyr473, Ala475, Asn487	Asn487	Phe456, Glu471, Tyr473, Ala475, Phe490	Arg454
-------------	----	---	--------	--	--------

The molecules listed in the table were binding within the RBD pocket hence might block ACE2 to connect with RBD, therefore, preventing the receptor ACE2 from interacting with Spike protein. Interestingly, lantadene A and lantadene B were discovered to bind directly to the hotspot location of the active pocket, which included residues namely, Arg403, Gly482, Gln493, Tyr495, Ser494, Gly496, Tyr505, Asn501, and Tyr449 through different interactions such as Tyr449 and Tyr505 participate in hydrophobic interaction and Arg403 in salt-bridge interaction for both the complexes, Though, other compounds also occupied the RBD pocket by forming interaction with the residues of RBD. On comparative analysis with known inhibitor like remdesivir for this protein, similar value of binding affinity has been recorded

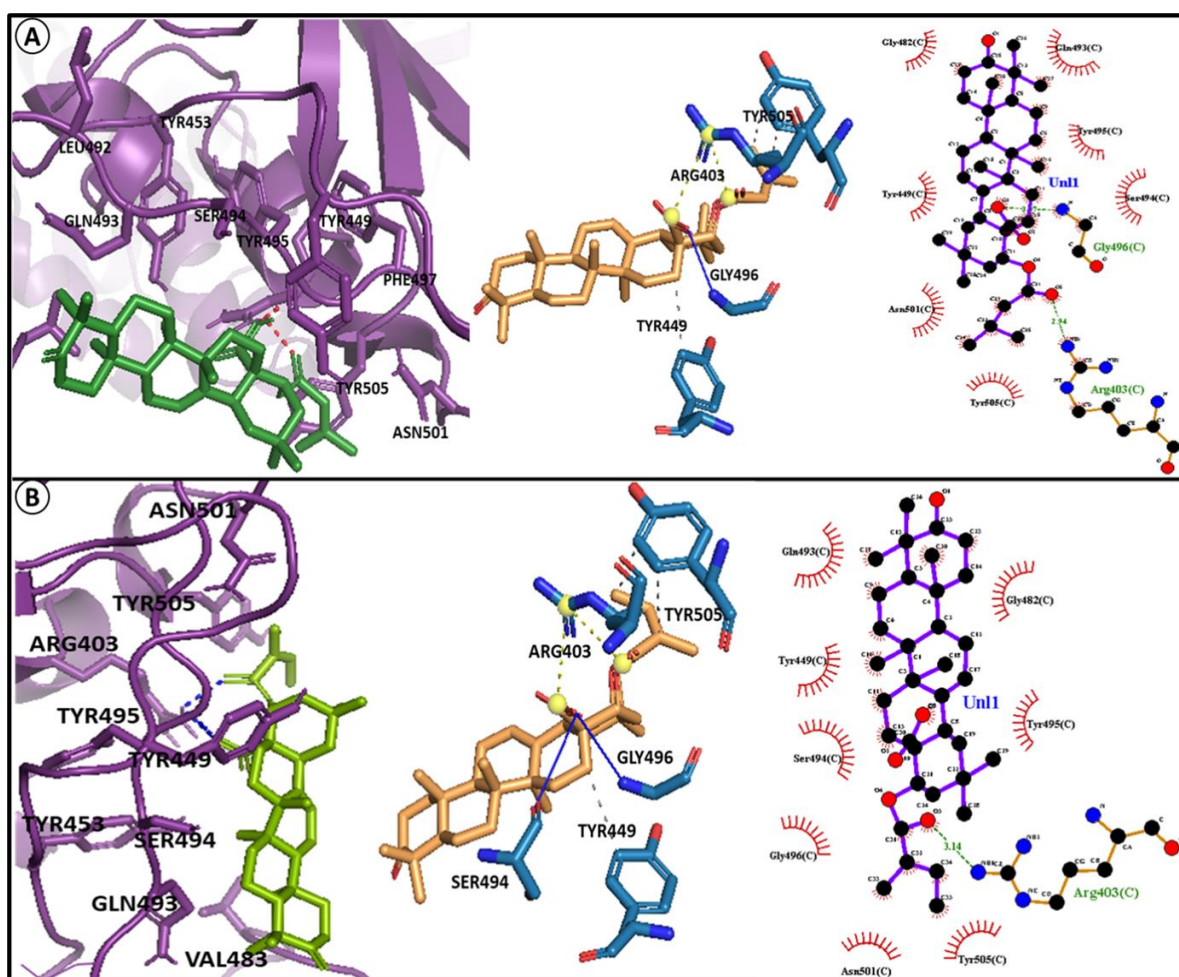


Figure. 3.5: Interaction within active pocket of RBD of spike glycoprotein. A. Lantadene B – SG-pro complex B. Lantadene A – SG-pro complex.

(Table 3.4). Besides, lantadene A and lantadene B were also involved in stable hydrogen bonding through Ser494 and Gly496, therefore these compounds were assumed to interrupt the activity of target and deemed for further study (Figure. 3.5, Table 3.7).

3.3.2. Pharmacokinetics analysis of shortlisted essential oils compounds

In the current investigation, the pharmacokinetics and physicochemical properties of phytochemicals were taken into consideration, for which computational prediction was implemented on the essential oil phytochemicals that were exhibiting probable drug-likeness for the intranasal treatment, although, in this scenario, it was not essential to strictly follow ADME rules, therefore such evaluation was considered only in preliminary screening criteria. All 2,363 compounds were initially checked for violations such as following, Lipinski violation rule, Egan violation rule, Ghose violations, Veber violations, Muegge violations, Bioavailability score, and Leadlikeness violations by evaluating the physicochemical properties using SwissADME. As shown in the Figure 3.6., approximately, 50% of essential oils compounds followed all the drug-likeness rules except Muegge's rule. Most of the

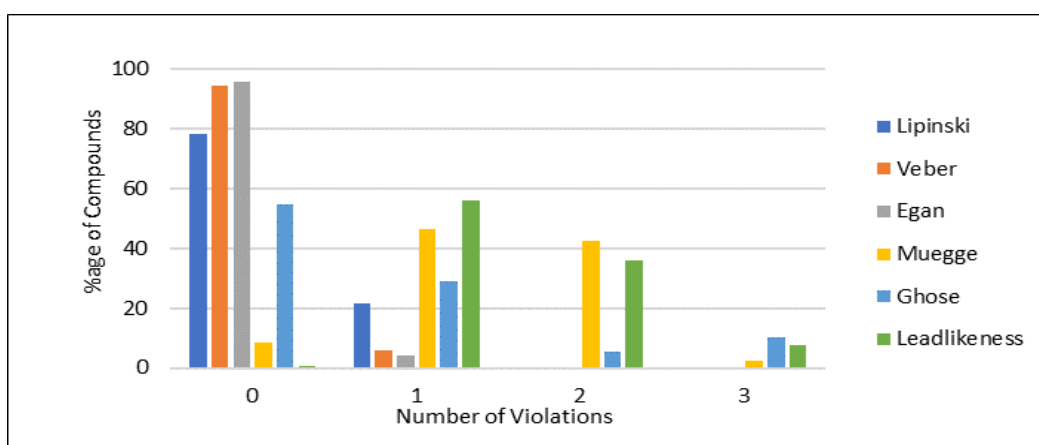


Figure 3.6: Distribution of dataset based on number of violations of stated rules for drug-likeness compounds showed less than two violations which is acceptable, a smaller number of compounds have been noticed to show three violations. In terms of toxicity, there were 644 top compounds resulting from docking study that exhibited binding affinity in the range of -7 and -9 kcal/mol. Moreover, qualified compounds from docking analysis discussed in section 3.1.1., were further subjected to verification of their available pharmacokinetic properties using PKCSM. Furthermore, Table 3.8 demonstrated the violations of rules, bioavailability, and toxicity parameters lying in the recommended range. It was also noticed

that none of the nominated compounds showed AMES toxicity, indicating that those can be used in human medication (Table 3.8). The study of CYP inhibitors suggested that the potential leads have possibilities to interact with CYP isoforms, CYP3A4 is involved predominantly in interaction. Activation of CYP3A4 is required for leads to avoid toxicity as its inactivation is responsible for drug toxicity through co-administered drug interactions [282]. According to pharmacokinetic and physiological properties these compounds are reliable as it is suggested that the druglike parameters are only guidelines for prior shortlisting not strict cut-offs for druglike nature of compounds [224], [228].

3.3.3. Investigation of stability and flexibility of ligand – receptor complexes in virtual biological system

Despite current experimental methodologies, a precise knowledge of the stability of the protein-ligand complex remains a challenge. This constraint is overcome via molecular dynamic simulation, which allows for a considerable degree of system flexibility. Owing to this knowledge, the selected complexes (11 complex) from docking analysis were subjected to MD simulation to evaluate and visualize the stability of complexes in biological system for 100 ns. Multiple replicate analyses of the same trajectory are expected to reduce misinterpretations caused by false positive results, which can occur in high-throughput computational research due to slight deviations in initial trajectory velocities or underlying hardware configurations, etc., [283]. We performed a 100 ns MD simulation of all eleven complexes in two replicates (replicate 1 and 2 demonstrated in red and green respectively) with the same parameters to explore the substantial changes in two trajectories of the same complexes under the same biological circumstances. The amino acid sequences of these proteins varied from 305 to 1147 amino acids thus performing replicate MD simulations was certainly computationally challenging and cumbersome in concordance with remarks from Knapp et al., (2018) [283]. In the analysis, the complex structure stability is determined by RMSD, RMSF of C- α atoms and hydrogen bonds in the complex. Root Mean Square Deviation (RMSD) and Root Mean Square Fluctuations (RMSF) are two key measures to structural fluctuations and deviations [241], [284], [285]. In addition to this other parameter were also considered such as radius of gyration that provides the measure of compactness of protein during the simulation, as well as hydrogen bonds in the complex were also analyzed

Table 3.8: Pharmacological properties of resulting essential oils compounds

Properties	F3O	BS	JM	ATE	LA	LAR	FG	LD	LB	PC
Molecular Weight	426.729	414.718	328.364	270.46	552.796	554.812	284.443	540.785	552.796	290.491
LogP	8.457	8.0248	3.3845	5.8402	7.9297	7.7215	5.6264	7.6195	7.9297	5.1702
#Rotatable Bonds	0	6	2	1	3	3	1	3	3	0
#Acceptors	1	1	5	0	4	4	1	4	4	1
#Donors	0	1	0	0	1	2	1	1	1	1
Surface Area	192.455	187.039	139.422	124.529	241.131	241.764	128.634	235.456	241.131	130.444
Water solubility	-5.856	-6.513	-4.026	-6.764	-3.875	-3.708	-6.083	-3.826	-3.875	-5.69
Caco2 permeability	1.236	1.18	0.995	1.372	0.622	0.617	1.57	0.603	0.622	1.496
Intestinal absorption (human)	97.452	93.658	98.249	96.618	100	97.011	91.358	100	100	95.189
Skin Permeability	-2.722	-2.76	-2.821	-2.482	-2.735	-2.735	-2.404	-2.735	-2.735	-2.773
P-glycoprotein substrate	No	No	No	No	No	No	No	No	No	No
P-glycoprotein I inhibitor	Yes	Yes	No	No	No	No	No	No	No	No
P-glycoprotein II inhibitor	Yes	Yes	No	No	Yes	Yes	No	Yes	Yes	Yes
VDss (human)	-0.023	0.091	-0.232	1.116	-1.104	-0.961	1.25	-1.209	-1.104	0.401

Fraction unbound (human)	0	0	0.16	0	0	0	0	0	0	0.006
BBB permeability	0.73	0.792	-0.017	0.721	-0.126	-0.053	0.308	-0.108	-0.126	0.695
CNS permeability	-1.471	-1.754	-2.058	-0.991	-1.201	-1.187	-1.604	-1.247	-1.201	-1.717
CYP2D6 substrate	No	No	No	No	No	No	No	No	No	No
CYP3A4 substrate	Yes	Yes	Yes	Yes	Yes	Yes	Yes	Yes	Yes	Yes
CYP1A2 inhibitor	No	No	Yes	Yes	No	No	No	No	No	Yes
CYP2C19 inhibitor	No	No	Yes	No	No	No	Yes	No	No	Yes
CYP2C9 inhibitor	No	No	No	No	No	No	No	No	No	Yes
CYP2D6 inhibitor	No	No	No	No	No	No	No	No	No	No
CYP3A4 inhibitor	No	No	No	No	No	No	No	No	No	No
Total Clearance	-0.04	0.628	1.044	0.961	-0.17	-0.103	0.787	-0.278	-0.256	0.457
Renal OCT2 substrate	No	No	No	No	No	No	No	No	No	No
AMES toxicity	No	No	No	No	No	No	No	No	No	No
Max. tolerated dose (human)	-0.374	-0.726	-0.137	-0.212	0.427	0.815	-0.308	0.428	0.427	-0.861
hERG I inhibitor	No	No	No	No	No	No	No	No	No	No
hERG II inhibitor	Yes	Yes	No	Yes	No	No	Yes	No	No	Yes
Hepatotoxicity	No	No	Yes	No	No	No	No	No	No	No
Skin Sensitisation	No	No	No	No	No	No	Yes	No	No	Yes
T.Pyriformis toxicity	0.308	0.383	0.784	0.995	0.286	0.285	1.386	0.286	0.286	0.81
Minnow toxicity	-1.944	-1.866	0.43	-0.934	-1.221	-1.205	-0.866	-1.028	-1.221	-0.281

during the course of simulation. Our overall results indicated negligible variation in the outcome of both replicate analyses, as have been discussed in the following sections.

3.3.3.1. Molecular dynamics simulation of main protease complexes

In this section, firstly the RMSD and RMSF trends were taken into consideration and represented in black, red and green color for native Mpro, replicate 1 and replicate 2 of corresponding complexes, respectively. Interestingly, RMSD curves for all Mpro-ligand complexes equilibrated after 26 ns, with fluctuation range between 0.15 and 0.4 nm indicating the instantaneous formation of a lowest potential energy stable complex in comparison to native Mpro. However, RMSD of native Mpro increased up to 25 ns then slightly decreased and persisted below 0.2 nm, and again increased after 60 ns remained at 0.4 nm. Average RMSD of native Mpro was 0.26 nm, whereas jatamansin-Mpro, beta-sitosterol-Mpro, 6,7-dehydroferruginol -Mpro, and phyllocladanol-Mpro complex showed 0.22, 0.28, 0.30 and 0.34 nm, respectively. Phyllocladanol followed the same pattern of fluctuation as Mpro. Jatamansin and beta-sitosterol displayed stable line in both replicates throughout the simulation except little bit fluctuations (Figure 3.7). The RMSD values of all complexes were lying in the range and apart from this it was inferred from the data that jatamansin, 6,7-dehydroferruginol and beta-sitosterol were more stable complexes comparatively. Further study of RMSF of complexes and native Mpro showed that residues in active pocket had RMSF fluctuations between 0.01 and 0.35 nm. An insignificant but slightly higher RMSF around residue number 50 was observed for the jatamansin-Mpro complex in comparison to native Mpro, (Figure 3.7B right panel) probably indicating to His41 of Mpro which has resorted to both hydrophobic interactions and salt bridge formation with jatamansin in the jatamansin-Mpro complex. Similarly, RMSF calculation of beta-sitosterol-Mpro suggested insignificant fluctuations at around residues 50 and 170 (Figure 3.7A). The average fluctuations of active site residues in all complexes were higher than unbound Mpro, which is indicating the conformational changes in protein that might destabilize the protein. The observations depicted stable binding of molecules to Mpro and close contact of ligands and Mpro. In terms of H-bonding analysis, minimum 0 and maximum 3 H-bonds were observed in jatamansin, 6,7-dehydroferruginol, and phyllocladanol-Mpro complexes throughout the 100 ns simulation in two replicates. The RMSD and H-bond plots

of 6,7-dehydroferruginol–Mpro exposed the similar pattern of stability within ~40 ns (Figure 3.8).

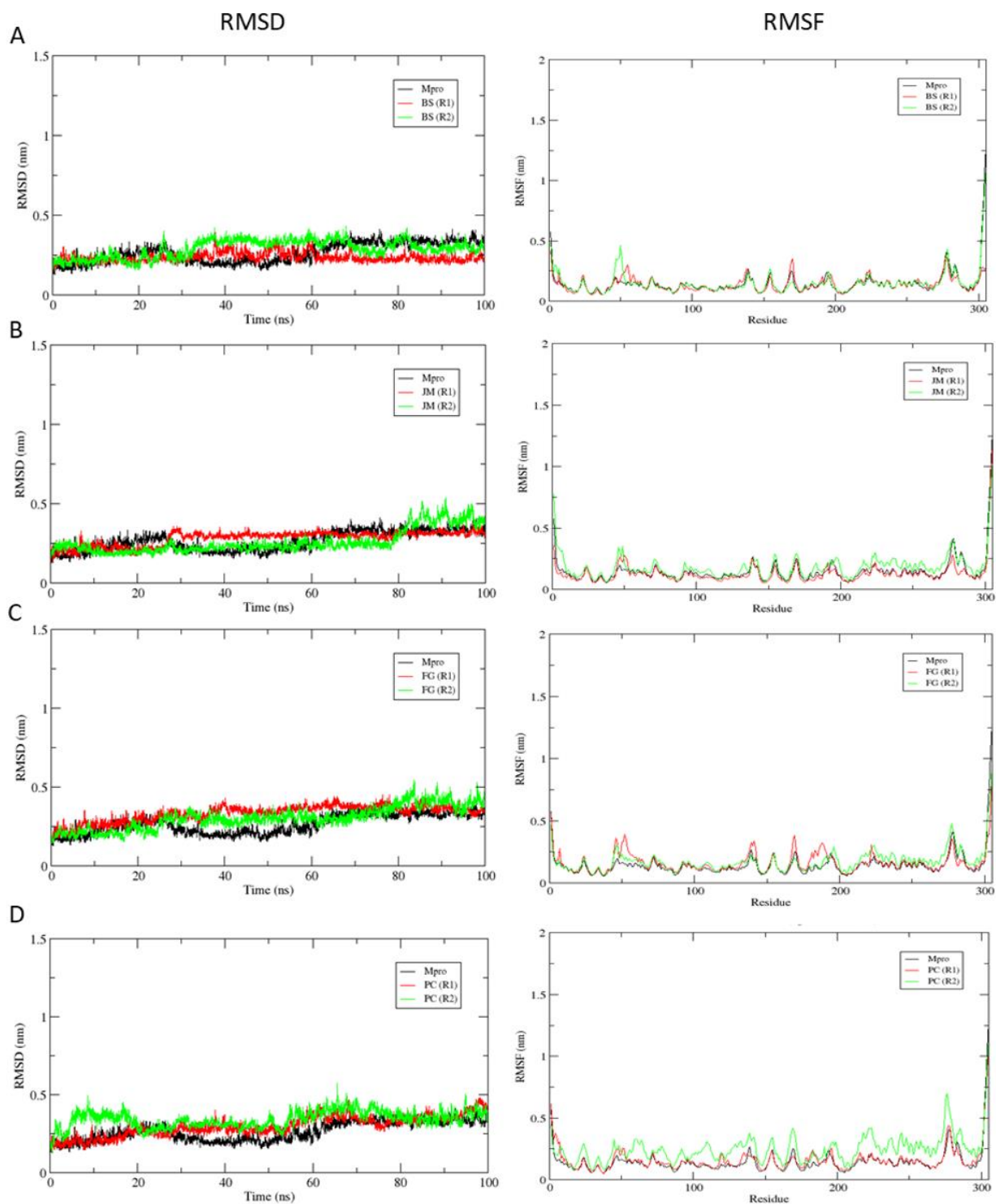


Figure 3.7: RMSD and RMSF profile of free Mpro and complexes. Native Mpro in black and complexes in red (Replica 1) and green (Replica 2) colour lines. A. Beta-Sitosterol – Mpro B. Jatamansin - Mpro C. 6,7-dehydroferruginol – Mpro D. Phyllocladanol – Mpro

Other complexes exhibit average of ~ 2 H-bonds. Furthermore, all four Mpro to ligand complexes exhibited similar RoG, temperature and pressure profiles with respect to time indicating compact packaging within optimum pressure and temperature of the newly formed complexes (Appendix Figure A2).

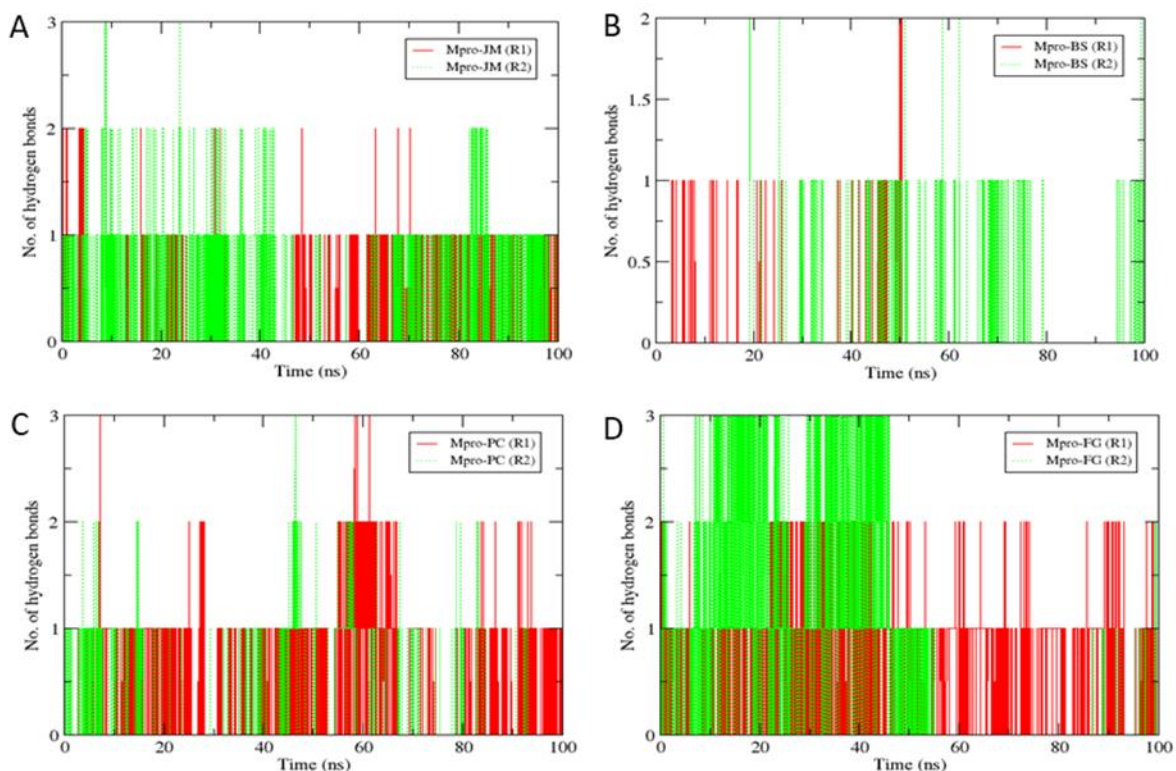


Figure 3.8: Hydrogen Bond Analysis of Mpro-complexes in two replications, Replica 1 (red) and Replica 2 (green). A. Jatamansin - Mpro B. Beta-Sitosterol – Mpro C. Phyllocladanol – Mpro D. 6,7-dehydroferruginol – Mpro

3.3.3.2. Molecular dynamics simulation of papain-like protease complexes

To examine the stability of complexes, RMSD, RMSF, gyration and other graphs were interpreted, and it was observed that RMSD of native PLpro remained almost stable with value less than 0.5 nm. Lantadene D-PLpro complex stabilized with slightly lower average rmsd (0.30 nm) compared to PLpro alone (0.32 nm). Since Trp107, Cys112, His273 and Asp287 are the reported catalytic sites in PLpro, and lantadene D interacted close to His273 and Asp 287 utilizing H-bonding and hydrophobic interactions in these regions. Active site residues like 268, 272, 271 were showing meagre difference in fluctuations compared to

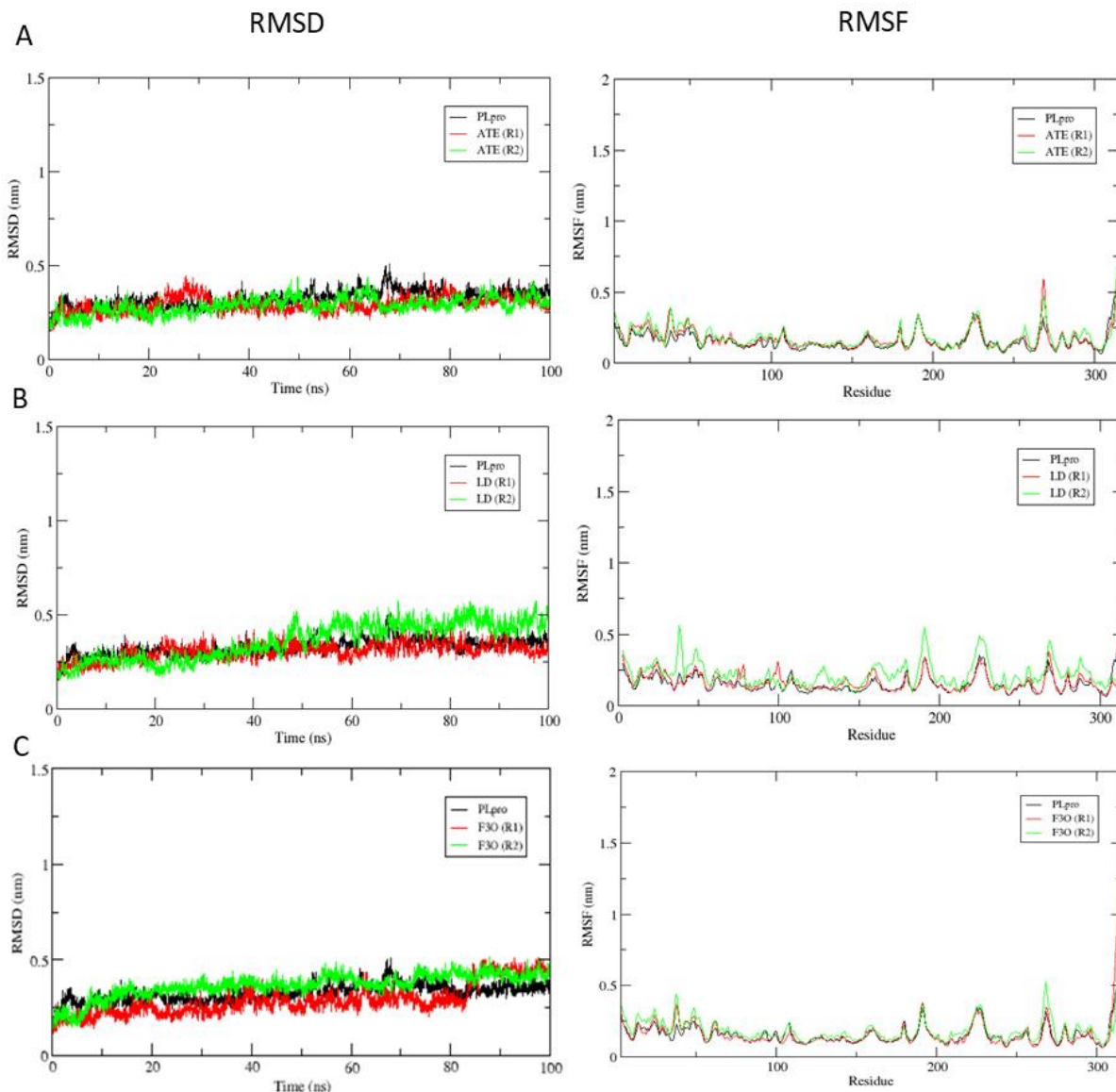


Figure 3.9: RMSD and RMSF profile of free PLpro and complexes. Native PLpro in black and complexes in red (Replica 1) and green (Replica 2) colour lines. A. Abietatriene – PLpro B. Lantadene D – PLpro C. Friedelan-3-one – PLpro.

unbound PLpro (Figure 3.9B), indicating stable confirmation of ligand and receptor within binding pocket.

On the other hand, the abietatriene-PLpro and friedelan-3-one-PLpro complexes had an average RMSD of 0.28 and 0.27 nm, respectively. The RMSD of abietatriene remained stable up to 20 ns then slight increase and decrease for 10ns and finally reached its constant state after 35 ns with slight fluctuations. While a seemingly equilibrated friedelan-3-one-PLpro rmsd graph with respect to time abnormally flipped equilibrium states to a higher rmsd value after around 85 ns and again got stability quickly, it was not observed in second replica. An

inexplicable rmsf around residue 40 similar to abietatriene-PLpro complex have also been observed for the friedelan-3-one-PLpro complex. Lys105 related dual interactions contributed to comparatively lower rmsf residue-wise values around 105 which should have been preferred depending on previous successful in vitro experimentation data on SARS-CoV. It is apparent from the figures that active and adjacent residues are fluctuating in limited range (0.1 - 0.4 nm) which is obvious to disrupt the native protein confirmation. Although, results of both replicas are also showing the same pattern of peaks in all graphs, the difference in value exists (Figure 3.9). Although, good RMSD was observed in abietatriene-PLpro complex, hydrogen bonds were not observed at all therefore it was filtered out from further consideration. The number of hydrogen bonds in lantadene D-PLpro and friedelan-3-one-

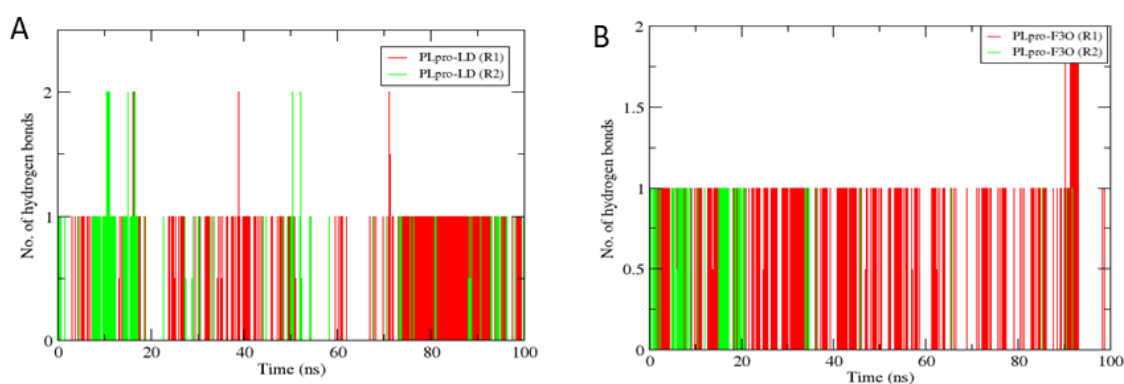


Figure 3.10: Hydrogen Bond Analysis of PLpro – Complexes in two replications, Replica 1 (red) and Replica 2 (green). A. Lantadene D – PLpro B. Friedelan-3-one – PLpro

PLpro complex are depicted in Figure 3.10. Radius of gyration clearly showed the recommended range of complexes for compactness and temperature and pressure plots were also generated to study the equilibrated system (Appendix Figure A4).

3.3.3.3. Molecular dynamics simulation of RNA dependent RNA polymerase complexes

Based on our previous docking analysis, two compounds were selected for further assessment. From the MD simulation analysis, both compounds were found to be in the range, Lantadene A was observed stable throughout the simulation however in second replica slight increase in average rmsd (0.11 nm) was detected. Reduced lantadene A was coinciding with native RdRp in replica 2 and looked more stable at some point, however, the difference between average rmsd of both replicas was very small i.e 0.07 nm. The average RMSD of free RdRp, lantadene-RdRp and reduced lantadene A-RdRp complex were 0.45, 0.42 and

0.40 nm, respectively. The lower value and minimal difference in average RMSD value suggested that both complexes are stable. The RMSD of reduced lantadene A-RdRp remained converged with native RdRp throughout the simulation whereas lantadene A-RdRp

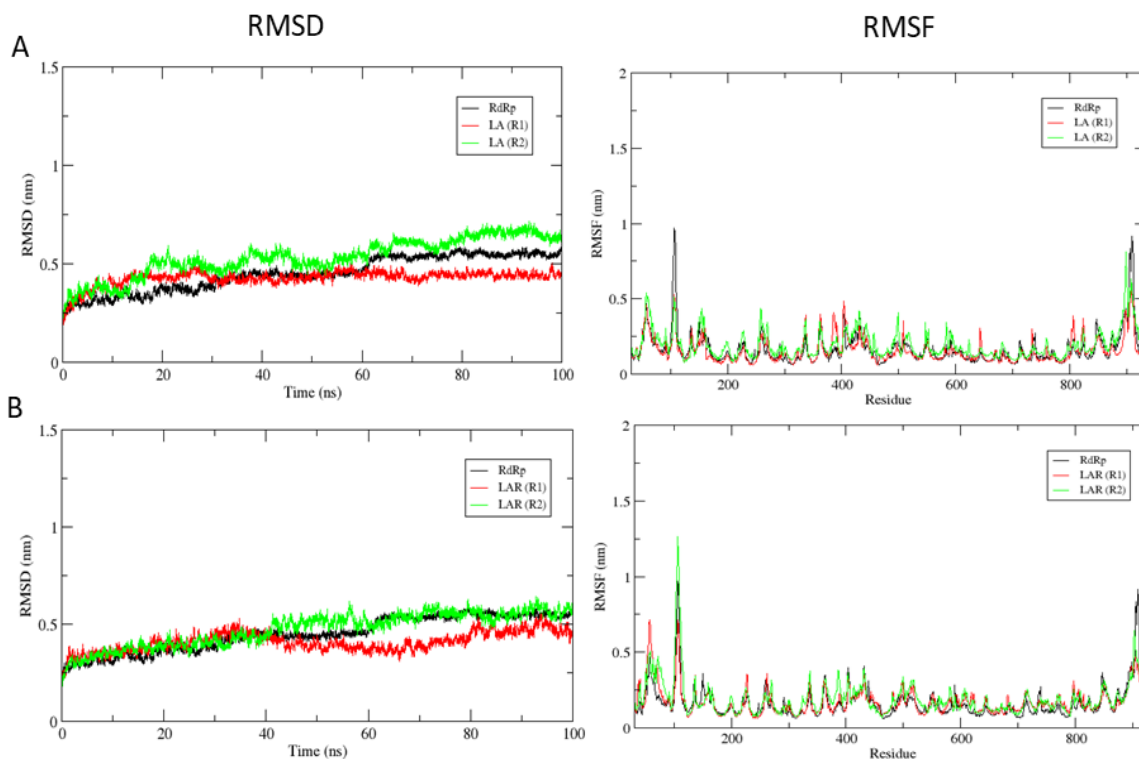


Figure 3.11: RMSD and RMSF profile of free RdRp and complexes. Native RdRp in black, and complexes in red (Replica 1) and green (Replica 2). A. Lantadene A – RdRp B. Reduced Lantadene A – RdRp

equilibrated after 26 ns. The average fluctuation in overall residues were identified for unbound RdRp, lantadene A-RdRp and Reduced lantadene A-RdRp as 0.16, 0.15 and 0.17 nm (Figure 3.11). RMSF of reduced lantadene A-RdRp was overall similar to lantadene A-RdRp or unbound RdRp, higher value of reduced lantadene A-RdRp might be due to fluctuation at reported active site region of RdRp, implying a compact dynamic association of both compounds to RdRp (Figure 3.11). Specifically, reduced lantadene A-RdRp had higher rmsf around Lys621 compared to either lantadene A-RdRp or unbound RdRp because of congregation of H-bonding and salt bridge with the same residue (Lys621). This statement can be better explained from the H-bond plot of reduced lantadene A-RdRp complex as minimum 0 and maximum 4 H-bonds have been observed in 100 ns time window of MD simulation whereas H-bonds in lantadene A-RdRp were observed up to 3 in both, indicating the stable complexes (Figure 3.12). RoG plot displayed the compactness of native structure

and complexes, the average value of unbound RdRp was 3.06 nm while, complexes lantadene A-RdRp and reduced lantadene A-RdRp exhibited slightly higher value, 3.16 and 3.08 nm

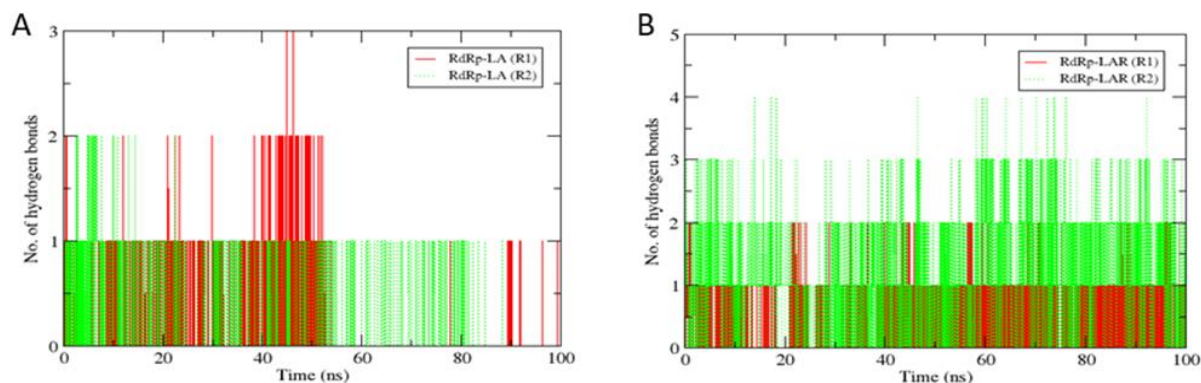


Figure 3.12: Hydrogen Bond Analysis of RdRp – Complexes in two replications, Replica 1 (red) and Replica 2 (green). A. Lantadene A – RdRp B. Reduced Lantadene A – RdRp

respectively, indicating the interaction of ligand and disruption of stability of protein however, the value of native RdRp is very close with reduced lantadene A-RdRp complex which can be potential stable and compact candidate. Temperature and Pressure plots revealed that the complexes reached the target value quickly and persisted suggesting that the system is equilibrated (Appendix Figure A5).

3.3.3.4. Molecular dynamics simulation of spike glycoprotein complexes

In the present study, the RMSD of SG-pro (unbound) remained constant till 13 ns then experienced a slight increase up to 24 ns and then decreased and continued with the constant value within 1 or 2 nm range with some fluctuations. The RMSD of complex lantadene A-SG-pro remained less than 1.5 nm throughout the simulation whereas lantadene B-SG-pro experienced RMSD value up to 2.1 nm at some instances. The average RMSD of unbound SG-pro, lantadene A-SG-pro and lantadene B-SG-pro was 1.7, 1.2, and 1.6 nm, respectively. From these observations, it can be inferred that both complexes are more stable than native SG-pro, preferably lantadene A-SG-pro (Figure 3.13).

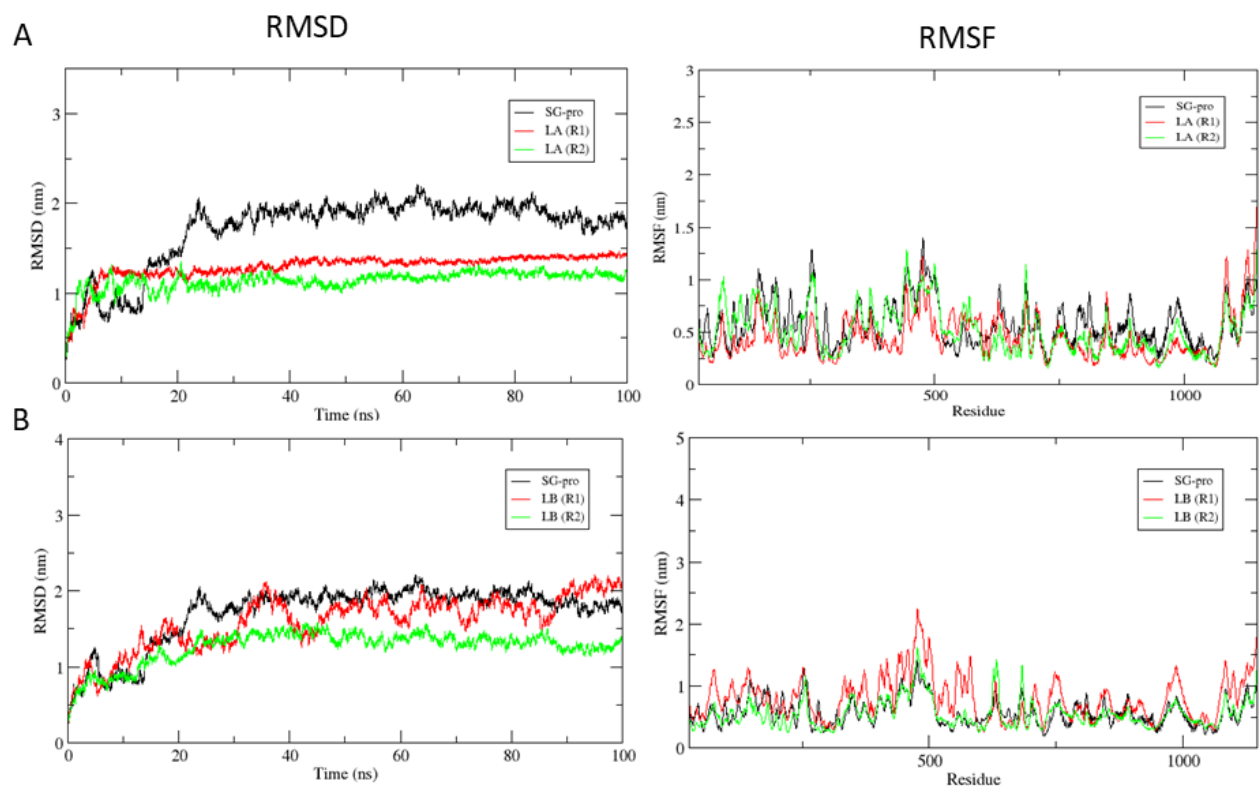


Figure 3.13: RMSD and RMSF profile of free Spike and complexes. Native SG-pro in black, complexes in red (Replica 1) and green (Replica 2). A. Lantadene A – SGpro B. Lantadene B – SGpro.

RMSF evaluation of lantadene A-SG-pro indicated lowest value (0.5 nm) in binding region (318-514) suggesting stable binding of lantadene A with SG-pro whereas lantadene B-SG-pro showed higher RMSF (1.1 nm), the other residues away from this mentioned region also had higher RMSF compared to either lantadene A-SG-pro complex or to unbound SG-pro

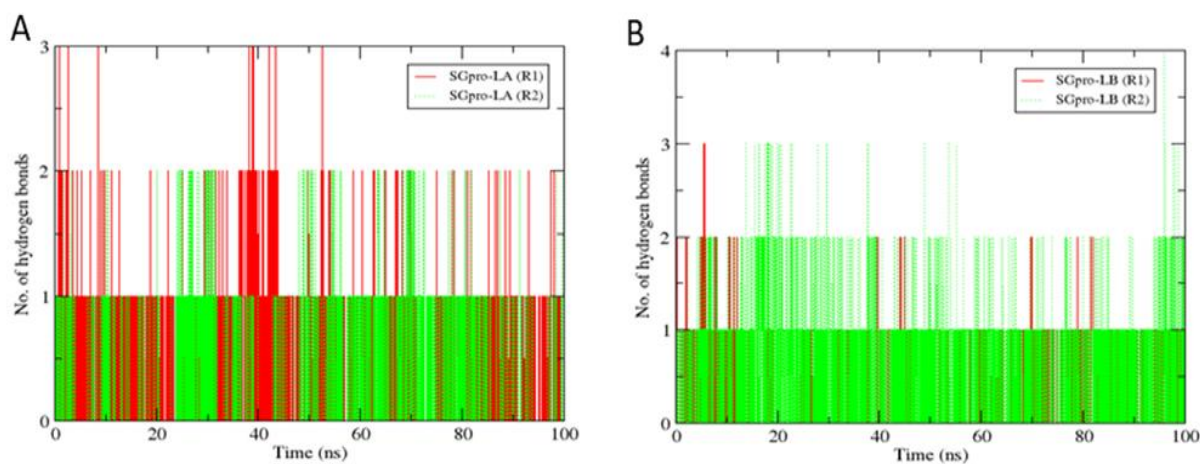


Figure 3.14: Hydrogen Bond Analysis of SGpro – Complexes in two replications, Replica 1 (red) and Replica 2 (green). A. Lantadene A – SGpro B. Lantadene B – SGpro

(Figure 3.13). The number of hydrogen bonds were observed up to 3 in both complexes throughout the simulation. In lantadene B-SG-pro complex, the plot almost overlapped in both replicates (Figure 3.14). The RoG of lantadene A-SG-pro significantly decreased compared to SG-pro alone and lantadene B-SG-pro indicating compact packaging of the complex. Lantadene B-SG-pro R1 and R2 RoG-time graphs over the 100 ns window were markedly distinct from each other, however, the difference in the average values was 0.4 nm only. Temperature and Pressure – time graphs indicated optimum values throughout the simulation (Appendix Figure A6).

3.3.4. Binding Free Energy Analysis

The binding free energy is the cumulative sum of all the energies contributing to the formation of interaction between receptor and ligand including van der walls, electrostatic, polar solvation, and SASA energy. Among them, all components of total binding energy contributed favourably except Polar solvation energy. The lower binding energy significantly addressed the stability of receptor-ligand complexes. Hence, complex with low binding energy would be preferable to other. Figure 3.15 presents an overview of all the energies of each of the complex. The total binding energy of EO compounds (jatamansin, phyllocladanol,

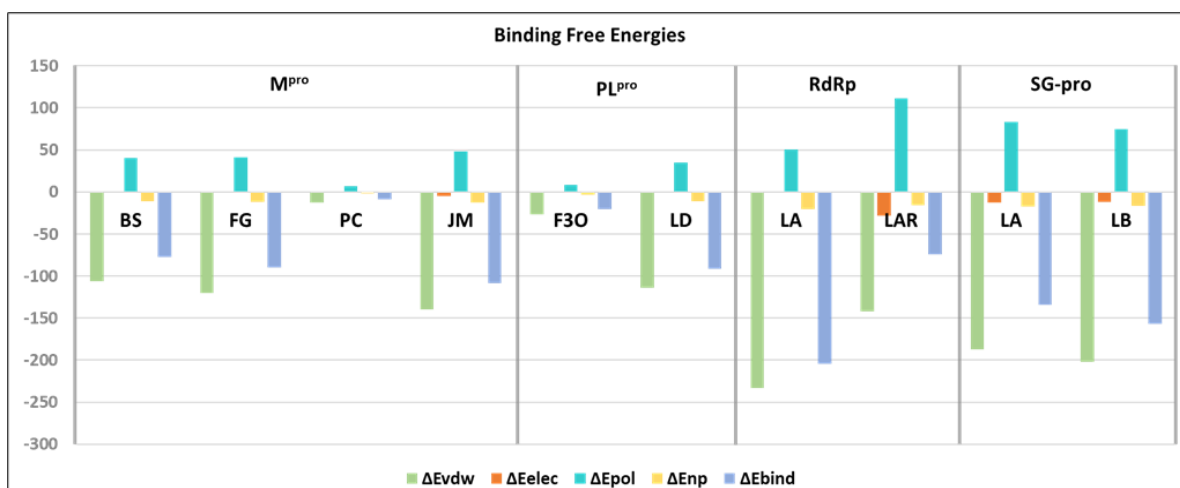


Figure 3.15: Binding energies evaluated from MM-PBSA method of selected complexes. Van der wall energy is indicating highest contribution in total free binding energy. ΔE_{vdw} , ΔE_{elec} , ΔE_{pol} , ΔE_{np} , and ΔE_{bind} represents van der wall energy, electrostatic energy, polar solvation energy, nonpolar solvation energy, and total binding energy respectively.

beta-sitosterol, and 6,7-dehydroferruginol) – Mpro complex suggested that jatamansin-Mpro presented the lowest binding energy whereas phyllocladanol-Mpro showed the highest of all. Other two complexes 6,7-dehydroferruginol-Mpro and beta-sitosterol-Mpro showed

comparatively intermediate values. Furthermore, total binding energy of PLpro complexes, lantadene D-PLpro exhibited lower value than friedelan-3-one-PLpro, however after consideration of previous observation both compounds were equally preferential. Surprisingly, in case of RdRp significant difference of binding energy has been observed in both complexes in which lantadene A-RdRp displayed very less value compared to the reduced lantadene A-RdRp complex, however both values are appropriate. In addition to this, binding free energy of complexes of lantadene A-SG-pro and lantadene B-SG-pro were showing binding energy of -134.101 and -156.525 kJ/mol indicating difference of around 20 kJ/mol (Table 3.9).

Table 3.9: Binding Free Energies calculated from MM-PBSA Method of different complexes

Receptor	Complex	Binding Free energy (kJ/mol)
Mpro	Beta-sitosterol-Mpro	-77.445 +/- 17.02
	6,7-dehydroferruginol-Mpro	-89.986 +/- 10.968
	Phyllocladanol-Mpro	-8.523 +/- 40.564
	Jatamansin-Mpro	-108.476 +/- 14.146
PLpro	Friedelan-3-one-PLpro	-20.743 +/- 42.519
	Lantadene D-PLpro	-91.322 +/- 36.35
RdRp	Lantadene A-RdRp	-204.038 +/- 20.951
	Reduced Lantadene A-RdRp	-74.122 +/- 15.722
SG-pro	Lantadene A-SG-pro	-134.101 +/- 16.312
	Lantadene B-SG-pro	-156.525 +/- 12.651

3.4. CONCLUSIONS

In the current study, molecular docking analysis of 2,363 EOs compounds from 1,050 medicinal and aromatic plant species against four major proteins of SARS-CoV-2 revealed four compounds to be potential candidates against Mpro, and three compounds against PLpro, while two compounds for RdRp and SG-pro where lantadene A is common to both. These compounds were also compared with the well-known drugs available to inhibit their respective protein targets. Further MD simulation and binding free energy analysis exposed more preferential compounds such as jatamansin and 6,7-dehydroferruginol for Mpro, lantadene D and friedelan-3-one for PLpro, lantadene A and reduced lantadene A might inhibit RdRp function effectively, and lantadene A could be potential inhibitor for SG-pro. Lantadene A has been shortlisted for both RdRp and SG-pro thus, it could be effective for both RdRp and SG-pro. We have considered various pros and cons of our data and have

arrived at the final conclusion that these EO compounds can be potential leads for intranasal therapy, after *in-vitro* and *in-vivo* testing against virus because nasal route has been recognized as the main entry route for SARS-CoV-2 infection as well as due to the inherent property of the EO compounds to travel longer distances via air.

CHAPTER 4

IDENTIFICATION OF ACTIVE COMPONENTS IN
***Picrorhiza kurroa* EXTRACTS AND THEIR POSSIBLE**
MECHANISTIC ACTIONS FOR THE TREATMENT OF
NAFLD/ NASH

4.1. INTRODUCTION

NAFLD has become one of the most frequent causes of chronic liver disease. Approximately, 25% of the adult population worldwide with highest occurrence in middle east and lowest in Africa [286][287]. According to recent study, the prevalence in India ranges from 9% to 53 % in different geographical regions where urban population found at higher risk than rural [288]. It progresses to different stages including NASH, liver cirrhosis and HCC [286], [289]. As mentioned in the literature review, prevalence of NAFLD is associated with various metabolic syndromes like, obesity, T2D, insulin resistance, hyperlipidemia, hypertension chronic kidney disease etc., [290]–[292]. From the studies, it was noticed that the occurrence of fatty liver ranges between 30 to 100% in obese patients, 10 to 75% in T2D, 20 to 90% in hyperlipidemia [288], [293]. Recent research on the Indian population revealed that 43% population had metabolic syndrome while 93% had found to exhibit at least one metabolic risk factor with NAFLD [288]. Besides, genetic factors also play a vital role in prevalence of NAFLD, for example, PNPLA3 and TM6SF2 genes and their variants have been significantly shown to be associated with NAFLD [288]. Overall, the aforementioned survey studies corroborated the fact that the NAFLD has various type of comorbidities. Hence, the treatment has been quite difficult. Although, insulin sensitizers, antioxidants, lipid-lowering drugs, pentoxifylline, and angiotensin receptor blockers appear to be the promising therapeutic agents for NAFLD/ NASH, however, those frequently cause undesirable effects [294]. Therefore, presently, the suggested treatments are limited to lifestyle modifications such as healthy diet, physical exercise, and use of medications to improve comorbidities and to prevent the progression of NAFLD [295], [296]. The conventional techniques that focus on one gene or component at a time have been ineffective in dealing with the multifaceted complexities of NAFLD since earlier research has revealed that progression of disease involves multiple factors and pathologies [297]. We would like to quote the words of Parlati et al., here “an ideal drug candidate for NAFLD should improve steatosis, hepatic inflammation and fibrosis, while ameliorating glucose metabolism, insulin resistance and obesity”. Hence indicating the involvement of multiple key players from different disease associated pathways in development and progression of NAFLD/ NASH [298]. As mentioned previously, currently there is no drug available to treat NAFLD however few are in phase II and III clinical trials [298].

Herbal medicines (including crude extracts, herbal formulations, pure isolated compounds from medicinal plants) have been proven to be effective in NAFLD/ NASH treatment through multiple components, targets, and regulating several pathways [42]. For instance, *Picrorhiza kurroa* is a medicinal herb, reported to show hepatoprotective activity, and its isolated compounds (Picroside-I and Picroside-II) are also reported as promising for treating NAFLD [44]–[46], [299]–[301], however exhibit poor bioavailability and less bio efficacy as compared to extracts (explained in detail in chapter 2) [152], [157], [158]. Even though, compounds in *Picrorhiza kurroa* have medicinal properties, the actual mechanism through which compounds in *Picrorhiza kurroa* extracts exhibit therapeutic effects on NAFLD/ NASH is unclear.

Since, network pharmacology has emerged as a powerful approach and gained widespread attention in dealing with disease complexities via influencing multiple components [302], [303]. Network pharmacology emphasizes paradigm change from traditional “single-target”, “single-drug” approach to “multi-target”, “multi-component” approach [149], [304]–[307]. In this direction, we utilized a network pharmacology approach to understand the intricacies in biological system involved in pathology and to capture the mechanism of action of active components of *Picrorhiza kurroa* in the treatment of NAFLD/ NASH. Firstly, compound structure similarity with drugs and drug-like compounds was done to check the new chemical entities which can be potential leads. Thereafter, pharmacokinetic profile of compounds was predicted to analyze the drug-likeness of compounds. Thereafter, we predicted the molecular targets of *Picrorhiza kurroa* compounds and investigated their combinatorial role on multiple targets. Afterwards, we identified the intersecting pathways and networks shared by molecular targets of *Picrorhiza kurroa* compounds and NAFLD/ NASH. Apart from this, molecular docking was performed to examine the interactions that allows active compounds to bind to their predicted targets, followed by 50ns MD simulation to analyze the stability and flexibility of complexes in biological systems. The outcome of current study can be useful in understanding the mechanism of *Picrorhiza kurroa* compounds in the treatment of NAFLD/ NASH to facilitate the development of new medications.

4.2. MATERIALS AND METHODS

4.2.1. Curation of significant compounds present in *Picrorhiza kurroa*

The list of *Picrorhiza kurroa* compounds was extracted from three databases namely Phytochemica [308], NPASS [309] and IMPAAT [310]. The biological or medicinal activities were retrieved from the literature of all the metabolites (Appendix Table A1). Based on their reported activity related to liver diseases, twenty-four active compounds were selected to explore in the current study.

4.2.2. Structure similarity analysis of *Picrorhiza kurroa* compounds with approved drugs for liver diseases

The structures of compounds present in *Picrorhiza kurroa* extracts were mapped with structures of known drugs for liver diseases retrieved from DrugBank (<https://go.drugbank.com/>) using R packages “ChemmineR” [311]. Molecular similarity of desired compounds with known drugs has been suggested as a key concept in identifying new leads [312]. The assumptions in this concept are that structurally similar molecules have similar activity and properties. Therefore, we used Tanimoto coefficient which is the most extensively used and popular similarity metric. For this, the molecular fingerprints of x, y, and z coordinates of atoms were calculated and the ratio of common fingerprints in both and the differences of common and unique fingerprints in both were evaluated. The structure with score greater than 0.7 and between 0.5-0.7 were considered to exhibit identical pharmacophores and similar structure, respectively.

4.2.3. *In silico* pharmacokinetic profiling of *Picrorhiza kurroa* compounds

It has been mentioned in above sections that bioavailability of isolated compounds is less therefore, physicochemical and pharmacokinetic properties of compounds were calculated using PKCSM tool [234]. Several parameters have been regarded related to absorption, distribution, metabolism, excretion, and toxicity. Apart from this, the Lipinski’s rule of five (RO5) is specifically considered as guidelines to predict the oral bioavailability of the compounds as stated in [228].

4.2.4. Network Pharmacology

4.2.4.1. Shortlisting of active constituents of *Picrorhiza kurroa* and prediction of their putative corresponding gene/ protein targets

The pharmacological targets of compounds were predicted from Polypharmacology Browser (PPB2) (<https://ppb2.gdb.tools/>) [313], Similarity ensemble approach (SEA) (<https://sea.bkslab.org/>) [314] and Swiss Target Prediction (<http://www.swisstargetprediction.ch/>) [315]. The predicted targets and compounds were uploaded in Cytoscape 3.7.1 (<https://www.cytoscape.org>) [316] and finally, compound-target network was generated, where nodes represent the genes and proteins, and edges represent the interactions between them. The size of nodes indicates the “Degree” value which shows the number of connections between nodes, larger the number, larger the size of node, more chances to become the key target in the network. The different color of nodes indicates the compounds and targets.

4.2.4.2. Screening biological targets of *Picrorhiza kurroa* compounds in treating NAFLD/ NASH

The pathogenic targets involved in NAFLD, and NASH directly/ indirectly were collected from GeneCard (<https://www.genecards.org/>) [317], Therapeutic Target Database (TTD) (<http://db.idrblab.net/ttd/>) [318], and DisGenNET databases (<https://www.disgenet.org/>) [319], by searching through keywords such as “non-alcoholic fatty liver”, “non-alcoholic steatohepatitis”, “nafld”, “nash”. Thereafter, all the targets of NAFLD/ NASH and active compounds were assessed by comparative analysis in order to extract the compounds treating targets of NAFLD and NASH. The Venn diagram was generated to show the overlapping pathological targets of NAFLD/ NASH and active compounds.

4.2.4.3. Capturing interactive protein targets of NAFLD/ NASH

The Protein-Protein Interaction (PPI) network of NAFLD and NASH targets was constructed by utilizing Search Tool for the Retrieval of Interacting Genes (STRING) (<https://string-db.org/>) [320] by setting the confidence score to >0.9 and disabling the text mining option. Thereafter, overlapping genes of NAFLD/ NASH and compounds were used as bait to capture additional interactive target genes from the interaction network. In addition to this, the nodes exhibiting “experimentally determined” interaction value >0.1 were selected for

further analysis. The network was visualized in Cytoscape, and topological parameters were evaluated using “Network Analyzer” of Cytoscape. The nodes with degree of freedom >4 , which is half of the median, were considered as significant nodes then the interaction between these nodes was visualized in Cytoscape to find the most potential hubs in the networks.

4.2.4.4. Gene ontology and KEGG enrichment analysis of shortlisted proteins

The shortlisted nodes were input to Database for Annotation, Visualization, and Integrated Discovery website (DAVID) for Gene Ontology (GO) and Kyoto encyclopedia of genes and genomes (KEGG) analysis to identify related biological process, function, and pathways of genes. We uploaded the gene list and converted it into gene ids in DAVID and used as input by setting the species to *Homo sapiens*. The suggested targets for top 20 GO (BP, MF and CC) and KEGG enrichments were considered for further study.

4.2.4.5. Construction of Compound-Target-Disease-Pathways Network

The network of compound-target-disease-pathways-other diseases was generated to depict the therapeutic mechanism of compounds for NAFLD and NASH. The nodes (compounds, target genes, NAFLD, NASH, biological/disease pathways, other diseases associated with NAFLD/ NASH) were segregated with different color and shape in the network and edges between the nodes reflect the interaction as well.

4.2.5. Molecular docking and molecular dynamics simulation analysis

The significant targets of NAFLD/ NASH interacting with related pathways, compounds, and other diseases were considered as potential key targets to uncover the mechanism of compounds of *Picrorhiza kurroa*. The docking simulation of 10 targets was done with 24 compounds to evaluate the binding profile of ligand and receptor. The PDB structures of targets were downloaded from RCSB PDB and the compound structures were extracted from PubChem. Protein structures were prepared by removing already attached small molecules, water molecules, adding H- bonds and Kollman charges and saved in pdbqt format, and the compounds were prepared and converted in pdbqt using AutoDock tools. The docking simulation was performed in AutoDock Vina [21] by using python script. Additionally, the docking of reference compounds was done with the targets for comparative analysis. The

complexes were visualized in ligprep. Finally, the compounds with higher docking score and good interaction were deemed as active components for interacting with their corresponding receptors. To examine the stability and flexibility of the protein-ligand complex and interactions, the selected compounds were subjected to MD simulation using the GROningen MAchine for Chemical Simulations (GROMACS). MD simulation was performed using GROMACS 2018.2 suite with GROMOS96 54a7 force field on gpu (nvidia dgx server). The ligand parameters and topology files were generated using PRODRG. Furthermore, the system was built utilizing Simple Point Charge (SPC) water molecules within a 1.0 nm dodecahedron box. Ions were added to the complex for neutralization afterward, energy minimization was performed to relax the system and remove the initial conflicts using 50,000 (maximum no. of steps) steps of steepest descent algorithm with tolerance of $>1000\text{kl/mol/nm}$. Equilibration was carried out in two phases, first with NVT (constant number of particles, pressure, and temperature). Finally, an MD simulation was run for 50ns with a time frame of 2fs and trajectories were created every 10 ps. The trajectories, Root Mean Square Deviation (RMSD) and Root Mean Square Fluctuation (RMSF) of confirmations of protein-ligand complexes were examined. The final trajectories were analyzed with UCSF Chimera, graphs were generated with GROMACS 2018.2 and visualized in Grace. The detailed methodology is presented in Figure 4.1.

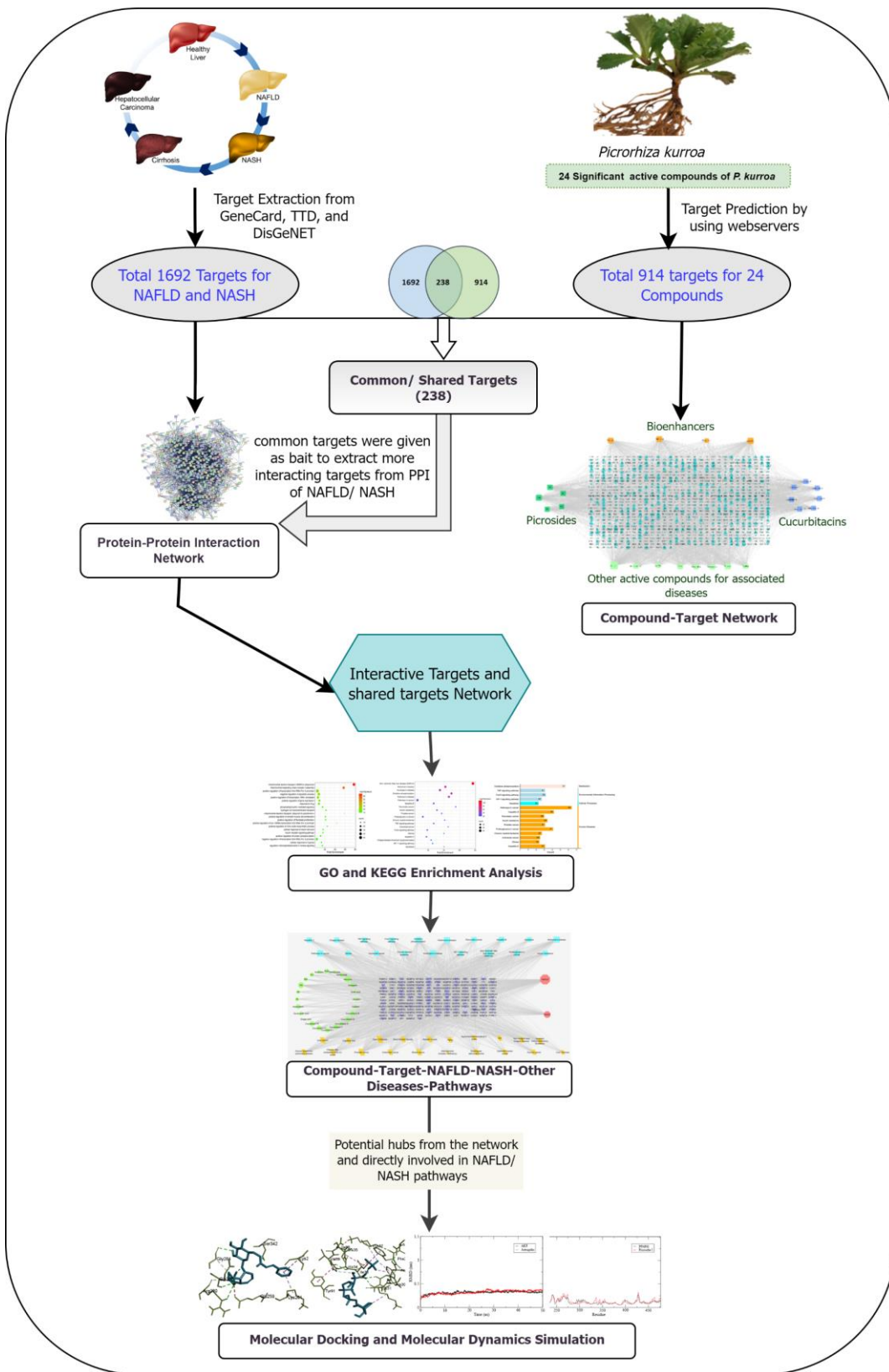


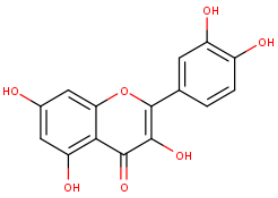
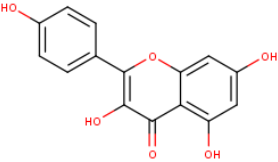
Figure 4.1: Workflow of network pharmacology strategy to capture *Picrorhiza kurroa* compounds and their mechanism in NAFLD/ NASH treatments

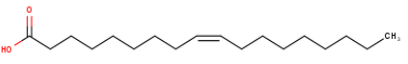
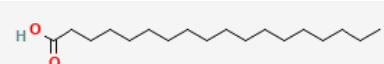
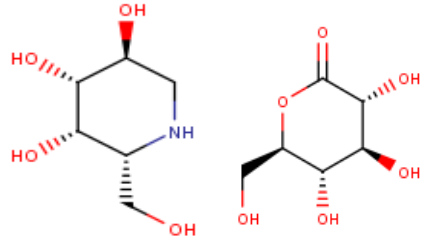
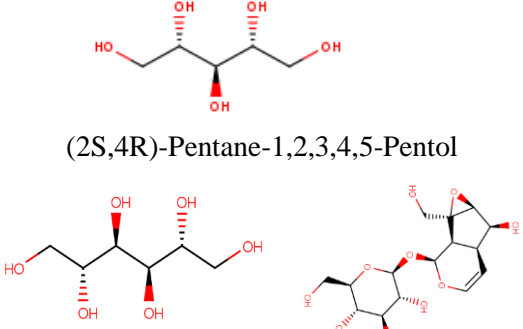
4.3. RESULTS AND DISCUSSION

4.3.1. Compound structure similarity with known drugs of liver diseases revealed presence of active compounds in *Picrorhiza kurroa*

The results of our analysis revealed that there are few compounds sharing similarity (Table 4.1) with the known drugs. These drugs are either approved or in use as control for experimental and investigational purpose according to DrugBank (<https://go.drugbank.com/>). Kaempferol and Quercetin showed identical pharmacophore as both are flavonoids, incidently Quercetin is also present in *Picrorhiza kurroa*. Quercetin has antioxidant, anti-inflammatory and radical scavenging activities as well as is a natural bioenhancer since it is dual inhibitor of CYP3A4 and P-gp [321]. According to a research, Quercetin pretreatment half an hour before verapamil delivery in rabbits increased the absolute and relative bioavailability values of verapamil compared to verapamil alone group[322]. Similar effects have been noticed with pretreatment/co-treatment with several drugs for cancer, cardiovascular diseases, hypertension or high blood pressure including diltiazem, paclitaxel, digoxin, doxorubicin, and tamoxifen [323]–[327]. Furthermore, Oleic acid used for Colorectal or Adenomatous Polyps [328], Migalastat is an approved drug for Fabry disease whereas Gluconolactone (DB04564) is used as antioxidants [329]. Hence, the similar or identical structures might exhibit similar property and biological activity. Almost all the compounds were having very low tanimoto coefficient. It can be assumed that these compounds could be new chemical entities which is giving scope to this field.

Table 4.1: Structure similarity in compounds and drugs based on tanimoto coefficient

Drugs	Metabolites	Tanimoto Coefficient
 Quercetin	 Kaempferol (Quercetin is also present in the <i>Picrorhiza kurroa</i>)	0.8

 <p>Oleic acid</p>	 <p>Stearic acid</p>	0.68
 <p>Migalastat</p> <p>Gluconolactone</p>	 <p>(2S,4R)-Pentane-1,2,3,4,5-Pentol</p> <p>Mannitol</p> <p>Catalpol</p>	0.53-0.59

4.3.2. *In silico* pharmacokinetic analysis of *Picrorhiza kurroa* compounds

It has been observed from the literature that bioavailability of compounds delivered through extravascular routes is less as compared to intravenous routes (details are mentioned in chapter 2). Most of the drugs, formulations and plant extracts are available for oral dose only, therefore, the bioavailability measure of any compound can be fruitful in pre-clinical studies. Generally, the Phase I and Phase II metabolic reactions break the molecule in polar or hydrophilic form so that it can eliminate easily from the body [330], but in case of picrosides there is extensive metabolism seen where molecule is not able to show that much effect and eliminates early [48]. For this, three main reasons were noticed firstly, hydrophilic nature resulting in less permeability through membrane and poor gastrointestinal absorption, secondly, intestinal bacteria's glucosidase and esterase activity was found to be liable for substantial metabolism and conversion into aglycones (inactive form of iridoid glycosides) and third, extensive metabolism by glucuronidation as the predominant excretion was observed of glucuronide and sulfate conjugates. The tabular data (mentioned in chapter 2) revealed bioavailability to some extent based on concentration in plasma that picroside-I and picroside-II are more orally bioavailable in extracts as compared to isolated forms. In light of above-mentioned issues, we modified the structures inspired from study of Han et al., (2018) [331], the lipophilicity reduced however the problem of less bioavailability still

persisted according to experimental study of Han et al. as well as prediction in current study. Hence, it was clear that extracts comprise some synergistic compounds to increase the bioavailability. In this context, the study was shifted to other direction i.e., exploration of involvement of enzymes that metabolizes the drugs. Since cytochrome enzymes in the liver metabolize the xenobiotics. In support of above-mentioned statements, we observed in computational pharmacokinetics profiling that picroside-I and picroside-II were not inhibiting any cytochrome isoform or transporters which may be leading to extensive metabolism whereas extracts contain some other metabolites which were influencing the cytochrome enzymes and P-gp transporters and showing more affinity with other responsible enzyme for the metabolism of picroside-I and picroside-II (Table 4.2). The findings were corroborating the probable reason suggested in literature that the occurrence of other metabolites in *Picrorhiza kurroa* extract which are probably inhibiting the extensive metabolism of picroside-I and picroside-II. Therefore, further network pharmacology strategies were designed to explore the individual mechanism and behavior of compounds.

4.3.3. Network pharmacology to unravel mechanisms of action of *Picrorhiza kurroa* compounds in possible treatment of NAFLD/ NASH

4.3.3.1. Gene/ Protein target prediction of *Picrorhiza kurroa* compounds and fishing targets of NAFLD/ NASH

A total of 24 compounds regarded as active components of *Picrorhiza kurroa* based on their biological activity for liver and associated diseases were considered in analysis. 3340 targets were predicted for all 24 active compounds of *Picrorhiza kurroa*, after removing duplicates, 914 targets were considered for further analysis. Figure 4.2 presents the component-target network, where the compounds are categorized into 4 categories based on their medicinal value, Picrosides, Cucurbitacins, Bioenhancers and other active compounds reported for other associated diseases. These four categories comprise compounds from different chemical classes such as Picrosides belong to iridoid glycosides, Cucurbitacins belong to triterpenoids, third category i.e., Bioenhancers belong to flavonoids and Phenols and the last category which is a combination of compounds from three chemical classes namely, iridoid glycosides, phenolic glycosides and flavonoids. Apart from this, a total of 1644 and 645 targets respectively for NAFL and NASH were retrieved from GeneCard, TTD and

Drugbank. Eventually, 1692 target genes were considered after removing redundancy. Thereafter, both datasets were compared, and 238 overlapping targets were selected as potentially key players in therapeutics affected by *Picrorhiza kurroa*.

4.3.3.2. Compounds – Targets Network analysis

4.3.3.2.1. Compounds in *Picrorhiza kurroa* extracts act in synergistic manner to treat complexities and co-morbidities of NAFLD/ NASH

An interactive network of compounds of *Picrorhiza kurroa* and their corresponding predicted targets was constructed and visualized in Cytoscape with 938 nodes (24 compounds and 914 targets) and 3339 edges (Figure 4.2). Moreover, a venn diagram was generated to capture the commonality and uniqueness in compounds and gene targets (Figure 4.3). It revealed that the

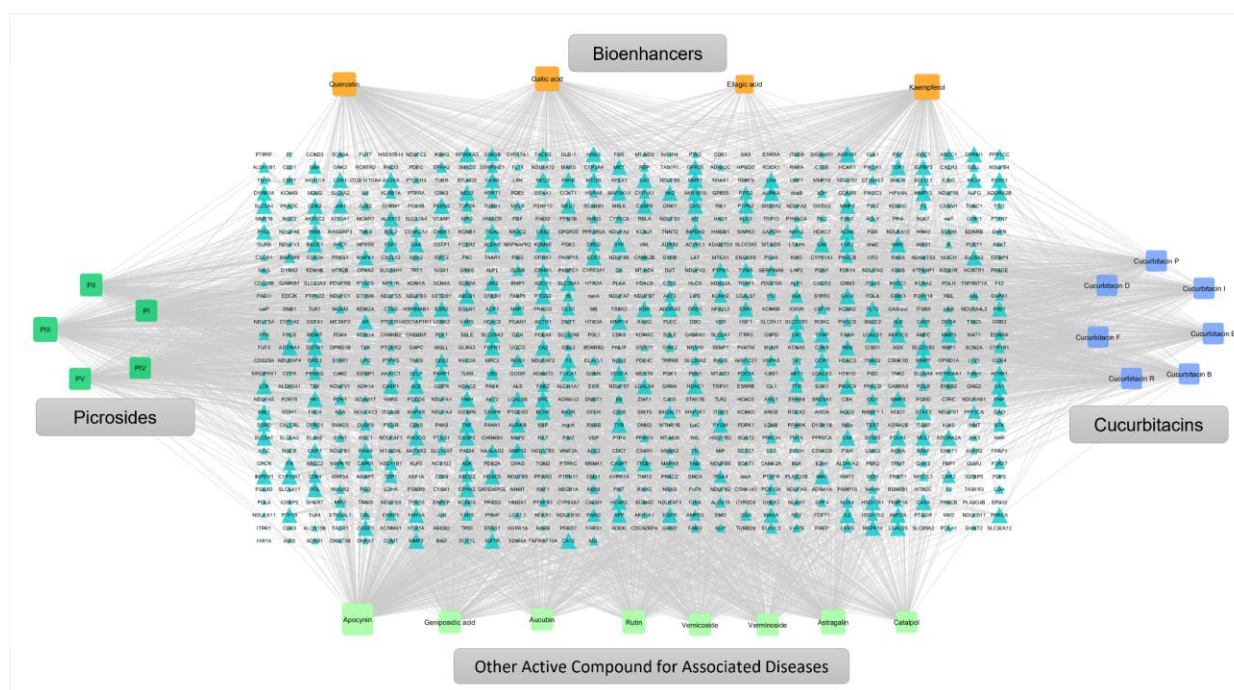


Figure 4.2: Compound-Target-Network of *Picrorhiza kurroa* compounds. Green rectangle represents the Picosides; Light blue rectangle stands for Cucurbitacins; Top orange rectangle stands for Bioenhancers; Light green rectangle represents the other active compounds from extracts for important for NAFLD associated diseases; In center, light cyan triangles represent the predicted targets of all 24 compounds; and edges represents the interaction between compounds and corresponding targets whereas size of all nodes indicate the number of interactions.

potential 56 targets are shared by all four categories, whereas different numbers are shown for different combinations. Contrastingly, 43, 71, 99 and 182 targets were unique for Picosides, Bioenhancers, Cucurbitacins and Other synergistic compounds, respectively.

Table 4.2: Prediction of physicochemical and ADMET properties of significant compounds in *Picrorhiza kurroa* extracts

	P-I	P-II	P-III	P-IV	P-V	G A	E A	KF	QR	CB	CD	CE	CF	CI	CR	CP	VN	V M	AB	GC A	AC	RT	AG	CP	
MOL_WEIGHT	492.477	512.464	536.53	508.476	664.613	17.012	30.421	286.239	166.176	558.712	516.675	556.696	518.691	514.659	528.686	520.707	466.439	524.475	346.332	374.342	166.176	610.521	448.38	362.331	
LOGP	-1.326	-2.0114	-0.9482	-1.6204	0.5662	0.5016	0.044	2.2824	1.6034	3.4993	2.9285	4.1902	2.7203	3.6194	4.0095	2.9443	-1.7256	-1.9148	-2.8015	-2.3175	1.6034	-1.6871	-0.2445	-3.5903	
#ROTATABLE_BONDS	7	7	8	7	11	1	0	1	2	5	4	5	4	4	4	5	6	7	4	5	2	6	4	4	
#ACCEPTORS	11	13	12	12	16	4	6	6	3	8	7	8	7	7	7	7	11	13	9	9	3	16	11	10	
#DONORS	5	6	6	6	1	4	4	4	1	3	4	3	5	4	4	5	5	7	6	6	1	10	7	6	
Water solubility	3.08	2.969	3.049	2.948	4.131	2.283	3.934	3.04	2.925	4.914	4.683	5.042	4.691	4.832	4.77	4.675	3.109	2.604	2.108	2.235	0.66	2.894	2.901	2.176	
Caco2 permeability	0.266	0.622	0.166	0.378	-0.193	0.061	0.382	0.032	-0.229	0.544	0.739	0.501	0.687	0.706	0.678	0.666	0.493	0.199	0.476	-0.398	1.262	-0.957	-1.003	0.397	
Intestinal absorption (human)	32.325	40.505	55.463	41.356	90.98	54.956	69.996	74.29	77.207	92.445	78.169	95.667	72.684	81.391	82.143	73.461	55.65	35.347	33.085	11.661	93.081	22.165	43.415	31.129	
P-glycoprotein substrate	Yes	Yes	Yes	Yes	No	Yes	Yes	Yes	Yes	Yes	Yes	Yes	Yes	Yes	Yes	Yes	Yes	Yes	Yes	Yes	No	No	Yes	Yes	Yes
P-glycoprotein I inhibitor	No	No	No	Yes	Yes	No	No	No	No	Yes	Yes	Yes	Yes	Yes	Yes	Yes	No	No	No	No	No	No	No	No	No
P-glycoprotein II inhibitor	No	No	No	No	No	No	No	No	No	Yes	Yes	Yes	Yes	Yes	Yes	Yes	No	No	No	No	No	No	No	No	No
VDss (human)	0.203	0.039	0.365	0.238	0.008	0.745	0.195	1.274	1.559	0.313	0.382	0.291	0.368	0.36	0.375	0.353	0.395	0.5	0.087	0.394	0.181	1.417	1.512	0.002	
Fraction unbound (human)	0.469	0.471	0.456	0.471	0.15	0.661	0.621	0.178	0.206	0.1	0.169	0.074	0.2	0.143	0.128	0.195	0.396	0.536	0.754	0.689	0.413	0.136	0.19	0.74	
BBB permeability	-1.264	-1.368	-1.784	-1.376	-2.794	-0.939	-0.974	-0.939	-1.098	-0.934	-0.789	-1.029	-0.752	-0.884	-0.914	-0.813	-1.324	-1.713	-0.803	-1.191	0.323	-2.254	-1.858	-1.126	
CNS permeability	4.096	4.177	4.382	4.209	3.422	3.453	3.247	2.228	3.065	2.973	3.042	2.956	3.103	3.026	3.014	3.116	4.199	4.525	4.166	4.212	2.259	5.281	3.897	4.275	

CYP2D6 substrate	No	No	No	No	No	No	No	No	No	No	No	No	No	No	No	No	No	No	No	No	No	No	No	No	No
CYP3A4 substrate	No	No	Yes	Yes	Yes	No	No	No	No	Yes	Yes	Yes	Yes	Yes	Yes	Yes	No	No	No	No	No	No	No	No	No
CYP1A2 inhibitor	No	No	No	No	No	No	No	Yes	Yes	No	No	No	No	No	No	No	No	No	No	No	No	No	No	No	No
CYP2C19 inhibitor	No	No	No	No	No	No	No	No	No	No	No	No	No	No	No	No	No	No	No	No	No	No	No	No	No
CYP2C9 inhibitor	No	No	No	No	No	No	No	No	No	No	No	No	No	No	No	No	No	No	No	No	No	No	No	No	No
CYP2D6 inhibitor	No	No	No	No	Yes	No	No	No	No	No	No	No	No	No	No	No	No	No	No	No	No	No	No	No	No
CYP3A4 inhibitor	No	No	No	No	No	No	No	No	No	No	No	No	No	No	No	No	No	No	No	No	No	No	No	No	No
Total Clearance	0.9 75	0.8 5	0.7 89	0.9 4	0.5 99	0.5 68	0.3 94	0.4 77	0.4 07	0.1 41	0.2 68	0.1 01	0.3 36	0.1 8	0.1 22	0.3 2	1.3 06	0.6 85	1.3 84	1.3 25	0.5 76	- 0.4 09	0.4 62	1.2 38	
Renal OCT2 substrate	No	No	No	No	No	No	No	No	No	No	No	No	No	No	No	No	No	No	No	No	No	No	No	No	No
AMES toxicity	No	No	No	No	No	No	No	No	No	No	No	No	No	No	No	No	No	No	No	No	No	No	No	No	No
Max. tolerated dose (human)	- 0.4 98	- 0.3 32	- 0.2 88	- 0.6 53	0.7 79	0.8 5	0.2 5	0.5 31	0.4 99	- 1.0 08	- 1.0 75	- 1.0 34	- 1.0 68	- 1.0 91	- 1.1 05	- 1.0 45	- 0.1 07	- 0.4 21	1.2 45	0.4 72	1.0 53	0.4 51	0.6 38	0.8 78	
hERG I inhibitor	No	No	No	No	No	No	No	No	No	No	No	No	No	No	No	No	No	No	No	No	No	No	No	No	No
hERG II inhibitor	Yes	No	Yes	No	No	No	No	No	No	No	No	No	No	No	No	No	No	Yes	No	No	No	Yes	No	No	
Oral Rat Acute Toxicity (LD50)	3.4 96	3.2 61	3.6 02	3.0 68	3.3 88	2.1 47	2.3 6	2.4 49	2.4 71	2.9 54	2.7 3	3.0 25	2.7 83	2.8 29	2.9 15	2.7 76	3.4 86	3.0 35	2.8 8	1.9 95	1.9 52	2.4 95	2.5 51	3.2 43	
Oral Rat Chronic Toxicity (LOAEL)	3.6 46	3.8 93	4.0 62	3.4 36	1.3 54	2.5 19	2.1 45	2.5 05	2.6 12	1.7 81	1.6 47	1.7 37	1.7 4	1.6 02	1.5 32	1.7 18	4.4 48	3.5 78	3.2 6	3.4 5	2.6 58	3.7 15	4.4 8	3.4 58	
Hepatotoxicity	No	No	No	No	No	No	No	No	No	No	No	No	No	No	No	No	No	No	No	No	No	No	No	No	No
Skin Sensitisation	No	No	No	No	No	No	No	No	No	No	No	No	No	No	No	No	No	No	No	No	No	Yes	No	No	No
<i>T.Pyrifor mis</i> toxicity	0.2 85	0.2 85	0.2 85	0.2 85	0.2 85	0.0 07	0.2 86	0.3 12	0.2 88	0.2 87	0.2 96	0.2 87	0.2 91	0.2 96	0.2 95	0.2 91	0.2 85	0.2 85	0.2 85	0.2 85	0.1 84	0.2 85	0.2 85	0.2 85	
Minnow toxicity	6.8 66	7.8 13	5.8 36	5.4 44	4.5 95	2.5 45	4.2 23	2.8 85	3.7 21	1.9 18	3.1 37	1.7 68	3.2 81	2.9 87	3.0 07	3.1 54	5.4 63	6.1 72	5.3 41	5.2 88	1.5 31	8.5 03	7.3 01	7.2 06	

Furthermore, Figure 4.2 illustrates 914 predicted targets of compounds act on multiple targets. In the network, the value of degree of freedom indicates the number of interactions between compounds and targets. Apocynin was found to have the largest number of potential targets with DoF = 320, followed by kaempferol, astragalín, picrosides and so on with DoF between 100-200. Ellagic acid had lesser interactive targets (DoF = 52) compared to others; however, number was quite good. Apocynin, kaempferol, astragalín, picroside-I, picroside-II, picroside-III, picroside-V, gallic acid, quercetin, rutin, verminoside, geniposidic acid, vernicoside, and aucubin interacted with at least 125 targets. These compounds have a vast variety of uses in treatment of various diseases (Table 4.3).

Table 4.3: Biological or Medicinal activity of compounds of *Picrorhiza kurroa*

Categories	Chemical classes	<i>Picrorhiza kurroa</i> Compounds	Common use/ Bioactivity	References
Picrosides	Iridoid Glycosides (monoterpenes)	Picroside-I (P-I)	Antioxidant	[332]
			Anti-cancer	[333]–[336]
			Hepatoprotective	[6], [45], [300], [337]–[339]
			Anti-inflammatory	[340]
			Neuroprotective	[341], [342]
		Picroside-II (P-II)	Anti-inflammatory	[343]–[350]
			Neuroprotective	[351]–[355]
			Hepatoprotective	[6], [339], [356]–[359]
			Cardio-protective	[360]
			Antioxidant	[361]–[367]
			Anti-apoptotic	[347]
		Picroside-III (P-III)	Anti-inflammatory	[350], [368]
			Hepatoprotective	[6], [301], [339], [357], [359], [369]
			Antihypoglycaemic	[370]
			Antimutagenic	[371]
Antispasmodic	[336]			
Picroside-IV (P-IV)	Anti-inflammatory	[350]		
Picroside-V (P-V)	Anti-inflammatory	[350]		
Bioenhancers	Carboxylic acids	Gallic acid (GA)	Antioxidant	[372]
			Bioenhancer	[327], [373]–[375]
	Glycosides	Ellagic acid (EA)	Antioxidant	[376]
			Hepatoprotective	[377]
			Antisteatotic	[376]
			Anticholestatic	[376]
			Antifibrogenic	[376]

			Anti-hepatocarcinogenic	[376]		
			Antiviral	[376]		
			Flavonoid	Kaempferol (KF)	Anti-cancer	[378], [379]
					Anti-tumor	[380], [381]
					Antioxidant	[380], [381]
					Anti-inflammatory	[380], [381]
					Cardioprotective	[380]
					Neuroprotective	[380]
			Quercetin (QC)	Antioxidant	[382]–[384]	
				Bioenhancer	[327], [374], [385]	
Anti-inflammatory	[386]					
Cucurbitacins	Terpenoids (triterpenes)	Cucurbitacin B (CB)	Anti-inflammatory	[387]		
			Antiproliferative	[388]		
			Anti-cancer	[389], [390]		
		Cucurbitacin D (CD)	Anti-inflammatory	[387]		
			Anti-tumor	[391]		
		Cucurbitacin E (CE)	Anti-inflammatory	[387]		
			Anti-tumor	[392]		
			Antiproliferative	[388]		
		Cucurbitacin F (CF)	Antihyperglycemic (Diabetes mellitus)	[393]		
		Cucurbitacin I (CI)	Anti-inflammatory	[387]		
		Cucurbitacin R (CR)	Hepatoprotective	[394], [395]		
			Anti-inflammatory	[396]		
Cucurbitacin P (CP)	Anti-dibetic	[387]				
Other active compounds for associated diseases	Iridoid Glycosides (monoterpenes)	Veronicoside (VN)	Anti-oxidant	[397]		
		Verminoside (VM)	Hepatoprotective	[397]		
			Anti-inflammatory	[398]		
			Anti-amoebic	[399]		
			Anti-hepatocarcinogenic	[397]		
			Anti-inflammatory	[398]		
			Anti-amoebic	[399]		
		Aucubin (AB)	Antiproliferative	[400]		
			Anti-inflammatory	[401]		
		Geniposidic acid (GCA)	Anti-tumor	[402]		
			Anti-inflammatory	[401], [403], [404]		
			Antidiabetic	[405], [406]		
			Hepatoprotective	[405]		
			Anti-cholestasis	[405]		
		Neuroprotective	[405]			

		Catalpol (CT)	Antioxidant	[407], [408]
			Anti-tumor	[402]
			Anti-alzheimer	[409]
			Anti-depressant	[409]
			Anti-diabetic	[409]
			Cardioprotective	[409]
	Phenolic Glycosides	Apocynin (AC)	Antioxidant	[410], [411]
			Neuroprotective	[412]
			Anti-inflammatory	[413], [414]
	Flavonoid	Rutin (RT)	Anti-alzheimer	[415]
			Anti-depressant	[416]
			Anti-diabetic	[417]
			Anti-arthritis	[418]
			Anti-hypercholesterolemic	[419]
Astragallic acid (AG)		Anti-inflammatory	[420]	
		Neuroprotective	[421]	
		Anti-obesity	[422]	
			Antioxidant	[423]

4.3.3.2.2. Noticeable role of bioenhancers in bioavailability of picrosides through compound -target network

Picrosides are the signature compounds of this herb which are reported for hepatoprotective activity in isolated form as well as crude extract and formulations. It was observed that bioavailability of picrosides is less in isolated form as compared to extract and formulations, the probable reason suggested in literature has been the occurrence of other metabolites in *Picrorhiza kurroa* extract that are likely to hinder the extensive metabolism of picroside-I and picroside-II probably by showing higher affinity with drug metabolizing enzymes. Moreover, due to validated report of antibacterial activity of *Picrorhiza kurroa* extract [152], [424], thereby presuming that additional compounds present in extract might show antibacterial activity against intestinal bacteria which are possibly responsible for metabolism of picrosides [48], [151], [152], [154], [157], [425]. The current study's findings corroborate this assertion, as quercetin, gallic acid, and ellagic acid, all identified as natural bioenhancers, are also found in *Picrorhiza kurroa*. These bioenhancers work as inhibitors of efflux transporter (P-gp) and CYP450 enzymes in intestinal epithelium and liver [373], [375], [426], [427]. In our study, quercetin, kaempferol, gallic acid and ellagic acid are categorized in Bioenhancer class, kaempferol is also a bioflavonoid, thus might have similar property

like that of quercetin and genistein. Figure 4.2 presents the Compound – Target network which has shown several interactions of bioenhancers with various isoforms of CYP450 enzymes as well as proteins of ABC family, thus in support of above argument it is clearly

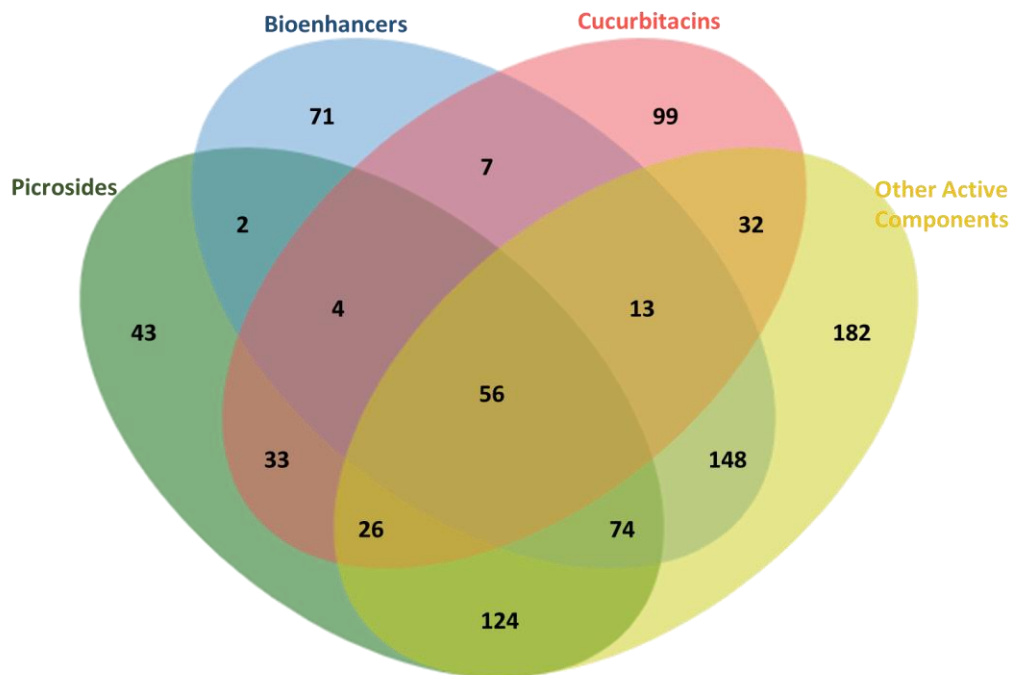


Figure 4.3: Venn diagram signifies the distribution of predicted targets according to corresponding compounds

suggested that these compounds play a critical role in enhancing the bioavailability of extracts. Apart from this, picroside-IV, and some of the cucurbitacins have been observed to interact with most significant drug metabolizing enzyme, CYP3A4, hence indicating the therapeutic efficacy of formulations based on picrosides. Moreover, Cucurbitacins and other active compounds are reported for various bioactivity and synergistic effects with drugs [398], [428]–[430]. Figure 4.2 and 4.3, clearly demonstrated the interaction of one compound with multiple targets and multiple compounds with common target, thus, several compounds of *Picrorhiza kurroa* may act on several targets to counteract NAFLD (Appendix Table A7). In a comparison of compound targets and NAFL/ NASH targets, 238 targets (Figure 4.1) were found to be potential in the mechanistic action of *Picrorhiza kurroa* in the treatment. These overlapping targets were considered for further study. In the above observations, the interactive behavior of compounds and targets indicates the significant role of these bioactive compounds of *Picrorhiza kurroa* in therapeutics.

4.3.3.3. Protein – Protein Interaction (PPI) network of shared targets

A total of 1692 targets of NAFLD/ NASH were provided to STRING and Protein-Protein interaction network was constructed with 1374 nodes and 5998 edges. After removing singletons, network of 946 nodes and 5998 edges was left. Thereafter, 238 interrelated targets of compounds and NAFLD/ NASH were used as prey to capture more interacting genes encoding protein targets to analyze the behavior of mechanism. Finally, a network was constructed in Cytoscape with a total of 532 nodes and 2268 edges then to explore the potential hubs, nodes with DoF > 4 (greater than half of the mean) were extracted to keep the precise data with additional targets. Eventually, a complete interactive network of targets was

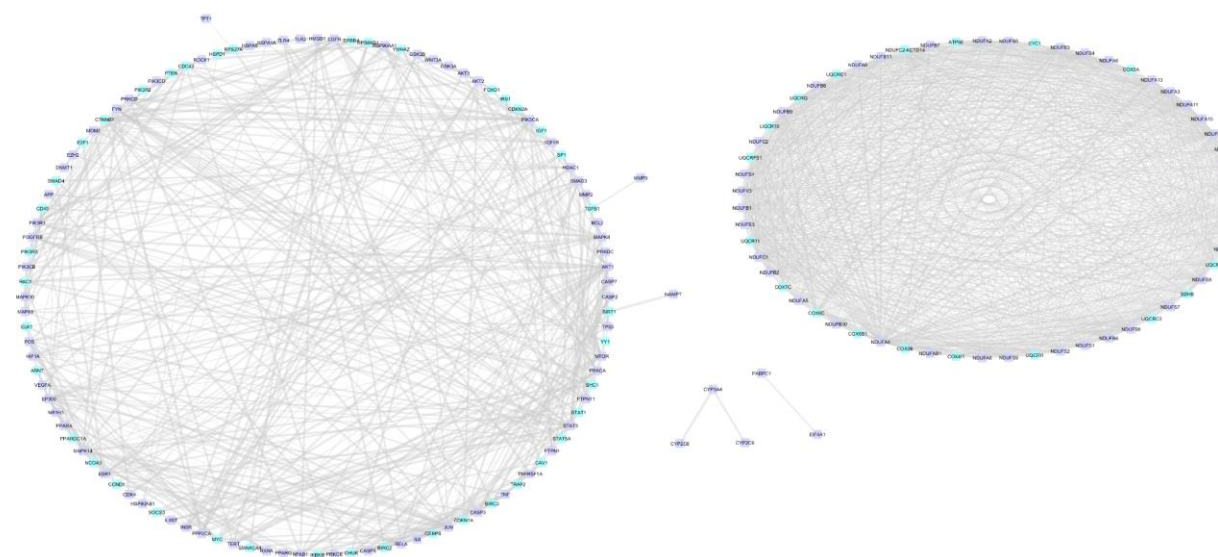


Figure 4.4: Interactive-Network of targets. Purple color nodes indicate the *P. kurroa* treating targets of NAFLD (shared targets) whereas, cyan color nodes indicate the additional interactive proteins came from Protein-Protein-Interaction Network

visualized in Cytoscape with 175 nodes and 1712 edges (Figure 4.4). In the network, two clusters were shown prominently; among them, the small subnetwork comprises 60 nodes from which 19 were interactive additional nodes came from PPI network and 41 nodes were potential gene encoding proteins of NAFL/ NASH targeted by bioactive compounds of *Picrorhiza kurroa*. This subnetwork comprised oxidoreductases namely NADH: ubiquinone oxidoreductase subunits, cytochrome c oxidase subunits (COX) and ubiquinol-cytochrome c reductase (UBQC) proteins. NADH: ubiquinone oxidoreductase subunits play an important role in stability of oxidative phosphorylation, degradation of subunits destabilise the oxidative phosphorylation resulting in impaired mitochondrial function, [431], [432], cyclooxygenases have been reported to play critical role in progression of disease towards

fibrosis and HCC [433]. On the other hand, another cluster comprised various types of targets involved in other associated diseases and signaling pathways, such as TGFB, NFKB, PIK3CA and its subunits, FOS, several Caspases. FOXO1, EGFR, PPARA, PPARG and many more. The additional interacting nodes from PPI and common nodes of NAFL/ NASH and compounds can be distinguished by color coding of nodes. Furthermore, three important isoforms of Cytochrome P450 were found interconnected indicating their role in metabolism of compounds in liver. In further study, involvement of these gene targets in pathways and their biological processes and molecular functions can be better understood by GO and KEGG enrichment analysis.

4.3.3.4. Gene Ontology and KEGG enrichment analysis of shortlisted targets

The shortlisted 175 gene targets were analyzed for GO and KEGG enrichment. A total of 667 GO terms were observed ($P < 0.05$), among them 490 belonged to Biological Process, 123 to Molecular Function and 53 to Cellular Components. As shown in Figure 4.5, In Biological Process (BP), potential targets were mainly involved in mitochondrial electron transportation, mitochondrial respiratory chain complex assembly, positive regulation of transcription by RNA polymerase II promoters, negative regulation of apoptotic process and so on. In Molecular Function (MF), potential targets were involved in NADH ubiquinone activity, enzyme binding, transcription factor binding, NADH dehydrogenase activity and so on. In the case of Cellular Components (CC), these potential shortlisted compounds were majorly involved in mitochondrial chain complexes, mitochondrial inner membrane, mitochondria, nucleoplasm, cytosol etc., consequently, overall observations were supporting the experimental literature. Koopman et al. (2007) has proposed mechanism i.e., reduction in activity of complex 1 enhances the ROS (reactive oxygen species) production which increases the mitochondrial fragmentation, disrupts the enzymatic activity involved in lipid metabolism and plays a vital role in CVD [434]. Similar findings have been observed in the current investigation with GO enrichment analysis, that few targets were critically involved in biological process, molecular functions and cellular process related to mitochondria namely “mitochondrial electron transport NADH to ubiquinone” and “complex 1 assembly process”, “NADH (ubiquinone) dehydrogenase activity”, “mitochondrial respiratory chain complex 1” respectively. Pérez-Carreras et al. (2003) observed the defective mitochondrial

respiratory chain complexes in liver of NASH patients as well as potential key player i.e., TNFA in mitochondrial dysfunction [432]. The results of network analysis depicted apocynin

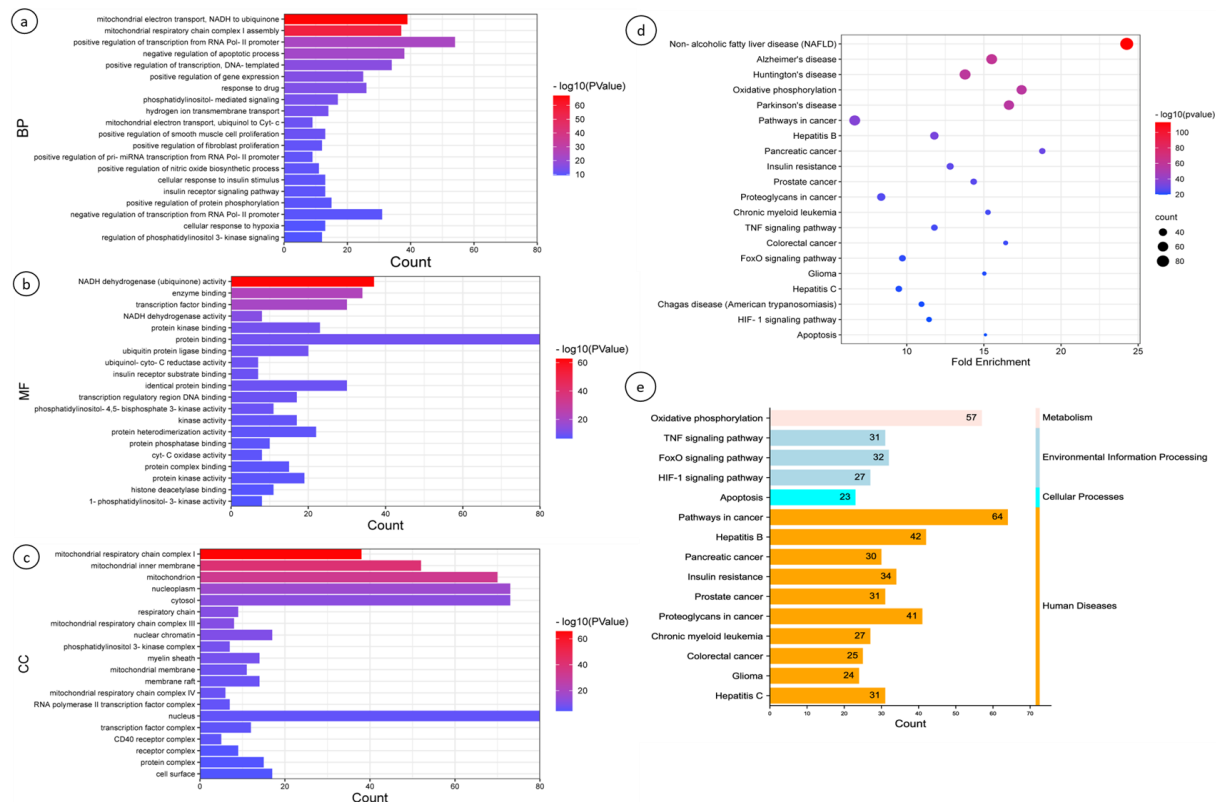


Figure 4.5: GO and KEGG enrichment analysis of shortlisted gene encoding targets involved in: (A) Biological Process, (B) Molecular Function (C) Cellular Component, (D&E) signaling and disease pathways. (A-D) represents the outcomes in color scales (according to different p-values) and the sizes of the dots represent the gene count of each term. (E) represents the distribution of targets in different pathways

and picoside-III interaction with all NDUFs in the network that are reported antioxidants, and work as superoxide dismutase, since the overproduction of ROS reduces the activity of antioxidant enzymes involved in maintaining the oxidative/ antioxidant balance in liver cell. Apocynin, as a NADPH oxidase inhibitor, reduces liver damage caused by excessive cholesterol intake in rats and also plays a significant role in reducing inflammation in the liver and adipose tissue and improving insulin resistance [435]–[437]. Picoside-II is also reported to reduce ROS production in NAFLD HepG2 model [356].

Furthermore, a total of 107 different pathways were observed based on p value < 0.05. Among them, top 20 pathways are presented in Figure 4.5, size of nodes represents the number of genes involved and fold enrichment indicates the coverage of target genes in all annotated genes of the pathways. The graph demonstrated, NAFLD pathway on top followed by some disease pathways including Alzheimer's disease, Huntington's disease and Hepatitis

B. Metabolic pathway was also observed for oxidative phosphorylation prominently with 57 gene targets. Apart from this, three signaling pathways including TNF signaling and FoxO signaling were noticed that might be crucial for diseases. The enrichment analysis suggested how the compounds of *Picrorhiza kurroa* play role in the therapeutics of NAFLD/ NASH. Therefore, the above-mentioned results indicate morbidities and mortality of NAFLD/ NASH.

4.3.3.5. Comprehensive Network (Compound – Target – Diseases – Pathways – Other associated diseases) Analysis

The network is shown in Figure 4.6, which comprises 240 nodes, including 174 target nodes (purple V-shaped), 20 nodes of pathways (cyan round rectangle), 20 nodes of related diseases (yellow diagonal), 24 nodes of active components (green circle) and 2 nodes of NAFLD and NASH (1 for each, red hexagon) and lines indicated connection between them. From the interpretation of network, it has been observed that 98 targets were controlled by multiple compounds of *Picrorhiza kurroa* and the compounds from iridoid glycoside, terpenoid and flavonoid classes namely, apocyanin, picroside-III, isoforms of cucurbitacin, kaempferol were regarded as more effective as they interacted with 57, 51, 18-25, 18 targets, respectively. However, all compounds were found to interact with at least 5 targets, which suggests that the compounds in the network were potentially effective and work in combination against

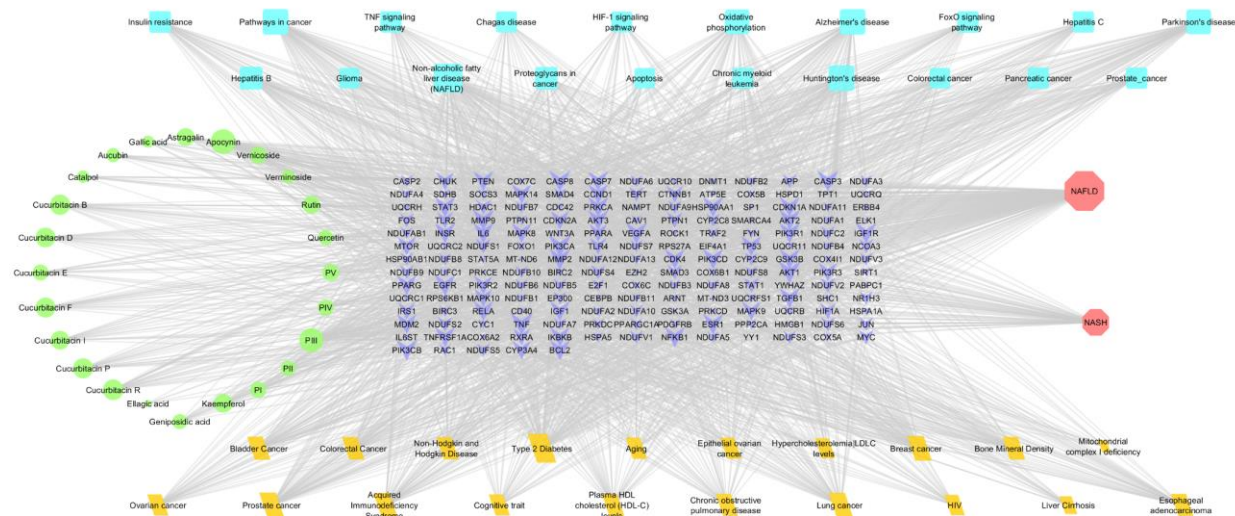


Figure 4.6: A comprehensive network of compound-disease-pathway-associated diseases. Color codes for all the nodes given in text, edges represent the interaction between all nodes whereas size of nodes indicate the number of interactions

each target involved in NAFLD/ NASH. Additionally, Cytochromes and their isoforms were found to interact with cucurbitacins (D, F, P), picroside-IV, astragaloside, kaempferol, quercetin, and rutin. Apart from this, 23 targets were involved in each pathway related to NAFLD/ NASH, and 89 targets were directly involved in NAFLD pathway whereas other targets in other related pathways. Besides, at least 11 targets were involved in each associated disease, where maximum 88 targets were of type 2 diabetes (T2D), several other targets were related to cancer, 17 were of Liver Cirrhosis, that addressed the comorbidities. Overall, the network analysis represented that all compounds interact to influence various diseases via influencing single and multiple targets. The top 15 targets, namely PIK3CA, TNF, AKT1, MMP9, CASP8, VEGFA, CASP3, MMP2, IGF1R, NFKB1, AKT2, EGFR, PIK3CB, IL6, and TP53, were regarded as hubs and all connected to compounds as well as implicated in various signaling and disease pathways displayed in the network.

4.3.4. *In silico* validation of potential candidates using molecular docking and molecular dynamics simulation

A total of ten genes encoding protein targets interacting with other targets, active components, associated disease and pathways, and which were directly involved in the NAFLD, and NASH pathways were considered for further study. The targets were namely, Interleukin-6 (IL6), serine/threonine protein kinase (AKT), Peroxisome proliferator-activated receptor gamma (PPARG), Peroxisome proliferator-activated receptor alpha (PPARA), Caspase-3 (CASP3), Caspase-8 (CASP8), Epidermal growth factor receptor (EGFR), Transforming growth factor beta-1 (TGFB), Tumor necrosis factor alpha (TNFA), Heat shock protein HSP 90-alpha (HSP90) (Figure 4.7). PPARA and PPARG are directly involved in NAFLD, PPARA agonists lower triglycerides and induce lipid clearance whereas PPARG agonists improve insulin resistance and T2DM. Therefore, various studies have shown that PPARA/G dual agonists can ameliorate lipid metabolism, reduce plasma triglycerides and can prevent cardiovascular complications and other metabolic disorders [438]. For now, Saroglitazar is the only dual agonist of PPARA and PPARG [439]. Furthermore, it was reported that TNFA and IL6 play critical role in development of NAFLD and insulin resistance through upregulation of key molecules associated with lipid metabolism, liver fibrosis and inflammation [440], [441]. In metabolic disorders,

inflammatory cytokine IL-6 and its signal transduction play a complex function in the progression of chronic inflammatory illnesses such as rheumatoid arthritis and inflammatory bowel disease [442]. In addition, recent study demonstrated a central role of TGFB1 in progression of NAFLD (via promoting hepatic stellate cells and extracellular matrix) and chronic liver condition and is regarded as a marker in fibrosis and HCC [443]. According to

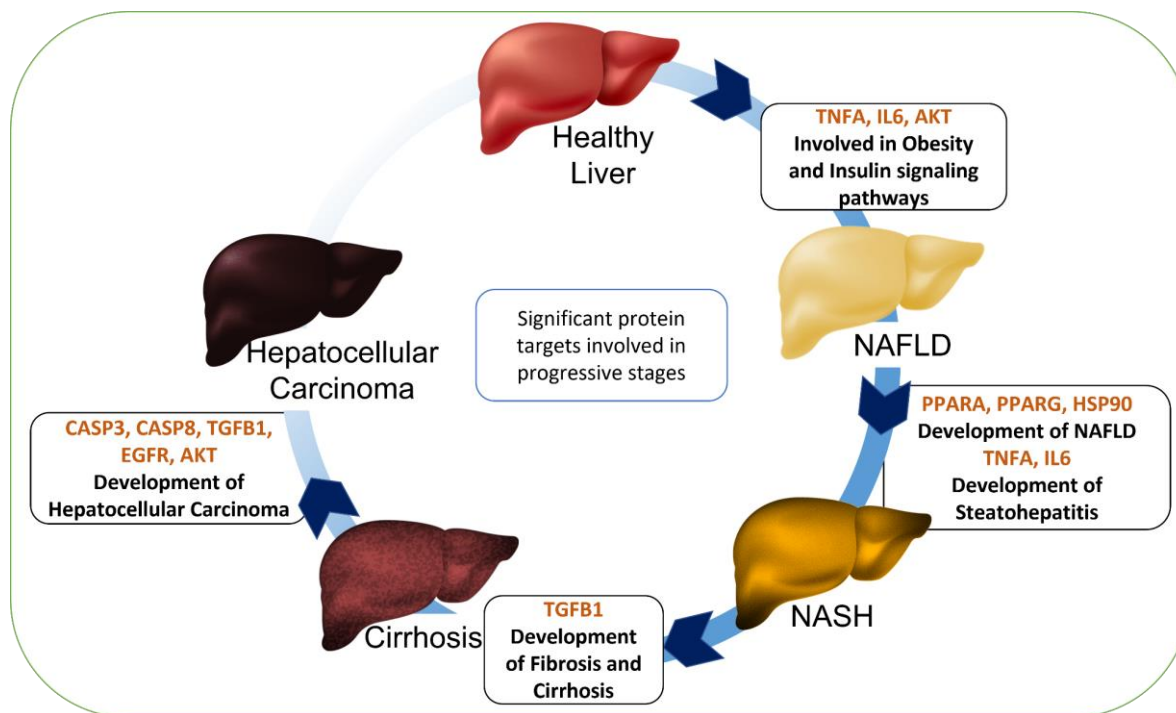


Figure 4.7: Mapping of critical protein targets to their role in corresponding progressive stages

reports, CASP3 inactivation ameliorates fibrogenesis in diet induced NASH model and inhibition of CASP8 reduces liver apoptosis, emeriscan (pancaspase inhibitor) supports the study by suppressing NAFLD [444]–[446]. Bhushan et al. (2019), suggested the inhibition of EGFR as a potential treatment strategy of NAFLD [447]. In a recent study, Adiponectin is observed to improve NAFLD via inhibition of Akt1/FoxO1 signaling [448]. HSP90 is reported as a potential therapeutic target in various types of diseases, including HCC and Hepatitis C, because of its regulation of different proinflammatory cytokines. Therefore, on the basis of therapeutic knowledge and current network analysis these chosen targets were subjected to docking simulation to check the binding with 24 active compounds of *Picrorhiza kurroa*. The protein structures were downloaded from RCSB PDB with the following corresponding ids IL6 (pdb id:1alu) [449], AKT (pdb id: 4ejn) [450], PPARG (pdb id: 2f4b) [451], PPARA (pdb id: 6lx8) [452], CASP3 (pdb id: 3kjf) [453], CASP8 (pdb id: 3kjn) [453],

EGFR (pdb id: 6tg0) [454], TGFB (pdb id: 3kfd) [455], TNFA (pdb id: 7jra) [456], HSP90 (pdb id: 5lnz) [457]. The grid was generated over the desired binding pocket reported for activity of respective proteins. The binding affinities and interactions of top five compounds

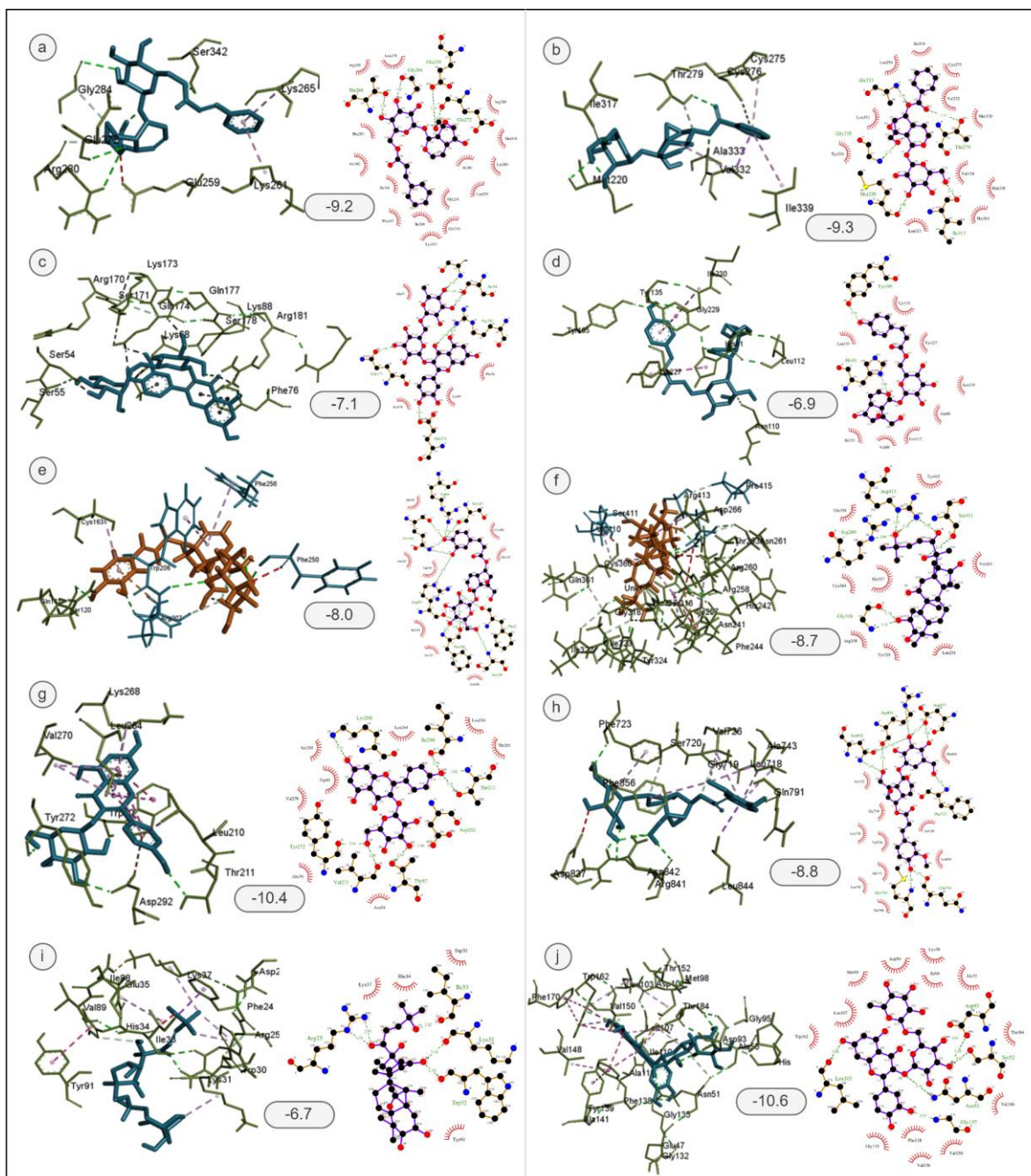


Figure 4.8: Interaction of potential compounds of *Picrorhiza kurroa* with putative targets in therapeutics of NAFLD/ NASH. Binding affinity of corresponding complex is mentioned in the center of individual figure. Left: 3D visualization and Right: 2D visualization of interaction (A) PPARG and Picroside-I complex (B) PPARA and Vernicoside complex (C) IL6 and Rutin complex (D) TNFA and Picroside-IV (E) CASP3 and Verminoside complex (F) CASP8 and Cucurbitacin I complex (G) AKT and Astragalin complex (H) EGFR and Picroside-III (I) TGFB and Cucurbitacin F (J) HSP90 and Rutin

with each target are displayed in Table 4.4. Figure 4.8 presents the detailed overview of the best compound docked in the active site pocket of corresponding target; the analysis is not only based on the docking score but also on interactions between the receptor and ligand. Picoside-I is considered best docked compound for PPARG with binding affinity -9.2 kcal/mol and four hydrogen bond (HB) interactions including Glu259 and 14 other interactions like hydrophobic, salt bridges and pi-pi stacking. Although, picoside-II and picoside-IV are also observed with good binding affinity, interacting with nearby residues in the pocket. Further, picoside-IV is also observed to have HB interaction with His91 and Tyr195 and hydrophobic interactions with various other residues including Leu133 and Tyr195 of TNFA. It can be concluded that picoside-I and picoside-IV had a good binding affinity with PPARG whereas vernicoside had with PPARA. All three compounds had interaction within same binding pocket as Saroglitazar [458]. The RMSD and RMSF of these complexes lie in the range. Hence, combination of these compounds might show similar dual-target mechanism. Moreover, cucurbitacin I and F bind in active site pocket of CASP8 and TGFB with binding affinity of -8.7 and -6.7 kcal/mol, respectively whereas vernicoside and verminoside bind in desired pocket of PPARA and CASP3 with binding affinity of -9.3 and -8.0 kcal/mol, respectively. Besides, picoside-III binds within the pocket of EGFR with a good number of hydrogen bonds and hydrophobic interaction including Arg841 and Thr790, astragalin binds with AKT through excellent binding affinity of -10.4 including active site residues like Thr211, Ile164, Val270, Tyr272. In addition to this, rutin is found to bind with HSP90 and IL6 both within the corresponding active pocket through binding affinity of -10.6 and -7.1. Aside from that, since the binding of prototype ligands is also examined, the tested compounds have superior binding and interactions with the respective targets (Figure 4.8). Overall, from the above observation it can be concluded that, multiple/ combination of compounds are affecting the targets which are directly involved in NAFLD/ NASH pathways as well as further progressive stages.

In the current study, 50 ns MD simulation of selected complexes from docking analysis has been performed to assess the stability and flexibility of complexes in biological system. MD trajectories were evaluated with the aid of Root-Mean Square Deviation (RMSD) and Root-Mean Square Fluctuations (RMSF). RMSD represents a total of atomic variations throughout

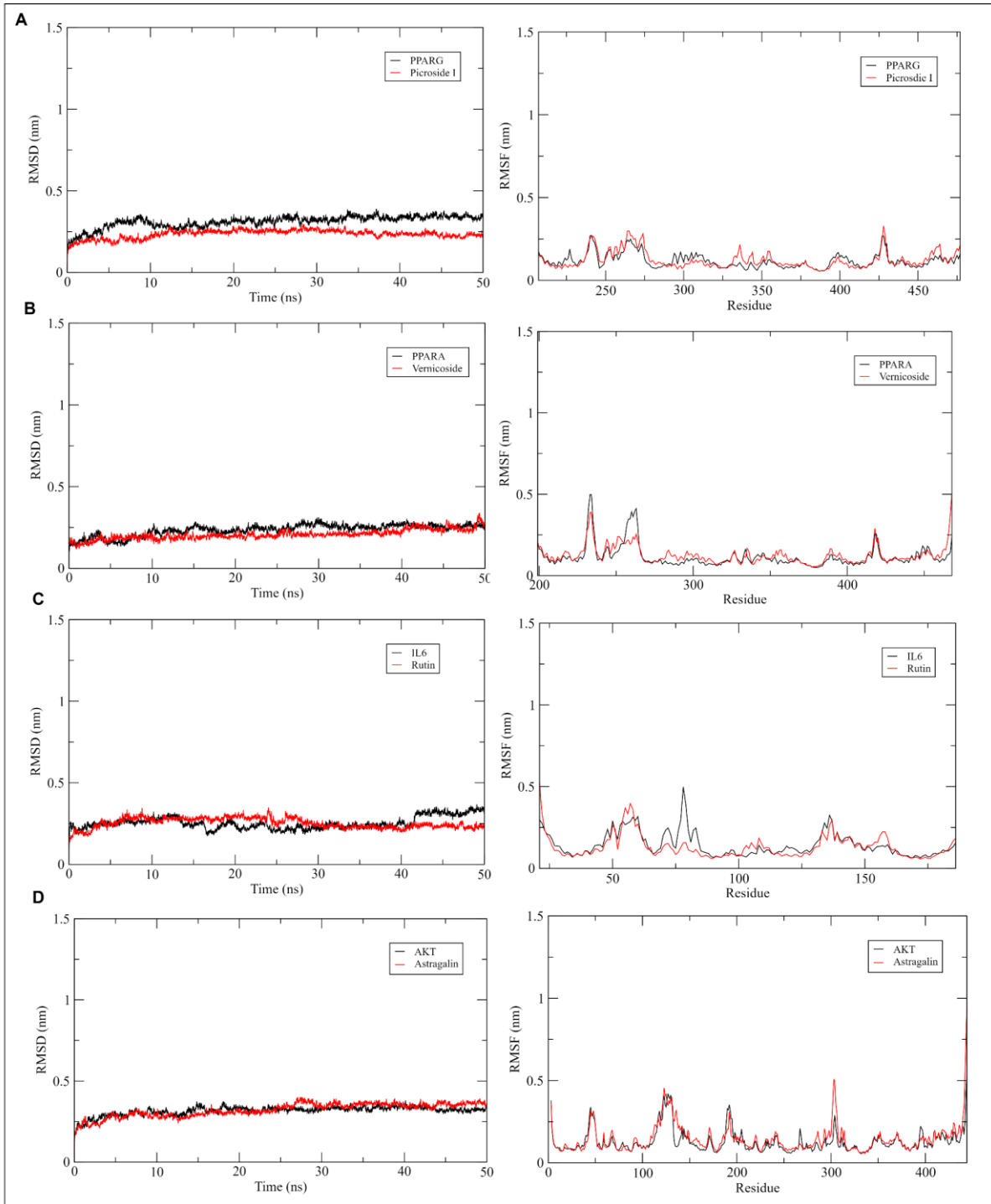
Table 4.4: Binding affinity and interactions of *Picrorhiza kurroa* compounds as well as reference compounds with their respective proteins

Targets	Refernce Compounds (BA)	Compounds	BA (kcal/mol)	Binding Pocket	H-bonds	Hydrophobic, pi-pi stacking, salt bridges
IL6	TLA (-4.5)	Cucurbitacin R	-7.6	Glu53, Arg42, Leu39, Arg40, Leu180, Arg184, Arg181, Ala182, Gln177, Ser178, Arg179, Gln175, Trp153, Leu167, Lys171	Glu95, Asn65	Pro67, Leu66, Thr145, Leu146, Val98
		Cucurbitacin E	-7.5		Asn65, Glu95, Thr140	Glu61, Leu66, Pro67, Tyr99, Thr140, Pro141, Asp142, Thr145,
		Cucurbitacin D	-7.4		Asn65, Glu95, Tyr99	Thr145, Asn146, Leu149, Val98, Pro141, Asp142
		Cucurbitacin I	-7.2		Glu108, Glu44, Arg106, Asp162, Gln158, Lys48	Thr45, Phe107, Thr165, Ser49, Ser109
		Rutin	-7.1		Ser54, Ser55, Arg181, Gln177, Glu174	Glu57, Ser178, Lys68, Phe76
PPARG	EHA (-7.3)	Picroside-I	-9.2	Ile249, Leu255, Glu259, Ile162, Arg280, Gly284, Cys285, Gln286, Arg288, Ser289, His323, Ile326, Tyr327, Leu330, Val339, Leu340, Ile341, Ser342, Met348, Phe363, Met364, His449, His465, Leu469, Tyr473	Glu259, Gly284, Thr268, Glu272	Phe247, Ile249, Leu255, Gly258, Lys261, Leu270, Arg280, Ile281, Arg288, Phe287, Ile341, Ser342, Gln345, Met348
		Picroside-IV	-9.1		Ser342, Lys265, Gln345, Thr268, Gly258	Phe247, Lys261, Glu259, Phe264, Ile267, Leu270, Ile341
		Kaempferol	-8.2		Thr268, Gln345	Phe247, Lys261, Ile262, His266, Lys265, Ile267, Leu270, Glu272, Ser342
		Ellagic acid	-8.3		Glu259, Glu272, Gln345, Thr268	Ile262, Lys265, His266, Ile267, Leu270, Arg280
		Picroside II	-7.9		Gln283, Met463, Asp462, Ser464, Leu465	Phe269, Lys275, Gln276, Gln286, Phe287, Val290, His466
CASP3	B92 (-6.7)	Cucurbitacin I	-8.9	Ser30, Asn33, Arg36, Arg64, Gly94, His121, Gly122, Gln161, Cys163, Ser205, Arg207	Glu248, Phe250	Cys163, Tyr204, Trp206, Arg207, Arg208, Ser249, Phe256
		Cucurbitacin P	-8.6		Ser205, Arg207, Phe250	His121, Cys163, Tyr204, Trp206, Asn208, Trp214, Glu248, Ser249, Ser251
		Cucurbitacin R	-8.5		Trp214, Asn208, Ser209, Arg207, Thr62	Trp206, His121, Ser249, Phe250, Ser251, Phe256
		Verminoside	-8		Arg64, Ser120, Gln161, Arg207, Phe250, Ser209, Phe256	His121, Ala162, Cys163, Ser205, Trp206, Asn208, Ser249, Ser251,
		Picroside V	-7.9		Arg64, Arg207	Thr62, Ser120, His121, Cys163, Tyr204, Ser205, Trp206, Phe250, Ser251, Phe252,

CASP8	B93 (-7.4)	Cucurbitacin I	-8.7	Lys224, Arg248, Asp285, Lys253, Leu254, His255, Ser256, Ile257, Arg258, Asp259, Arg260 , Leu315, His317, Gly318 , Asp319, Tyr324, Gln358 , Ala359, Cys360, Gly362, Cys409, Ser411 , Arg413	Arg413 , Arg260 , Gly318, Ser411	Leu254, Arg258, His317, Gln358 , Tyr324, Cys360, Val410, Tyr412
		Cucurbitacin B	-8.7		Ser411	Ile257, Arg258, His317, Gly318 , Tyr324, Cys360, Gly362, Asp363, Tyr412, Asn414, Arg413 , Trp420
		Cucurbitacin D	-8.5		Arg413 , Gly318 , Gly362	Leu254, Ile257, Arg258, His317, Asp319, Tyr324, Cys360, Asp363, Val410, Ser411 , Tyr412
		Cucurbitacin R	-8.5		Gly318 , Asp319, Tyr324, Arg413	Lys253, Leu254, Ile257, Arg258, His317, Cys360, Asp363, Val410, Tyr412
		Cucurbitacin P	-8.4		Asp259, Asn261, Arg413 , Ser411 , Gly318	Arg258, His317, Tyr324, Asp363, Val410, Tyr412, Pro415
EGFR	N78 (-8.2)	Cucurbitacin E	-8.9	Leu718, Gly724, Val726, Ala743, Lys745 , Met766, Cys775, Leu777, Leu788, Met790 , Met793 , Gly796 , Cys797 , Arg841 , Asn842, Leu844, Thr854 , Phe856	Phe723, Arg841 , Asn842, Gly857	Ala722, Cys797, Asp837, Phe856, Leu858
		Picroside-III	-8.8		Phe723, Gln791, Met793, Asp837, Arg841 , Asn842	Leu718, Gly719, Ser720, Ala722, Val726, Ala743, Thr790 , Leu792, Leu844, Phe856
		Cucurbitacin P	-8.4		Ser720, Asp837, Arg841	Leu718, Gly719, Gly721, Phe723, Asn842, Leu844, Phe856
		Cucurbitacin R	-8.3		Asp837, Arg841 , Asn842	Gly721, Ala722, Phe723, Cys797 , Phe856, Lys875, Val876, Pro877
		Verminoside	-8.3		Lys745, Asn842	Gly719, Phe723, Val726, Ala743, Cys775, Thr790, Arg841, Leu844, Phe850, Thr854, Phe856
AKT	OR4 (-10)	Astragalin	-10.4	Gln59, Leu78, Gln79, Trp80, Ile84 , Arg86, Leu202, Ser205, Leu210, Thr211 , Thr263, Leu264 , Val270 , Tyr272 , Glu278, Asn274, Ile288, Asp292, Cys296, Gly311, Glu322, Asp325	Thr82, Thr211 , Lys268, Val271, Tyr272 , Ile290, Asp292	Asn54, Gln79, Trp80, Ser205, Leu210, Leu264 , Val270 , Thr291,
		Ellagic acid	-10.1		Ser205, Thr211 , Ile290, Thr291	Trp80, Leu210, Leu264, Lys268, Val270 , Tyr272 , Asp292
		Verminoside	-10		Asn54, Gln79, His207, Tyr263, Val271, Tyr272	Trp80, Ser205, Arg206, Leu210, Thr211 , Leu264 , Val270 , Arg273, Asp274, Cys296, Asp292
		Picroside I	-9.7		Asn54, Gln79, Tyr272 , Arg273	Arg15, Gly16, Glu17, Trp80, Thr82, Ile84 , Glu85, Asp274, Asp292, Cys296
		Quercetin	-9.4		Gln79, Thr211 , Tyr272	Trp80, Leu210, Val270 , Val271, Asp292
PPARA	OLA (-4.6)	Veronicoside	-9.3	Asn219, Asn221, Ile241, Leu247, Ala250, Glu251, Leu254, Val255, Ile272, Cys275, Ser280 , Thr283, Glu286, Tyr314 , Ile317,	Ala333, Gly335, Met220, Thr279, Ile317	Leu254, Cys275, Thr283, Met320, Leu321 , Val332 , Val324, Met330, Leu331, Tyr334, Ile339,
		Cucurbitacin P	-7.9		Arg434, Glu315, Arg388, Tyr311, Asp466	Asp387, Pro389, Val437, Met467, Tyr468

		Cucurbitacin D	-7.7	Phe318, Met320, Leu321 , Val324, Met330, Val332 , Gly335, Ile339, Ile354, Met355, His440 , Val444 Tyr464	Thr200, Lys204, Ser414	Leu203, Ala207, Lys208, Tyr211, Ser373, His411
		Cucurbitacin I	-7.5		Ser373, Asn415, Asp374, His411, Lys204	Ala207, Lys208, Tyr211, Val407, Leu410, Ser414
		Picroside-III	-7		Tyr311, Arg388, Glu315, Met467	Arg434, Val437, Thr438, Gln445, Tyr468
TNFA	VGY (-6.1)	Rutin	-7.3	Leu133 , Tyr135 , Tyr195 , Gly197, Val199, Ile231, Ala232, Leu233	Lys141, Leu218, Asp219	Glu99, Gly100, Pro215, Asp216, Tyr217, Phe220
		Cucurbitacin R	-7		Phe220, Leu218	Glu99, Lys141, Gly142, Gln143, Asp216, Tyr217, Asp219, Ala221
		Picroside-IV	-6.9		His91, Tyr195	Val89, Ala90, Asn110, Leu112, Leu133 , Tyr135 , Tyr227, Ile231
		Quercetin	-6.9		Gly100, Leu218, Asp219, Phe220, Ala221	Glu99, Asp216
		Cucurbitacin I	-6.7		His91, Tyr135	Lys87, Val89, Ala90, Ile231, Ala232
HSP90	70Z (-9.7)	Rutin	-10.6	Asn51 , Ala55 , Lys58 , Val92, Asp93 , Gly95, Ile96 , Met98 , Ala101, Leu107, Ile110, Gly132, Gly135, Val136, Phe138 , Tyr139, Val150, His154, Ala161, Ile170, Thr184 , Lys185	Asn51 , Ser52, Leu103, Gly137	Asp54, Ala55 , Lys58 , Ile96 , Met98 , Leu107, Gly135, Val136, Phe138 , Val150, Trp162, Thr184 , Val186
		Astragalins	-9.5		Asn51 , Ser52, Asp93	Ala55 , Met98 , Leu107, Gly135, Phe138 , Val150, Trp162, Thr184 , Val186
		Picroside I	-9.3		Asn51 , Gly97, Phe138 , Thr184	Asp54, Ala55 , Ile96 , Met98 , Leu107, Val150, Trp162, Val186
		Cucurbitacin F	-9		Met98, Gly135, Tyr139	Asn51 , Asp54, Ala55 , Lys58 , Ile96, Leu107, Ala111, Val136, Phe138
		Quercetin	-9		Leu48, Ser52, Asp93 , Gly135	Asn51 , Met98 , Val136, Phe138 , Tyr139, Thr184 , Val186
TGFB	metformin (-4.6)	Rutin	-7	Tyr21, Arg25 , Lys26, Trp30 , Lys31, Trp32 , Ile33, His34 , Val89, Tyr90 , Tyr91 , Val92, Gly93 , Arg94 , Pro96, Leu101	Arg25 , Trp30 , Lys31, Ile33, Glu35, Lys37	Asp23, Phe24, Trp32 , His34
		Cucurbitacin D	-7		Tyr39, Ala41, Asn103, Met104	Leu28, Asn42, Phe43, Cys44, Val79, Pro80, Ile105, Val106,
		Cucurbitacin P	-6.9		Tyr39, Ala41, Cys44	Leu20, Ile22, Leu28, Trp30 , Phe43, Cys78, Pro80, Met104, Val106
		Cucurbitacin F	-6.7		Arg25 , Lys31, Trp32 , Ile33	Trp30 , His34 , Lys37, Tyr91
		Cucurbitacin I	-6.5		Lys31, Trp32 , Ile33, Tyr91	Arg25 , His34 , Trp30

50 ns simulation between the current conformation and desired conformation, which is a crucial basis for determining the system's stability, whereas RMSF represents the flexibility of protein residues by measuring the average deviation of the particle from the reference position during the course of the simulation. As shown in Figure 4.9, all the systems get equilibrated after 20 ns except IL6-Rutin which is equilibrated at 30 ns and TGFβ-Cucurbitacin F which encounters high fluctuations, however it was also within the range. Moreover, all the bound complexes showed average RMSD less than 0.32 nm. The average RMSD of all native proteins was observed in the range of 0.22 – 0.42 nm; however, the average RMSD of bound complexes was observed in the range of 0.20 – 0.32 nm. It is apparent from the figures that all systems remained almost stable throughout the simulation with slight deviation for a little time except TGFβ – Cucurbitacin F which exhibit average RMSD of 0.32 nm, however, it showed small deviations within the range. Further analysis of RMSF of complexes and apo-proteins showed that residue fluctuations are in acceptable range, with average RMSF between 0.12 – 0.17 nm for all complexes which is little bit higher than native proteins at some residues indicating the flexibility of native protein after binding with compounds. Thus, ligand binding has had a considerable impact on residue fluctuation. The results revealed that all complexes exhibit low RMSD and RMSF, hence can be considered stable complexes.



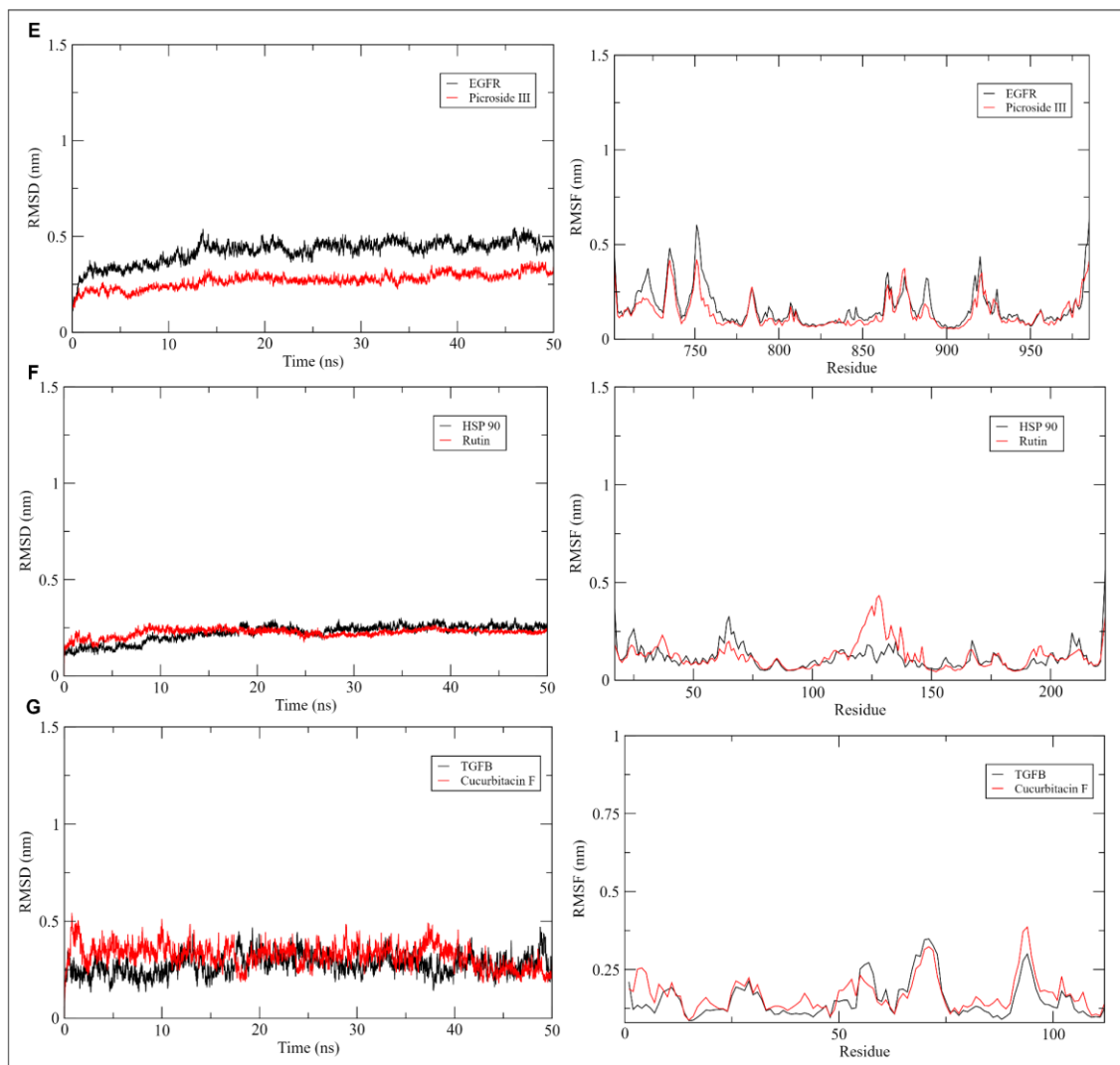


Figure 4.9: Molecular dynamics simulation analysis. RMSD and RMSF profile of apo-proteins and respective complexes. Apo-protein is represented in black and complexes in red color lines.

4.4. CONCLUSIONS

This study was set out to determine the mechanism of *Picrorhiza kurroa* compounds reported in extracts for the treatment of NAFLD/ NASH using comprehensive network pharmacology. The findings revealed that phytochemicals might have pharmacological effects in NAFLD via multi-component-multi-target mechanism by regulating various pathways, including liver apoptosis, inflammation, drug metabolism and so on. Briefly, picroside-I and Vernicoside have been observed as potential agonists of PPARG and PPARA whereas, picroside-III, Astragaloside and Cucurbitacin F as potential inhibitors of EGFR, AKT, and

TGFB, respectively. Rutin is observed to inhibit putatively both IL6 and HSP90. Furthermore, the study revealed synergistic action of compounds in addressing comorbidities of disease. However, this study had limitations as the compound and target information was retrieved from the databases, which might be different from actual biological system. To corroborate results, additional experimental verification and clinical trials can provide functional leads as potential therapeutics for complex diseases of NAFLD/ NASH.

CHAPTER 5
CONCLUSIONS AND FUTURE PROSPECTS

5.1. CONCLUSIONS

In present investigation, the aim was to map phytochemicals from extracts of different plant species into potential leads. Towards this, two types of studies were carried out to resolve the critical issue in two diseases, COVID-19 and NAFLD. The study explored phytochemicals from essential oils and aromatic plant species as well as from a medicinal herb, *Picrorhiza kurroa* known for its hepatoprotective activity using different approaches of computational drug discovery. The shortlisted compounds can be potential leads to consider for drug development.

- The selected essential oils compounds can be putative compounds for nasal therapy since nasal route is the main entry route of SARS-CoV-2 as well as due to the inherent property of the EO compounds to travel longer distances via air.
- The SARS-COV-2 receptor also exists in brain that is why brain disorders were also noticed among some patients during covid, the essential oil compounds can possibly reach to brain through olfactory lobes.
- On the other hand, the study of *Picrorhiza kurroa* compounds revealed combinatorial effect on targets via multi-component-multi-target mechanism by regulating various pathways, including liver apoptosis, inflammation, drug metabolism.
- Furthermore, the study revealed synergistic action of compounds in herbal extracts of *Picrorhiza kurroa*, thereby addressing comorbidities of disease.

5.2. FUTURE PROSPECTS

This research will serve as a base for future *in-vitro* and *in-vivo* studies. These findings provide the following insights for future research:

- Further experimental validation and clinical trials are required to corroborate the results towards development of novel drugs for treatment of above-mentioned diseases.
- Similar strategy can be applied to address the complexities of other complicated diseases.

- The selected hubs and interacting components can be used to develop biomarkers for each development stages of NAFLD/ NASH.
- The similar pharmacophore or chemical entities with shortlisted compounds can be used to develop new drugs via ligand-based drug discovery and fragment-based drug discovery.

REFERENCES

- [1] D. S. Fabricant and N. R. Farnsworth, “The value of plants used in traditional medicine for drug discovery”, *Environ. Health Perspect.*, vol. 109, no. suppl 1, pp. 69–75, 2001.
- [2] A. G. Atanasov et al., “Natural products in drug discovery: advances and opportunities”, *Nat. Rev. Drug Discov.* 2021 203, vol. 20, no. 3, pp. 200–216, Jan. 2021.
- [3] I. Banjari et al., “Antidiabetic Effects of Aronia melanocarpa and Its Other Therapeutic Properties”, *Front. Nutr.*, vol. 4, no. 1, p. 53, Nov. 2017.
- [4] N. E. Thomford et al., “African Lettuce (*Launaea taraxacifolia*) Displays Possible Anticancer Effects and Herb-Drug Interaction Potential by CYP1A2, CYP2C9, and CYP2C19 Inhibition”, *OMICS*, vol. 20, no. 9, pp. 528–537, Sep. 2016.
- [5] S. Ji et al., “Antioxidant effect of aqueous extract of four plants with therapeutic potential on gynecological diseases; Semen persicae, Leonurus cardiaca, Hedyotis diffusa, and Curcuma zedoaria”, *Eur. J. Med. Res.*, vol. 22, no. 1, pp. 1–8, Nov. 2017.
- [6] Y. Dwivedi, R. Rastogi, N. K. Garg, and B. N. Dhawan, “Picroliv and its Components Kutkoside and Picroside I Protect Liver Against Galactosamine-Induced Damage in Rats”, *Pharmacol. Toxicol.*, vol. 71, no. 5, pp. 383–387, 1992.
- [7] D. J. Newman and G. M. Cragg, “Natural Products as Sources of New Drugs over the Nearly Four Decades from 01/1981 to 09/2019”, *J. Nat. Prod.*, vol. 83, no. 3, pp. 770–803, Mar. 2020.
- [8] E. Patridge, P. Gareiss, M. S. Kinch, and D. Hoyer, “An analysis of FDA-approved drugs: natural products and their derivatives”, *Drug Discov. Today*, vol. 21, no. 2, pp. 204–207, 2016.
- [9] H. Kiyohara, T. Matsumoto, and H. Yamada, “Combination Effects of Herbs in a Multi-herbal Formula: Expression of Juzen-taiho-to’s Immuno-modulatory Activity on the Intestinal Immune System”, *Evid. Based. Complement. Alternat. Med.*, vol. 1, no. 1, p. 91, 2004.

- [10] M. Leonti and R. Verpoorte, “Traditional Mediterranean and European herbal medicines”, *J. Ethnopharmacol.*, vol. 199, pp. 161–167, Mar. 2017.
- [11] D. A. Dias, S. Urban, and U. Roessner, “A Historical overview of natural products in drug discovery”, *Metabolites*, vol. 2, no. 2, pp. 303–336, 2012.
- [12] Y. Tu, “The discovery of artemisinin (qinghaosu) and gifts from Chinese medicine”, *Nat. Med.*, vol. 17, no. 10, pp. 1217–1220, Oct. 2011.
- [13] C. M. Song, S. J. Lim, and J. C. Tong, “Recent advances in computer-aided drug design”, *Brief. Bioinform.*, vol. 10, no. 5, pp. 579–591, Sep. 2009.
- [14] J. A. DiMasi, R. W. Hansen, and H. G. Grabowski, “The price of innovation: new estimates of drug development costs”, *J. Health Econ.*, vol. 22, no. 2, pp. 151–185, 2003.
- [15] N. E. Thomford et al., “Natural products for drug discovery in the 21st century: Innovations for novel drug discovery”, *Int. J. Mol. Sci.*, vol. 19, no. 6, 2018.
- [16] D. J. Newman, “Natural products as leads to potential drugs: An old process or the new hope for drug discovery?”, *J. Med. Chem.*, vol. 51, no. 9, pp. 2589–2599, May 2008.
- [17] A. L. Harvey, R. Edrada-Ebel, and R. J. Quinn, “The re-emergence of natural products for drug discovery in the genomics era”, *Nat. Rev. Drug Discov.*, vol. 14, no. 2, pp. 111–129, 2015.
- [18] C. L. Hung and C. C. Chen, “Computational approaches for drug discovery”, *Drug Dev. Res.*, vol. 75, no. 6, pp. 412–418, 2014.
- [19] W. Yu and A. D. Mackerell, “Computer-Aided Drug Design Methods”, *Methods Mol. Biol.*, vol. 1520, p. 106, 2017.
- [20] T. Pantsar and A. Poso, “Binding Affinity via Docking: Fact and Fiction”, *Mol. A J. Synth. Chem. Nat. Prod. Chem.*, vol. 23, no. 8, p. 1899, 2018.

- [21] O. Trott and A. J. Olson, "AutoDock Vina: Improving the speed and accuracy of docking with a new scoring function, efficient optimization, and multithreading", *J. Comput. Chem.*, 2009.
- [22] M. Karplus and J. A. McCammon, "Molecular dynamics simulations of biomolecules", *Nat. Struct. Biol.* 2002 99, vol. 9, no. 9, pp. 646–652, 2002.
- [23] S. J. Y. Macalino, V. Gosu, S. Hong, and S. Choi, "Role of computer-aided drug design in modern drug discovery", *Arch. Pharm. Res.*, vol. 38, no. 9, pp. 1686–1701, Sep. 2015.
- [24] W. Duch, K. Swaminathan, and J. Meller, "Artificial intelligence approaches for rational drug design and discovery", *Curr. Pharm. Des.*, vol. 13, no. 14, pp. 1497–1508, May 2007.
- [25] M. Hassan Baig et al., "Computer Aided Drug Design: Success and Limitations", *Curr. Pharm. Des.*, vol. 22, no. 5, pp. 572–581, Jan. 2016.
- [26] A. A. Sayampanathan, C. S. Heng, P. H. Pin, J. Pang, T. Y. Leong, and V. J. Lee, "Infectivity of asymptomatic versus symptomatic COVID-19", *Lancet*, vol. 397, no. 10269, pp. 93–94, 2021.
- [27] C. A. Devaux, J. M. Rolain, P. Colson, and D. Raoult, "New insights on the antiviral effects of chloroquine against coronavirus: what to expect for COVID-19?", *Int. J. Antimicrob. Agents*, vol. 55, no. 5, p. 105938, 2020.
- [28] B. Shah, P. Modi, and S. R. Sagar, "In silico studies on therapeutic agents for COVID-19: Drug repurposing approach", *Life Sci.*, vol. 262, no. 1, p. 117652, 2020.
- [29] M. M. A. K. Shawan, S. K. Halder, and M. A. Hasan, "Luteolin and abyssinone II as potential inhibitors of SARS-CoV-2: an in silico molecular modeling approach in battling the COVID-19 outbreak", *Bull. Natl. Res. Cent.*, vol. 45, no. 1, p. 27, 2021.
- [30] V. K. Bhardwaj, R. Singh, J. Sharma, V. Rajendran, R. Purohit, and S. Kumar, "Bioactive Molecules of Tea as Potential Inhibitors for RNA-Dependent RNA Polymerase of SARS-CoV-2", *Front. Med.*, vol. 8, no. 1, p. 684020, 2021.

- [31] V. K. Bhardwaj, R. Singh, P. Das, and R. Purohit, "Evaluation of acridinedione analogs as potential SARS-CoV-2 main protease inhibitors and their comparison with repurposed anti-viral drugs", *Comput. Biol. Med.*, vol. 128, no. 1, p. 104117, 2021.
- [32] J. K. R. da Silva, P. L. B. Figueiredo, K. G. Byler, and W. N. Setzer, "Essential oils as antiviral agents. Potential of essential oils to treat sars-cov-2 infection: An in-silico investigation", *Int. J. Mol. Sci.*, vol. 21, no. 10, 2020.
- [33] W. Sungnak et al., "SARS-CoV-2 entry factors are highly expressed in nasal epithelial cells together with innate immune genes", *Nat. Med.*, vol. 26, no. 5, pp. 681–687, 2020.
- [34] W. Dhifi, S. Bellili, S. Jazi, N. Bahloul, and W. Mnif, "Essential Oils' Chemical Characterization and Investigation of Some Biological Activities: A Critical Review", *Medicines*, vol. 3, no. 4, p. 25, Sep. 2016.
- [35] M. Moghaddam and L. Mehdizadeh, "Chemistry of Essential Oils and Factors Influencing Their Constituents", in *Soft Chemistry and Food Fermentation*, pp. 379–419, 2017.
- [36] G. Horváth and K. Ács, "Essential oils in the treatment of respiratory tract diseases highlighting their role in bacterial infections and their anti-inflammatory action: a review", *Flavour Fragr. J.*, vol. 30, no. 5, p. 341, Sep. 2015.
- [37] S. Bittmann, "COVID-19: Expression of ACE2-receptors in the Brain Suggest Neurotropic Damage", *J. Regen. Biol. Med.*, vol. 2, no. 3, p. 027, 2020.
- [38] Y. C. Li, W. Z. Bai, and T. Hashikawa, "The neuroinvasive potential of SARS-CoV2 may play a role in the respiratory failure of COVID-19 patients", *J. Med. Virol.*, vol. 92, no. 6, pp. 552–555, 2020.
- [39] S. K. Asrani, H. Devarbhavi, J. Eaton, and P. S. Kamath, "Burden of liver diseases in the world", *J. Hepatol.*, vol. 70, no. 1, pp. 151–171, Jan. 2019.
- [40] X. Ge, L. Zheng, M. Wang, Y. Du, and J. Jiang, "Prevalence trends in non-alcoholic fatty liver disease at the global, regional and national levels, 1990–2017: a

- population-based observational study”, *BMJ Open*, vol. 10, no. 8, p. e036663, Aug. 2020.
- [41] C. D. Byrne and G. Targher, “Review NAFLD: A multisystem disease”, *J. Hepatol.*, vol. 62, no. 1, pp. S47–S64, 2015.
- [42] Y. Xu et al., “Herbal Medicine in the Treatment of Non-Alcoholic Fatty Liver Diseases-Efficacy, Action Mechanism, and Clinical Application”, *Front. Pharmacol.*, vol. 11, no. 1, p. 601, 2020.
- [43] X. X. Yang et al., “Mitochondrial metabolomic profiling for elucidating the alleviating potential of *Polygonatum kingianum* against high-fat diet-induced nonalcoholic fatty liver disease”, *World J. Gastroenterol.*, vol. 25, no. 43, pp. 6404–6415, Nov. 2019.
- [44] H. Dhama-Shah et al., “Intervention by picroside II on FFAs induced lipid accumulation and lipotoxicity in HepG2 cells”, *J. Ayurveda Integr. Med.*, vol. 12, no. 3, pp. 465–473, 2021.
- [45] S. N. Shetty, S. Mengi, R. Vaidya, and A. D. B. Vaidya, “A study of standardized extracts of *Picrorhiza kurroa* Royle ex Benth in experimental nonalcoholic fatty liver disease”, *J. Ayurveda Integr. Med.*, vol. 1, no. 3, pp. 203–210, 2010.
- [46] S. Sinha, J. Bhat, M. Joshi, V. Sinkar, and S. Ghaskadbi, “Hepatoprotective activity of *Picrorhiza kurroa* Royle Ex. Benth extract against alcohol cytotoxicity in mouse liver slice culture”, *Int. J. Green Pharm.*, vol. 5, no. 3, pp. 244–253, 2011.
- [47] A. Raut et al., “*Picrorhiza kurroa*, Royle ex Benth: Traditional uses, phytopharmacology, and translational potential in therapy of fatty liver disease”, *J. Ayurveda Integr. Med.*, p. 100558, Jun. 2022.
- [48] D. Upadhyay, S. Anandjiwala, H. Padh, and M. Nivsarkar, “In vitro - In vivo metabolism and pharmacokinetics of picroside i and II using LC-ESI-MS method”, *Chem. Biol. Interact.*, vol. 254, pp. 83–92, 2016.
- [49] N. R. Farnsworth, O. Akerele, A. S. Bingel, D. D. Soejarto, and Z. Guo, “Medicinal plants in therapy”, *Bull. World Health Organ.*, vol. 63, no. 6, p. 981, 1985.

- [50] M. Lahlou, “The Success of Natural Products in Drug Discovery”, *Pharmacol. Pharm.*, vol. 4, pp. 17–31, 2013, doi: 10.4236/pp.2013.43A003.
- [51] G. M. Cragg and D. J. Newman, “Natural products: a continuing source of novel drug leads.”, *Biochim. Biophys. Acta*, vol. 1830, no. 6, pp. 3670–3695, Jun. 2013.
- [52] C. Katiyar, A. Gupta, S. Kanjilal, and S. Katiyar, “Drug discovery from plant sources: An integrated approach”, vol. 33, no. 1, 2012.
- [53] M. Fitzgerald, M. Heinrich, and A. Booker, “Medicinal plant analysis: A historical and regional discussion of emergent complex techniques”, *Front. Pharmacol.*, vol. 10, p. 1480, 2019.
- [54] A. D. Kinghorn, L. Pan, J. N. Fletcher, and H. Chai, “The relevance of higher plants in lead compound discovery programs”, *J. Nat. Prod.*, vol. 74, no. 6, pp. 1539–1555, Jun. 2011.
- [55] G. M. Cragg and D. J. Newman, “Biodiversity: A continuing source of novel drug leads”, *Pure Appl. Chem.*, vol. 77, no. 1, pp. 7–24, Jan. 2005.
- [56] J. K. Borchardt, “The Beginnings of Drug Therapy: Ancient Mesopotamian Medicine”, *Drug News Perspect.*, vol. 15, no. 3, p. 192, 2002.
- [57] S. Dev, “Ancient-modern concordance in Ayurvedic plants: some examples.”, *Environ. Health Perspect.*, vol. 107, no. 10, p. 789, 1999.
- [58] G. M. Cragg and D. J. Newman, “Plants as a source of anti-cancer agents”, *J. Ethnopharmacol.*, vol. 100, no. 1–2, pp. 72–79, 2005.
- [59] D. J. Newman and G. M. Cragg, “Natural Products as Sources of New Drugs from 1981 to 2014”, *J. Nat. Prod.*, vol. 79, no. 3, pp. 629–661, 2016.
- [60] M. A. Ashraf, “Phytochemicals as Potential Anticancer Drugs: Time to Ponder Nature’s Bounty”, *Biomed Res. Int.*, vol. 2020, pp. 1–7, 2020.
- [61] D. L. Klayman, “Qinghaosu (artemisinin): An antimalarial drug from China”, *Science*, vol. 228, no. 4703, pp. 1049–1055, 1985.

- [62] P. M. O'Neill and G. H. Posner, "A medicinal chemistry perspective on artemisinin and related endoperoxides", *J. Med. Chem.*, vol. 47, no. 12, pp. 2945–2964, Jun. 2004.
- [63] P. M. O'Neill, V. E. Barton, and S. A. Ward, "The molecular mechanism of action of artemisinin--the debate continues", *Molecules*, vol. 15, no. 3, pp. 1705–1721, Mar. 2010.
- [64] J. Wang et al., "Artemisinin directly targets malarial mitochondria through its specific mitochondrial activation", *PLoS One*, vol. 5, no. 3, p. e9582, Mar. 2010.
- [65] N. H. Oberlies and D. J. Kroll, "Camptothecin and Taxol: Historic Achievements in Natural Products Research", *J. Nat. Prod.*, vol. 67, no. 2, pp. 129–135, Feb. 2004.
- [66] P. D. Senter, "Potent antibody drug conjugates for cancer therapy", *Curr. Opin. Chem. Biol.*, vol. 13, no. 3, pp. 235–244, Jun. 2009.
- [67] P. B. Schiff and S. B. Horwitz, "Taxol stabilizes microtubules in mouse fibroblast cells", *Proc. Natl. Acad. Sci. U. S. A.*, vol. 77, no. 3, pp. 1561–1565, 1980.
- [68] L. Müller-Kuhrt, "Putting nature back into drug discovery", *Nat. Biotechnol.*, vol. 21, no. 6, pp. 602–602, Jun. 2003.
- [69] M. L. Lee and G. Schneider, "Scaffold architecture and pharmacophoric properties of natural products and trade drugs: Application in the design of natural product-based combinatorial libraries", *J. Comb. Chem.*, vol. 3, no. 3, pp. 284–289, May 2001.
- [70] T. Henkel, Brunne M. Roger, H. Muller, and F. Reichel, "Statistical Investigation into the Structural Complementarity of Natural Products and Synthetic Compounds - PubMed", *Angew. Chemie Int. Ed. English*, vol. 38, no. 5, pp. 643–647, 1999, Accessed: Jul. 09, 2022.
- [71] M. Feher and J. M. Schmidt, "Property Distributions: Differences between Drugs, Natural Products, and Molecules from Combinatorial Chemistry", *J. Chem. Inf. Comput. Sci.*, vol. 43, no. 1, pp. 218–227, Jan. 2003.

- [72] G. A. Cordell, "Sustainable medicines and global health care", *Planta Med.*, vol. 77, no. 11, pp. 1129–1138, 2011.
- [73] A. G. Atanasov et al., "Discovery and resupply of pharmacologically active plant-derived natural products: A review", *Biotechnol. Adv.*, vol. 33, no. 8, pp. 1582–1614, 2015.
- [74] M. S. Butler, "The role of natural product chemistry in drug discovery", *J. Nat. Prod.*, vol. 67, no. 12, pp. 2141–2153, Dec. 2004.
- [75] C. J. Henrich and J. A. Beutler, "Matching the power of high throughput screening to the chemical diversity of natural products", *Nat. Prod. Rep.*, vol. 30, no. 10, pp. 1284–1298, Sep. 2013.
- [76] J. W. H. Li and J. C. Vederas, "Drug discovery and natural products: End of an era or an endless frontier?", *Science*, vol. 325, no. 5937, pp. 161–165, 2009.
- [77] F. E. Koehn and G. T. Carter, "Rediscovering natural products as a source of new drugs", *Discov. Med.*, vol. 5, no. 26, pp. 159–164, 2005.
- [78] F. E. Koehn and G. T. Carter, "The evolving role of natural products in drug discovery", *Nat. Rev. Drug Discov.*, vol. 4, no. 3, pp. 206–220, 2005.
- [79] J. W. Scannell, A. Blanckley, H. Boldon, and B. Warrington, "Diagnosing the decline in pharmaceutical R&D efficiency", *Nat. Rev. Drug Discov.*, vol. 11, no. 3, pp. 191–200, Mar. 2012.
- [80] B. David, J. L. Wolfender, and D. A. Dias, "The pharmaceutical industry and natural products: historical status and new trends", *Phytochem. Rev.* 2014 142, vol. 14, no. 2, pp. 299–315, Jun. 2014.
- [81] D. G. I. Kingston, "Modern natural products drug discovery and its relevance to biodiversity conservation", *J. Nat. Prod.*, vol. 74, no. 3, pp. 496–511, Mar. 2011.
- [82] J. Clardy and C. Walsh, "Lessons from natural molecules", *Nat.* 2004 4327019, vol. 432, no. 7019, pp. 829–837, Dec. 2004.

- [83] T. W. Corson and C. M. Crews, "Molecular Understanding and Modern Application of Traditional Medicines: Triumphs and Trials", *Cell*, vol. 130, no. 5, pp. 769–774, Sep. 2007.
- [84] B. Patwardhan, "Ethnopharmacology and drug discovery", *J. Ethnopharmacol.*, vol. 100, no. 1–2, pp. 50–52, Aug. 2005.
- [85] D. J. Newman and G. M. Cragg, "Natural products as sources of new drugs over the 30 years from 1981 to 2010", *J. Nat. Prod.*, vol. 75, no. 3, pp. 311–335, Mar. 2012.
- [86] I. Paterson and E. A. Anderson, "The renaissance of natural products as drug candidates", *Science*, vol. 310, no. 5747, pp. 451–453, Oct. 2005.
- [87] M. A. Strege, "High-performance liquid chromatographic–electrospray ionization mass spectrometric analyses for the integration of natural products with modern high-throughput screening", *J. Chromatogr. B Biomed. Sci. Appl.*, vol. 725, no. 1, pp. 67–78, Apr. 1999.
- [88] H. He et al., "Mannopectimycin esters and carbonates, potent antibiotic agents against drug-resistant bacteria", *Bioorg. Med. Chem. Lett.*, vol. 14, no. 1, pp. 279–282, Jan. 2004.
- [89] M. Lahlou, "Screening of natural products for drug discovery", *Expert Opin. Drug Discov.*, vol. 2, no. 5, pp. 697–705, May 2007.
- [90] B. Patwardhan, A. D. B. Vaidya, and M. Chorghade, "Ayurveda and natural products drug discovery", *Curr. Sci.*, vol. 86, no. 6, pp. 789–799, Jul 2022.
- [91] D. P. Waller, "Methods in ethnopharmacology", *J. Ethnopharmacol.*, vol. 38, no. 2–3, pp. 189–195, 1993.
- [92] A. Kumar Shakya, "Medicinal plants: Future source of new drugs", *Int. J. Herb. Med.*, vol. 4, no. 4, pp. 59–64, 2016.
- [93] M. Leonti, "The future is written: impact of scripts on the cognition, selection, knowledge and transmission of medicinal plant use and its implications for

- ethnobotany and ethnopharmacology”, *J. Ethnopharmacol.*, vol. 134, no. 3, pp. 542–555, Apr. 2011.
- [94] R. R. Baumgartner et al., “Bioactivity-guided isolation of 1,2,3,4,6-Penta-O-galloyl-d- glucopyranose from paeonia lactiflora roots as a PTP1B inhibitor (*Journal of Natural Products* (2010) 73 (1578))”, *J. Nat. Prod.*, vol. 73, no. 10, p. 1742, Oct. 2010.
- [95] E. H. Heiss et al., “Identification of chromomoric acid C-I as an Nrf2 activator in *Chromolaena odorata*”, *J. Nat. Prod.*, vol. 77, no. 3, pp. 503–508, Mar. 2014.
- [96] A. F. Tawfike, C. Viegelmann, and R. Edrada-Ebel, “Metabolomics and dereplication strategies in natural products”, *Methods Mol. Biol.*, vol. 1055, pp. 227–244, 2013.
- [97] J. Gertsch, “Botanical drugs, synergy, and network pharmacology: forth and back to intelligent mixtures”, *Planta Med.*, vol. 77, no. 11, pp. 1086–1098, 2011.
- [98] Y. Liu and M. W. Wang, “Botanical drugs: challenges and opportunities: contribution to Linnaeus Memorial Symposium 2007”, *Life Sci.*, vol. 82, no. 9–10, pp. 445–449, Feb. 2008.
- [99] Z. Liu, “Preparation of botanical samples for biomedical research”, *Endocr. Metab. Immune Disord. Drug Targets*, vol. 8, no. 2, pp. 112–121, Jun. 2008.
- [100] B. Schmidt, D. M. Ribnicky, A. Poulev, S. Logendra, W. T. Cefalu, and I. Raskin, “A natural history of botanical therapeutics”, *Metabolism.*, vol. 57, no. 7 Suppl 1, p. S9, 2008.
- [101] C. M. Morel, Y. T. Touré, B. Dobrokhotov, and A. M. J. Oduola, “The mosquito genome--a breakthrough for public health”, *Science*, vol. 298, no. 5591, p. 79, Oct. 2002.
- [102] K. C. Nicolaou, J. A. Pfefferkorn, A. J. Roecker, G. Q. Cao, S. Barluenga, and H. J. Mitchell, “Natural product-like combinatorial libraries based on privileged structures. 1. General principles and solid-phase synthesis of benzopyrans”, *J. Am. Chem. Soc.*, vol. 122, no. 41, pp. 9939–9953, Oct. 2000.

- [103] K. C. Nicolaou et al., “Natural product-like combinatorial libraries based on privileged structures. 2. Construction of a 10 000-membered benzopyran library by directed split-and-pool chemistry using NanoKans and optical encoding”, *J. Am. Chem. Soc.*, vol. 122, no. 41, pp. 9954–9967, Oct. 2000.
- [104] S. Shechter, D. R. Thomas, and D. A. Jans, “Application of In Silico and HTS Approaches to Identify Nuclear Import Inhibitors for Venezuelan Equine Encephalitis Virus Capsid Protein: A Case Study”, *Front. Chem.*, vol. 8, p. 1049, Dec. 2020.
- [105] G. Sliwoski, S. Kothiwale, J. Meiler, and E. W. Lowe, “Computational methods in drug discovery”, *Pharmacol. Rev.*, vol. 66, no. 1, pp. 334–395, Jan. 2013.
- [106] S. P. Leelananda and S. Lindert, “Computational methods in drug discovery”, *Beilstein J. Org. Chem.* 12267, vol. 12, no. 1, pp. 2694–2718, Dec. 2016.
- [107] G. Shanmugam and J. Jeon, “Computer-Aided Drug Discovery in Plant Pathology”, *plant Pathol. J.*, vol. 33, no. 6, pp. 529–542, 2017.
- [108] C. Vénien-Bryan, Z. Li, L. Vuillard, and J. A. Boutin, “Cryo-electron microscopy and X-ray crystallography: Complementary approaches to structural biology and drug discovery”, *Acta Crystallogr. F Struct. Biol. Commun.*, vol. 73, no. 4, pp. 174–183, Apr. 2017.
- [109] E. P. Carpenter, K. Beis, A. D. Cameron, and S. Iwata, “Overcoming the challenges of membrane protein crystallography”, *Curr. Opin. Struct. Biol.*, vol. 18, no. 5, pp. 581–586, Oct. 2008.
- [110] A. M. Lesk and C. Chothia, “How different amino acid sequences determine similar protein structures: The structure and evolutionary dynamics of the globins”, *J. Mol. Biol.*, vol. 136, no. 3, pp. 225–270, Jan. 1980.
- [111] K. Illergård, D. H. Ardell, and A. Elofsson, “Structure is three to ten times more conserved than sequence—A study of structural response in protein cores”, *Proteins Struct. Funct. Bioinforma.*, vol. 77, no. 3, pp. 499–508, Nov. 2009.

- [112] Z. Xiang, “Advances in homology protein structure modeling”, *Curr. Protein Pept. Sci.*, vol. 7, no. 3, pp. 217–227, Jun. 2006.
- [113] J. U. Bowie, R. Lüthy, and D. Eisenberg, “A method to identify protein sequences that fold into a known three-dimensional structure”, *Science*, vol. 253, no. 5016, pp. 164–170, 1991.
- [114] K. Mizuguchi, “Fold recognition for drug discovery”, *Drug Discov. Today TARGETS*, vol. 3, no. 1, pp. 18–23, Feb. 2004.
- [115] T. Schwede, J. Kopp, N. Guex, and M. C. Peitsch, “SWISS-MODEL: An automated protein homology-modeling server”, *Nucleic Acids Res.*, 2003.
- [116] A. Šali and T. L. Blundell, “Comparative protein modelling by satisfaction of spatial restraints”, *J. Mol. Biol.*, vol. 234, no. 3, pp. 779–815, Dec. 1993.
- [117] J. Yang and Y. Zhang, “I-TASSER server: new development for protein structure and function predictions”, *Nucleic Acids Res.*, vol. 43, no. W1, pp. W174–W181, 2015.
- [118] J. Söding, A. Biegert, and A. N. Lupas, “The HHpred interactive server for protein homology detection and structure prediction”, *Nucleic Acids Res.*, vol. 33, no. Web Server issue, p. W249, Jul. 2005.
- [119] D. T. Jones, “GenTHREADER: an efficient and reliable protein fold recognition method for genomic sequences”, *J. Mol. Biol.*, vol. 287, no. 4, pp. 797–815, Apr. 1999.
- [120] C. A. Rohl, C. E. M. Strauss, K. M. S. Misura, and D. Baker, “Protein Structure Prediction Using Rosetta”, *Methods Enzymol.*, vol. 383, pp. 66–93, Jan. 2004.
- [121] S. Roughley, L. Wright, P. Brough, A. Massey, and R. E. Hubbard, “Hsp90 Inhibitors and Drugs from Fragment and Virtual Screening”, *Top. Curr. Chem.*, vol. 317, pp. 61–82, 2011.
- [122] M. Batool, B. Ahmad, and S. Choi, “A Structure-Based Drug Discovery Paradigm”, *Int. J. Mol. Sci.* 2019, Vol. 20, Page 2783, vol. 20, no. 11, p. 2783, Jun. 2019.

- [123] S. A. Hollingsworth and R. O. Dror, “Molecular Dynamics Simulation for All”, *Neuron*, vol. 99, no. 6, pp. 1129–1143, Sep. 2018.
- [124] J. S. Burg et al., “Structural biology. Structural basis for chemokine recognition and activation of a viral G protein-coupled receptor”, *Science*, vol. 347, no. 6226, pp. 1113–1117, Mar. 2015.
- [125] J. D. Durrant and J. A. McCammon, “Molecular dynamics simulations and drug discovery”, *BioMed Cent.*, vol. 27, no. 3, pp. 2985–2993, 1894.
- [126] O. M. H. Salo-Ahen et al., “Molecular Dynamics Simulations in Drug Discovery and Pharmaceutical Development”, *Processes*, vol. 9, no. 1, p. 71, Dec. 2020.
- [127] E. Vangrevelinghe, K. Zimmermann, J. Schoepfer, R. Portmann, D. Fabbro, and P. Furet, “Discovery of a potent and selective protein kinase CK2 inhibitor by high-throughput docking”, *J. Med. Chem.*, vol. 46, no. 13, pp. 2656–2662, Jun. 2003.
- [128] V. Karthick et al., “Virtual screening of the inhibitors targeting at the viral protein 40 of Ebola virus”, *Infect. Dis. Poverty*, vol. 5, no. 1, pp. 1–10, Feb. 2016.
- [129] K. A. Peele et al., “Molecular docking and dynamic simulations for antiviral compounds against SARS-CoV-2: A computational study”, *Informatics Med. unlocked*, vol. 19, p. 100345, Jan. 2020.
- [130] X. Wang et al., “Combination of antiviral drugs inhibits SARS-CoV-2 polymerase and exonuclease and demonstrates COVID-19 therapeutic potential in viral cell culture”, *Commun. Biol.*, vol. 5, no. 1, pp. 1–14, Feb. 2022.
- [131] Y. Lu and Z. Nikolovska-coleska, “Discovery of a Nanomolar Inhibitor of the Human Murine Double Minute 2 (MDM2)–p53 Interaction thr.PDF”, *J. Med. Chem.*, vol. 49, no. 13, pp. 3759–3762, 2006.
- [132] M. Shahbaaz, S. H. Qari, M. H. Abdellattif, and M. A. Hussien, “Structural analyses and classification of novel isoniazid resistance coupled mutational landscapes in *Mycobacterium tuberculosis*: a combined molecular docking and MD simulation study”, vol. 40, no. 11, pp. 4791–4800, 2020.

- [133] V. S. Aathmanathan, V. Arumugam, and M. Krishnan, "Computational approach to explore the inhibitory potential of biologically derived compounds against *Spodoptera litura* vitellogenin receptor (VgR) using structure based virtual screening and molecular dynamics", vol. 40, no. 11, pp. 4954–4960, 2020.
- [134] Y. L. Liu, S. Lindert, W. Zhu, K. Wang, J. A. McCammon, and E. Oldfield, "Taxodione and arenarone inhibit farnesyl diphosphate synthase by binding to the isopentenyl diphosphate site", *Proc. Natl. Acad. Sci. U. S. A.*, vol. 111, no. 25, pp. e2530–e2539, Jun. 2014.
- [135] G. H. Loew, H. O. Villar, and I. Alkorta, "Strategies for Indirect Computer-Aided Drug Design", *Pharm. Res.*, vol. 10, no. 4, pp. 475–486, 1993.
- [136] M. JS, G. AC, and M. EJ, "3-D pharmacophores in drug discovery", *Curr. Pharm. Des.*, vol. 7, no. 7, pp. 567–597, Mar. 2001.
- [137] C. Acharya, A. Coop, J. E. Polli, and A. D. MacKerell, "Recent advances in ligand-based drug design: relevance and utility of the conformationally sampled pharmacophore approach", *Curr. Comput. Aided. Drug Des.*, vol. 7, no. 1, pp. 10–22, Dec. 2011.
- [138] M. I. Skvortsova, I. V Stankevich, V. A. Palyulin, and N. S. Zefirov, "Molecular similarity concept and its use for predicting the properties of chemical compounds", *Russ. Chem. Rev.*, vol. 75, no. 11, pp. 961–979, 2006.
- [139] R. P. Sheridan and S. K. Kearsley, "Why do we need so many chemical similarity search methods?", *Drug Discov. Today*, vol. 7, no. 17, pp. 903–911, 2002.
- [140] M. Gütlein, A. Karwath, and S. Kramer, "CheS-Mapper - Chemical space mapping and visualization in 3D", *J. Cheminform.*, vol. 4, no. 3, pp. 1–16, 2012.
- [141] S.-K. Lin, "Pharmacophore Perception, Development and Use in Drug Design.", *Molecules*, vol. 5, no. 7, pp. 987–989, Jul. 2000.
- [142] R. P. Verma and C. Hansch, "Camptothecins: A SAR/QSAR study", *Chem. Rev.*, vol. 109, no. 1, pp. 213–235, Jan. 2009.

- [143] J. Verma, V. Khedkar, and E. Coutinho, “3D-QSAR in drug design--a review”, *Curr. Top. Med. Chem.*, vol. 10, no. 1, pp. 95–115, Jan. 2010.
- [144] N. S. Sakle, S. A. More, and S. N. Mokale, “A network pharmacology-based approach to explore potential targets of *Caesalpinia pulcherima*: an updated prototype in drug discovery”, *Sci. Rep.*, vol. 10, no. 1, pp. 1–16, Oct. 2020.
- [145] A. L. Hopkins, “Network pharmacology: the next paradigm in drug discovery”, *Nat. Chem. Biol.* 2008 411, vol. 4, no. 11, pp. 682–690, Oct. 2008.
- [146] S. Di et al., “A Network Pharmacology Approach to Uncover the Mechanisms of Shen-Qi-Di-Huang Decoction against Diabetic Nephropathy”, *Evid. Based. Complement. Alternat. Med.*, vol. 2018, no. 7043402, 2018.
- [147] X. F. Huang et al., “A network pharmacology strategy to investigate the anti-inflammatory mechanism of luteolin combined with in vitro transcriptomics and proteomics”, *Int. Immunopharmacol.*, vol. 86, no. 106727, Sep. 2020.
- [148] Y. Shi, M. Chen, Z. Zhao, J. Pan, and S. Huang, “Network Pharmacology and Molecular Docking Analyses of Mechanisms Underlying Effects of the Cyperi Rhizoma - Chuanxiong Rhizoma Herb Pair on Depression”, *Evid. Based. Complement. Alternat. Med.*, vol. 2021, no. 1, p. 5704578, 2021.
- [149] J. Lv, L. Pan, Y. Ye, and Y. Zhou, “A sensitive and selective RP-HPLC method for simultaneous determination of picroside-I and picroside-II in rat plasma and its application in pharmacokinetics studies”, *J. Sep. Sci.*, vol. 30, no. 15, pp. 2466–2472, 2007.
- [150] K. Vipul, M. Nitin, and R. C. Gupta, “A sensitive and selective LC-MS-MS method for simultaneous determination of picroside-I and kutkoside (active principles of herbal preparation picroliv) using solid phase extraction in rabbit plasma: Application to pharmacokinetic study”, *J. Chromatogr. B Anal. Technol. Biomed. Life Sci.*, vol. 820, no. 2, pp. 221–227, 2005.

- [151] D. Upadhyay, R. P. Dash, S. Anandjiwala, and M. Nivsarkar, “Comparative pharmacokinetic profiles of picrosides I and II from kutkin, *Picrorhiza kurroa* extract and its formulation in rats”, *Fitoterapia*, vol. 85, no. 1, pp. 76–83, 2013.
- [152] J. Zhu et al., “A pre-clinical pharmacokinetic study in rats of three naturally occurring iridoid glycosides, Picroside-I, II and III, using a validated simultaneous HPLC-MS/MS assay”, *J. Chromatogr. B Anal. Technol. Biomed. Life Sci.*, vol. 993–994, pp. 47–59, 2015.
- [153] S. Zahiruddin et al., “Pharmacokinetics and comparative metabolic profiling of iridoid enriched fraction of *Picrorhiza kurroa* – An Ayurvedic Herb”, *J. Ethnopharmacol.*, vol. 197, pp. 157–164, 2017.
- [154] F. C. Yang, S. L. Yang, and L. Z. Xu, “Determination of picroside II in dog plasma by HPLC and its application in a pharmacokinetics study”, *Biomed. Chromatogr.*, vol. 19, no. 4, pp. 279–284, 2005.
- [155] Q. L. Yu et al., “A sensitive LC-ESI-MS method for pharmacokinetic studies of picroside II in dog plasma”, *Chromatographia*, vol. 67, no. 11–12, pp. 1013–1016, 2008.
- [156] K. Xiong, Z. Ju, T. Zhang, Z. Wang, and H. Han, “Metabolic profiles and pharmacokinetics of picroside I in rats by liquid chromatography combined with electrospray ionization tandem mass spectrometry”, *J. Chromatogr. B Anal. Technol. Biomed. Life Sci.*, vol. 1095, no. 1, pp. 157–165, 2018.
- [157] Y. Ma, S. Cheng, M. L. Leski, D. Luo, and J. He, “Development and validation of a sensitive LC-tandem-MS method for the quantitative determination of picroside II in rat plasma”, *Chromatographia*, vol. 68, no. 11–12, pp. 1027–1032, 2008.
- [158] D. Tworowski et al., “COVID19 Drug Repository: Text-mining the literature in search of putative COVID19 therapeutics”, *Nucleic Acids Res.*, vol. 49, no. D1, pp. D113–D1121, 2021.
- [159] B. Chen et al., “Overview of lethal human coronaviruses”, *Signal Transduct. Target. Ther.*, vol. 5, no. 1, p. 89, 2020.

- [160] L. Yan et al., “Architecture of a SARS-CoV-2 mini replication and transcription complex”, *Nat. Commun.*, vol. 11, no. 5874, 2020.
- [161] D. Shin et al., “Papain-like protease regulates SARS-CoV-2 viral spread and innate immunity”, *Nature*, vol. 587, no. 1, pp. 657–672, 2020.
- [162] T. Klemm et al., “Mechanism and inhibition of the papain-like protease, PLpro, of SARS-CoV-2”, *EMBO J.*, vol. 39, no. 18, pp., 2020.
- [163] S. A. Kulkarni and K. Ingale, “CHAPTER 1: In Silico Approaches for Drug Repurposing for SARS-CoV-2 Infection”, in *The Coronavirus Pandemic and the Future: Virology, Epidemiology, Translational Toxicology and Therapeutics*, vol. 2, 2022, pp. 1–80.
- [164] C. K. Kang et al., “In vitro activity of lopinavir/ritonavir and hydroxychloroquine against severe acute respiratory syndrome coronavirus 2 at concentrations achievable by usual doses”, *Korean J. Intern. Med.*, vol. 35, no. 4, p. 787, 2020.
- [165] C. Marzolini et al., “Effect of Systemic Inflammatory Response to SARS-CoV-2 on Lopinavir and Hydroxychloroquine Plasma Concentrations”, *Antimicrob. Agents Chemother.*, vol. 64, no. 9, pp. e01177-20, Sep. 2020.
- [166] P. Panagopoulos et al., “Lopinavir/ritonavir as a third agent in the antiviral regimen for SARS-CoV-2 infection”, *J. Chemother.*, vol. 33, no. 3, pp. 193–197, 2021.
- [167] S. M. Reza Hashemian, T. Farhadi, and A. A. Velayati, “A Review on Remdesivir: A Possible Promising Agent for the Treatment of COVID-19”, *Drug Des. Devel. Ther.*, vol. 14, pp. 3215–3222, 2020.
- [168] W. C. Ko et al., “Arguments in favour of remdesivir for treating SARS-CoV-2 infections”, *Int. J. Antimicrob. Agents*, vol. 55, no. 4, p. 105933, Apr. 2020.
- [169] Y.-C. Wang et al., “Structural basis of SARS-CoV-2 main protease inhibition by a broad-spectrum anti-coronaviral drug”, *Am. J. Cancer Res.*, vol. 10, no. 8, p. 2545, 2020.

- [170] A. A. Elfiky, “Anti-HCV, nucleotide inhibitors, repurposing against COVID-19”, *Life Sci.*, vol. 248, p. 117477, May 2020.
- [171] J. S. Khalili, H. Zhu, N. S. A. Mak, Y. Yan, and Y. Zhu, “Novel coronavirus treatment with ribavirin: Groundwork for an evaluation concerning COVID-19”, *J. Med. Virol.*, vol. 92, no. 7, p. 746, Jul. 2020.
- [172] U. Agrawal, R. Raju, and Z. F. Udwadia, “Favipiravir: A new and emerging antiviral option in COVID-19”, *Med. journal, Armed Forces India*, vol. 76, no. 4, pp. 370–376, Oct. 2020.
- [173] E. A. Coomes and H. Haghbayan, “Favipiravir, an antiviral for COVID-19?”, *J. Antimicrob. Chemother.*, vol. 75, no. 7, pp. 2013–2014, Jul. 2020.
- [174] L. Li, X. Wang, R. Wang, Y. Hu, S. Jiang, and X. Lu, “Antiviral Agent Therapy Optimization in Special Populations of COVID-19 Patients”, *Drug Des. Devel. Ther.*, vol. 14, p. 3013, 2020.
- [175] S. Joshi et al., “Real-World Experience with Favipiravir for the Treatment of Mild-to-Moderate COVID-19 in India”, *Pragmatic Obs. Res.*, vol. 13, pp. 33–41, May 2022.
- [176] K. Uzunova, E. Filipova, V. Pavlova, and T. Vekov, “Insights into antiviral mechanisms of remdesivir, lopinavir/ritonavir and chloroquine/hydroxychloroquine affecting the new SARS-CoV-2”, *Biomed. Pharmacother.*, vol. 131, p. 110668, Nov. 2020.
- [177] E. Mantlo, N. Bukreyeva, J. Maruyama, S. Paessler, and C. Huang, “Antiviral activities of type I interferons to SARS-CoV-2 infection”, *Antiviral Res.*, vol. 179, p. 104811, Jul. 2020.
- [178] E. Sallard, F. X. Lescure, Y. Yazdanpanah, F. Mentre, and N. Peiffer-Smadja, “Type 1 interferons as a potential treatment against COVID-19”, *Antiviral Res.*, vol. 178, p. 104791, Jun. 2020.
- [179] M. J. Vincent et al., “Chloroquine is a potent inhibitor of SARS coronavirus infection and spread”, *Virol. J.*, vol. 2, p. 69, Aug. 2005.

- [180] M. E. Rebeaud and F. Zores, “SARS-CoV-2 and the Use of Chloroquine as an Antiviral Treatment”, *Front. Med.*, vol. 7, p. 184, Apr. 2020.
- [181] Y. Acharya and A. Sayed, “Chloroquine and hydroxychloroquine as a repurposed agent against COVID-19: a narrative review”, *Ther. Adv. Infect. Dis.*, vol. 7, 2020.
- [182] H. L. B. Braz et al., “In silico study of azithromycin, chloroquine and hydroxychloroquine and their potential mechanisms of action against SARS-CoV-2 infection”, *Int. J. Antimicrob. Agents*, vol. 56, no. 3, p. 106119, Sep. 2020.
- [183] C. A. Gentry, M. B. Humphrey, S. K. Thind, S. C. Hendrickson, G. Kurdgelashvili, and R. J. Williams, “Long-term hydroxychloroquine use in patients with rheumatic conditions and development of SARS-CoV-2 infection: a retrospective cohort study”, *Lancet Rheumatol.*, vol. 2, no. 11, pp. e689–e697, Nov. 2020.
- [184] A. K. Singh, A. Singh, A. Shaikh, R. Singh, and A. Misra, “Chloroquine and hydroxychloroquine in the treatment of COVID-19 with or without diabetes: A systematic search and a narrative review with a special reference to India and other developing countries”, *Diabetes Metab. Syndr.*, vol. 14, no. 3, p. 246, May 2020.
- [185] F. R. Bhuiyan, S. Howlader, T. Raihan, and M. Hasan, “Plants Metabolites: Possibility of Natural Therapeutics Against the COVID-19 Pandemic”, *Front. Med.*, vol. 7, no. 1, p. 444, Aug. 2020.
- [186] C. S. Sharanya, A. Sabu, and M. Haridas, “Potent phytochemicals against COVID-19 infection from phyto-materials used as antivirals in complementary medicines: a review”, *Futur. J. Pharm. Sci.* 2021 71, vol. 7, no. 1, pp. 1–20, Jun. 2021.
- [187] M. B. Majnooni et al., “Phytochemicals: Potential Therapeutic Interventions Against Coronavirus-Associated Lung Injury”, *Front. Pharmacol.*, vol. 11, p. 588467, Nov. 2020.
- [188] S. Jo, S. Kim, D. H. Shin, and M. S. Kim, “Inhibition of SARS-CoV 3CL protease by flavonoids”, *J. Enzyme Inhib. Med. Chem.*, vol. 35, no. 1, pp. 145–151, Jan. 2020.

- [189] A. Swargiary, S. Mahmud, and M. A. Saleh, “Screening of phytochemicals as potent inhibitor of 3-chymotrypsin and papain-like proteases of SARS-CoV2: an *in silico* approach to combat COVID-19”, *J. Biomol. Struct. Dyn.*, vol. 40, no. 5, p. 15, 2020.
- [190] A. Basu, A. Sarkar, and U. Maulik, “Molecular docking study of potential phytochemicals and their effects on the complex of SARS-CoV2 spike protein and human ACE2”, *Sci. Reports 2020 101*, vol. 10, no. 1, pp. 1–15, Oct. 2020.
- [191] S. Koulgi, V. Jani, V. N. Mallikarjunachari Uppuladinne, U. Sonavane, and R. Joshi, “Natural plant products as potential inhibitors of RNA dependent RNA polymerase of Severe Acute Respiratory Syndrome Coronavirus-2”, *PLoS One*, vol. 16, no. 5, pp. 1–18, 2021.
- [192] S. A. Mir et al., “Identification of SARS-CoV-2 RNA-dependent RNA polymerase inhibitors from the major phytochemicals of *Nigella sativa*: An *in silico* approach”, *Saudi J. Biol. Sci.*, vol. 29, no. 1, pp. 394–401, Jan. 2022.
- [193] S. Nallusamy et al., “Exploring Phytochemicals of Traditional Medicinal Plants Exhibiting Inhibitory Activity Against Main Protease, Spike Glycoprotein, RNA-dependent RNA Polymerase and Non-Structural Proteins of SARS-CoV-2 Through Virtual Screening”, *Front. Pharmacol.*, vol. 12, p. 667704, Jul. 2021.
- [194] P. Singh et al., “The dual role of phytochemicals on SARS-CoV-2 inhibition by targeting host and viral proteins”, *J. Tradit. Complement. Med.*, vol. 12, no. 1, pp. 90–99, Jan. 2022.
- [195] S. Gowrishankar et al., “Promising phytochemicals of traditional Indian herbal steam inhalation therapy to combat COVID-19 – An *in silico* study”, *Food Chem. Toxicol.*, vol. 148, no. 111966, 2021.
- [196] P. H. Johnson and S. C. Quay, “Advances in nasal drug delivery through tight junction technology”, *Expert Opin. Drug Deliv.*, vol. 2, no. 2, pp. 281–298, 2005.
- [197] A. A. H. Abdellatif, H. M. Tawfeek, A. Abdelfattah, G. El-Saber Batiha, and H. F. Hetta, “Recent updates in COVID-19 with emphasis on inhalation therapeutics:

- Nanostructured and targeting systems”, *J. Drug Deliv. Sci. Technol.*, vol. 63, p. 102435, Jun. 2021.
- [198] G. Pilcer and K. Amighi, “Formulation strategy and use of excipients in pulmonary drug delivery”, *Int. J. Pharm.*, vol. 392, no. 1–2, pp. 1–19, Jun. 2010.
- [199] A. J. Hickey, “Emerging trends in inhaled drug delivery”, *Adv. Drug Deliv. Rev.*, vol. 157, pp. 63–70, Jan. 2020.
- [200] B. B. Eedara, W. Alabsi, D. Encinas-Basurto, R. Polt, J. G. Ledford, and H. M. Mansour, “Inhalation Delivery for the Treatment and Prevention of COVID-19 Infection”, *Pharmaceutics*, vol. 13, no. 7, p. 1077, Jul. 2021.
- [201] M. Griesel et al., “Inhaled corticosteroids for the treatment of COVID-19”, *Cochrane database Syst. Rev.*, vol. 3, no. 3, Mar. 2022.
- [202] S. Ramakrishnan et al., “Inhaled budesonide in the treatment of early COVID-19 (STOIC): a phase 2, open-label, randomised controlled trial”, *Lancet Respir. Med.*, vol. 9, no. 7, pp. 763–772, Jul. 2021.
- [203] J. S. Raut and S. M. Karuppayil, “A status review on the medicinal properties of essential oils”, *Ind. Crops Prod.*, vol. 62, pp. 250–264, Dec. 2014.
- [204] P. K. Yadalam et al., “Antiviral Essential Oil Components Against SARS-CoV-2 in Pre-procedural Mouth Rinses for Dental Settings During COVID-19: A Computational Study”, *Front. Chem.*, vol. 9, p. 642026, Mar. 2021.
- [205] L. T. Neto, M. L. G. Monteiro, D. Galvan, and C. A. Conte-Junior, “An evaluation of the potential of essential oils against sars-cov-2 from in silico studies through the systematic review using a chemometric approach”, *Pharmaceutics*, vol. 14, no. 11, p. 1138, Nov. 2021.
- [206] B. T. P. Thuy et al., “Investigation into SARS-CoV-2 Resistance of Compounds in Garlic Essential Oil”, *ACS Omega*, vol. 5, no. 14, pp. 8312–8320, Apr. 2020.
- [207] S. Panikar et al., “Essential oils as an effective alternative for the treatment of COVID-19: Molecular interaction analysis of protease (Mpro) with pharmacokinetics

- and toxicological properties”, *J. Infect. Public Health*, vol. 14, no. 5, pp. 601–610, May 2021.
- [208] A. M. Baig, A. Khaleeq, U. Ali, and H. Syeda, “Evidence of the COVID-19 Virus Targeting the CNS: Tissue Distribution, Host-Virus Interaction, and Proposed Neurotropic Mechanisms”, *ACS Chem. Neurosci.*, vol. 11, no. 7, pp. 995–998, Apr. 2020.
- [209] Y. Wu et al., “Nervous system involvement after infection with COVID-19 and other coronaviruses”, *Brain. Behav. Immun.*, vol. 87, pp. 18–22, Jul. 2020.
- [210] H. M. Berman et al., “The Protein Data Bank”, *Nucleic Acids Res.*, vol. 28, no. 1, pp. 235–242, Jan. 2000.
- [211] A. D. Mesecarr, “A Taxonomically-Driven Approach to Development of Potent, Broad-Spectrum Inhibitors of Coronavirus Main Protease Including SARS-CoV-2 (COVID-19)”, 2020, doi: 10.2210/pdb6w63/pdb.
- [212] J. Osipiuk et al., “The crystal structure of papain-like protease of SARS CoV-2”, 2020, doi: 10.2210/pdb6w9c/pdb.
- [213] D. Wrapp et al., “Cryo-EM structure of the 2019-nCoV spike in the prefusion conformation”, *Science*, vol. 367, no. 6483, pp. 1260–1263, 2020.
- [214] Y. Gao et al., “Structure of the RNA-dependent RNA polymerase from COVID-19 virus”, *Science*, vol. 368, no. 6492, pp. 779–782, May 2020.
- [215] S. Kumari et al., “EssOilDB: a database of essential oils reflecting terpene composition and variability in the plant kingdom”, *Database (Oxford)*, vol. 2014, 2014.
- [216] S. Kim et al., “PubChem in 2021: New data content and improved web interfaces”, *Nucleic Acids Res.*, 2021.
- [217] H. E. Pence and A. Williams, “Chemspider: An online chemical information resource”, *J. Chem. Educ.*, vol. 87, no. 11, pp. 1123–1124, 2010.

- [218] G. Madhavi Sastry, M. Adzhigirey, T. Day, R. Annabhimoju, and W. Sherman, "Protein and ligand preparation: Parameters, protocols, and influence on virtual screening enrichments", *J. Comput. Aided. Mol. Des.*, vol. 27, no. 3, 2013.
- [219] G. M. Morris et al., "Software news and updates AutoDock4 and AutoDockTools4: Automated docking with selective receptor flexibility", *J. Comput. Chem.*, vol. 30, no. 16, pp. 2785–2791, 2009.
- [220] S. Forli, R. Huey, M. E. Pique, M. F. Sanner, D. S. Goodsell, and A. J. Olson, "Computational protein-ligand docking and virtual drug screening with the AutoDock suite", *Nat. Protoc.*, vol. 11, no. 5, pp. 905–919, 2016.
- [221] A. Daina, O. Michielin, and V. Zoete, "SwissADME: A free web tool to evaluate pharmacokinetics, drug-likeness and medicinal chemistry friendliness of small molecules", *Sci. Rep.*, vol. 7, no. 1, p. 42717, 2017.
- [222] H. van de Waterbeemd and E. Gifford, "ADMET in silico modelling: Towards prediction paradise?", *Nat. Rev. Drug Discov.*, vol. 2, no. 3, pp. 192–204, 2003.
- [223] Gary W. Caldwell, David M. Ritchie, John A. Masucci, William Hageman, and Zhengyin Yan, "The New Pre-Preclinical Paradigm: Compound Optimization in Early ...: Ingenta Connect", *Curr. Top. Med. Chem.*, vol. 1, no. 5, pp. 353–366, Nov. 2001, Accessed: May 09, 2022.
- [224] S. Fatima, P. Gupta, S. Sharma, A. Sharma, and S. M. Agarwal, "ADMET profiling of geographically diverse phytochemical using chemoinformatic tools", *Future Med. Chem.*, vol. 12, no. 1, pp. 69–87, 2019.
- [225] A. Sharma, S. Sharma, M. Gupta, S. Fatima, R. Saini, and S. M. Agarwal, "Pharmacokinetic profiling of anticancer phytochemicals using computational approach", *Phytochem. Anal.*, vol. 29, no. 6, pp. 559–568, 2018.
- [226] S. Sharma, M. Gupta, A. Sharma, and S. M. Agarwal, "Oral Bioavailability of Naturally Occurring Anticancer Phytomolecules", *Lett. Drug Des. Discov.*, vol. 15, no. 11, pp. 1180–1188, 2018.

- [227] C. A. Lipinski, F. Lombardo, B. W. Dominy, and P. J. Feeney, “Experimental and computational approaches to estimate solubility and permeability in drug discovery and development settings”, *Adv. Drug Deliv. Rev.*, vol. 23, no. 1–3, pp. 3–25, Jan. 1997.
- [228] W. J. Egan, K. M. Merz, and J. J. Baldwin, “Prediction of drug absorption using multivariate statistics”, *J. Med. Chem.*, vol. 43, no. 21, pp. 3867–3877, Oct. 2000.
- [229] D. F. Veber, S. R. Johnson, H. Y. Cheng, B. R. Smith, K. W. Ward, and K. D. Kopple, “Molecular properties that influence the oral bioavailability of drug candidates”, *J. Med. Chem.*, vol. 45, no. 12, pp. 2615–2623, Jun. 2002.
- [230] A. K. Ghose, V. N. Viswanadhan, and J. J. Wendoloski, “A knowledge-based approach in designing combinatorial or medicinal chemistry libraries for drug discovery. 1. A qualitative and quantitative characterization of known drug databases”, *J. Comb. Chem.*, vol. 1, no. 1, pp. 55–68, 1999.
- [231] I. Muegge, S. L. Heald, and D. Brittelli, “Simple selection criteria for drug-like chemical matter”, *J. Med. Chem.*, vol. 44, no. 12, pp. 1841–1846, Jun. 2001.
- [232] D. E. V. Pires, T. L. Blundell, and D. B. Ascher, “pkCSM: Predicting small-molecule pharmacokinetic and toxicity properties using graph-based signatures”, *J. Med. Chem.*, vol. 58, no. 9, pp. 4066–4072, 2015.
- [233] W. Huang, Z. Lin, and W. F. Van Gunsteren, “Validation of the GROMOS 54A7 Force Field with Respect to β -Peptide Folding”, *J. Chem. Theory Comput.*, vol. 7, no. 5, pp. 1237–1243, May 2011.
- [234] A. W. Schüttelkopf and D. M. F. Van Aalten, “PRODRG: a tool for high-throughput crystallography of protein-ligand complexes”, *Acta Crystallogr. D. Biol. Crystallogr.*, vol. 60, no. Pt 8, pp. 1355–1363, Aug. 2004.
- [235] D. Van Der Spoel, E. Lindahl, B. Hess, G. Groenhof, A. E. Mark, and H. J. C. Berendsen, “GROMACS: fast, flexible, and free”, *J. Comput. Chem.*, vol. 26, no. 16, pp. 1701–1718, Dec. 2005.

- [236] C. Wang et al., “Calculating protein-ligand binding affinities with MMPBSA: Method and error analysis”, *J. Comput. Chem.*, vol. 37, no. 27, pp. 2436–2446, Oct. 2016.
- [237] P. A. Kollman et al., “Calculating structures and free energies of complex molecules: Combining molecular mechanics and continuum models”, *Acc. Chem. Res.*, vol. 33, no. 12, pp. 889–897, 2000.
- [238] R. Kumari, R. Kumar, and A. Lynn, “G-mmpbsa -A GROMACS tool for high-throughput MM-PBSA calculations”, *J. Chem. Inf. Model.*, 2014.
- [239] L. Martínez, “Automatic Identification of Mobile and Rigid Substructures in Molecular Dynamics Simulations and Fractional Structural Fluctuation Analysis”, *PLoS One*, vol. 10, no. 3, p. e0119264, Mar. 2015.
- [240] D. Chen, N. Oezguen, P. Urvil, C. Ferguson, S. M. Dann, and T. C. Savidge, “Regulation of protein-ligand binding affinity by hydrogen bond pairing”, *Sci. Adv.*, vol. 2, no. 3, p. e1501240, 2016.
- [241] Z. Jiang, L. You, W. Dou, T. Sun, and P. Xu, “Effects of an electric field on the conformational transition of the protein: A molecular dynamics simulation study”, *Polymers (Basel)*, vol. 11, no. 2, pp. 1–13, 2019.
- [242] A. Ekalu, R. Gbekele-Oluwa Ayo, J. D. Habila, and I. Hamisu, “Bioactivity of Phaeophytin a, α -Amyrin and lupeol from *Brachystelma togoense* Schltr”, *J. Turkish Chem. Soc. Sect. A Chem.*, vol. 6, no. 3, pp. 411–418, Oct. 2019.
- [243] N. N. Okoye, D. L. Ajaghaku, H. N. Okeke, E. E. Ilodigwe, C. S. Nworu, and F. B. C. Okoye, “beta-Amyrin and alpha-amyrin acetate isolated from the stem bark of *Alstonia boonei* display profound anti-inflammatory activity”, *Pharm. Biol.*, vol. 52, no. 11, pp. 1478–1486, Nov. 2014.
- [244] B. Karen Cardoso et al., “Antioxidant activity of α and β -amyrin isolated from *Myrcianthes pungens* leaves”, *Nat. Prod. Res.*, vol. 34, no. 12, pp. 1777–1781, Jun. 2018.

- [245] M. Sharma, P. Dev Sharma, M. Pal Bansal, and J. Singh, "Synthesis and Antitumor Activity of Novel Pentacyclic Triterpenoid Lantadene D", *Lett. Drug Des. Discov.*, vol. 4, no. 3, pp. 201–206, Mar. 2007.
- [246] C. Grace-Lynn, I. Darah, Y. Chen, L. Y. Latha, S. L. Jothy, and S. Sasidharan, "In Vitro Antioxidant Activity Potential of Lantadene A, a Pentacyclic Triterpenoid of Lantana Plants", *Molecules*, vol. 17, no. 9, pp. 11185–11198, Sep. 2012.
- [247] M. Litaudon et al., "Cytotoxic pentacyclic triterpenoids from *Combretum sondaicum* and *Lantana camara* as inhibitors of Bcl-xL/BakBH3 domain peptide interaction", *J. Nat. Prod.*, vol. 72, no. 7, pp. 1314–1320, Jul. 2009.
- [248] C. O. Ichiko, A. T. A. Terrumun, O. I. John, and V. A. John, "In vitro antimicrobial properties of friedelan-3-one from *Pterocarpus santalinoides* LHerit, ex Dc", *African J. Biotechnol.*, vol. 15, no. 14, pp. 531–538, Apr. 2016.
- [249] S. S. Kumar, N. Tailor, H. B. Lee, and M. Sharma, "Reduced Lantadenes A and B: semi-synthetic synthesis, selective cytotoxicity, apoptosis induction and inhibition of NO, TNF- α production in HL-60 cells", *Med. Chem. Res.*, vol. 22, no. 7, pp. 3379–3388, Nov. 2012.
- [250] Monika, A. Sharma, S. K. Suthar, V. Aggarwal, H. B. Lee, and M. Sharma, "Synthesis of lantadene analogs with marked in vitro inhibition of lung adenocarcinoma and TNF- α induced nuclear factor-kappa B (NF- κ B) activation", *Bioorg. Med. Chem. Lett.*, vol. 24, no. 16, pp. 3814–3818, Aug. 2014.
- [251] R. G. S. Ferreira, W. F. Silva, V. F. Veiga, Á. A. N. Lima, and E. S. Lima, "Physicochemical Characterization and Biological Activities of the Triterpenic Mixture α,β -Amyrenone", *Molecules*, vol. 22, no. 2, p. 298, Feb. 2017.
- [252] N. L. M. Quintão et al., "Contribution of α, β -Amyrenone to the Anti-Inflammatory and Antihypersensitivity Effects of *Aleurites moluccana* (L.) Willd.", *Biomed Res. Int.*, vol. 2014, no. 636839, 2014.
- [253] C. M. A. Tanaka et al., "Abietatrienes diterpenoids from *Sagittaria montevidensis* SSP *Montevidensis*", *Quim. Nova*, vol. 33, no. 1, pp. 30–32, 2010.

- [254] M. A. González, “Aromatic abietane diterpenoids: their biological activity and synthesis”, *Nat. Prod. Rep.*, vol. 32, no. 5, pp. 684–704, May 2015.
- [255] S. I. Alqasoumi and M. S. Abdel-kader, “Terpenoids from *Juniperus procera* with hepatoprotective activity”, *Pak. J. Pharm. Sci.*, vol. 25, no. 2, pp. 315–322, Apr. 2012.
- [256] M. S. Abdel-Kader et al., “Characterization and hepatoprotective evaluation of sesquiterpenes and diterpenes from the aerial parts of *Juniperus sabina* L.”, *Saudi Pharm. J. SPJ*, vol. 27, no. 7, pp. 920–929, Nov. 2019.
- [257] J. Becerra et al., “Antifungal and antibacterial activity of diterpenes isolated from wood extractables of Chilean Podocarpaceae”, *J. Chil. Chem. Soc.*, vol. 47, no. 2, pp. 151–157, 2002.
- [258] M. Aurang Zeb, “Isolation and biological activity of β -sitosterol and stigmasterol from the roots of *Indigofera heterantha*”, *Pharm. Pharmacol. Int. J.*, vol. 5, no. 5, pp. 204–207, Nov. 2017.
- [259] W. U. Bari et al., “Anticholinesterase, antioxidant potentials, and molecular docking studies of isolated bioactive compounds from *Grewia optiva*”, *Int. J. Food Prop.*, vol. 22, no. 1, pp. 1386–1396, 2019.
- [260] S. Babu and S. Jayaraman, “An update on β -sitosterol: A potential herbal nutraceutical for diabetic management”, *Biomed. Pharmacother.*, vol. 131, no. 110702, Nov. 2020.
- [261] I. M. Villaseñor, J. Angelada, A. P. Canlas, and D. Echevoyen, “Bioactivity studies on beta-sitosterol and its glucoside”, *Phyther. Res.*, vol. 16, no. 5, pp. 417–421, Aug. 2002.
- [262] M. S. Bin Sayeed, S. M. R. Karim, T. Sharmin, and M. M. Morshed, “Critical Analysis on Characterization, Systemic Effect, and Therapeutic Potential of Beta-Sitosterol: A Plant-Derived Orphan Phytosterol”, *Medicines*, vol. 3, no. 4, p. 29, Nov. 2016.
- [263] I. Kubo, Y. Xu, and K. Shimizu, “Antibacterial activity of ent-kaurene diterpenoids from *Rabdosia rosthornii*”, *Phyther. Res.*, vol. 18, no. 2, pp. 180–183, Feb. 2004.

- [264] M. Chandra et al., “ β -Selinene-Rich Essential Oils from the Parts of *Callicarpa macrophylla* and Their Antioxidant and Pharmacological Activities”, *Medicines*, vol. 4, no. 3, p. 52, Jul. 2017.
- [265] K. P. Anupama, O. Shilpa, A. Antony, and H. P. Gurushankara, “Jatamansinol from *Nardostachys jatamansi*: a multi-targeted neuroprotective agent for Alzheimer’s disease”, *J. Biomol. Struct. Dyn.*, pp. 1–21, 2021.
- [266] S. Chaudhary et al., “Evaluation of antioxidant and anticancer activity of extract and fractions of *Nardostachys jatamansi* DC in breast carcinoma”, *BMC Complement. Altern. Med.*, vol. 15, no. 50, Dec. 2015.
- [267] S. S. Cheng and S. T. Chang, “Bioactivity and characterization of exudates from *Cryptomeria japonica* bark”, *Wood Sci. Technol.*, vol. 48, no. 4, pp. 831–840, 2014.
- [268] Y. I. Matsushita, Y. H. Hwang, K. Sugamoto, and T. Matsui, “Antimicrobial activity of heartwood components of sugi (*Cryptomeria japonica*) against several fungi and bacteria”, *J. Wood Sci.*, vol. 52, no. 6, pp. 552–556, Dec. 2006.
- [269] Y. Wang, R. Liu, F. Meng, and Z. Su, “Antiproliferative activity of an angular furanocoumarin-oroselol in human oral cancer cells is mediated via autophagy induction, inhibition of cell migration, invasion, and downregulation of PI3K/AKT signalling pathway”, *Acta Biochim. Pol.*, vol. 69, no. 1, pp. 85–89, 2022.
- [270] J. Wang et al., “Structure-activity relationship and synthetic methodologies of α -santonin derivatives with diverse bioactivities: A mini-review”, *Eur. J. Med. Chem.*, vol. 175, pp. 215–233, Aug. 2019.
- [271] V. C. Roa-Linares et al., “Anti-herpetic and anti-dengue activity of abietane ferruginol analogues synthesized from (+)-dehydroabietylamine”, *Eur. J. Med. Chem.*, vol. 108, pp. 79–88, Jan. 2016.
- [272] M. A. González, J. Clark, M. Connelly, and F. Rivas, “Antimalarial activity of abietane ferruginol analogues possessing a phthalimide group”, *Bioorg. Med. Chem. Lett.*, vol. 24, no. 22, pp. 5234–5237, Nov. 2014.

- [273] H. Saijo, H. Kofujita, K. Takahashi, and T. Ashitani, “Antioxidant activity and mechanism of the abietane-type diterpene ferruginol”, *Nat. Prod. Res.*, vol. 29, no. 18, pp. 1739–1743, Sep. 2014.
- [274] A. K. Ghosh, M. Brindisi, D. Shahabi, M. E. Chapman, and A. D. Mesecar, “Drug Development and Medicinal Chemistry Efforts toward SARS-Coronavirus and Covid-19 Therapeutics”, *ChemMedChem*, vol. 15, no. 11, pp. 907–932, 2020.
- [275] Y. M. Báez-Santos, S. E. St John, and A. D. Mesecar, “The SARS-coronavirus papain-like protease: structure, function and inhibition by designed antiviral compounds.”, *Antiviral Res.*, vol. 115, no. March, pp. 21–38, Mar. 2015.
- [276] X. Gao et al., “Crystal structure of SARS-CoV-2 papain-like protease”, *Acta Pharm. Sin. B*, vol. 11, no. 1, pp. 237–245, 2021.
- [277] J. Shang et al., “Cell entry mechanisms of SARS-CoV-2”, *Proc. Natl. Acad. Sci. U. S. A.*, vol. 117, no. 21, pp. 11727–11734, May 2020.
- [278] J. Lan et al., “Structure of the SARS-CoV-2 spike receptor-binding domain bound to the ACE2 receptor.”, *Nature*, vol. 581, no. 7807, pp. 215–220, 2020.
- [279] R. Singh, V. K. Bhardwaj, J. Sharma, D. Kumar, and R. Purohit, “Identification of potential plant bioactive as SARS-CoV-2 Spike protein and human ACE2 fusion inhibitors”, *Comput. Biol. Med.*, vol. 136, no. 1, p. 104631, 2021.
- [280] G. K. Dresser, J. D. Spence, and D. G. Bailey, “Pharmacokinetic-pharmacodynamic consequences and clinical relevance of cytochrome P450 3A4 inhibition”, *Clin. Pharmacokinet.*, vol. 38, no. 1, pp. 41–57, 2000.
- [281] B. Knapp, L. Ospina, and C. M. Deane, “Avoiding False Positive Conclusions in Molecular Simulation: The Importance of Replicas”, *J. Chem. Theory Comput.*, vol. 14, no. 12, pp. 6127–6138, 2018.
- [282] W. Humphrey, A. Dalke, and K. Schulten, “VMD: visual molecular dynamics”, *J. Mol. Graph.*, vol. 14, no. 1, pp. 33–38, 1996.

- [283] K. Sargsyan, C. Grauffel, and C. Lim, “How Molecular Size Impacts RMSD Applications in Molecular Dynamics Simulations”, *J. Chem. Theory Comput.*, vol. 13, no. 4, pp. 1518–1524, Apr. 2017.
- [284] Z. M. Younossi, A. B. Koenig, D. Abdelatif, Y. Fazel, L. Henry, and M. Wymer, “Global epidemiology of nonalcoholic fatty liver disease-Meta-analytic assessment of prevalence, incidence, and outcomes”, *Hepatology*, vol. 64, no. 1, pp. 73–84, Jul. 2016.
- [285] Z. M. Younossi, G. Marchesini, H. Pinto-Cortez, and S. Petta, “Epidemiology of Nonalcoholic Fatty Liver Disease and Nonalcoholic Steatohepatitis: Implications for Liver Transplantation”, *Transplantation*, vol. 103, no. 1, pp. 22–27, Jan. 2019.
- [286] A. De and A. Duseja, “Nonalcoholic Fatty Liver Disease: Indian Perspective”, *Clin. liver Dis.*, vol. 18, no. 3, pp. 158–163, Sep. 2021.
- [287] I. Pierantonelli and G. Svegliati-Baroni, “Nonalcoholic Fatty Liver Disease: Basic Pathogenetic Mechanisms in the Progression from NAFLD to NASH”, *Transplantation*, vol. 103, no. e1, pp. e1–e13, 2019.
- [288] H. C. Masuoka and N. Chalasani, “Nonalcoholic fatty liver disease: An emerging threat to obese and diabetic individuals”, *Ann. N. Y. Acad. Sci.*, vol. 1281, no. 1, pp. 106–122, 2013.
- [289] M. S. Mundi, S. Velapati, J. Patel, T. A. Kellogg, B. K. Abu Dayyeh, and R. T. Hurt, “Evolution of NAFLD and Its Management”, *Nutr. Clin. Pract.*, vol. 35, no. 1, pp. 72–84, Feb. 2020.
- [290] A. Duseja et al., “Non-alcoholic Fatty Liver Disease and Metabolic Syndrome- Position Paper of the Indian National Association for the Study of the Liver, Endocrine Society of India, Indian College of Cardiology and Indian Society of Gastroenterology”, *J. Clin. Exp. Hepatol.*, vol. 5, no. 1, pp. 51–68, Mar. 2015.
- [291] P. Angulo, “Nonalcoholic fatty liver disease”, *N. Engl. J. Med.*, vol. 346, no. 16, pp. 1221–1231, Apr. 2002.

- [292] Y. Takahashi, K. Sugimoto, H. Inui, and T. Fukusato, “Current pharmacological therapies for nonalcoholic fatty liver disease / nonalcoholic steatohepatitis”, *World J. Gastroenterol.*, vol. 21, no. 13, pp. 3777–3785, 2015.
- [293] N. Chalasani et al., “The diagnosis and management of nonalcoholic fatty liver disease: Practice guidance from the American Association for the Study of Liver Diseases”, *Hepatology*, vol. 67, no. 1, pp. 328–357, Jan. 2018.
- [294] Z. Younossi et al., “Global Perspectives on Nonalcoholic Fatty Liver Disease and Nonalcoholic Steatohepatitis”, *Hepatology*, vol. 69, no. 6, pp. 2672–2682, Jun. 2019.
- [295] L. C. Bertot and L. A. Adams, “The Natural Course of Non-Alcoholic Fatty Liver Disease”, *Int. J. Mol. Sci.*, vol. 17, no. 5, p. 774, May 2016.
- [296] L. Parlati, M. Régnier, H. Guillou, and C. Postic, “New targets for NAFLD”, *JHEP reports Innov. Hepatol.*, vol. 3, no. 6, p. 100346, Dec. 2021.
- [297] R. Chander et al., “Evaluation of hepatoprotective activity of picroliv(from *Picrorhiza kurroa*) in *Mastomys natalensis* infected with *plasmodium berghei*”, *Indian J. Med. Res.*, vol. 92, no. 1, pp. 34–37, 1990.
- [298] P. Verma, V. Basu, V. Gupta, G. Saxena, and L. Ur Rahman, “Pharmacology and Chemistry of a Potent Hepatoprotective Compound Picroliv Isolated from the Roots and Rhizomes of *Picrorhiza kurroa* Royle ex Benth. (Kutki)”, *Curr. Pharm. Biotechnol.*, vol. 10, no. 6, pp. 641–649, 2009.
- [299] H. Dhama-Shah et al., “Picroside II attenuates fatty acid accumulation in HEPG2 cells via modulation of fatty acid uptake and synthesis”, *Clin. Mol. Hepatol.*, vol. 24, no. 1, pp. 77–87, 2018.
- [300] X. ying Tian and L. Liu, “Drug discovery enters a new era with multi-target intervention strategy”, *Chin. J. Integr. Med.*, vol. 18, no. 7, pp. 539–542, Jul. 2012.
- [301] M. Blencowe, T. Karunanayake, J. Wier, N. Hsu, and X. Yang, “Network Modeling Approaches and Applications to Unravelling Non-Alcoholic Fatty Liver Disease”, *Genes (Basel)*, vol. 10, no. 12, p. 966, Dec. 2019.

- [302] X. Song, Y. Zhang, E. Dai, L. Wang, and H. Du, “Prediction of triptolide targets in rheumatoid arthritis using network pharmacology and molecular docking”, *Int. Immunopharmacol.*, vol. 80, p. 106179, Mar. 2020.
- [303] R. Li, C. Guo, Y. Li, X. Liang, L. Yang, and W. Huang, “Therapeutic target and molecular mechanism of vitamin C-treated pneumonia: a systematic study of network pharmacology”, *Food Funct.*, vol. 11, no. 5, pp. 4765–4772, 2020.
- [304] S. Xinqiang, Z. Yu, Y. Ningning, D. Erqin, W. Lei, and D. Hongtao, “Molecular mechanism of celastrol in the treatment of systemic lupus erythematosus based on network pharmacology and molecular docking technology”, *Life Sci.*, vol. 240, p. 117063, 2019.
- [305] M. Zhang et al., “Network pharmacology analysis of Chaihu Lizhong Tang treating non- alcoholic fatty liver disease”, *Comput. Biol. Chem.*, vol. 86, no. 1, p. 107248, 2020.
- [306] S. Pathania, S. M. Ramakrishnan, and G. Bagler, “Phytochemica: A platform to explore phytochemicals of medicinal plants”, *Database*, vol. 2015, pp. 1–8, 2015.
- [307] X. Zeng et al., “NPASS: Natural product activity and species source database for natural product research, discovery and tool development”, *Nucleic Acids Res.*, vol. 46, no. D1, pp. D1217–D1222, 2018.
- [308] K. Mohanraj et al., “IMPPAT: A curated database of Indian Medicinal Plants, Phytochemistry and Therapeutics”, *Sci. Rep.*, vol. 8, no. 1, pp. 1–17, 2018.
- [309] Y. Cao, A. Charisi, L.-C. Cheng, T. Jiang, and T. Girke, “ChemmineR: a compound mining framework for R”, *Bioinformatics*, vol. 24, no. 15, pp. 1733–1734, 2008.
- [310] F. Mao et al., “Chemical structure-related drug-like criteria of global approved drugs”, *Molecules*, vol. 21, no. 1, pp. 1–18, 2016.
- [311] M. Awale and J. L. Reymond, “Polypharmacology Browser PPB2: Target Prediction Combining Nearest Neighbors with Machine Learning”, *J. Chem. Inf. Model.*, vol. 59, no. 1, pp. 10–17, Jan. 2019.

- [312] M. J. Keiser, B. L. Roth, B. N. Armbruster, P. Ernsberger, J. J. Irwin, and B. K. Shoichet, “Relating protein pharmacology by ligand chemistry”, *Nat. Biotechnol.*, vol. 25, no. 2, pp. 197–206, Feb. 2007.
- [313] A. Daina, O. Michielin, and V. Zoete, “SwissTargetPrediction: updated data and new features for efficient prediction of protein targets of small molecules”, *Nucleic Acids Res.*, vol. 47, no. W1, pp. W357–W364, Jul. 2019.
- [314] P. Shannon et al., “Cytoscape: A software Environment for integrated models of biomolecular interaction networks”, *Genome Res.*, vol. 13, no. 11, pp. 2498–2504, 2003.
- [315] M. Safran et al., “GeneCards Version 3: the human gene integrator”, *Database J. Biol. Databases Curation*, vol. 2010, pp. 1–16, Aug. 2010.
- [316] Y. Zhou et al., “Therapeutic target database update 2022: facilitating drug discovery with enriched comparative data of targeted agents”, *Nucleic Acids Res.*, vol. 50, no. D1, pp. D1398–D1407, 2022.
- [317] J. Piñero et al., “DisGeNET: a discovery platform for the dynamical exploration of human diseases and their genes”, *Database J. Biol. Databases Curation*, vol. 2015, pp. 1–17, Apr. 2015.
- [318] D. Szklarczyk et al., “STRING v11: protein–protein association networks with increased coverage, supporting functional discovery in genome-wide experimental datasets”, *Nucleic Acids Res.*, vol. 47, no. Database issue, p. D613, Jan. 2019.
- [319] R. J. Nijveldt, E. Van Nood, D. E. C. Van Hoorn, P. G. Boelens, K. Van Norren, and P. A. M. Van Leeuwen, “Flavonoids: a review of probable mechanisms of action and potential applications”, *Am. J. Clin. Nutr.*, vol. 74, no. 4, pp. 418–425, 2001.
- [320] J.-S. Choi and H.-K. Han, “The effect of quercetin on the pharmacokinetics of verapamil and its major metabolite, norverapamil, in rabbits”, *J. Pharm. Pharmacol.*, vol. 56, no. 12, pp. 1537–1542, Feb. 2004.

- [321] J. S. Choi and X. Li, "Enhanced diltiazem bioavailability after oral administration of diltiazem with quercetin to rabbits", *Int. J. Pharm.*, vol. 297, no. 1–2, pp. 1–8, Jun. 2005.
- [322] J. S. Choi, B. W. Jo, and Y. C. Kim, "Enhanced paclitaxel bioavailability after oral administration of paclitaxel or prodrug to rats pretreated with quercetin", *Eur. J. Pharm. Biopharm.*, vol. 57, no. 2, pp. 313–318, 2004.
- [323] Y. H. Wang, P. D. L. Chao, S. L. Hsiu, K. C. Wen, and Y. C. Hou, "Lethal quercetin-digoxin interaction in pigs", *Life Sci.*, vol. 74, no. 10, pp. 1191–1197, Jan. 2004.
- [324] S. C. Shin, J. S. Choi, and X. Li, "Enhanced bioavailability of tamoxifen after oral administration of tamoxifen with quercetin in rats", *Int. J. Pharm.*, vol. 313, no. 1–2, pp. 144–149, Apr. 2006.
- [325] G. Randhawa, J. Kullar, and Rajkumar, "Bioenhancers from mother nature and their applicability in modern medicine", *Int. J. Appl. Basic Med. Res.*, vol. 1, no. 1, pp. 5–10, 2011.
- [326] H. J. Murff et al., "Dietary intake of PUFAs and colorectal polyp risk", *Am. J. Clin. Nutr.*, vol. 95, no. 3, p. 712, Mar. 2012.
- [327] E. H. McCafferty and L. J. Scott, "Migalastat: A Review in Fabry Disease", *Drugs*, vol. 79, no. 5, pp. 543–554, Apr. 2019.
- [328] Z. Zhang and W. Tang, "Drug metabolism in drug discovery and development", *Acta Pharm. Sin. B*, vol. 8, no. 5, p. 732, Sep. 2018.
- [329] H. Han et al., "Synthesis and biological evaluation of picroside derivatives as hepatoprotective agents", *Nat. Prod. Res.*, vol. 33, no. 19, pp. 2845–2850, 2019.
- [330] R. Chander, N. K. Kapoor, and B. N. Dhawan, "Picroliv, picroside-I and kutkoside from *Picrorhiza kurroa* are scavengers of superoxide anions", *Biochem. Pharmacol.*, vol. 44, no. 1, pp. 180–183, 1992.
- [331] J. P. Gaddipati, S. Madhavan, G. S. Sidhu, A. K. Singh, P. Seth, and R. K. Maheshwari, "Picroliv - A natural product protects cells and regulates the gene

- expression during hypoxia/reoxygenation”, *Mol. Cell. Biochem.*, vol. 194, no. 1–2, pp. 271–281, 1999.
- [332] M. N. Mallick et al., “HPTLC Analysis of Bioactivity Guided Anticancer Enriched Fraction of Hydroalcoholic Extract of *Picrorhiza kurroa*”, *Biomed Res. Int.*, vol. 2015, no. 513875, 2015.
- [333] D. Rathee, V. Lather, A. S. Grewal, and H. Dureja, “Enzymatic inhibitory activity of iridoid glycosides from *Picrorrhiza kurroa* against matrix metalloproteinases: Correlating in vitro targeted screening and docking”, *Comput. Biol. Chem.*, vol. 78, no. 1, pp. 28–38, 2019.
- [334] D. Rathee, M. Thanki, S. Bhuvra, S. Anandjiwala, and R. Agrawal, “Iridoid glycosides-Kutkin, Picroside I, and Kutkoside from *Picrorrhiza kurroa* Benth inhibits the invasion and migration of MCF-7 breast cancer cells through the down regulation of matrix metalloproteinases. 1st Cancer Update.”, *Arab. J. Chem.*, vol. 6, no. 1, pp. 49–58, 2013.
- [335] P. Bhandari, N. Kumar, B. Singh, A. P. Gupta, V. K. Kaul, and P. S. Ahuja, “Stability-indicating LC-PDA method for determination of picrosides in hepatoprotective Indian herbal preparations of *Picrorhiza kurroa*”, *Chromatographia*, vol. 69, no. 3, pp. 221–227, 2009.
- [336] P. L. Dong, Z. L. Gao, X. Yin, Z. Q. Li, and H. Han, “Hepatoprotective activity assessment of amino acids derivatives of picroside I and II”, *Chem. Biol. Drug Des.*, vol. 97, no. 2, 2021.
- [337] Y. Dwivedi, R. Rastogi, R. Mehrotra, N. K. Garg, and B. N. Dhawan, “Picroliv protects against aflatoxin B1 acute hepatotoxicity in rats”, *Pharmacol. Res.*, vol. 27, no. 2, pp. 189–199, 1993.
- [338] G. B. Singh et al., “Antiinflammatory activity of the iridoids kutkin, picroside-1 and kutkoside from *Picrorhiza kurroa*”, *Phyther. Res.*, vol. 7, no. 6, pp. 402–407, 1993.

- [339] P. Li, K. Matsunaga, T. Yamakuni, and Y. Ohizumi, "Potentiation of nerve growth factor-action by picrosides I and II, natural iridoids, in PC12D cells", *Eur. J. Pharmacol.*, vol. 406, no. 2, pp. 203–208, 2000.
- [340] P. Li, K. Matsunaga, T. Yamakuni, and Y. Ohizumi, "Picrosides I and II, selective enhancers of the mitogen-activated protein kinase-dependent signaling pathway in the action of neurotogenic substances on PC12D cells", *Life Sci.*, vol. 71, no. 15, pp. 1821–1835, 2002.
- [341] J. Choi et al., "Picroside II attenuates airway inflammation by downregulating the transcription factor GATA3 and Th2-Related cytokines in a mouse model of HDM-Induced allergic asthma", *PLoS One*, vol. 11, no. 11, p. e0167098, 2016.
- [342] Y. Guo, X. Xu, Q. Li, Z. Li, and F. Du, "Anti-inflammation effects of picroside 2 in cerebral ischemic injury rats", *Behav. Brain Funct.*, vol. 6, no. 43, 2010.
- [343] Y. Huang et al., "Picroside II protects against sepsis via suppressing inflammation in mice", *Am. J. Transl. Res.*, vol. 8, no. 12, pp. 5519–5531, 2016.
- [344] C. Ma and A. Shi, "Picroside II prevents inflammation injury in mice with diabetic nephropathy via TLR4/NF- κ B pathway", *Qual. Assur. Saf. Crop. Foods*, vol. 13, no. 4, pp. 38–43, 2021.
- [345] L. Wang et al., "Effect of picroside II on apoptosis induced by renal ischemia/reperfusion injury in rats", *Exp. Ther. Med.*, vol. 9, no. 3, pp. 817–822, 2015.
- [346] L. Zhao, X. Li, T. Wang, Y. Guo, F. Pang, and C. Chang, "The anti-inflammatory effect of picroside II and the optimizing of therapeutic dose and time window in cerebral ischemic injury in rats", *Mod. Res. Inflamm.*, vol. 2, no. 3, 2013.
- [347] X. Piao, B. Liu, L. Guo, F. Meng, and L. Gao, "Picroside II Shows Protective Functions for Severe Acute Pancreatitis in Rats by Preventing NF-KB-Dependent Autophagy", *Oxid. Med. Cell. Longev.*, vol. 2017, no. 7085709, 2017.
- [348] A. Viljoen, N. Mncwangi, and I. Vermaak, "Anti-inflammatory iridoids of botanical origin", *Curr. Med. Chem.*, vol. 19, no. 14, pp. 2104–2127, 2012.

- [349] Q. Li, Z. Li, X. ying Xu, Y. liang Guo, and F. Du, “Neuroprotective properties of picroside II in a rat model of focal cereabral ischemia”, *Int. J. Mol. Sci.*, vol. 11, no. 11, pp. 4580–4590, 2010.
- [350] T. Li, J. W. Liu, X. D. Zhang, M. C. Guo, and G. Ji, “The neuroprotective effect of picroside II from Hu-Huang-lian against oxidative stress”, *Am. J. Chin. Med.*, vol. 35, no. 4, pp. 681–691, 2007.
- [351] S. Li et al., “Picroside II Exerts a Neuroprotective Effect by Inhibiting mPTP Permeability and EndoG Release after Cerebral Ischemia/Reperfusion Injury in Rats”, *J. Mol. Neurosci.*, vol. 64, no. 1, pp. 144–155, 2018.
- [352] Y. Wang et al., “Neuroprotective effect of picroside II in brain injury in mice”, *Am. J. Transl. Res.*, vol. 8, no. 12, pp. 5532–5544, 2016.
- [353] L. Zhao, Y. Guo, X. Ji, and M. Zhang, “The neuroprotective effect of picroside II via regulating the expression of myelin basic protein after cerebral ischemia injury in rats”, *BMC Neurosci.*, vol. 15, no. 25, 2014.
- [354] H. Dhami-shah et al., “13. Picroside ii reduces lipid accumulation, oxidative stress and mitochondrial dysfunction in in vitro NAFLD HePG2 cell model”, *J. Clin. Exp. Hepatol.*, vol. 8, no. 1, pp. 40–41, 2018.
- [355] H. Gao and Y. W. Zhou, “Inhibitory effect of picroside II on hepatocyte apoptosis”, *Acta Pharmacol. Sin.*, vol. 26, no. 6, pp. 729–736, 2005.
- [356] R. Kumar, Y. K. Gupta, S. Singh, and S. Arunraja, “*Picrorhiza kurroa* Inhibits Experimental Arthritis Through Inhibition of Pro-inflammatory Cytokines, Angiogenesis and MMPs”, *Phyther. Res.*, vol. 30, no. 1, pp. 112–119, 2016.
- [357] A. B. Vaidya, “*Picrorhiza kurroa* (kutaki) royle ex. benth as a hepatoprotective agent - Experimental & clinical studies”, *J. Postgrad. Med.*, vol. 42, no. 4, pp. 105–108, 1996.
- [358] M. Nandave et al., “Cardioprotective effect of root extract of *Picrorhiza kurroa* (Royle Ex Benth) against isoproterenol-induced cardiotoxicity in rats”, *Indian J. Exp. Biol.*, vol. 51, no. 9, pp. 694–701, 2013.

- [359] F. M. Çomu et al., “Effect of picroside II on erythrocyte deformability and lipid peroxidation in rats subjected to hind limb ischemia reperfusion injury”, *Drug Des. Devel. Ther.*, vol. 10, no. 1, pp. 927–931, 2016.
- [360] K. L. Joy, N. V. Rajeshkumar, G. Kuttan, and R. Kuttan, “Effect of *Picrorrhiza kurroa* extract on transplanted tumours and chemical carcinogenesis in mice”, *J. Ethnopharmacol.*, vol. 71, no. 1–2, pp. 261–266, 2000.
- [361] V. Rajkumar, G. Guha, and R. Ashok Kumar, “Antioxidant and anti-neoplastic activities of *Picrorrhiza kurroa* extracts”, *Food Chem. Toxicol.*, vol. 49, no. 2, pp. 363–369, 2011.
- [362] Y. Kılıç et al., “Effect of picroside II on hind limb ischemia reperfusion injury in rats”, *Drug Des. Devel. Ther.*, vol. 11, no. 1, pp. 1917–1925, 2017.
- [363] S. Sanjay, S. H. Banu, and M. Chethankumar, “The study of potentiality of *Picrorrhiza kurroa* root proteins to inhibit free radicals and α -Amylase enzyme”, *Asian J. Pharm. Clin. Res.*, vol. 8, no. 2, 2015.
- [364] S. S. Tiwari, M. M. Pandey, S. Srivastava, and A. Rawat, “TLC densitometric quantification of picrosides (picroside-I and picroside-II) in *Picrorrhiza kurroa* and its substitute *Picrorrhiza scrophulariiflora* and their antioxidant studies”, *Biomed. Chromatogr.*, vol. 26, no. 1, pp. 61–68, 2012.
- [365] L. Wang et al., “Picroside II protects rat kidney against ischemia/reperfusion-induced oxidative stress and inflammation by the TLR4/NF- κ B pathway”, *Exp. Ther. Med.*, vol. 9, no. 4, pp. 1253–1258, 2015.
- [366] D. Soni and A. Grover, ““Picrosides” from *Picrorrhiza kurroa* as potential anti-carcinogenic agents”, *Biomed. Pharmacother.*, vol. 109, no. 1, pp. 1680–1687, 2019.
- [367] P. Gupta et al., “Synergistic protective effect of picrorrhiza with honey in acetaminophen induced hepatic injury”, *Indian J. Exp. Biol.*, vol. 54, no. 8, pp. 530–536, 2016.

- [368] V. Prakash, A. Kumari, H. Kaur, M. Kumar, S. Gupta, and R. Bala, “Chemical constituents and biological activities of genus *Picrorhiza*: An update”, *Indian J. Pharm. Sci.*, vol. 82, no. 4, pp. 562–577, 2020.
- [369] M. Masood et al., “*Picrorhiza kurroa*: An ethnopharmacologically important plant species of Himalayan region”, *Pure Appl. Biol.*, vol. 4, no. 3, pp. 407–417, 2015.
- [370] M. Asnaashari, R. Farhoosh, and A. Sharif, “Antioxidant activity of gallic acid and methyl gallate in triacylglycerols of Kilka fish oil and its oil-in-water emulsion”, *Food Chem.*, vol. 159, pp. 439–444, 2014.
- [371] Ajazuddin et al., “Role of herbal bioactives as a potential bioavailability enhancer for Active Pharmaceutical Ingredients”, *Fitoterapia*, vol. 97, pp. 1–14, 2014.
- [372] G. B. Dudhatra et al., “A comprehensive review on pharmacotherapeutics of herbal bioenhancers”, *Sci. World J.*, vol. 2012, p. 637953, 2012.
- [373] B. Peterson, M. Weyers, J. H. Steenekamp, J. D. Steyn, C. Gouws, and J. H. Hamman, “Drug bioavailability enhancing agents of natural origin (bioenhancers) that modulate drug membrane permeation and pre-systemic metabolism”, *Pharmaceutics*, vol. 11, no. 1, p. 33, 2019.
- [374] W. R. García-Niño and C. Zazueta, “Ellagic acid: Pharmacological activities and molecular mechanisms involved in liver protection”, *Pharmacol. Res.*, vol. 97, no. 1, pp. 84–103, 2015.
- [375] K. Singh, A. K. Khanna, and R. Chander, “Hepatoprotective activity of ellagic acid against carbon tetrachloride induced hepatotoxicity in rats”, *Indian J. Exp. Biol.*, vol. 37, no. 10, pp. 1025–1026, 1999.
- [376] A. Y. Chen and Y. C. Chen, “A review of the dietary flavonoid, kaempferol on human health and cancer chemoprevention”, *Food Chem.*, vol. 138, no. 4, pp. 2099–2107, 2013.
- [377] M. Imran et al., “Kaempferol: A key emphasis to its anticancer potential”, *Molecules*, vol. 24, no. 12, p. 2277, 2019.

- [378] J. M. Calderon-Montano, E. Burgos-Moron, C. Perez-Guerrero, and M. Lopez-Lazaro, "A Review on the Dietary Flavonoid Kaempferol", *Mini-Reviews Med. Chem.*, vol. 11, no. 4, pp. 298–344, 2011.
- [379] J. Wang et al., "Antitumor, antioxidant and anti-inflammatory activities of kaempferol and its corresponding glycosides and the enzymatic preparation of kaempferol", *PLoS One*, vol. 13, no. 5, p. e0197563, 2018.
- [380] A. A. Boligon et al., "Protective effects of extracts and flavonoids isolated from *scutia buxifolia* reissek against chromosome damage in human lymphocytes exposed to hydrogen peroxide", *Molecules*, vol. 17, no. 5, pp. 5757–5769, 2012.
- [381] A. W. Boots, G. R. M. M. Haenen, and A. Bast, "Health effects of quercetin: From antioxidant to nutraceutical", *Eur. J. Pharmacol.*, vol. 585, no. 2–3, pp. 325–337, 2008.
- [382] S. H. Jung, B. J. Kim, E. H. Lee, and N. N. Osborne, "Isoquercitrin is the most effective antioxidant in the plant *Thuja orientalis* and able to counteract oxidative-induced damage to a transformed cell line (RGC-5 cells)", *Neurochem. Int.*, vol. 57, no. 7, pp. 713–721, 2010.
- [383] R. Bhimanwar, L. Kothapalli, and A. Khawshi, "Quercetin as natural bioavailability modulator: An overview", *Res. J. Pharm. Technol.*, vol. 13, no. 4, pp. 2045–2052, 2020.
- [384] A. P. Rogerio et al., "Anti-inflammatory activity of quercetin and isoquercitrin in experimental murine allergic asthma", *Inflamm. Res.*, vol. 56, no. 10, pp. 402–408, 2007.
- [385] B. Jayaprakasam, N. P. Seeram, and M. G. Nair, "Anticancer and antiinflammatory activities of cucurbitacins from *Cucurbita andreana*", *Cancer Lett.*, vol. 189, no. 1, pp. 11–16, 2003.
- [386] K. L. K. Duncan, M. D. Duncan, M. C. Alley, and E. A. Sausville, "Cucurbitacin E-induced disruption of the actin and vimentin cytoskeleton in prostate carcinoma cells", *Biochem. Pharmacol.*, vol. 52, no. 10, pp. 1553–1560, 1996.

- [387] S. Duangmano, S. Dakeng, W. Jiratchariyakul, A. Suksamrarn, D. R. Smith, and P. Patmasiriwat, "Antiproliferative effects of cucurbitacin B in breast cancer cells: Down-regulation of the c-Myc/hTERT/telomerase pathway and obstruction of the cell cycle", *Int. J. Mol. Sci.*, vol. 11, no. 12, pp. 5323–5338, 2010.
- [388] U. Kaushik, V. Aeri, and S. R. Mir, "Cucurbitacins - An insight into medicinal leads from nature", *Pharmacogn. Rev.*, vol. 9, no. 17, pp. 12–18, 2015.
- [389] C. S. Park et al., "Inhibition of Nitric Oxide Generation by 23,24-Dihydrocucurbitacin D in Mouse Peritoneal Macrophages", *J. Pharmacol. Exp. Ther.*, vol. 309, no. 2, pp. 705–710, 2004.
- [390] Y. Dong et al., "Cucurbitacin E, a tetracyclic triterpenes compound from Chinese medicine, inhibits tumor angiogenesis through VEGFR2-mediated Jak2-STAT3 signaling pathway", *Carcinogenesis*, vol. 31, no. 12, pp. 2097–2104, 2010.
- [391] J. Guerrero-Analco et al., "Antidiabetic properties of selected Mexican copalchis of the Rubiaceae family", *Phytochemistry*, vol. 68, no. 15, pp. 2087–2095, 2007.
- [392] A. Agil et al., "Isolation of an anti-hepatotoxic principle from the juice of *Ecballium elaterium*", *Planta Med.*, vol. 65, no. 7, pp. 673–675, 1999.
- [393] M. Miró, "Cucurbitacins and their pharmacological effects", *Phyther. Res.*, vol. 9, no. 3, pp. 159–168, 1995.
- [394] J. M. Escandell et al., "Activated kRas protects colon cancer cells from cucurbitacin-induced apoptosis: The role of p53 and p21", *Biochem. Pharmacol.*, vol. 76, no. 2, pp. 198–207, 2008.
- [395] L. Yin et al., "Bioactivity-guided isolation of antioxidant and anti-hepatocarcinoma constituents from *Veronica ciliata*", *Chem. Cent. J.*, vol. 10, no. 27, 2016.
- [396] P. Picerno, G. Autore, S. Marzocco, M. Meloni, R. Sanogo, and R. P. Aquino, "Anti-inflammatory activity of verminoside from *Kigelia africana* and evaluation of cutaneous irritation in cell cultures and reconstituted human epidermis", *J. Nat. Prod.*, vol. 68, no. 11, pp. 1610–1614, 2005.

- [397] N. Bharti, S. Singh, F. Naqvi, and A. Azam, "Isolation and in vitro antiamoebic activity of iridoids isolated from *Kigelia pinnata*", *Arkivoc*, vol. 2006, no. 10, pp. 69–76, 2006.
- [398] J. Y. Hung, C. J. Yang, Y. M. Tsai, H. W. Huang, and M. S. Huang, "Antiproliferative activity of aucubin is through cell cycle arrest and apoptosis in human non-small cell lung cancer A549 cells", *Clin. Exp. Pharmacol. Physiol.*, vol. 35, no. 9, pp. 995–1001, 2008.
- [399] H. J. Koo, K. H. Lim, H. J. Jung, and E. H. Park, "Anti-inflammatory evaluation of gardenia extract, geniposide and genipin", *J. Ethnopharmacol.*, vol. 103, no. 3, pp. 496–500, 2006.
- [400] H. Y. Hsu, J. J. Yang, S. Y. Lin, and C. C. Lin, "Comparisons of geniposidic acid and geniposide on antitumor and radioprotection after sublethal irradiation", *Cancer Lett.*, vol. 113, no. 1–2, pp. 31–37, 1997.
- [401] H. T. Liu et al., "Geniposide inhibits interleukin-6 and interleukin-8 production in lipopolysaccharide-induced human umbilical vein endothelial cells by blocking p38 and ERK1/2 signaling pathways", *Inflamm. Res.*, vol. 59, no. 6, pp. 451–461, 2010.
- [402] B. Xu et al., "Geniposide ameliorates TNBS-induced experimental colitis in rats via reducing inflammatory cytokine release and restoring impaired intestinal barrier function", *Acta Pharmacol. Sin.*, vol. 38, no. 5, pp. 688–698, 2017.
- [403] C. Zhao et al., "Geniposide ameliorates cognitive deficits by attenuating the cholinergic defect and amyloidosis in middle-aged Alzheimer model mice", *Neuropharmacology*, vol. 116, no. 1, pp. 18–29, 2017.
- [404] Y. Zhang et al., "Geniposide acutely stimulates insulin secretion in pancreatic β -cells by regulating GLP-1 receptor/cAMP signaling and ion channels", *Mol. Cell. Endocrinol.*, vol. 430, no. 1, pp. 89–96, 2016.
- [405] J. Liu, F. Yin, X. Zheng, J. Jing, and Y. Hu, "Geniposide, a novel agonist for GLP-1 receptor, prevents PC12 cells from oxidative damage via MAP kinase pathway", *Neurochem. Int.*, vol. 51, no. 6–7, pp. 361–369, 2007.

- [406] N. K. Lee, "Preservation effects of geniposidic acid on human keratinocytes (HaCaT) against UVB", *Biomed. Dermatology*, vol. 5, no. 2, 2018.
- [407] S. K. Bhattamisra, K. H. Yap, V. Rao, and H. Choudhury, "Multiple Biological Effects of an Iridoid Glucoside, Catalpol and Its Underlying Molecular Mechanisms", *Biomolecules*, vol. 10, no. 1, p. 32, Jan. 2019.
- [408] R. Fan et al., "Protective effect of apocynin in an established alcoholic steatohepatitis rat model", *Immunopharmacol. Immunotoxicol.*, vol. 34, no. 4, pp. 633–638, 2012.
- [409] Y. Sun et al., "Therapeutic effect of apocynin through antioxidant activity and suppression of apoptosis and inflammation after spinal cord injury", *Exp. Ther. Med.*, vol. 13, no. 3, pp. 952–960, 2017.
- [410] A. Simonyi et al., "The neuroprotective effects of apocynin", *Front. Biosci. - Elit.*, vol. 4, no. 1, pp. 2183–2193, 2012.
- [411] B. A. 'T Hart, S. Copray, and I. Philippens, "Apocynin, a low molecular oral treatment for neurodegenerative disease", *Biomed Res. Int.*, vol. 2014, no. 298020, 2014.
- [412] S. Hougee et al., "Oral administration of the NADPH-oxidase inhibitor apocynin partially restores diminished cartilage proteoglycan synthesis and reduces inflammation in mice", *Eur. J. Pharmacol.*, vol. 531, no. 1–3, pp. 264–269, 2006.
- [413] S. W. Wang et al., "Rutin inhibits β -amyloid aggregation and cytotoxicity, attenuates oxidative stress, and decreases the production of nitric oxide and proinflammatory cytokines", *Neurotoxicology*, vol. 33, no. 3, pp. 482–490, Jun. 2012.
- [414] D. G. Machado et al., "Antidepressant-like effect of rutin isolated from the ethanolic extract from *Schinus molle* L. in mice: Evidence for the involvement of the serotonergic and noradrenergic systems", *Eur. J. Pharmacol.*, vol. 587, no. 1–3, pp. 163–168, Jun. 2008.
- [415] N. T. Niture, A. A. Ansari, and S. R. Naik, "Anti-hyperglycemic activity of rutin in streptozotocin-induced diabetic rats: an effect mediated through cytokines,

- antioxidants and lipid biomarkers - PubMed”, *Indian J. Exp. Biol.*, vol. 52, no. 7, pp. 720–727, 2014, Accessed: Jul. 2022.
- [416] E. A. Ostrakhovitch and I. B. Afanas’ev, “Oxidative stress in rheumatoid arthritis leukocytes: suppression by rutin and other antioxidants and chelators”, *Biochem. Pharmacol.*, vol. 62, no. 6, pp. 743–746, Sep. 2001.
- [417] A. Kanashiro et al., “Modulatory effects of rutin on biochemical and hematological parameters in hypercholesterolemic Golden Syrian hamsters”, *An. Acad. Bras. Cienc.*, vol. 81, no. 1, pp. 67–72, 2009.
- [418] L. Fengyang et al., “Astragalín suppresses inflammatory responses via down-regulation of NF- κ B signaling pathway in lipopolysaccharide-induced mastitis in a murine model”, *Int. Immunopharmacol.*, vol. 17, no. 2, pp. 478–482, Oct. 2013.
- [419] A. Riaz et al., “Astragalín: A Bioactive Phytochemical with Potential Therapeutic Activities”, *Adv. Pharmacol. Sci.*, vol. 2018, no. 9794625, 2018.
- [420] E. Ohkoshi, H. Miyazaki, K. Shindo, H. Watanabe, A. Yoshida, and H. Yajima, “Constituents from the Leaves of *Nelumbo nucifera* Stimulate Lipolysis in the White Adipose Tissue of Mice”, *Planta Med.*, vol. 73, no. 12, pp. 1255–1259, Oct. 2007.
- [421] J. Choi, H. J. Kang, S. Z. Kim, T. O. Kwon, S. Il Jeong, and S. Il Jang, “Antioxidant effect of astragalín isolated from the leaves of *Morus alba* L. against free radical-induced oxidative hemolysis of human red blood cells”, *Arch. Pharm. Res.*, vol. 36, no. 7, pp. 912–917, Mar. 2013.
- [422] P. V. Kumar, A. Sivaraj, G. Madhumitha, A. M. Saral, and B. S. Kumar, “In-vitro anti-bacterial activities of *Picrorhiza kurroa* rhizome extract using agar well diffusion method”, *Int. J. Curr. Pharm. Res.*, vol. 2, no. 1, pp. 30–33, 2010.
- [423] R. Tundis, M. Loizzo, F. Menichini, G. Statti, and F. Menichini, “Biological and Pharmacological Activities of Iridoids: Recent Developments”, *Mini-Reviews Med. Chem.*, vol. 8, no. 4, pp. 399–420, 2008.
- [424] B. L. Athukuri and P. Neerati, “Enhanced Oral Bioavailability of Diltiazem by the Influence of Gallic Acid and Ellagic Acid in Male Wistar Rats: Involvement of

- CYP3A and P-gp Inhibition”, *Phytother. Res.*, vol. 31, no. 9, pp. 1441–1448, Sep. 2017.
- [425] B. L. Athukuri and P. Neerati, “Enhanced oral bioavailability of metoprolol with gallic acid and ellagic acid in male Wistar rats: involvement of CYP2D6 inhibition”, *Drug Metab. Pers. Ther.*, vol. 31, no. 4, pp. 229–234, Dec. 2016.
- [426] S. Jing et al., “Cucurbitacins: Bioactivities and synergistic effect with small-molecule drugs”, *J. Funct. Foods*, vol. 72, no. 1, p. 104042, Sep. 2020.
- [427] J. Stefanska and R. Pawliczak, “Apocynin: Molecular Aptitudes”, *Mediators Inflamm.*, vol. 2008, p. 106507, 2008, doi: 10.1155/2008/106507.
- [428] S. Sharma, A. Ali, J. Ali, J. K. Sahni, and S. Baboota, “Rutin : therapeutic potential and recent advances in drug delivery”, *Expert Opin. Investig. Drugs*, vol. 22, no. 8, pp. 1063–1079, Aug. 2013.
- [429] K. Lee et al., “Hepatic mitochondrial defects in a nonalcoholic fatty liver disease mouse model are associated with increased degradation of oxidative phosphorylation subunits”, *Mol. Cell. Proteomics*, vol. 17, no. 12, pp. 2371–2386, 2018.
- [430] M. Pérez-Carreras et al., “Defective hepatic mitochondrial respiratory chain in patients with nonalcoholic steatohepatitis”, *Hepatology*, vol. 38, no. 4, pp. 999–1004, 2003.
- [431] P. Martín-Sanz, M. Casado, and L. Boscá, “Cyclooxygenase 2 in liver dysfunction and carcinogenesis: Facts and perspectives”, *World J. Gastroenterol.*, vol. 23, no. 20, p. 3580, May 2017.
- [432] W. J. H. Koopman et al., “Human NADH:ubiquinone oxidoreductase deficiency: Radical changes in mitochondrial morphology?”, *Am. J. Physiol. - Cell Physiol.*, vol. 293, no. 1, pp. C22–C29, 2007.
- [433] M. S. Petrônio, M. L. Zeraik, L. M. Da Fonseca, and V. F. Ximenes, “Apocynin: Chemical and biophysical properties of a NADPH oxidase inhibitor”, *Molecules*, vol. 18, no. 3, pp. 2821–2839, 2013.

- [434] L. S. Lu et al., “Apocynin alleviated hepatic oxidative burden and reduced liver injury in hypercholesterolaemia”, *Liver Int.*, vol. 27, no. 4, pp. 529–537, 2007.
- [435] D. L. Zhu, R. Meng, Y. Bi, D. H. Yang, and Y. P. Wang, “Apocynin improves insulin resistance through suppressing inflammation in high-fat diet-induced obese mice”, *Mediators Inflamm.*, vol. 2010, no. 1, p. 858735, 2010.
- [436] P. Balakumar, M. Rose, S. S. Ganti, P. Krishan, and M. Singh, “PPAR dual agonists: are they opening Pandora’s Box?”, *Pharmacol. Res.*, vol. 56, no. 2, pp. 91–98, Aug. 2007.
- [437] M. R. Jain et al., “Saroglitazar, a novel PPAR α / γ agonist with predominant PPAR α activity, shows lipid-lowering and insulin-sensitizing effects in preclinical models”, *Pharmacol. Res. Perspect.*, vol. 3, no. 3, p. e00136, 2015.
- [438] S. Kakino et al., “Pivotal Role of TNF- α in the Development and Progression of Nonalcoholic Fatty Liver Disease in a Murine Model”, *Horm. Metab. Res.*, vol. 50, no. 1, pp. 80–87, 2018.
- [439] J. Khura, T. R. Khurana, S. Mehra, and P. Singh, “Evaluation of Pro-Inflammatory Markers IL-6 and TNF- α and their Correlation with Non-Alcoholic Fatty Liver Disease”, *J. Adv. Res. Med.*, vol. 6, no. 2, pp. 1–6, 2019.
- [440] K. Ishihara and T. Hirano, “IL-6 in autoimmune disease and chronic inflammatory proliferative disease”, *Cytokine Growth Factor Rev.*, vol. 13, no. 4–5, pp. 357–368, Aug. 2002.
- [441] B. Nair and L. Nath R., “Inevitable role of TGF- β 1 in progression of nonalcoholic fatty liver disease”, *J. Recept. Signal Transduct.*, vol. 40, no. 3, pp. 195–200, 2020.
- [442] S. Thapaliya et al., “Caspase 3 inactivation protects against hepatic cell death and ameliorates fibrogenesis in a diet-induced NASH model”, *Dig. Dis. Sci.*, vol. 59, no. 6, pp. 1197–1206, 2014.
- [443] M. Shiffman et al., “Randomised clinical trial: emricasan versus placebo significantly decreases ALT and caspase 3/7 activation in subjects with non-alcoholic fatty liver disease”, *Aliment. Pharmacol. Ther.*, vol. 49, no. 1, pp. 64–73, 2019.

- [444] N. Nasiri-Ansari et al., “Empagliflozin attenuates non-alcoholic fatty liver disease (NAFLD) in high fat diet fed ApoE(-/-) mice by activating autophagy and reducing ER stress and apoptosis”, *Int. J. Mol. Sci.*, vol. 22, no. 2, p. 818, 2021.
- [445] B. Bhushan et al., “Pharmacologic Inhibition of Epidermal Growth Factor Receptor Suppresses Nonalcoholic Fatty Liver Disease in a Murine Fast-Food Diet Model”, *Hepatology*, vol. 70, no. 5, pp. 1456–1563, 2019.
- [446] X. Xie et al., “Enhancement of Adiponectin Ameliorates Nonalcoholic Fatty Liver Disease via Inhibition of FoxO1 in Type I Diabetic Rats”, *J. Diabetes Res.*, vol. 2018, no. 1, p. 6254340, 2018.
- [447] W. Somers, M. Stahl, and J. S. Seehra, “1.9 Å crystal structure of interleukin 6: Implications for a novel mode of receptor dimerization and signaling”, *EMBO J.*, vol. 16, no. 5, pp. 989–997, 1997.
- [448] M. A. Ashwell et al., “Discovery and optimization of a series of 3-(3-phenyl-3H-imidazo[4,5-b]pyridin-2-yl)pyridin-2-amines: orally bioavailable, selective, and potent ATP-independent Akt inhibitors”, *J. Med. Chem.*, vol. 55, no. 11, pp. 5291–5310, Jun. 2012.
- [449] N. Mahindroo et al., “Indol-1-yl acetic acids as peroxisome proliferator-activated receptor agonists: Design, synthesis, structural biology, and molecular docking studies”, *J. Med. Chem.*, vol. 49, no. 3, pp. 1212–1216, 2006.
- [450] S. Kamata et al., “PPAR α Ligand-Binding Domain Structures with Endogenous Fatty Acids and Fibrates”, *iScience*, vol. 23, no. 11, p. 101727, 2020.
- [451] Z. Wang et al., “Kinetic and structural characterization of caspase-3 and caspase-8 inhibition by a novel class of irreversible inhibitors”, *Biochim. Biophys. Acta*, vol. 1804, no. 9, pp. 1817–1831, 2010.
- [452] J. Lategahn et al., “Targeting Her2-insYVMA with Covalent Inhibitors - A Focused Compound Screening and Structure-Based Design Approach”, *J. Med. Chem.*, vol. 63, no. 20, pp. 11725–11755, 2020.

- [453] S. Radaev, Z. Zou, T. Huang, E. M. Lafer, A. P. Hinck, and P. D. Sun, “Ternary complex of transforming growth factor- β 1 reveals isoform-specific ligand recognition and receptor recruitment in the superfamily”, *J. Biol. Chem.*, vol. 285, no. 19, pp. 14806–14814, 2010.
- [454] H. Y. Xiao et al., “Biologic-like in Vivo Efficacy with Small Molecule Inhibitors of TNF α Identified Using Scaffold Hopping and Structure-Based Drug Design Approaches”, *J. Med. Chem.*, vol. 63, no. 23, pp. 15050–15071, 2020.
- [455] D. A. Schuetz et al., “Ligand Desolvation Steers On-Rate and Impacts Drug Residence Time of Heat Shock Protein 90 (Hsp90) Inhibitors”, *J. Med. Chem.*, vol. 61, no. 10, pp. 4397–4411, May 2018.
- [456] F. Xiao-yan, D. Ting-ting, L. Ya-ya, X. Wei-ren, and C. Xian-chao, “In-silico Identification of peroxisome proliferatoractivated receptor (PPAR) α/γ agonists from Ligand Expo Components database”, *J. Biomol. Struct. Dyn.*, vol. 39, no. 5, pp. 1853–1864, 2020.

APPENDICES

Table A1: Medicinal value of *Picrorhiza kurroa* compounds

Chemical class	Chemical Name	Biaoactivity
Irodoid Glycosides (monoterpenes)	Picroside I	anti-oxidant
		anti-cancer
		hepatoprotective
		anti-inflammatory
	Picroside II	anti neronalapoptosis
		anti-inflammatory
		Neuroprotective
		hepatoprotective
		Cardio-protective
		anti-oxidant
		anti-apoptotic
	Picroside III	anti-inflammatory
		hepatoprotective
		antihypoglycaemic
		antimutagenic
		antispasmodic
		anti-tumor
		antiviral
		immunomodulatory
	purgative effects	
	Picroside IV	anti-inflammatory
	Picroside V	anti-inflammatory
	Kutkoside	anti-oxidant
		anti-cancer
		anti-inflammatory
	Geniposidic acid	anti-inflammatory
		Sedative
		antidibetic
antiphlogistic		
hepatoprotective		
Anti-cholestasis		
neuroprotectice		
anti-oxidant		
antithrombotic		
anti-tumor		
6-ferulloylcatalpol	anti-inflammatory	
Veronicoside	anti-oxidant	
Minecoside	anti-inflammatory	
Verminoside	anti-hepatocarcinogenic	
	anti-inflammatory	
	anti-amoebic	

	Specioside	anti-amoebic
	Catalpol	antihyperglycemic (Diabetes mellitus)
		neuroprotective
		anti-cancer
		antiapoptosis
	Boschnalosite	Antisenile agent
	Aucubin	antiproliferative
		antihyperglycemic (Diabetes mellitus)
		hypertension
		anti-oxidant
		anti-inflammatory
Glycosides	Ellagic acid	anti-oxidant
		hepatoprotective
		antisteatotic
		anticholestatic
		antifibrogenic
		anti-hepatocarcinogenic
		antiviral
	4-hydroxyl-3-methoxy-acetophenone	anti-asthmatic
	Kutkiol	hepatoprotective
Kutkisterol	hepatoprotective	
Anhydromaggiemycin	anti-tumor	
Trifolin	antifungal	
Cucurbitacin Glycosides	Cucurbitacin glycoside 1	Tumor inhibition
		hepatoprotective
		anti-inflammatory
	2-O-glucoside of cucurbitacin B	anti-inflammatory
		anti-tumor
		hepatoprotective
		anti-inflammatory
	anti-tumor	
	hepatoprotective	
Phenolic Glycosides	Picein	anti-oxidant
	Apocynin	anti-oxidant
		anti-inflammatory
	Androsin	antiallergen
antiasthmatic		
Phenyletanoid glycoside	Plantainoside D	anti-oxidant
		cardioprotective
		anti-apoptotic

Phenols	Catechol	anti-oxidant
Oxazines	Chandrananimycin D	anticancer
organooxygen	Acetovanillone	anti-inflammatory
		anti-rheumatic
Terpenoids (triterpenes)	Cucurbitacin B	anti-inflammatory
		anti-tumor
		antiproliferative
		anti-cancer
		Anti-atherosclerotic
		anti-inflammatory
	Cucurbitacin D	anti-tumor
		anti-inflammatory
	Cucurbitacin E	anti-tumor
		antiproliferative
		Anti-atherosclerotic
		antihyperglycemic (Diabetes mellitus)
	Cucurbitacin F	anti-inflammatory
	Cucurbitacin I	anticancer/antitumor
anti-cancer		
Cucurbitacin R	hepatoprotective	
	anti-inflammatory	
	anti-dibetic	
Cucurbitacin P	anti-dibetic	
Steroids	FORMOCORTAL	anticancer
		anti-inflammatory
Flavonoid	Kaempferol	anti-cancer
		anti-tumor
		anti-oxidant
		anti-inflammatory
		cardioprotective
		neuroprotective
	Astragaln	anti-cancer
		anti-inflammatory
		anti-oxidant
		neuroprotective
		anti-dibetic
		cardioprotective
		antiulcer
		anti-fibrotic
	Rutin	antioxidant
		anti-inflammatory
		Hepatoprotective
		vasoprotective

		anticarcinogenic
		neuroprotective
		cardioprotective
		anti-cancer
		anti-arthritic
		anti-asthmatic
		gastroprotective (antiulcer)
	Isoquercetin	anti-oxidant
	Isoquercetin	anti-inflammatory
	Isoquercetin	anti-asthmatic
	Isoquercetin	anti-tumor
	Isoquercetin	diuretic
	Nicotifloroside	hepatoprotective
	Nicotifloroside	neuroprotective
	Quercetin	anti-oxidant
	Quercetin	anti-inflammatory
	Formononetin	anti-cancer
Cinnamic acids	6'-Cinnamoylcatalpol	anti-inflammatory
Carboxylic acids	Cinnamic acid	anti-oxidant
		antimicrobial
	Vanillic acid	antibacterial
		antimicrobial
		chemopreventive
		anti-inflammatory
Gallic acid	anti-oxidant	
Alcohols	D-mannitol	anti-oxidant

Table A2: Compounds with highest binding affinity with residues present other than active site pocket of Mpro

Compound Name	Binding Energy
reduced lantadene a	-9.5
lantadene a	-9.3
friedelan-3-one	-9.3
lantadene c	-9.2
lantadene d	-8.9
lantadene b	-8.9
reduced lantadene b	-8.9
alpha-amyrenone	-8.5
beta-amyrin	-8.5
alpha-amyrin	-8.5

Table A3: Compounds with highest binding affinity with residues present other than active site pocket of Pappain-Like Protease

Compound Name	Binding Energy
alpha-amyrenone	-7.8
reduced lantadene a	-7.7
beta-amyrin	-7.6
alpha-amyrin	-7.6
reduced lantadene b	-7.5
abietal	-7.4
lantadene a	-7.4
lantadene d	-7.4
lantadene b	-7.4
lantadene c	-7.3
abietol	-7.2
6,7-dehydroferruginol	-7.2
isopimaradiene	-7.2
beta-sitosterol	-7.1
abietadiene	-7.1
dehydroabietol	-7.1
friedelan-3-one	-7.1

Table A4: Compounds with highest binding affinity with residues present other than active site pocket of RNA dependent RNA polymerase

Compound Name	Binding Energy
friedelan-3-one	-9.1
beta-amyrin	-9
alpha-amyrenone	-8.7
abieta-8,12-diene	-8.5
isokaurene	-8.5
khusinol	-8.5
alpha-amyrin	-8.5
abietatriene	-8.4
kaur-16-ene	-8.4
pimara-8,15-diene	-8.4
isophyllocladene	-8.2
reduced lantadene a	-8.2
dehydroabietal	-8.2
nezukol	-8.2
isohibaene	-8.2
trans-totarol	-8.1
abietadiene	-8.1
lantadene a	-8.1
rimuene	-8.1
lantadene b	-8.1
(11E,13Z)-Labdadien-8-ol	-8.1

Table A5: Compounds with highest binding affinity with residues present other than active site pocket of Spike Glycoprotein

Compound Name	Binding Energy
alpha-amyrone	-8.9
beta-amyrin	-8.8
reduced lantadene b	-8.6
perfluorotributylamine	-8.6
alpha-amyrin	-8.6
friedelan-3-one	-8.6
reduced lantadene a	-8.4
kaur-15-ene	-8.3
beyerene	-8.3
kaurene	-8.2
isophyllocladene	-8.2
lantadene a	-8.1
lantadene b	-8.1
lantadene c	-8
lantadene d	-8

Table A7: Compound-Target Interaction. Relationship of 914 protein targets of all compounds with other compounds in the extracts. Individual compound has multiple targets and vice-versa.

		P-I	P-II	P-III	P-IV	P-V	CB	CD	CE	CF	CI	CP	CR	EA	GA	GCA	KF	QR	RT	AC	AG	AB	CP	VM	VN	
1	JUN		✓																	✓						
2	ABAT														✓					✓						
3	ABCB1					✓					✓	✓	✓				✓	✓		✓	✓					
4	ABCB1A																		✓							
5	ABCB2																				✓					
6	ABCC1																✓	✓	✓	✓	✓					
7	ABCC2																		✓	✓	✓					
8	ABCG2																✓	✓	✓	✓	✓					
9	ABL1	✓	✓	✓	✓	✓			✓															✓	✓	
10	ACE	✓		✓	✓											✓	✓			✓		✓	✓	✓	✓	✓
11	ACE2		✓		✓																				✓	
12	ACHE			✓			✓	✓	✓	✓	✓	✓	✓	✓	✓				✓	✓	✓	✓				
13	ACLY															✓	✓		✓	✓			✓			
14	ACP1											✓						✓	✓	✓		✓				
15	ACVRL1							✓		✓		✓														
16	ADA															✓						✓	✓			
17	ADAM10					✓			✓																	
18	ADAM17				✓	✓							✓													
19	ADAMTS4						✓						✓													
20	ADAMTS5						✓						✓													
21	ADCY1						✓	✓	✓	✓	✓	✓														
22	ADCYAP1R1																			✓						
23	ADH1A													✓												
24	ADK	✓	✓		✓											✓							✓	✓		✓
25	ADOK																					✓				
26	ADORA1	✓	✓	✓	✓				✓					✓		✓	✓	✓	✓		✓	✓	✓	✓	✓	
27	ADORA2A	✓	✓	✓	✓	✓		✓	✓							✓	✓	✓	✓			✓	✓	✓	✓	✓
28	ADORA2B	✓	✓		✓	✓	✓	✓														✓		✓	✓	✓
29	ADORA3	✓	✓	✓	✓	✓				✓		✓				✓	✓		✓		✓	✓	✓	✓	✓	✓
30	ADRA1A														✓											
31	ADRA1D														✓											
32	ADRA2A														✓				✓		✓					
33	ADRA2B														✓											
34	ADRA2C														✓				✓		✓					
35	ADRB1		✓												✓					✓						
36	ADRB2		✓												✓							✓			✓	
37	AGL															✓					✓	✓	✓			

38	AGTR1	✓	✓		✓				✓	✓	✓											✓
39	AHCY											✓		✓	✓						✓	
40	AHR																					
41	AKR1A1														✓	✓						✓
42	AKR1B1	✓	✓	✓	✓	✓					✓		✓	✓	✓	✓	✓	✓	✓	✓	✓	✓
43	AKR1B10	✓	✓	✓	✓					✓			✓	✓	✓					✓	✓	✓
44	AKR1C1										✓				✓					✓		
45	AKR1C2										✓				✓		✓	✓			✓	
46	AKR1C21													✓	✓	✓				✓		
47	AKR1C3	✓	✓		✓						✓				✓		✓	✓	✓	✓	✓	✓
48	AKR1C4														✓					✓		✓
49	AKT1					✓	✓		✓	✓	✓				✓							
50	AKT2									✓												
51	AKT3			✓					✓	✓					✓	✓						
52	ALB		✓		✓							✓								✓		✓
53	ALDH1A1																✓	✓				
54	ALDH1A2		✓														✓		✓			✓
55	ALDH1B1		✓														✓		✓			✓
56	ALDH2		✓	✓	✓										✓		✓		✓			✓
57	ALDH5A1											✓							✓			
58	ALK								✓	✓	✓		✓									
59	ALOX12				✓										✓	✓	✓	✓	✓	✓	✓	✓
60	ALOX15														✓	✓	✓	✓	✓			
61	ALOX15B														✓	✓		✓				
62	ALOX5					✓	✓	✓	✓	✓	✓	✓	✓	✓	✓	✓	✓	✓	✓			
63	ALP1																✓	✓	✓			
64	ALPG																		✓			
65	ALPI														✓	✓	✓		✓			
66	ALPL																		✓			
67	ALS																		✓			
68	AMPC										✓					✓						
69	AMPD3		✓		✓															✓	✓	✓
70	AMY1A					✓						✓	✓	✓	✓				✓	✓		✓
71	AMY2A		✓										✓	✓		✓			✓	✓	✓	✓
72	ANTXR2					✓						✓			✓	✓						
73	AOX																			✓		
74	APEX1															✓			✓			
75	APP		✓	✓												✓	✓	✓	✓			✓
76	AR						✓	✓	✓	✓	✓	✓										
77	ARG1														✓	✓	✓		✓			
78	AROA												✓									
79	AROB												✓									

248	ERAP1		✓														✓		✓	✓			✓	
249	ERBB2					✓	✓		✓															
250	ERN1													✓					✓		✓			
251	ESR1								✓	✓	✓			✓		✓	✓	✓						
252	ESR2						✓	✓	✓	✓	✓	✓		✓		✓	✓							
253	ESRRA																							
254	ESRRB																✓							
255	EZH1													✓		✓								
256	EZH2													✓		✓								
257	F10						✓											✓		✓				
258	F12																			✓				
259	F2						✓			✓								✓	✓					
260	F3	✓	✓	✓	✓									✓									✓	✓
261	F7				✓		✓																	
262	F9				✓																		✓	
263	FAAH								✓		✓													
264	FABG													✓				✓	✓		✓			
265	FABH														✓					✓	✓			
266	FABI													✓		✓	✓	✓	✓	✓	✓			
267	FABZ													✓		✓	✓	✓	✓	✓				
268	FASN		✓					✓						✓		✓	✓	✓		✓			✓	
269	FBP1																						✓	
270	FCER2			✓			✓																	
271	FDFT1										✓													
272	FDPS																✓	✓						
273	FGF1	✓	✓			✓											✓		✓	✓	✓	✓	✓	
274	FGF2	✓	✓			✓											✓	✓		✓	✓	✓	✓	
275	FGFR1	✓	✓	✓	✓					✓													✓	✓
276	FGR														✓									
277	FHIT			✓																			✓	
278	FIMH	✓	✓			✓									✓			✓		✓	✓	✓	✓	
279	FKBP1A						✓			✓	✓		✓											
280	FKBP5						✓																	
281	FLT3						✓	✓		✓		✓					✓	✓	✓					
282	FLT4							✓									✓	✓						
283	FNTA	✓								✓		✓												
284	FNTB	✓								✓		✓		✓										
285	FOLA																						✓	
286	FOLH1	✓	✓	✓	✓									✓	✓	✓	✓					✓	✓	
287	FOS																						✓	
288	FPGS																✓	✓						
289	FRAP1						✓																	

290	FTO													✓							✓	✓			
291	FUCA1	✓	✓		✓									✓	✓	✓						✓	✓		✓
292	FUT4													✓											
293	FUT6			✓																					
294	FUT7													✓											
295	FYN				✓									✓								✓	✓		✓
296	G6PD								✓																
297	G6PD-6PGL																					✓			
298	GAA			✓										✓	✓						✓	✓	✓	✓	
299	GABRA1																					✓			
300	GABRA5																					✓			
301	GABRB1													✓											
302	GAG-pol													✓											
303	GAPC		✓																						
304	GAPDH								✓														✓		✓
305	GBA	✓			✓					✓													✓	✓	✓
306	GBA2				✓																		✓	✓	
307	GCGR																								
308	GFAG																						✓		
309	GFER																						✓		
310	GGH																						✓	✓	
311	GGTA1		✓												✓							✓	✓	✓	✓
312	GJB2														✓								✓	✓	✓
313	GLD-1																						✓		
314	GLMU																						✓		
315	GLO1				✓											✓	✓	✓	✓	✓	✓				
316	GLRA3														✓										
317	GLRB														✓										
318	GNB1																						✓		
319	GNG2																						✓		
320	GNPAT															✓	✓						✓		
321	GPCR																						✓		
322	GPCR35																							✓	
323	GPR35															✓		✓	✓	✓	✓		✓	✓	✓
324	GPR55				✓																				
325	GRB2																						✓		
326	GRIK1															✓	✓						✓	✓	
327	GRIK2															✓	✓						✓	✓	
328	GRIK3															✓	✓						✓	✓	
329	GRK1																							✓	
330	GRK2																								✓
331	GRK6																								

332	GRM2													✓				✓						
333	GRM3																	✓						
334	GRM4																	✓						
335	GRM5																	✓						
336	GSK3A					✓	✓																	
337	GSK3B																							
338	GSTA1																							
339	GSTM2																							
340	GSTO1																							
341	GSTP1																							
342	GUSB																							
343	GYRB		✓	✓																				
344	HAO1																							
345	HARS	✓																						
346	HCAR1																							
347	HCAR2	✓	✓	✓	✓																			
348	HCRTR1																							
349	HCRTR2																							
350	HDAC1	✓	✓																					
351	HDAC2																							
352	HDAC3																							
353	HDAC5																							
354	HDAC6																							
355	HDAC7																							
356	HDAC8																							
357	HDAC9																							
358	HIF1A																							
359	HIF1AN																							
360	HK1	✓																						
361	HK2	✓																						
362	HLCS	✓																						
363	HMGB1																							
364	HMGCR																							
365	HMOX1																							
366	HPGDS																							
367	HPRT1																							
368	HRAS	✓	✓																					
369	HRH3																							
370	HSD11B1																							
371	HSD11B2																							
372	HSD17B1	✓																						
373	HSD17B14																							

416	ITGB1	✓	✓	✓	✓	✓														✓			✓
417	ITGB3			✓																✓			✓
418	ITGB5			✓																			
419	ITGB6			✓																	✓		
420	ITGB7				✓																		✓
421	ITK	✓				✓	✓		✓		✓		✓										
422	ITPR1																				✓		
423	ITPR3																						✓
424	JAK1						✓	✓		✓	✓	✓	✓								✓		
425	JAK2						✓	✓		✓	✓	✓	✓								✓		
426	JAK3					✓		✓													✓		
427	KCNA3																				✓	✓	✓
428	KCNA5								✓														
429	KCNB1																				✓		
430	KCND3														✓	✓	✓				✓		
431	KCNH2			✓			✓	✓			✓		✓										
432	KCNJ1												✓		✓								
433	KCNK2			✓																		✓	
434	KCNK3																					✓	
435	KCNK9																					✓	
436	KCNMA1																					✓	
437	KDM1A								✓														
438	KDM2A														✓								
439	KDM3A														✓							✓	
440	KDM4A														✓								
441	KDM4B																					✓	
442	KDM4C														✓								
443	KDM4D														✓							✓	
444	KDM4E														✓	✓	✓	✓	✓		✓	✓	✓
445	KDM5C														✓							✓	
446	KDM6B														✓								
447	KDR	✓	✓	✓	✓	✓	✓	✓	✓		✓	✓	✓		✓		✓	✓	✓				✓
448	KISS1R																				✓		
449	KIT											✓		✓									✓
450	KLF5																					✓	
451	KLK3			✓				✓		✓	✓												
452	KLK5																					✓	
453	KLK7																					✓	
454	KLRB1A		✓												✓						✓	✓	✓
455	KMO																					✓	
456	KMT2A														✓	✓							
457	KMT5A																					✓	

500	MDH1																	✓				
501	MDM2						✓					✓										
502	MELK																					
503	MERTK						✓	✓														
504	MET		✓			✓	✓								✓			✓	✓			
505	METAP2					✓																
506	MGAM												✓		✓	✓					✓	
507	MGLL																				✓	
508	MGMT	✓	✓	✓	✓																✓	✓
509	mgrA														✓							
510	MIP																					✓
511	MKKN1																					✓
512	MKKN2												✓	✓								✓
513	MLNR												✓	✓								
514	MME	✓	✓	✓	✓																✓	✓
515	MMP1	✓	✓		✓	✓	✓	✓	✓	✓	✓	✓	✓	✓							✓	✓
516	MMP12	✓	✓	✓	✓																	✓
517	MMP13		✓	✓	✓	✓	✓														✓	✓
518	MMP14	✓			✓	✓	✓						✓	✓	✓						✓	✓
519	MMP15												✓									
520	MMP16				✓								✓									✓
521	MMP2	✓		✓	✓			✓	✓	✓	✓	✓	✓	✓							✓	✓
522	MMP3				✓	✓	✓	✓	✓	✓	✓	✓	✓	✓							✓	✓
523	MMP7	✓	✓		✓	✓	✓	✓	✓	✓	✓	✓	✓								✓	✓
524	MMP8	✓	✓	✓	✓	✓	✓	✓	✓	✓	✓	✓	✓	✓							✓	✓
525	MMP9	✓				✓	✓	✓	✓	✓	✓	✓	✓	✓							✓	✓
526	MPC2					✓																
527	MPG																					✓
528	MPO																					✓
529	MRGPRX1		✓																			✓
530	MTCA1																					✓
531	MT-ND1			✓																		✓
532	MT-ND2			✓																		✓
533	MT-ND3			✓																		✓
534	MT-ND4			✓																		✓
535	MT-ND4L			✓																		✓
536	MT-ND5			✓																		✓
537	MT-ND6			✓																		✓
538	MTNR1B																					✓
539	MTOR						✓	✓	✓												✓	✓
540	MVD																					✓
541	MYLK																					✓

878	TOP2A			✓											✓	✓	✓		✓						
879	TP53																✓								
880	TPMT												✓							✓					
881	TPT1												✓												
882	TRAP1						✓				✓		✓												
883	TREH																						✓	✓	
884	TRPM8																							✓	
885	TRPV1																							✓	
886	TRPV2																							✓	
887	TSSK2																							✓	
888	TTL						✓		✓		✓		✓												
889	TTR					✓							✓		✓	✓							✓		✓
890	TUBB																							✓	
891	TUBB1												✓											✓	
892	TUBB2B																							✓	
893	TXK											✓		✓											
894	TYK2																							✓	
895	TYMP	✓	✓	✓																				✓	✓
896	TYMS			✓									✓		✓	✓							✓	✓	✓
897	TYR	✓	✓	✓	✓								✓	✓	✓	✓	✓	✓	✓	✓	✓	✓	✓	✓	✓
898	TYRO3						✓	✓					✓												
899	UGCG			✓																					✓
900	UPP1	✓																							✓
901	VAR5	✓	✓			✓																			✓
902	VCAM1																								✓
903	VCP																								✓
904	VDR												✓	✓											
905	VEGFA	✓	✓												✓	✓	✓						✓	✓	✓
906	V-FPS																✓	✓	✓				✓		
907	VHL																								✓
908	WEE1						✓						✓												
909	WNT3A																								✓
910	XDH																✓	✓	✓				✓		
911	YARS		✓			✓									✓	✓									✓
912	YARS1																								✓
913	ZWF1																								✓

Figures

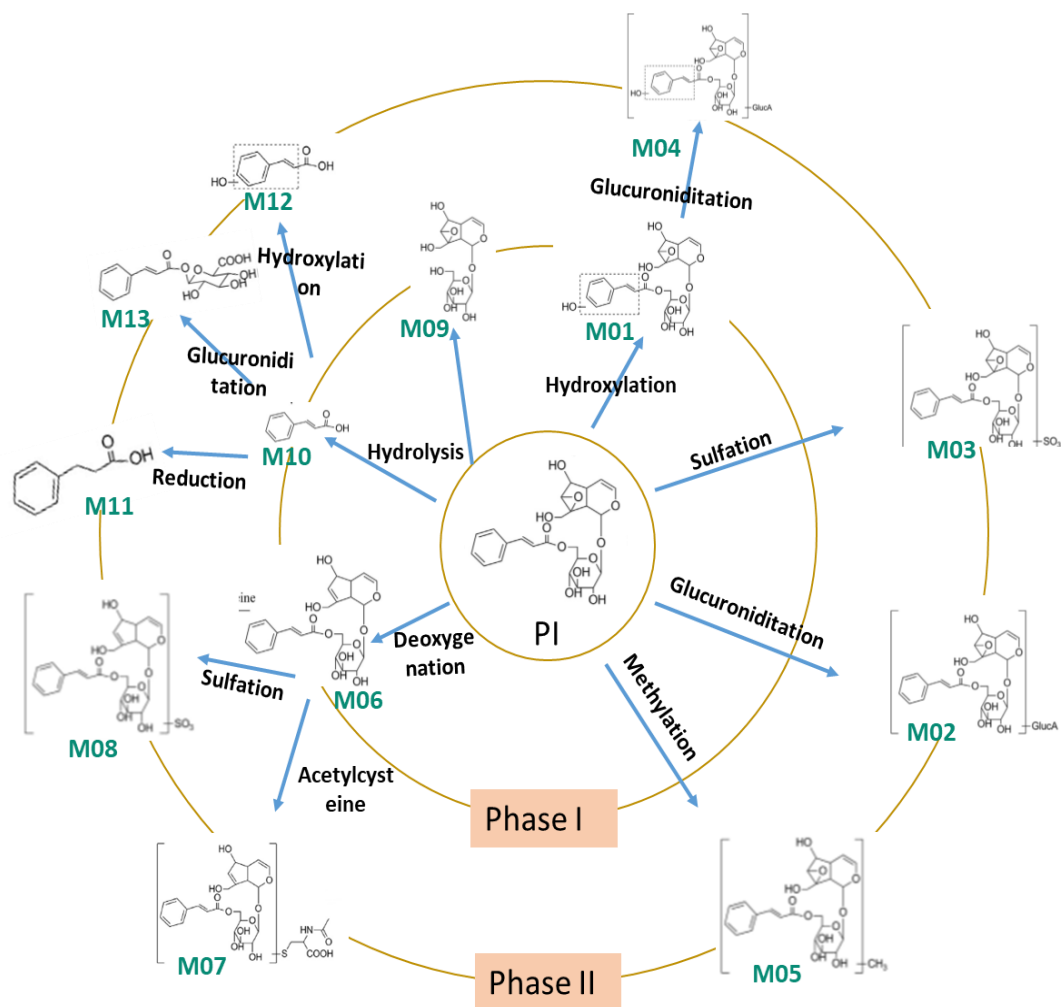


Figure A1: Sub-metabolites of Picoside I in proposed metabolic pathway (according to Xiong et al, 2018); M01 – Hydroxylated PI, M02 – Glucuronated PI, M03 – Sulfanated PI, M04 – Glucuronated product of M01, M05 – Methylated PI, M06 – Deoxygenated PI, M08 – Sulfanated PI, M09 – Catalpol, M10 – Cinnamic acid, M11 – Reduced form of cinnamic acid

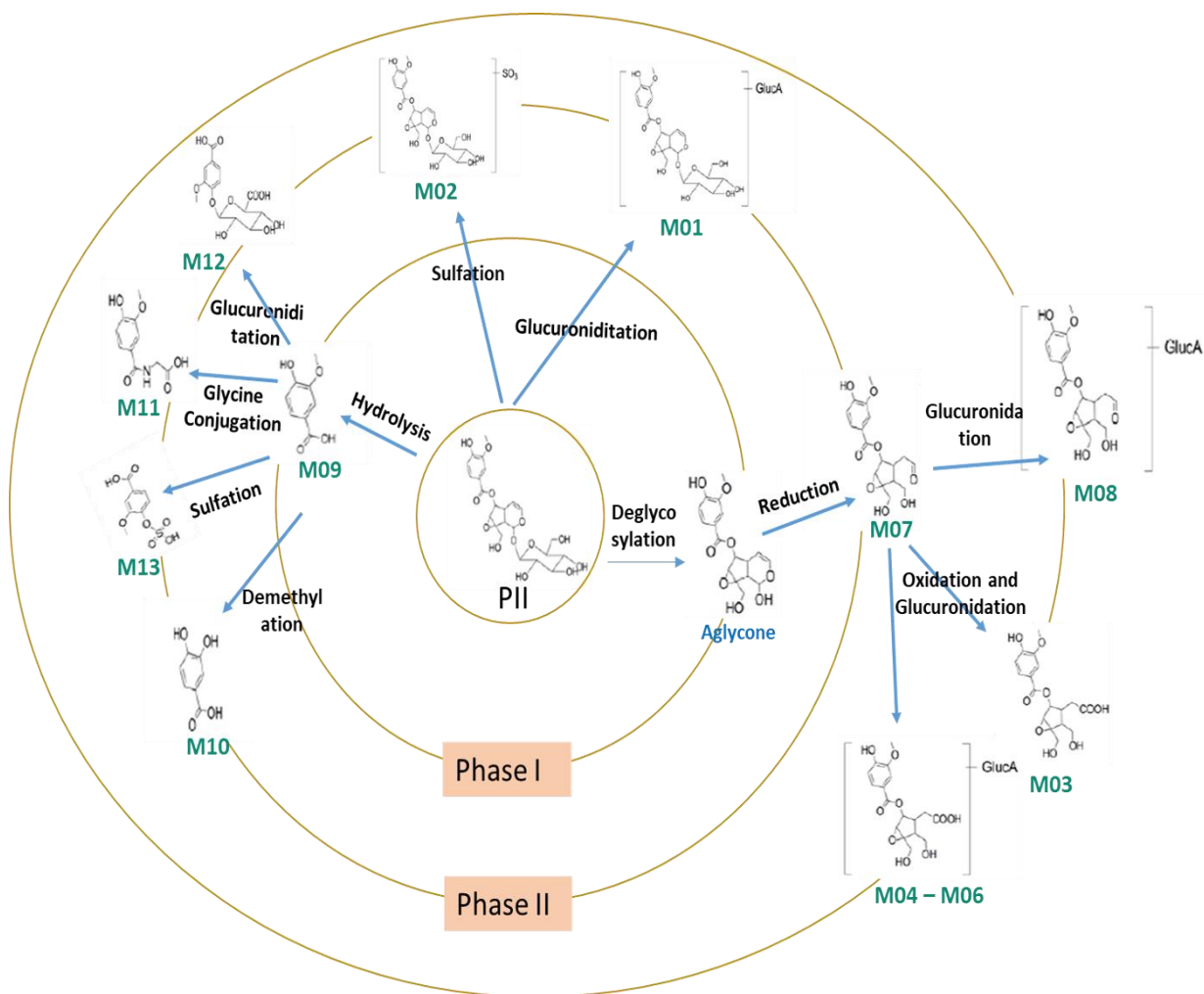


Figure A2: Sub-metabolites of Picoside II in proposed metabolic pathway (according to Gao et al., 2016); M01 – Glucuronated PII, M02 – Sulfate Conjugate of PII, M03 – Oxidised form of M07, M04 - M06 – Glucuronic acid conjugates of M03, M07 – Reduced product of Aglycone, M08 – Glucuronic acid conjugate of M07, M09 – Vanillic acid, M10 – Demethylated metabolite of vanillic acid, M11 – Glycine conjugate of vanillic acid, M12 – Glucuronic acid conjugate of vanillic acid, M13 – Sulfate conjugate of vanillic acid

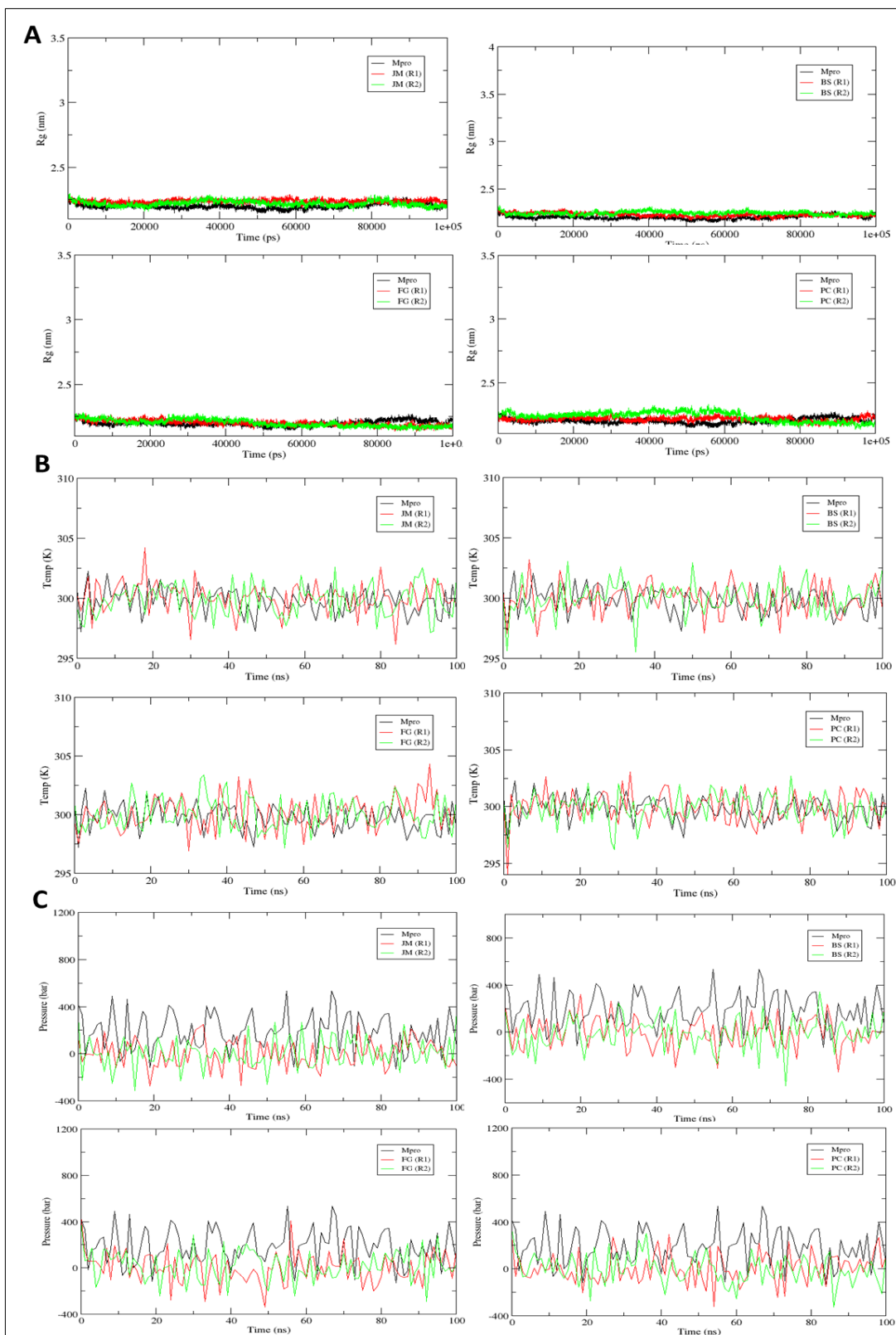


Figure A3: Graphs of native M^{pro} (black) and M^{pro}-ligand complexes in two replicates R1 (red) and R2 (green). A. Radius of gyration in 100 ns MD simulation. B. Temperature C. Pressure

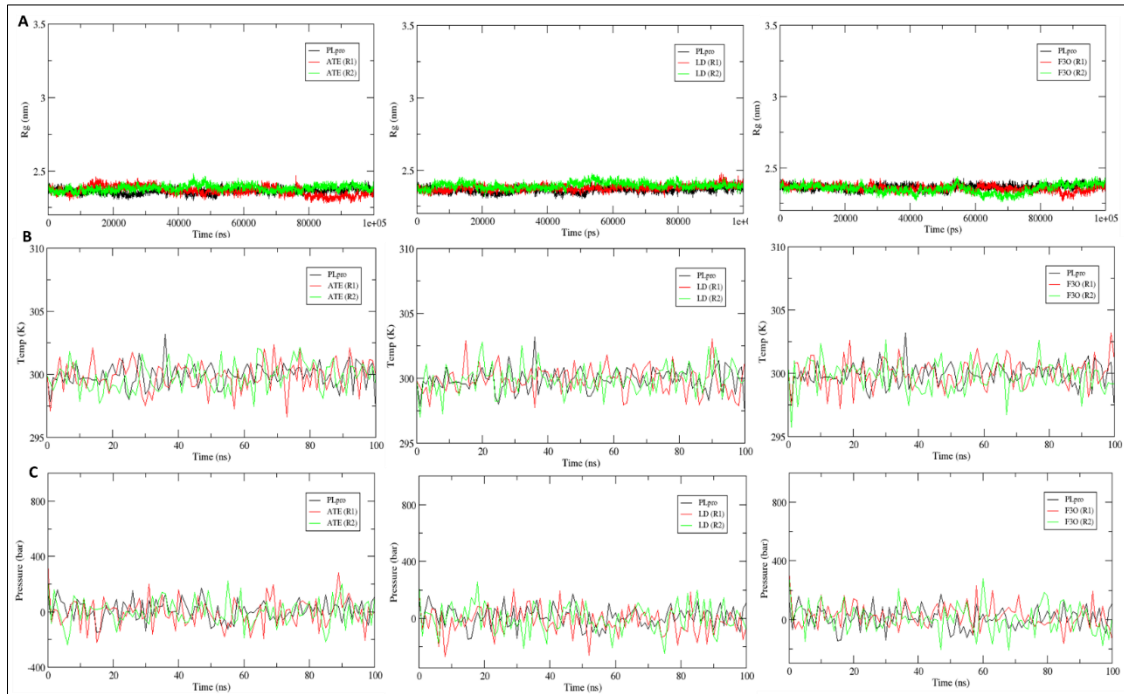


Figure A4: Graphs of native PLpro (black) and PLpro-ligand complexes in two replicates R1 (red) and R2 (green). A. Radius of gyration in 100 ns MD simulation. B. Temperature C. Pressure

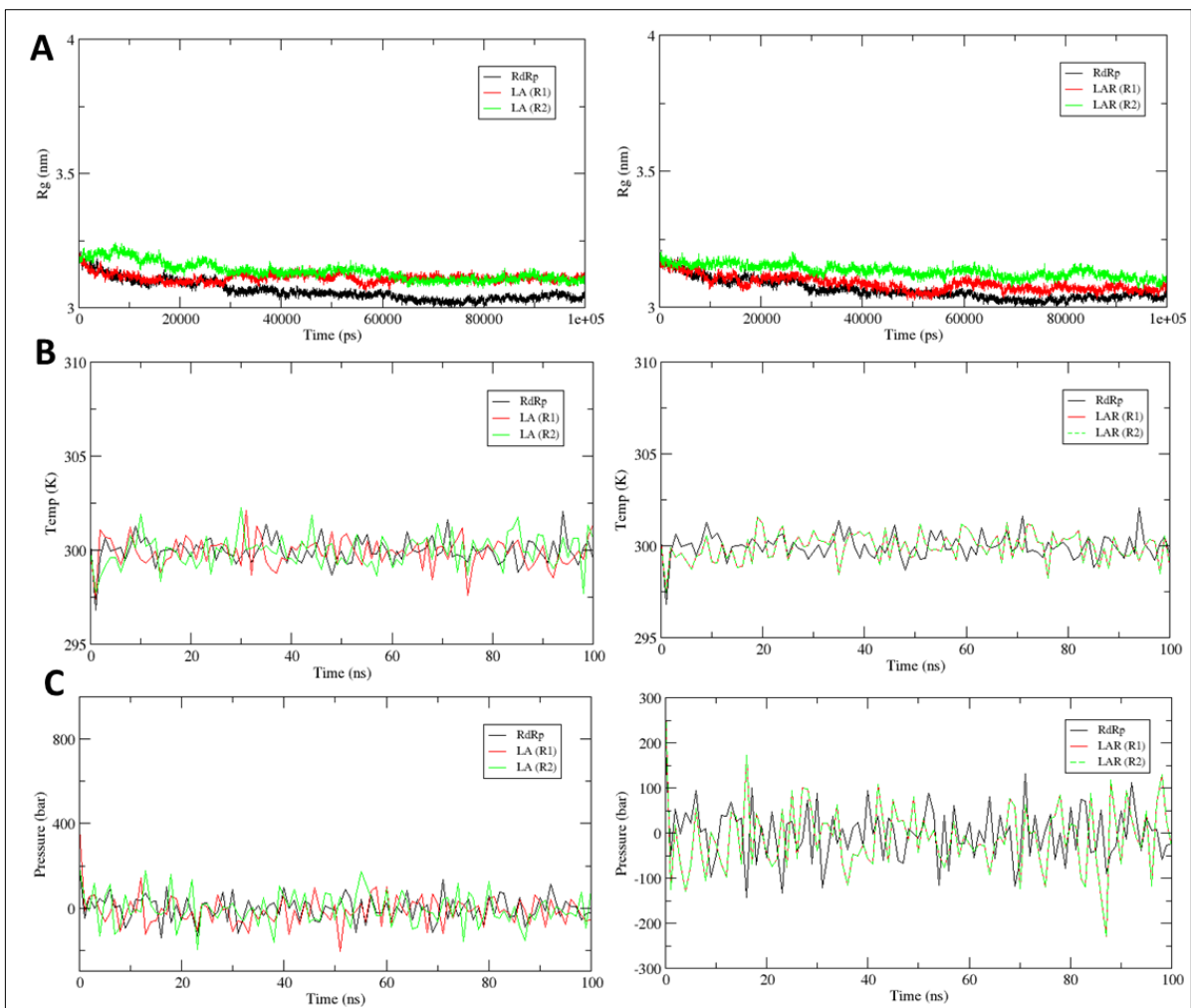


Figure A5: Graphs of native RdRp (black) and RdRp-ligand complexes in two replicates R1 (red) and R2 (green). A. Radius of gyration in 100 ns MD simulation. B. Temperature C. Pressure

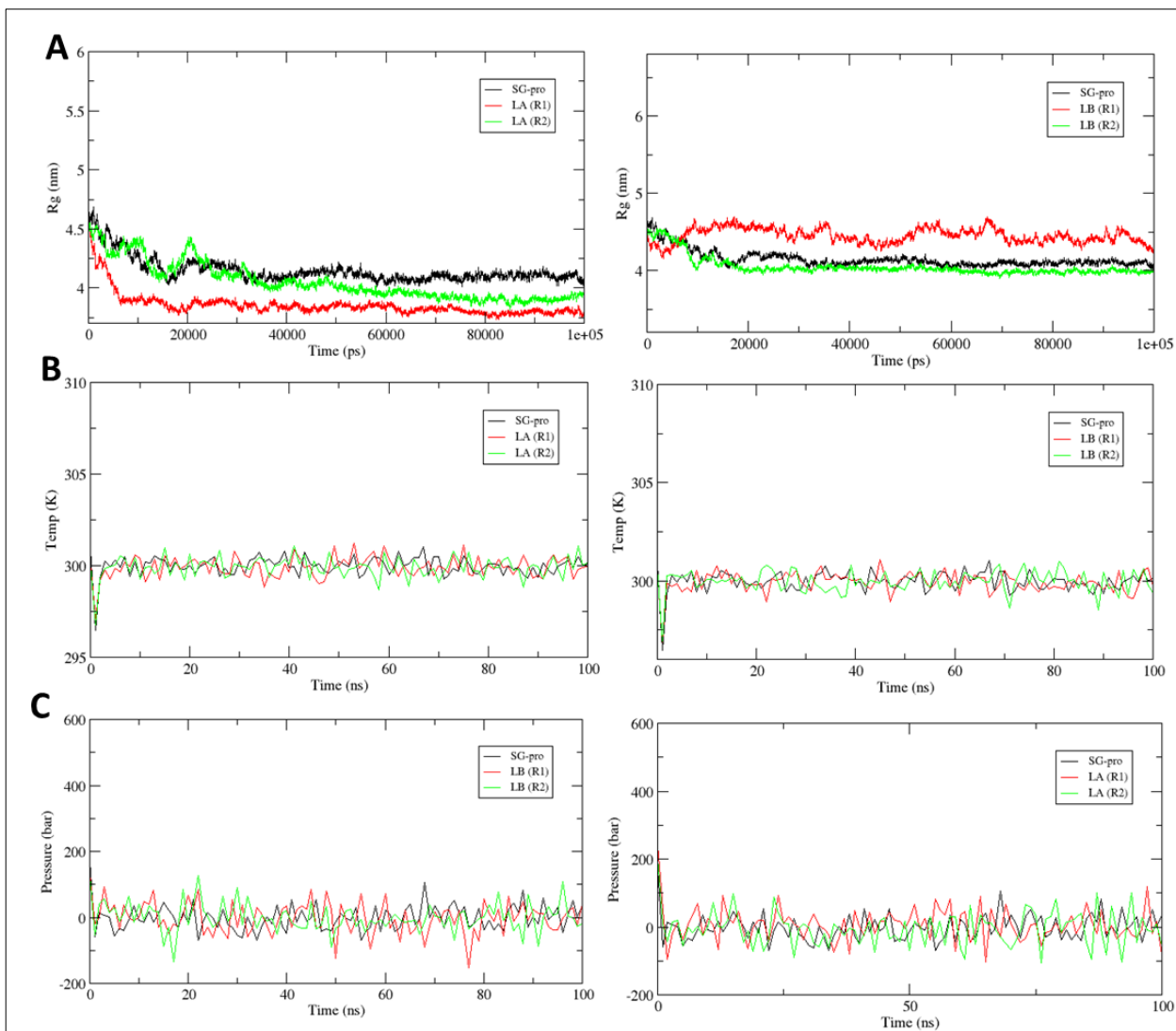


Figure A6: Graphs of native S-Protein (black) and S-Protein-ligand complexes in two replicates R1 (red) and R2 (green). A. Radius of gyration in 100 ns MD simulation. B. Temperature C. Pressure

LIST OF PUBLICATIONS

International Journal Papers

- S. Sharma, A. Sharma, D. Bhattacharyya, and R. S. Chauhan, “Computational identification of potential inhibitory compounds in Indian medicinal and aromatic plant species against major pathogenicity determinants of SARS-CoV-2”, *J. Biomol. Struct. Dyn.*, pp. 1–19, 2021.
- S. Sharma, A. Sharma, and R. S. Chauhan, “Network Pharmacology and Molecular Simulations unravel mechanistic actions of bioactive compounds in a hepatoprotective herb, *Picrorhiza kurroa* for the treatment of NAFLD/ NASH”, *Curr. Comput.-Aided Drug Des.* (Under Revision).

Conferences/Workshops

- S. Sharma, R.S. Chauhan, “Computational Identification of potential therapeutic compounds among essential oils of medicinal and aromatic plants to neutralize major protein targets of SARS-CoV-2”, Presented in International Conference on Innovations in Biotechnology and Life Sciences at Delhi Technical University, Dec. 18-20, 2020.
- S. Sharma, and R.S. Chauhan, presented a poster on “Network Pharmacology addresses the mechanistic action of *Picrorhiza kurroa* compounds and complexities of NAFLD/ NASH” at National Symposium of “Metabolic Associated Fatty Liver Disease”, Translational Health Science and Technology Institute (THSTI), Faridabad, June 2022.
- Participated in CSIR sponsored National Workshop-cum-Training Programme on “Computational Workshop on Genomics, Proteomics, and Metagenomics”, held at CSIR-IGIB, New Delhi, July 20-23, 2022.
- Attended Symposium on “Current Trends in Therapeutics and Diagnostics of NAFLD” at Translational Health Science and Technology Institute (THSTI), Faridabad, June 2019

Patent

- S. Sharma, A. Sharma, D. Bhattacharyya, R.S. Chauhan, “A composition of essential oil compounds targeting major proteins of SARS-COV-2 and a process of preparation thereof”, Ref. No./Application no. assigned: 20211101575.

Research Papers (Other than PhD work)

- A. Sharma, **S. Sharma**, H. Sood, R.S. Chauhan, “Comparative coexpression networks pinpoint acyltransferases decorating structures of major iridoid glycosides in a medicinal herb, *Picrorhiza kurroa*”, *Plant Gene*, 31, 100366, 2022.
- A. Kharb, **S. Sharma**, A. Sharma, N. Nirwal, R. Pandey, D. Bhattacharyya, R. S. Chauhan, “Capturing acyltransferase (s) transforming final step in the biosynthesis of a major Iridoid Glycoside, (Picoside-II) in a Himalayan Medicinal Herb, *Picrorhiza kurroa*”, 1-10, 2022 [IF: 2.7]
- A. Sharma, D. Bhattacharyya, **S. Sharma**, R.S. Chauhan, “Transcriptome profiling reveal key hub genes in co-expression networks involved in Iridoid glycosides biosynthetic machinery in *Picrorhiza kurroa*”, *Genomics*, 113, 5, 3381-3394. [IF:5.7]
- A. Aggarwal, **S. Sharma**, D. Khare, “Virtual screening of novel phytocompound(s) with potential to combat Mycobacterium tuberculosis infection”, *Lett. Drug Des. Discov.*, 19, 2022. [IF: 1.1]

Scholar Biography

Shilpa Sharma was born on 13th Dec 1995, in Meerut, Uttar Pradesh India. She did BSc. (H) Zoology from Dyal Singh College, University of Delhi in the year 2015. She acquired master's degree in MSc. Bioinformatics from Jamia Millia Islamia in 2017. She did research internship from National Institute of Cancer and Research, Noida and INMAS DRDO. Currently, she is pursuing her Ph.D. degree in bioinformatics in the Department of Biotechnology of Bennett University, Greater Noida. Her area of interest includes Computer-aided drug discovery, Pharmacophore modeling, Next Generation Sequencing analysis, Transcriptomics, Proteomics, and Metagenomics. She has published various papers in journals and conferences. The personal email IDs are: e19soe816@bennett.edu.in; shilpa2713@gmail.com.

COMPUTATIONAL MAPPING OF PHYTOCHEMICALS IN PLANTS /HERBAL EXTRACTS TO POTENTIAL LEAD COMPOUNDS

Thesis submitted in partial fulfilment of the requirements for the Degree of

DOCTOR OF PHILOSOPHY

By

**SHILPA SHARMA
(E19SOE816)**



**BENNETT
UNIVERSITY**
TIMES OF INDIA GROUP

Department of Biotechnology,
School of Engineering and Applied Sciences

Bennett University
(Established under UP Act No 24, 2016)
Plot Nos 8-11, Tech Zone II
Greater Noida-201310, Uttar Pradesh, India
July 2022

CHAPTER 5
CONCLUSIONS AND FUTURE PROSPECTS

5.1. CONCLUSIONS

In present investigation, the aim was to map phytochemicals from extracts of different plant species into potential leads. Towards this, two types of studies were carried out to resolve the critical issue in two diseases, COVID-19 and NAFLD. The study explored phytochemicals from essential oils and aromatic plant species as well as from a medicinal herb, *Picrorhiza kurroa* known for its hepatoprotective activity using different approaches of computational drug discovery. The shortlisted compounds can be potential leads to consider for drug development.

- The selected essential oils compounds can be putative compounds for nasal therapy since nasal route is the main entry route of SARS-CoV-2 as well as due to the inherent property of the EO compounds to travel longer distances via air.
- The SARS-COV-2 receptor also exists in brain that is why brain disorders were also noticed among some patients during covid, the essential oil compounds can possibly reach to brain through olfactory lobes.
- On the other hand, the study of *Picrorhiza kurroa* compounds revealed combinatorial effect on targets via multi-component-multi-target mechanism by regulating various pathways, including liver apoptosis, inflammation, drug metabolism.
- Furthermore, the study revealed synergistic action of compounds in herbal extracts of *Picrorhiza kurroa*, thereby addressing comorbidities of disease.

5.2. FUTURE PROSPECTS

This research will serve as a base for future *in-vitro* and *in-vivo* studies. These findings provide the following insights for future research:

- Further experimental validation and clinical trials are required to corroborate the results towards development of novel drugs for treatment of above-mentioned diseases.
- Similar strategy can be applied to address the complexities of other complicated diseases.

- The selected hubs and interacting components can be used to develop biomarkers for each development stages of NAFLD/ NASH.
- The similar pharmacophore or chemical entities with shortlisted compounds can be used to develop new drugs via ligand-based drug discovery and fragment-based drug discovery.